

Cardiff University

Institute of Cancer and Genetics

School of Medicine

**Parameters affecting tumour control and toxicity
in oesophageal cancer: a multi-dimensional
outcome analysis**

A dissertation presented to the Institute of Cancer and Genetics at the
School of Medicine, Cardiff University in partial fulfilment of the
requirements for the degree of Doctor of Philosophy

Dewi Rhys Carrington

Ph. D. 2016



DECLARATION

This work has not been submitted in substance for any other degree or award at this or any other university or place of learning, nor is being submitted concurrently in candidature for any degree or other award.

Signed (candidate) Date

STATEMENT 1

This thesis is being submitted in partial fulfilment of the requirements for the degree of(insert MCh, MD, MPhil, PhD etc, as appropriate)

Signed (candidate) Date

STATEMENT 2

This thesis is the result of my own independent work/investigation, except where otherwise stated.
Other sources are acknowledged by explicit references. The views expressed are my own.

Signed (candidate) Date

STATEMENT 3

I hereby give consent for my thesis, if accepted, to be available for photocopying and for inter-library loan, and for the title and summary to be made available to outside organisations.

Signed (candidate) Date

STATEMENT 4: PREVIOUSLY APPROVED BAR ON ACCESS

I hereby give consent for my thesis, if accepted, to be available for photocopying and for inter-library loans **after expiry of a bar on access previously approved by the Academic Standards & Quality Committee.**

Signed (candidate) Date

Contents

Acknowledgments	9
List of Figures	10
List of Tables	14
List of Acronyms	16
Breakdown of Contribution	19
Study Aims and Objectives	20
Abstract	21
1: Introduction	22
1.1 Oesophageal cancer	22
1.2 Radiotherapy	23
1.3 Radiotherapy in practice	25
1.3.1 Measuring the radiotherapy dose	25
1.3.2 How does radiotherapy work	25
1.3.3 The linear accelerator	27
1.4 Treatment planning	33
1.4.1 Target volumes	34
1.4.2 Dose analysis and homogeneity	37
1.4.3 Treatment plan optimisation	38
1.5 Statistical analysis	39
1.5.1 Mann-Whitney U test	40

1.5.2	Kaplan-Meier and the log-rank test	40
1.5.3	Cox proportional hazard	42
1.6	Clinical trials	42
1.6.1	Phases of a clinical trial	44
1.7	The SCOPE 1 clinical trial	45
1.8	Relating radiotherapy treatment to outcome	47
2:	Data and software preparation	50
2.1	Clinical data management	50
2.2	Data preparation in the SCOPE 1 analysis	51
2.2.1	Radiotherapy trial data	51
2.2.2	Outcome data preparation	56
2.3	Testing the data pathway	57
2.4	Program and script development	62
2.4.1	Automatic dose volume histogram calculation	63
2.4.2	DVH import in EUCLID	65
2.4.3	Addition of hazard ratio calculation	73
2.5	Testing the survival analysis module	74
2.6	Conformity indices	75
2.7	Type A and Type B algorithms	80
3:	Dose distribution and patient outcome	86
3.1	Introduction	86

3.2	Correlating plan quality with outcome	87
3.2.1	Quantifying plan quality	87
3.2.2	Analysis of conformity index values across the database	88
3.2.3	Comparing JCI and MDC	91
3.2.4	Outcome data	95
3.2.5	Deciding on CI breakpoint	95
3.4	Results	96
3.4.1	OverMDC and UnderMDC and overall survival	96
3.5	Analysis of OverMDC values	98
3.5.1	Clinical factors	98
3.5.2	Technological factors	101
3.6	Re-planning of Type B patients in OMP	102
3.6.1	Obtaining a VMAT solution in OMP	103
3.6.2	Class solution in Radiotherapy planning	103
3.6.3	What makes a good treatment plan?	104
3.6.4	VMAT optimising volumes	105
3.6.5	Multicriteria Optimization and creating a pareto curve	106
3.6.6	Re-planning worst performing OverMDC patients	114
3.7	Multivariate analysis	116
3.8	Discussion	116
3.9	Conclusion	119

4: The effect of dose escalation on gastric toxicity	120
4.1 Introduction	120
4.1.1 Tumour control probability	120
4.1.2 Normal tissue complication probability	122
4.1.3 Clinical derivation and use of TCP and NTCP	123
4.2 The need for dose escalation	124
4.3 Modelling the impact of dose escalation	126
4.3.1 Study dataset	126
4.3.2 Treatment planning	127
4.3.3 Radiobiological modelling	130
4.4 Results	131
4.5 Discussion	139
4.6 Quantification of stomach movement	145
4.7 Cone Beam Computed Tomography	147
4.8 Preparing for analysis	148
4.8.1 Outlining the stomach volume	148
4.8.2 Image registration	148
4.8.3 Quantifying the stomach position	150
4.9 Results	152
4.9.1 Difference in max and min XYZ coordinates and COM	152
4.9.2 Average displacement of XYZ and COM coordinates	154
4.9.3 Difference in total volume	155
4.9.4 Difference in overlap volumes	156
4.10 Discussion	158

4.11	Conclusion	160
------	------------	-----

5: CT image heterogeneity and patient outcome **162**

5.1	Introduction	162
-----	--------------	-----

5.2	Texture analysis of the SCOPE 1 data	164
-----	--------------------------------------	-----

5.2.1	TexRAD software package	164
-------	-------------------------	-----

5.2.2	Considering contrast and cetuximab	166
-------	------------------------------------	-----

5.2.3	Importing GTV outlines	167
-------	------------------------	-----

5.2.4	Texture analysis algorithm settings for oesophageal cancer	174
-------	--	-----

5.2.5	Analysed sample size	174
-------	----------------------	-----

5.3	Results	175
-----	---------	-----

5.3.1	Texture analysis in TexRAD	175
-------	----------------------------	-----

5.3.2	Multivariate analysis	180
-------	-----------------------	-----

5.4	Discussion	181
-----	------------	-----

5.5	Conclusion	185
-----	------------	-----

6. Conclusions and further work **186**

6.1	Conclusions	186
-----	-------------	-----

6.2	Further work	188
-----	--------------	-----

7. Dissemination of work and attended courses, seminars and conferences	191
7.1 Publications	191
7.2 Attended courses, seminars and conferences	193
Appendix	195
A1 Computer coding	195
A2 SCOPE 1 Radiotherapy Protocol	195
References	235

Acknowledgments

This project would not have been possible without the funding I received from Cancer Research Wales for which I am extremely grateful. Their continued support of research in Wales is important and greatly appreciated. I have been lucky in having a fantastic team of supervisors in Dr John Staffurth, Dr Emiliano Spezi, Dr Tom Crosby and Dr Sarah Gwynne. From the outset the advice and support I received has been exemplary. In particular I would like to thank John and Emiliano, I would not have got here without your guidance and encouragement.

I was based at Velindre Cancer Centre throughout this project therefore I would also like to thank all the staff of the Medical Physics department. In particular to Phil Wheeler for his help with the VMAT class solution work and Paddy Downes for problem solving when importing DICOM data. The Cancer Research Wales library staff Bernadette and Anne were also invaluable in tracking down and accessing papers in the literature that might otherwise have been out of reach. I feel great pride in now calling the centre my workplace as a Medical Physicist in the NHS and look forward to developing my career as a member of the team there.

I would like to thank my parents. Their unconditional support, particularly during the early stages of my academic education, set me on the path to where I am today. Diolch o waelod fy nghalon am bopeth.

Finally I would like to thank and dedicate this PhD to my wife Kat and our family. Your unbounded love and optimism is an inspiration and I would not be who I am without you. I love you.

List of Figures

Figure 1.1 – Schematic of radiation damage to DNA

Figure 1.2 – Schematic of linear accelerator head for (a) photon beam treatment (b) electron beam treatment

Figure 1.3 – Graphic of linear accelerator head

Figure 1.4 – Illustrating the principles of IMRT

Figure 1.5 – Schematic of treatment volumes

Figure 1.6 – Schematic of SCOPE 1 clinical trial

Figure 2.1 – Gold standard structure naming

Figure 2.2 – Example of non-uniform naming of patient structures

Figure 2.3 – Spreadsheet for testing of data pathway

Figure 2.4 – EUCLID interface

Figure 2.5 – Statistical analysis options in EUCLID

Figure 2.6 – Test DVH analysis with pneumonitis grade

Figure 2.7 – Test Kaplan Meier split by Lung V30 values

Figure 2.8 – Formatting of data in Excel spreadsheet

Figure 2.9 – Addition of filepath column to Excel spreadsheet

Figure 2.10 – Manual import of DVH data

Figure 2.11 – Automatic import of DVH data

Figure 2.12 – DVH from manual and automatic import

Figure 2.13 – DVH for TotalLung from manual and automatic import

Figure 2.14 – Kaplan Meier plot from EUCLID

Figure 2.15 – Kaplan Meier plot from SPSS

Figure 2.16 –Schematic for Jaccard Conformity Index

Figure 2.17 – Schematic of MDC showing OverMDC and UnderMDC

Figure 2.18 – Variation of MDC with change in JCI for two spherical volumes

Figure 2.19a – Plan using Type A algorithm showing PTV and 95% isodose line

Figure 2.19b – Plan using Type B algorithm showing PTV and 95% isodose line

Figure 2.20 – Consort diagram showing patient treatment and tumour demographics

Figure 3.1 – Distribution of JCI values across the database

Figure 3.2 – Distribution of UnderMDC values across the database

Figure 3.3 – Distribution of OverMDC values across the database

Figure 3.4 – Profile of outlier patient in CER with dose wash

Figure 3.5 – Distribution of UnderMDC and OverMDC values across the database

Figure 3.6 – Plot of OverMDC vs JCI

Figure 3.7 – Plot of UnderMDC vs JCI

Figure 3.8 – Plot of Mean MDC vs JCI

Figure 3.9 – Kaplan Meier according to OverMDC

Figure 3.10 – Kaplan Meier according to UnderMDC

Figure 3.11 – Distribution of tumour site in OverMDC >4.4mm

Figure 3.12 – Distribution of tumour site in OverMDC <4.4mm

Figure 3.13 – OverMDC and GTV length for patients

Figure 3.14 – OverMDC and PTV volume for patients

Figure 3.15 – OverMDC and dose delivery method for patients

Figure 3.16 - % volume receiving dose constraint for each structure

Figure 3.17 – Mean Lung dose vs Mean Heart dose

Figure 3.18 a-e – Showing spilling of dose into lung with increased heart weight

Figure 3.19 – Mean Lung dose vs Mean Heart dose for patient 1

Figure 3.20 – Mean Lung dose vs Mean Heart dose for patient 2

Figure 3.21 – Effect of re-planning from 3D-CRT to VMAT on OverMDC

Figure 4.1 – Schematic of StomachWall-In and StomachWall-Out volumes

Figure 4.2 a-c – Comparison of 50Gy_{3D}, 50Gy_{RA} and 60Gy_{RA} radiotherapy plans

Figure 4.3 – TCP values of 50Gy_{3D}, 50Gy_{RA} and 60Gy_{RA} radiotherapy plans

Figure 4.4 – NTCP for heart for 50Gy_{3D}, 50Gy_{RA} and 60Gy_{RA} radiotherapy plans

Figure 4.5 – NTCP for lung for 50Gy_{3D}, 50Gy_{RA} and 60Gy_{RA} radiotherapy plans

Figure 4.6 – NTCP for stomach for 50Gy_{3D}, 50Gy_{RA} and 60Gy_{RA} radiotherapy plans

Figure 4.7 – NTCP for whole stomach for 50Gy_{3D}, 50Gy_{RA} and 60Gy_{RA} radiotherapy plans

Figure 4.8 – NTCP for stomach wall minus PTV2 for 50Gy_{3D}, 50Gy_{RA} and 60Gy_{RA} radiotherapy plans

Figure 4.9 – NTCP vs whole stomach wall/PTV1 overlap structure volume for 60Gy_{RA} radiotherapy plans

Figure 4.10 – NTCP vs whole stomach wall/PTV2 overlap structure volume for 60Gy_{RA} radiotherapy plans

Figure 4.11 – Schematic of CBCT and conventional ‘fan’ CT

Figure 4.12 – Pre registration of planning CT and CBCT images

Figure 4.13 – Post registration of planning CT and CBCT images

Figure 4.14 – Screen grab from CERR showing all stomach volumes

Figure 4.15 – Absolute volume of stomach across treatment

Figure 4.16 – Absolute volume of PTV/Stomach overlap across treatment

Figure 4.17 – Absolute volume of PTV2/Stomach overlap across treatment

Figure 5.1 – GTV outline in OsiriX

Figure 5.2 – XML output from OsiriX

Figure 5.3 – Incorrect orientation of structure in TexRAD

Figure 5.4 – TexRAD XML format

Figure 5.5 – Correct import of structure into TexRAD

List of Tables

Table 1.0 – Outline of typical phases of clinical trials

Table 2.0 – Dose bins for automatic and manual import of DVH

Table 2.1 – Dose volume constraints for SCOPE 1 trial

Table 2.2 – Mann Whitney U test for MDC metrics between Type A and Type B dose algorithms

Table 3.0 – Number of patients included in analysis in Chapter 3

Table 3.1 – Dose volume constraints for VMAT planning

Table 3.2 – Objectives and weighting of structures in VMAT plan

Table 3.3 – OverMDC after re-planning with VMAT class solution

Table 3.4 – Results of multivariate analysis

Table 4.0 – Number of patients included in analysis in Chapter 4

Table 4.1 – Dose constraints for dose escalated radiotherapy plans

Table 4.2 – Comparison of dose volume metrics and TCP and NTCP values for all radiotherapy plans

Table 4.3 – Pearson correlation coefficients between stomach, stomach wall volumes and dose metrics.

Table 4.4 – Difference in minimum, maximum and COM coordinates (mm) for stomach structures (Patient 1)

Table 4.5 – Difference in minimum, maximum and COM xyz coordinates (mm) for stomach structures (Patient 2)

Table 4.6 – Difference in minimum, maximum and COM xyz coordinates (mm) for stomach structures (Patient 3)

Table 4.7 – Difference in minimum, maximum and COM xyz coordinates (mm) for stomach structures (Patient 4)

Table 4.8 – Average displacement of minimum, maximum and COM xyz coordinates

Table 4.9– Average xyz coordinates across all image sets

Table 4.10 – Average COM coordinates across all images

Table 4.11 – Percentage difference in stomach volume between CBCT and planning image

Table 4.12 – Percentage difference in PTV/stomach overlap volume between CBCT and planning image

Table 4.13 – Percentage difference in PTV2/stomach overlap volume between CBCT and planning image

Table 5.0 – Number of patients included in analysis in Chapter 5

Table 5.1 – TexRAD image analysis parameters

Table 5.2 – Subgroups of patients

Table 5.3 – Statistically significant results for all patients imaged with contrast

Table 5.4 – Statistically significant results for all patients not imaged with contrast

Table 5.5 – Statistically significant results for patients imaged with contrast and not administered cetuximab

Table 5.6 – Statistically significant results for patients imaged with contrast and administered cetuximab

Table 5.7 – Statistically significant results for patients imaged with contrast and not administered cetuximab

Table 5.8 – Statistically significant results for patients not imaged with contrast and not administered cetuximab

List of Acronyms

CRT – Chemoradiotherapy

dCRT – Definitive Chemoradiotherapy

Gy – Gray

MLC – Multi Leaf Collimator

3D-CRT – 3D Conformal Radiotherapy

IMRT – Intensity Modulated Radiotherapy

VMAT – Volume Modulated Radiotherapy

CT – Computed Tomography

ICRU – International Commission on Radiation Units and Measurements

GTV – Gross Tumour Volume

CTV – Clinical Target Volume

PTV – Planning Treatment Volume

TV – Treated Volume

IV – Irradiated Volume

OAR – Organ at Risk

PRV – Planning Organ at Risk Volume

DVH – Dose Volume Histogram

TCP – Tumour Control Probability

NTCP – Normal Tissue Complication Probability

D_{\max} – Maximum Dose

OMP – Oncentra MasterPlan

WCTU – Wales Cancer Trials Unit

EGFR – Epidermal Growth Factor Receptor

CDM – Clinical Data Management

DICOM – Digital Imaging and Communications in Medicine

RTOG – Radiation Therapy Oncology Group

CERR – Computational Environment for Radiotherapy Research

MRI – Magnetic Resonance Imaging

RTTQA – Radiotherapy Trial Quality Assurance

CRF – Case Report Form

CTCAE – Common Terminology Criteria for Adverse Event

CN – Conformation Number

RCI – Radiation Conformity Index

JCI – Jaccard Conformity Index

MDC – Mean Distance to Conformity

MCO – Multicriteria Optimisation

GEJ – Gastroesophageal Junction

EUS – Endoscopic Ultrasound

SIB – Simultaneous Integrated Boost

QUANTEC – Quantitative Analyses of Normal Tissue Effects in the Clinic

IGRT – Image Guided Radiotherapy

CBCT – Cone Beam Computed Tomography

COM – Centre of Mass

TA – Texture Analysis

ROI – Region of Interest

SSF – Spatial Scaling Factor

XML – Extensible Markup Language

HU – Hounsfield Units

Breakdown of contribution

Dewi Rhys Carrington – Carried out study and drafting of thesis manuscript.

John Staffurth, Cardiff University – Involved in conception and design of overall study and drafting of manuscript. Provided clinical support.

Emiliano Spezi, Cardiff University - Involved in conception and design of overall study and drafting of manuscript. Provided technical support.

Sarah Gwynne, Abertawe and Bro Morgannwg University Health Board - Involved in conception and design of overall study and drafting of manuscript.

Thomas Crosby, Velindre NHS Trust - Involved in conception and design of overall study and drafting of manuscript.

Chris Hurt, WCTU – Substantially involved in acquisition of all trial data and providing statistical guidance.

Peter Dutton, WCTU - Substantially involved in acquisition of all trial data and providing statistical guidance.

Philip Wheeler, Velindre NHS Trust – Provided technical support for conception of radiotherapy planning class solution in Chapter 3.

Betsan Thomas, Velindre NHS Trust – Provided clinical support and knowledge for organ at risk outlining in lower oesophageal work in Chapter 4.

Samantha Warren, Oxford University – Involved in conception and design of dose escalation study in Chapter 4. Provided technical support.

Mike Partridge, Oxford University - Involved in conception and design of dose escalation study in Chapter 4. Provided technical support.

Maria Hawkins, Oxford University - Involved in conception and design of dose escalation study in Chapter 4. Provided technical support.

Study aims and objectives

The aim of this study was to investigate clinical and technical factors that may influence patient toxicity and outcome within an oesophageal cancer clinical trial dataset. The objectives of the study were:

1. To assess interdepartmental variation in radiotherapy treatment planning techniques
2. Identify clinical factors that may influence radiotherapy treatment outcome
3. To implement new metrics that may allow quantification of treatment planning variation
4. To incorporate treatment planning variation data, dose data and other biological and clinical factors into a multivariate analysis linked with patient outcome
5. To investigate the role of radiotherapy dose escalation in improving patient outcome
6. To identify and explore new metrics that relate patient factors to outcome

Abstract

The work contained within this thesis explores the relationship between clinical and technological parameters of radiotherapy treatment planning and patient outcome in patients who were treated for cancer of the oesophagus as part of the SCOPE 1 clinical trial. However the methods and concepts of the work could also have applications at other tumour sites.

By developing ideas from previous studies, a novel method of applying a conformity index found a significant relationship between the quality of a radiotherapy plan and patient outcome in terms of overall survival. Furthermore it was found that the plan quality could be improved by utilising a relatively new method of dose delivery. This dose delivery method also allowed the improving of tumour control via dose escalation to be explored via radiobiological modelling. The results of this work showed that although the probability of controlling the tumour is increased, there is also a significantly higher risk of increased gastric toxicity for patients with lower oesophageal tumours. Interfraction gastric movement was also investigated with the end result being a recommendation for stomach movement and toxicity to be minimised by using a pre-treatment protocol. This is being taken forward in a nationwide multicentre clinical trial. Finally a texture analysis software package was used to investigate whether there was relationship between the image heterogeneity parameters of computed tomography images and patient outcome. This work could potentially aid the decision making process of radiotherapy treatment, allowing a more informed judgement to be made on the most beneficial treatment for the patient.

Chapter 1

Introduction

1.1 Oesophageal Cancer

Worldwide, oesophageal cancer is the eighth most common cancer and it has the fifth highest mortality rate of any tumour sites (1). The disease can present in two main histological sub types, squamous-cell carcinoma, more common in the developing world and arises from the skin cells that line the upper and middle third of the oesophagus, and adenocarcinoma, which is more common in the developed world and arises from glandular cells present in the lower third of the oesophagus. The main risk factors associated with squamous cell carcinomas include tobacco smoking, alcohol consumption and poor nutrition whilst the main risk factors for adenocarcinomas include smoking, obesity and gastroesophageal reflux disease (2). The incidence of squamous cell carcinoma in the UK remains stable or is falling whilst the incidence of adenocarcinomas affecting the lower oesophagus and gastro-oesophageal junction has increased substantially over recent decades (3). Where the patient remains fit and healthy, surgical resection of the tumour remains the first choice of curative therapy. However surgery is only appropriate for 10-20% of the patient population and despite low postoperative mortality rates, the long-term outcomes from surgical-based treatment due to both systematic relapse and locally

advanced disease at presentation remains poor (4). Most patients will therefore present with in-operable disease or may not be fit enough to undergo surgery.

Chemoradiotherapy (CRT), the combination of chemotherapy and radiotherapy, is used widely in combination with surgery to try and improve the low survival rates of surgery alone. CRT can be combined with surgery both as neoadjuvant, before surgery, or adjuvant, after surgery, therapy. Recent studies and trials however have shown definitive CRT (dCRT), where chemo-radiation is the sole method of treatment, is not only more effective than chemotherapy (5) or radiotherapy (6) alone in treating oesophageal cancer, but also results in significantly higher overall survival rate compared to surgery alone (7) & (8).

The majority of patients who relapse do so within the previously irradiated area (9) (10), with the reported local failure rate in patients treated with CRT being 45-58%. Therefore, although radiotherapy undoubtedly does and will continue to play an important part in the treatment of oesophageal cancer, it is vital that the delivery of radiation to the tumour sites is done in a manner that will maximise the tumour control whilst reducing the risk of normal tissue toxicity.

1.2 Radiotherapy

Radiotherapy, together with surgery and chemotherapy, is one of three main modalities used in the treatment of cancer. It uses photons, electrons or ions to destroy tumour cells within the body. Ionising radiation in the form of photons and electrons has been used in the treatment of patients since the beginning of the 20th century, soon after the initial discovery of x-rays. This early treatment mostly consisted of either kilovoltage x-ray sets or the application of radium either on or

near the lesions on the patient. It was not until 1956 that the first patient was treated with a linear accelerator, which uses the high-speed impact of electrons on a small piece of high-density material to produce high-energy x-ray photons that can be focused to enter a patient. A key step forward was the use of higher energies, giving skin sparing for deep seated tumours. However, tight dose distributions are needed to spare normal tissue of irradiation, with geometric accuracies of 2-3mm required for the delivery of successful treatment plans (11) and dosimetric differences of 5-7% known to cause significant changes in tumour control and normal tissue (12) & (13).

Radiotherapy is usually performed as part of a fractionated schedule, in which the treatment is spread over a number of days. This is important as it allows both the healthy tissue to recover from some unavoidable exposure but also to ensure that tumour cells that may have been in the radio-resistant phase of their cell cycles to be in the radio-sensitive cycle when the next radiation dose is given (14). Fractionation schedules will vary between tumour sites and can also be changed as a result of clinical trials in which a particular schedule is found to be more beneficial.

Clinical trials are an extremely important part of clinical science and research. They are essential in evaluating the efficacy of new treatment methods and carefully conducted clinical trials are the quickest and safest method of determining whether the new treatment should be given to the extended population. Radiotherapy can be prescribed to patients either as a stand-alone therapy or as part of a treatment schedule that includes chemotherapy. As a result, radiotherapy can be included in a clinical trial in two ways; as part of standard care where all patients receive the same

radiotherapy schedule, or as the research arm itself, where patients will receive different radiotherapy schedules to determine the efficacy of one over the other.

1.3 Radiotherapy in practice

1.3.1 Measuring the radiotherapy dose

In order to safely treat a patient it is critical that the dose of radiotherapy administered to that patient is quantified. The SI unit for radiotherapy is the Gray (Gy), and it is defined as the absorption of one joule of radiation energy by one kilogram of matter ($1\text{Gy} = 1 \text{ J/Kg}$) (15). This standard unit is used to prescribe radiotherapy to patients, with the amount of dose prescribed usually dependent on the tumour site.

1.3.2 How does radiotherapy work?

It is the interaction of the x-ray radiation produced for radiotherapy with a patient's tissue that enables radiotherapy to be an effective form of treatment.

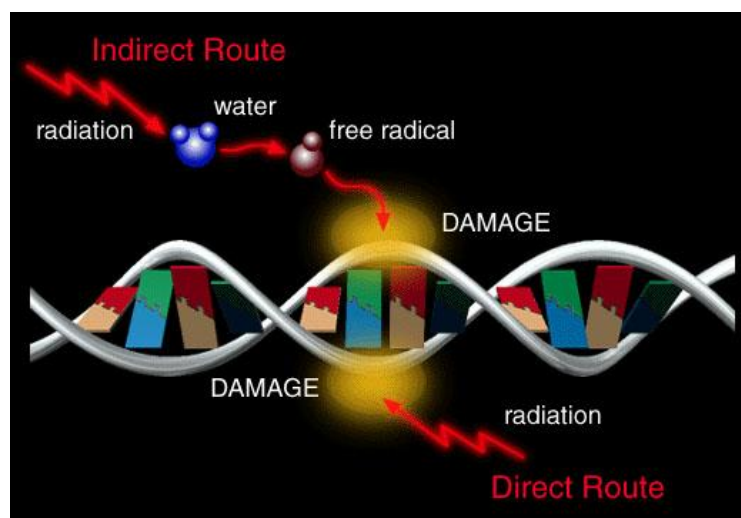


Figure 1.1 - Schematic of radiation damage to DNA (16)

Radiation can cause damage either via the indirect or direct route as shown in Figure 1.1.

The effects of radiation on tissue can be divided into four phases (17):

1. The physical phase – radiation absorption in tissue leads to ionisation (ejection of orbital electrons) and excitation (raising electrons to higher energy levels within the atom).
2. The chemical phase – these damaged atoms and molecules react with other cellular components leading to the breakage of chemical bonds and the formation of ‘free-radicals’. These free radicals are highly reactive oxygen species that go on to interact with the DNA.
3. The biological phase – this includes all subsequent processes, beginning with enzymatic reactions that act on the residual chemical damage. The vast majority of DNA damage is repaired successfully but some lesions fail to repair and this leads to cell death. In most tissues, several cell divisions may occur prior to cell death.
4. The clinical phase – this covers the clinical effects of the delivered radiation. Tumour effects are thought to be generally due to cell death caused directly by DNA damage, although indirect effects such as reduction of tumour vascularity or enhanced immune recognition may also be important. Normal tissue effects may be acute due to direct cell death to mucosal surface or late, thought to be due to indirect effects on the vasculature or on the stem cell component, reducing the capacity to

repair future damage. Radiation is also potentially carcinogenic and there is a risk of radiation-induced second malignancies, especially in younger patients and those expected to live a further 10 years.

The maximum radiation dose that can be tolerated at any given tumour site within an individual is largely unknown. This is mostly due to the difficulty of carrying out studies that are not limited by the toxicity of the surrounding normal tissue. As a result, the commonly accepted maximum doses that are prescribed to any particular area have been derived empirically during the history of radiation therapy and these will be based on limited retrospective data and clinical observations. There are published guidelines that have been used as reasonable estimates of the risk of developing a particular toxicity (18), however these are based on small populations of patients, treated with out-dated techniques. A major consideration when prescribing radiation to patients is the type of tissue exposed and the impact of uncontrolled cancer, as this may influence the decision on how much radiation is necessary and tolerable. For example in some tissues such as the lung, quite a lot of damage after irradiation may be acceptable if the probability of tumour control is reasonably high. However, the consequences of a high dose to the central nervous system can be severe, and it must therefore be tailored to minimise the likelihood of damage.

1.3.3 The linear accelerator

Linear accelerators are the most widely used machine for producing x-rays in a radiotherapy department. The megavoltage x-rays are produced by the deceleration

of electrons in a tungsten target and the energy spectrum of the photons will be determined by the electron energy, target and filter composition. Electrons produced by an electron gun are accelerated up to relativistic velocities along a waveguide by a magnetic field generated by microwaves. The microwaves are produced in either a klystron or magnetron. Typically electrons will enter the waveguide at around $0.4c$ and will leave having been accelerated up to $0.995c$ (where c = speed of light). It is important that the electron beam is steered so that it enters and leaves the waveguide correctly, and that it also strikes the target or scattering foil in such a way that it creates the required high quality beam. There are therefore usually two steering coils either side of the waveguide and then a bending magnet in order to focus the beam on to the target.

Electrons lose their energy as they pass through the target via three primary interaction mechanisms, the most important of which for the production of clinically useable x-ray photons is the bremsstrahlung mechanism. Bremsstrahlung X rays result from Coulomb interactions between the incident electron and the nuclei of the target material. During the Coulomb interaction between the incident electron and the nucleus, the incident electron is decelerated and loses part of its kinetic energy in the form of bremsstrahlung photons. A range of photon energies is produced, with the maximum energy being equal to the energy of the electrons incident on the target. However the x-rays are transmitted in a very non-uniform beam that is unsatisfactory for x-ray therapy. The beam is therefore passed through a flattening filter, which will produce a flat x-ray beam at a certain depth, usually 5 or 10cm, in water.

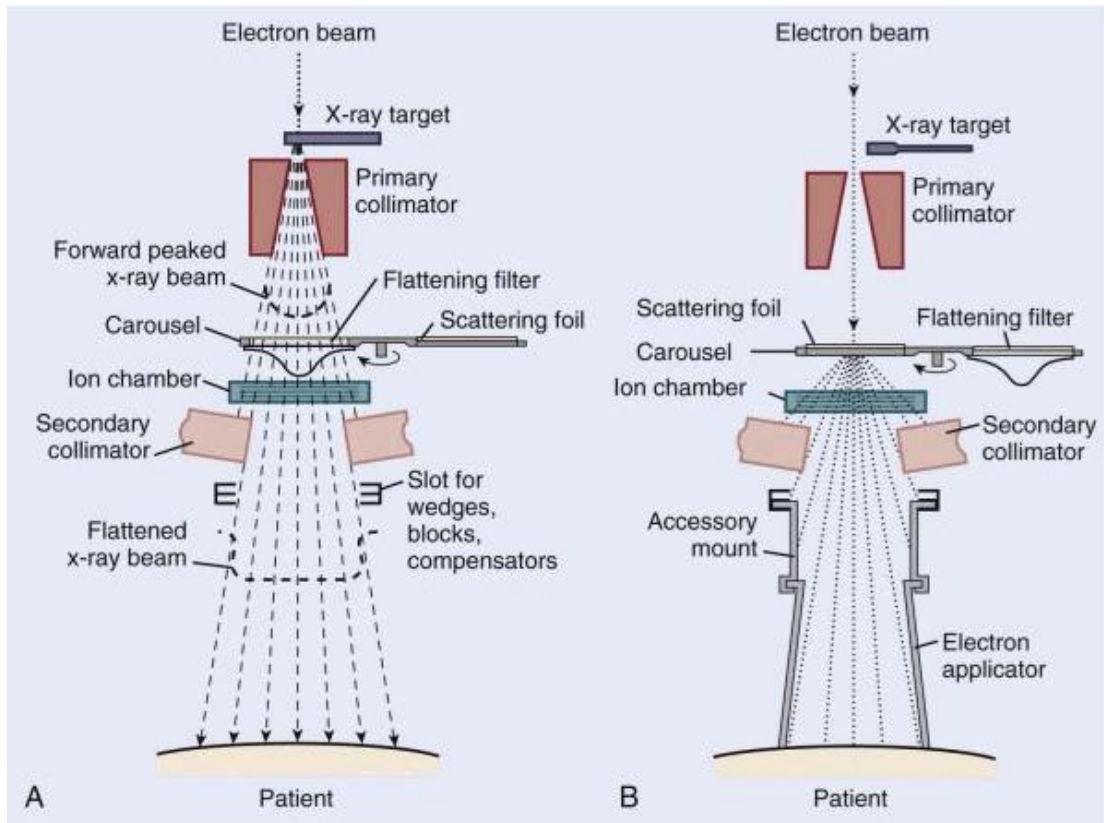


Fig 1.2 – Schematic of linear accelerator head for (a) photon beam treatment (b) electron beam treatment (19)

After the flattening filter the beam will move through an ionisation chamber to measure the dose output of the linac followed by a set of collimators to shape the beam (see Figure 1.2). A set of primary collimators determines the maximum field size, usually $(40 \times 40) \text{cm}^2$ at the isocentre with secondary collimators then being used to define the photon beam as required. The secondary collimators can also be used to provide an enhanced dynamic wedge. In this mode the collimator is driven across the field whilst the beam is still on, mimicking the effect of placing a metal wedge block in the beam.

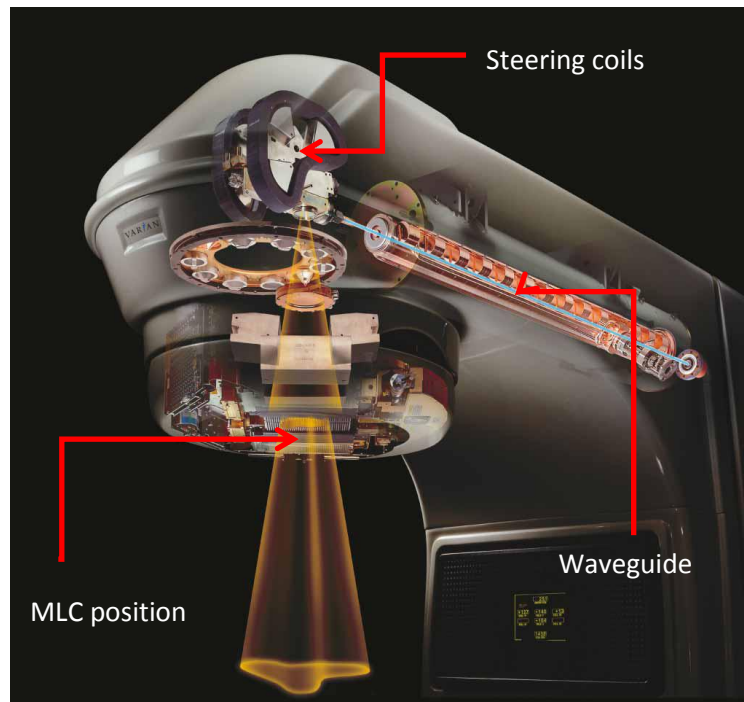


Fig 1.3 – Graphic of linear accelerator head (20)

Most modern Linacs will also have a set of Multi Leaf Collimators (MLCs) to further collimate the beam (See Figure 1.3). These are independent blades that are in a set either side of the beam. They can be moved independently and by utilising these millimetres wide adjustable metal leaves close to the point at which the x-rays are generated, they allow the beam of x-rays to be shaped and focused to a high degree, thereby improving the precision at which the dose to the patient can be delivered.

Dose delivery techniques

Initially, the only way to conform the radiation beam created from a linear accelerator to the required treatment area or volume on the patient was by utilising the secondary collimators, blocks and wedges. However the addition of the MLCs to most modern day linear accelerators has resulted in the advent of more advanced

dose delivery techniques such as 3D conformal radiotherapy (3D-CRT), intensity modulated radiotherapy (IMRT) and volume modulated arc therapy (VMAT).

3D-CRT

In essence this type of radiotherapy delivery is simply the utilisation of all the available 'blocking' tools in the linear accelerator. Before the MLC, radiotherapy would be administered by trying to simply match the height and width of the tumour within the patient. In fact, the earliest linear accelerators would administer radiotherapy treatments with only a relatively low quality x-ray to guide the oncologist and physicist as to the location and size of the tumour. The MLC, together with Computed Tomography (CT) based imaging, allows a much better match to be made between the shape of the tumour and the x-ray field delivered from the linac, hence the term 'conformal'. Typically administered using 2-5 beams, 3D-CRT is still used widely to treat breast, lung, rectum and oesophageal tumours.

IMRT

As the name implies, this method allows the user to modulate the intensity of each radiation beam. This results in each field having areas of high and low intensity (or fluence) within the same field, allowing for a greater degree of control of the dose distribution within the target. By modulating the fluence across some or all of the fields, the high dose volume created by the superposition of the beams can have areas of convexity. Treatment would therefore be planned so that the area of high dose wraps around the tumour, and by arranging the areas of normal tissue within

the convex areas, it allows them to receive a relatively lower dose to that of the tumour.

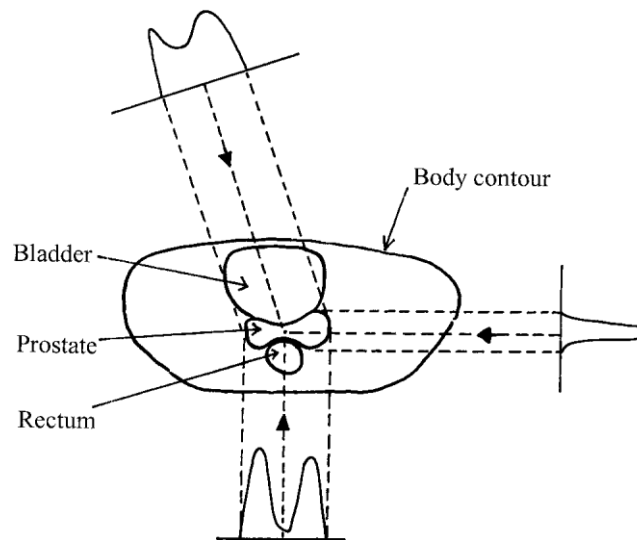


Figure 1.4 – Illustrating the principles of IMRT (21)

Figure 1.4 is an illustration of the principles of IMRT, in this case when treating the prostate. It can be seen how the prostate has a concave outline and how the use of modulated fluence on each beam allows the high dose area to be sculpted around the rectum and bladder, both of which should ideally receive as little dose as possible. IMRT treatments will generally use a larger number of beams than 3D-CRT with 9 sometimes being used for some tumours located in the head and neck region where there are many sensitive organs to consider.

VMAT

The basic concept of arc therapy is the delivery of radiation from a continuous rotation of the radiation source and allows the patient to be treated from a full 360°

angle (22). Essentially an alternative form of IMRT, VMAT is an extremely conformal form of radiotherapy administration, and allows the simultaneous variation of three parameters during treatment delivery i.e. gantry rotation speed, treatment aperture shape and dose rate. Another major advantage of VMAT is the improvement in treatment delivery time as a result of treatment being delivered faster in a continuous arc compared to multiple stationary beam positions (23).

1.4 Treatment planning

Successful radiotherapy delivery depends on the patient receiving a high dose of radiation to the tumour cells whilst ensuring that sensitive healthy cells nearby do not receive the same dose. It is therefore imperative that any dose delivered to the patient is done so in a manner that will meet this clinical objective. As a result, an essential part of radiotherapy treatment is the planning of the dose delivery. Each treatment plan must be individually designed for each patient taking into account the location of the tumour and their individual anatomy. The plans are prepared on specific computer software that model the behaviour of the treatment machine and simulate the effect of the applied radiation fields within the patient, thereby giving the clinical and physics staff the best possible approximation of the treatment delivery. Plans are generated on diagnostic quality computed tomography (CT) images acquired for each patient. These are used to both visually deduce the area where treatment is required and to correct for tissue inhomogeneities by quantifying the relationship between CT Hounsfield units and electron densities (24). When designing the radiation therapy fields, the clinical and physics staff must take into account several important biological and technical factors (25). These include: likely

patterns of regional tumour spread, to ensure coverage of local tumour extensions not detectable with current imaging techniques; uncertainties in positioning the patient for each treatment; and tumour and organ movement during and between treatments. In order to accurately and safely plan the delivery and take into account these factors amongst other there are specific structures that will be created in each treatment plan.

1.4.1 Target volumes

Target volumes are used when planning to outline any relevant volumes within the patient that should be taken into consideration when administering dose. The International Commission on Radiation Units and Measurements (ICRU) reports 50 and 62 give specific definitions of volumes to which the dose should be restricted as well as those in which it should be maximised. These are shown in Figure 1.5

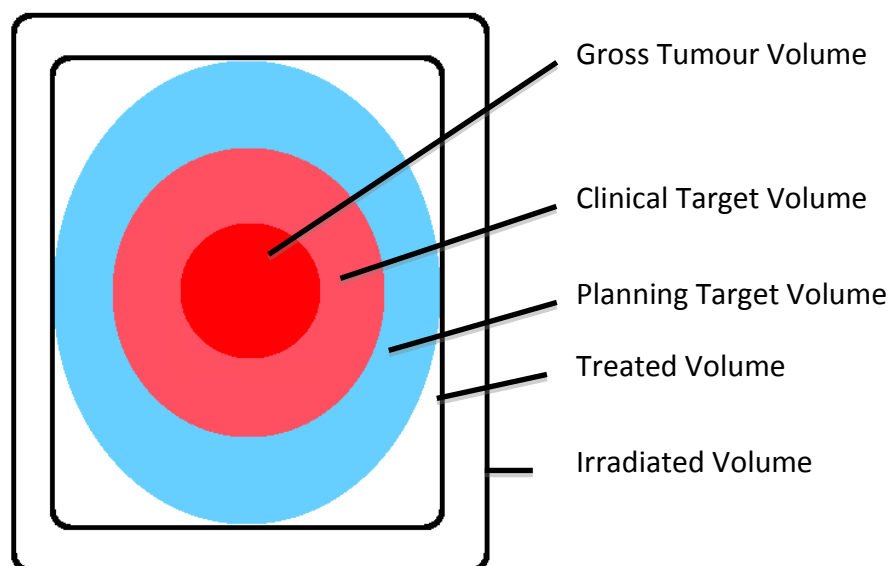


Figure 1.5 – Schematic of treatment volumes

Gross Tumour Volume (GTV)

The GTV is defined as *'The gross palpable or visible/demonstrable extent and location of malignant growth'*. Clinical examination, imaging or both can determine the size and extent of the GTV.

Clinical Target Volume (CTV)

The CTV is defined as *'A tissue volume that contains a demonstrable GTV and/or subclinical microscopic malignant disease, which has to be eliminated. This volume thus has to be treated adequately in order to achieve the aim of the radiotherapy, cure or palliation.'* This margin is added to the GTV but can also be created without a GTV present should the original tumour have been removed.

Planning Treatment Volume (PTV)

The PTV is defined as *'A geometrical concept used for treatment planning, and it is defined to select appropriate beam sizes and beam arrangements, to ensure that the prescribed dose is actually delivered to the CTV.'* A margin is added to the CTV primarily to account for uncertainties that arise as a result of patient movement and set up errors within the CTV. Specifically, an Internal Margin (IM) accounts for movement of the CTV with respect to the internal or external reference points used for aligning patients, and a Set-up Margin (SM) accounts for uncertainty in the position of the beam relative to the reference points/structures on the patient.

Treated Volume (TV)

The treated volume is defined as *'The volume enclosed by an isodose surface, selected and specified by the radiation oncologist as being appropriate to achieve the purpose of treatment.'* The TV is the volume that is receiving dose in order to ensure that the PTV receives the required dose. It is a region enclosed by the 95% isodose line on the treatment plan.

Irradiated volume (IV)

The irradiated volume is defined as *'The tissue volume which receives a dose that is considered significant in relation to normal tissue tolerance.'* This volume should be kept as small as possible in order to minimise the damage to normal tissue.

Organs At Risk (OAR)

'Normal tissues whose radiation sensitivity may significantly influence treatment planning and/or dose.' These are specific organs that due to their location, function and radiosensitivity will have an influence on how the tumour volume is treated. They are usually contoured within the Treatment Planning System (TPS) and will have specific dose constraints dependent on the particular organ. An additional volume known as the **Planning Organ at Risk Volume (PRV)** is also used. This is a margin added to the OAR to account for movements and changes in shape and/or size of the OAR, as well as set-up uncertainties.

For a more extensive description of the target volumes and OARs relevant to this thesis, please refer to appendix A2 Sections 3 and 4.

1.4.2 Dose analysis and homogeneity

When the necessary structures and OARs have been outlined, the dose can be calculated and optimised. There are important considerations that should be met to ensure that the plan is optimal, both in terms of delivering dose to the tumour and sparing normal tissue. Although the distribution of the dose in the plan can be visualised on the CT images using isodose lines, the most common method of quantifying the distribution is by using a Dose Volume Histogram (DVH).

Dose Volume Histogram – A DVH is a histogram relating radiation dose to tissue volume (26). They are extensively used in treatment planning to graphically summarize the radiation distribution within a volume of interest that would result from a proposed radiation treatment plan. They can also be used as input to modelling techniques such as Tumour Control Probability (TCP) and Normal Tissue Complication Probability (NTCP) (see Section 4.1).

Within the PTV – It is aimed that 99% of the PTV volume receives 95% of the dose. Analysing the DVH can ensure this is met. The dose within PTV should also be made to be as homogeneous as possible, following the -5% and +7% homogeneity as set out in ICRU 50.

Outside the PTV – Areas outside the PTV that have a minimum diameter of 15mm and exceed the prescribed dose are known as ‘hot spots’. They should be minimised as much as possible.

Maximum Dose (D_{max}) – This is the maximum dose to a volume of 1.8cc and should not exceed 107% within the PTV.

1.4.3 Treatment plan optimisation

As mentioned, an objective of successful radiotherapy treatment is the delivery of a high dose to the tumour whilst minimising dose to healthy tissue. In order to achieve this, a patient will usually be irradiated from several directions with beams that overlap at the tumour site to maximise the dose relative to the surrounding area. There are two main sets of parameters that require configuration in radiotherapy planning; the directions from which to irradiate the patient and the shapes and intensity profiles of the beams. Optimising these parameters is a significant mathematical challenge using complex algorithms and techniques that are automated using computer programs. Although these will usually be carried out using specific radiotherapy planning software with a graphical interface that makes the implementation of these techniques relatively easy, it is still essential that the user have a good understanding of the underlying methods in which a radiotherapy plan is designed and implemented.

There are two types of radiation treatment planning process; forward planning and inverse planning (27). In forward planning, plans are constructed largely using a trial and error method, albeit one utilising the knowledge and experience of the planner. In a clinical setting, the initial stages of a standard radiotherapy plan will follow a pre determined set of beam arrangements that have been developed to provide a good starting point. The plan can therefore be improved by following an iterative process

where the user will adjust numerous parameters, re-calculate the dose and repeat until they are confident that the optimal plan for that patient has been generated. Although this process is used widely in clinical practice, it is generally very time consuming and does not necessarily create the best plans. This may be due to the lack of the planner's experience and knowledge or from time constraints before the plan has to be reviewed by an oncologist and delivered.

Due to considerable advances in technology, both computational and engineering, a new method of planning known as inverse planning is now becoming more widespread. In contrast to forward planning, where a plan will be generated and dose objectives to selected structures and OARs are taken into consideration towards the end of the planning process, the inverse planning process begins with specific dose objectives and constraints relating to the relative importance of each structure. An optimisation process is then run within the treatment planning system to find the treatment plan which best matches all the input criteria.

Two treatment planning systems are used extensively in this investigation. These are Oncentra MasterPlan (OMP) (Elekta AB, Stockholm, Sweden), and Eclipse (Varian, Palo Alto, USA).

1.5 Statistical analysis

The nature of this whole study requires various statistical tests to be conducted. This section gives a brief introduction to all the tests used within this thesis.

1.5.1 Mann-Whitney U test

The Mann-Whitney U test is essentially a test for assessing whether two independent samples come from the same distribution. For example, a possible use would be to test whether the toxicity values of a set of patients are dependent on the gender of the patients. The logic behind the test is to rank the data for each condition, and then see how different the two rank totals are. If there is a systematic difference between the two conditions, then most of the high ranks will belong to one condition and most of the low rank will belong to the other. As a result, the rank total will be different. A p value is calculated to inform whether this difference is significant.

1.5.2 Kaplan-Meier plots and the log-rank test

The Kaplan-Meier method combined with the logrank test is the most commonly used method for displaying and statistically testing the comparison in survival distributions of two or more groups.

In analysing survival data, two functions that are dependent on time are of particular interest: the survival function and the hazard function (28). The survival function $S(t)$ is defined as the probability of surviving at least to time t . The hazard function $h(t)$ is the conditional probability of dying at time t having survived to that time. Plotting $S(t)$ against t results in a survival curve and the Kaplan-Meier method can be used to estimate this curve from the observed survival times. The method is based on the idea that the probability of surviving k or more periods from entering the study is a product of the k observed survival rates for each period, given by

$$S(k) = p_1 \cdot p_2 \cdot p_3 \cdot \dots \cdot p_k \quad (1.0)$$

Where p_1 is the proportion surviving the first period, p_2 the proportion surviving the second period etc.

To plot a Kaplan-Meier curve the survival times, including the censored values (indicating missing data), must be ordered in increasing duration. Plotting the cumulative proportion surviving against the survival times then gives the stepped survival curve as seen in any Kaplan-Meier plot.

The log rank test is used to test the null hypothesis that there is no difference between the groups in the probability of an event (usually death) at any time point.

The test statistic is calculated as follows:

$$\chi^2(\logrank) = \frac{(O_1 - E_1)^2}{E_1} + \frac{(O_2 - E_2)^2}{E_2} \quad (1.1)$$

where the O_1 and O_2 are the total numbers of observed events in groups 1 and 2, respectively, and E_1 and E_2 the total numbers of expected events. The test is widely used however it does not allow other explanatory variables to be taken into account.

In these instances the Cox proportional hazard test should be used.

1.5.3 Cox proportional hazard

The Cox proportional hazard enables the difference between survival times of particular groups of patients to be tested whilst allowing for other explanatory factors. In this model, the response (dependent) variable is the 'hazard'. The hazard is the probability of dying (or experiencing the event in question) given that the patients have survived up to a given point in time, or the risk for death at that moment. The hazard ratio calculated in the cox model does not depend on time, as it is assumed that if the risk of dying at a particular point in time in one group is for example twice that in the other group, then at any other time it will still be twice that in the other group. The hazard ratio is therefore a method of quantifying the difference between two groups.

1.6 Clinical trials

A clinical trial is a research study done to evaluate new treatments. They are essential in growing our understanding of potential new treatment methods and can be considered gateways through which these new treatment methods become the standard method of care. Not only do they allow us to test the efficacy of new protocols but also to test existing protocols that may be being applied in a different setting under new circumstances. If a particular protocol is found to be successful there is a high probability that it may become standard procedure, especially if the positive outcome can be confirmed via other clinical trials. However, whether the protocol is new or that the trial is re examining an existing one, it is essential that there should be precise, thorough and systematic evaluation of the protocol being tested. If the protocol is well designed and followed precisely by everyone involved,

the resulting data will be a true representation of the patient cohort included. Although clinical trials aren't the only form of research in which new treatment methods can be implemented, their ability to provide high quality evidence based conclusions from often large databases means that they are considered the gold standard of clinical study.

A clinical trial will be conducted to answer a specific question and to address a specific hypothesis. It is therefore imperative that the hypothesis is clear, well thought out and preferably backed by scientific theory or evidence. It is also important that the data or evidence produced by the trial is adequate in answering the initial question. If this is achieved, then the trial will be able to show that the clinical protocol alone was responsible for the observed results, which is the main aim of any trial. Trial design is therefore potentially extremely complex, requiring a large amount of scientific understanding and rigour. In addition, they can be expensive to run and often require external funding and specific teams or institutions to run them. Clinical trials of the highest quality, where data are acquired over a number of years are therefore a specialised undertaking. As a result there are institutions where their sole undertaking is the preparation, organisation and analysis of trial data. In the case of this thesis and the investigation included within it using the SCOPE 1 trial data, this institution was the Wales Cancer Trials Unit (WCTU) based within Cardiff University. WCTU is responsible for running a number of clinical trials within the UK and provided me with the data from the SCOPE 1 trial in order to conduct the investigations within this thesis.

1.6.1 Phases of a clinical trial

	Phase I	Phase II	Phase III	Phase IV
Number of participants	20-80	100-300	1000-3000	1000+
Time	Up to several months	Up to 2 years	1-4 years	1+ years
Purpose	Studies the safety of medication/treatment	Studies the efficacy	Studies the safety, efficacy and dosing	Studies the long term effectiveness
Phase Success Rate	70%	33%	25-30%	70-90%

Table 1.0 – Outline of typical phases of clinical trials

Table 1.0 shows the typical phases within a clinical trial. Trials can be split into 4 main phases:

Phase I: Researchers test a new drug or treatment in a small group of people for the first time to evaluate its safety, determine a safe dosage range, and identify side effects.

Phase II: The drug or treatment is given to a larger group of people to see if it has some level of efficacy and to further evaluate its safety.

Phase III: The drug or treatment is given to large groups of people to confirm its effectiveness, monitor side effects, compare it to commonly used treatments, and collect information that will allow the drug or treatment to be used safely.

Phase IV: These studies are done after the drug or treatment has been marketed to gather information on the drug's effect in various populations and any side effects associated with long-term use.

Due to the stringent requirements of clinical trials and the analysis of the data they produce, many will not reach phase III and IV. It is only when the efficacy of the new drug or technique is proved that the trial may move on to the next phase. Indeed, trials may also be stopped mid phase if the incoming results show that it would be un-ethical to proceed.

1.7 The SCOPE 1 clinical trial

The SCOPE 1 trial was a National Cancer Research Institute and Cancer Research UK funded Phase II/III two arm trial of dCRT with and without cetuximab in oesophageal cancer (29). See Figure 1.6 for a schematic of the trial.

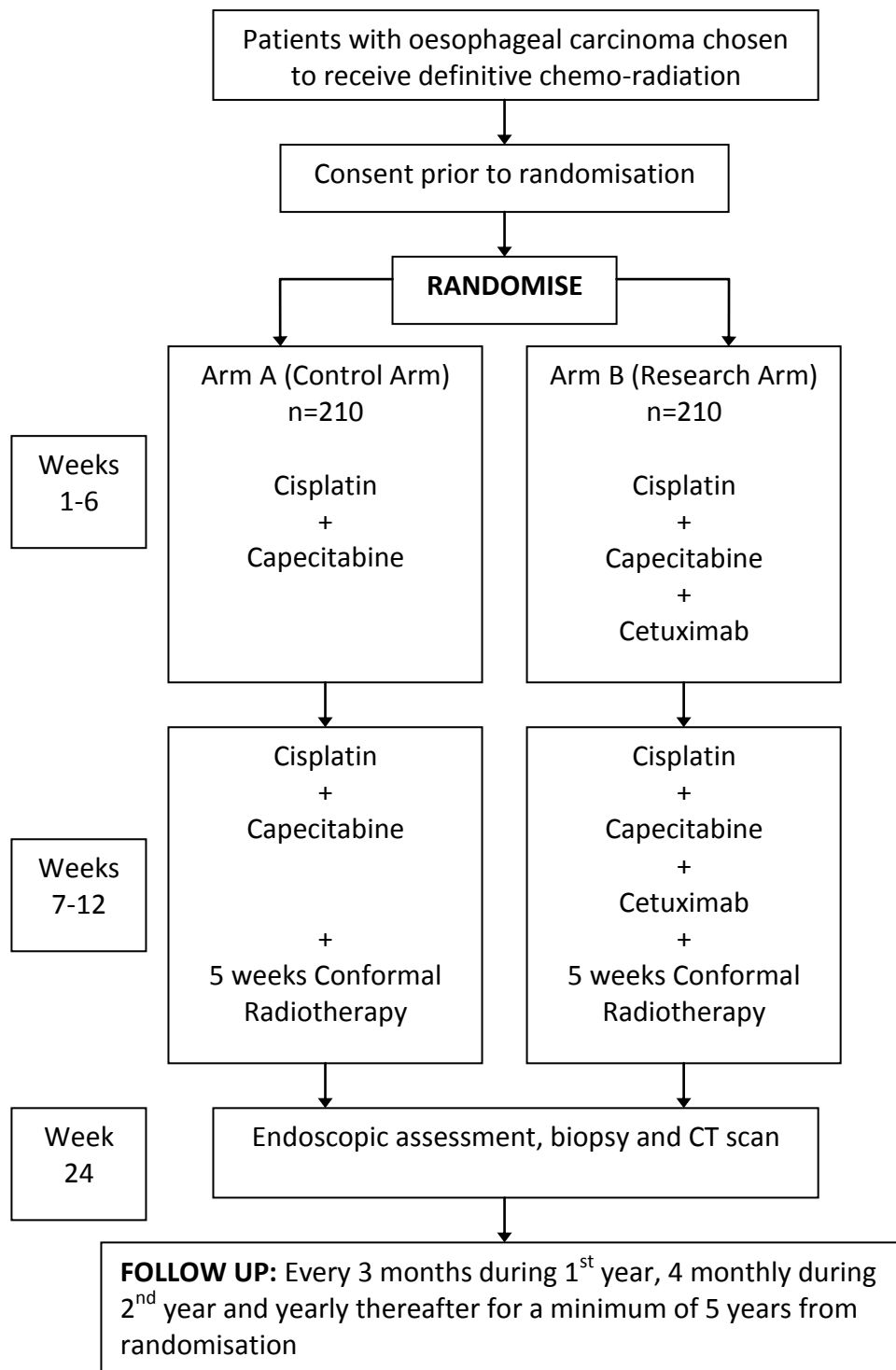


Figure 1.6 – Schematic of SCOPE 1 clinical trial

Cetuximab is a monoclonal antibody and epidermal growth factor receptor (EGFR) inhibitor that has been shown to prevent radiotherapy induced growth stimulation. For example Bonner et al reported improved local control and overall survival in the

cetuximab arm of a trial of 424 randomised patients receiving 70-76.8Gy of radiotherapy for locally advanced squamous cell carcinoma of the head and neck (30). However, although head and neck cancer is a disease with many similarities to oesophageal cancer, the results of the SCOPE 1 trial were not as positive in terms of cetuximab administration. 258 patients were recruited from 36 UK centres between February 7, 2008 and February 22, 2012 with patients being randomly assigned via a central computerised system using stratified minimisation to receive CRT alone or CRT with cetuximab (see Figure 1.6). CRT consisted of cisplatin 60mg/m² (day 1) and capecitabine 625mg/m² twice daily (days 1-21) for four cycles with cycles three and four being given concurrently with 50Gy in 25 fractions of radiotherapy. The primary endpoint was the proportion of patients who were treatment failure free at week 24 for the phase 2 trial and overall survival for the phase 3 trial. The results showed that the 24 week failure free survival was significantly better in the CRT only arm compared to the CRT plus cetuximab arm (76.9% (90% confidence interval 69.7-83.0) vs 66.4% (58.6-73.6)). The CRT plus cetuximab group also had shorter median overall survival (22.1 months (95% confidence interval 15.1-24.5) vs 25.4 months (20.5-37.9)). However, despite this, the trial showed relatively low rates of acute and late toxicity (defined according to CTCAE grading) and the two year overall survival was 56% in the control arm, higher than previously published studies.

1.8 Relating radiotherapy treatment to outcome

Whether the aim of treatment is curative or palliative, it is clear that the purpose of radiotherapy is to improve the well being of patients. Depending on the condition and health of a patient, a course of radiotherapy treatment will be prescribed that to

the best knowledge of the clinical staff is most likely to achieve the desired outcome. With the now widespread use of three-dimensional (3D) treatment planning, volumetric-based radiotherapy datasets that can be used to directly relate treatment to outcome are becoming increasingly available (31). However with so many variables and factors both clinical and technological involved in radiotherapy treatment, the analysis of these datasets quickly becomes complex. Yet the ability to utilise these datasets and further our knowledge of the relationship between treatment factors and outcome has the potential to greatly enhance the treatment of cancer. Importantly, this may open the way for patient-specific, individualised treatment planning decisions based on estimates of the risks of complications vs increases in local control (32). This type of highly individualised treatment however can only be achieved by validating predictions against relevant outcome datasets (33).

Broadly speaking, the relating of treatment to outcome falls into two fields; a.) the correlation of patient and treatment factors to toxicity and outcome via statistical tests, and b.) the approximation of toxicity and tumour control resulting from treatment via radiobiological modelling. There is a significant amount of work in the literature in both these fields. The correlation of treatment and predictive factors to outcome via statistical testing is mostly concentrated on the retrospective analysis of clinical data sets, and these studies have been carried out on a wide number of tumour sites. The type of patient specific predicting factor that is investigated also varies widely and have increased in number in recent years due to progress in genetics and imaging technology (34). They include predictors such as tumour length

((35)-(36)) and volume (37) and the number of counted metastasis (38), variations in treatment administration that may increase toxicity (39), metabolic imaging (40) and dosimetric predictors (41). El Naqa (31, 33, 42-46) together with Deasy (47-50) have made a significant contribution to both these fields and their work in multivariable modelling of radiotherapy outcomes (33) in particular was important.

Chapter 2

Database and software preparation

2.1 Clinical data management

Clinical data management (CDM) is an essential part of any clinical trial. CDM is the process of collection, cleaning, and management of subject data in compliance with regulatory standards. The process should start with the end goal in mind and conducted correctly, it leads to generation of high-quality, reliable, and statistically sound data (51). The main objective is keeping the amount of errors and missing data to a minimum, therefore maximising the amount of analysable data (52). If this objective is achieved, the main research question posed by the clinical trial will be answerable. High quality data should be accurate and be ready for statistical analysis. It should be decided from the outset what to do with any data that deviates from the initial protocol. It may be decided to exclude all such data or that there is a set number or value of allowed deviations before they are excluded. Although it is important to maximise the amount of analysable data within the database, it is also important that these data are consistent and that any deviations from the protocol will not affect the statistical outcome of the original research question. The inclusion or exclusion of these patients should therefore be given serious consideration in every clinical trial.

2.2 Data preparation in the SCOPE 1 analysis

The main data set for this thesis was the result of a nationwide clinical trial of the effect of including cetuximab in the chemotherapy regimen of dCRT for oesophageal cancer. Named 'SCOPE 1: A phase II/III trial of chemoradiotherapy in esophageal cancer plus or minus cetuximab.', the trial data were collated and organised by WCTU.

2.2.1 Radiotherapy trial data

The radiotherapy planning data were stored on a network drive in the exact format in which it was received from the Radiotherapy centres participating in the trial. Depending on the centre from which the data were received this was either in Digital Imaging and Communications in Medicine (DICOM) (53) or Radiation Therapy Oncology Group (RTOG) format (54), both of which are standard for handling, storing and transmitting information in medical imaging. In order to use these data within the Matlab based programs in which most of the analysis would be undertaken, it was required that all the DICOM and RTOG data be converted into Matlab files (.mat). This was carried out for the entire database using the 'import' function within the Computational Environment for Radiotherapy Research (CERR) program and saving each case into a separate folder.

DICOM data format

DICOM is a standard for handling, storing, printing and transmitting information in medical imaging. It is used in all modern medical imaging systems like x-rays,

ultrasound, CT and Magnetic Resonance Imaging (MRI). The core of DICOM is a file format and networking protocol:

DICOM file format: DICOM files contain more than just images. Every DICOM file holds patient information (name, ID, sex and birth date), important acquisition data (type of equipment used and its settings), and context of the imaging study that is used to link the image to the medical treatment it was part of.

DICOM network protocol: All medical imaging application that are connected to the hospital network use the DICOM protocol to exchange information, mainly images but also patient and procedure information. The network protocol is used to search for imaging studies in the archive and restore imaging studies to the workstation in order to display it. More advanced network commands are also available to control and follow the treatment schedule procedures, report statuses and share the workload between imaging devices.

Uniform data

It is becoming increasingly apparent that there is a need for a standardised naming convention in radiation oncology in order to facilitate comparison of dosimetry across patient datasets (55). This is important, as variations can lead to confusion when analysing datasets, where the analysis of the correct information is critical. Although the SCOPE 1 trial required a radiotherapy plan to be made for each patient,

and the analysis of these plans was known from the outset, there was no naming convention for the essential SCOPE 1 structures and dose sets decided upon when the trial started. As there were 34 centres involved in the trial, with each centre and potentially each individual radiotherapy planner within each centre having a different method of naming each structure and dose set, they were originally not uniformly named across the database. In order for the data analysis within Matlab to work successfully, it was essential that the same structures and dose sets from one patient to the next across the data database were named exactly the same.

Structure naming

The first task was therefore ensuring that the names of each structure with the radiotherapy plans were uniform across the database.

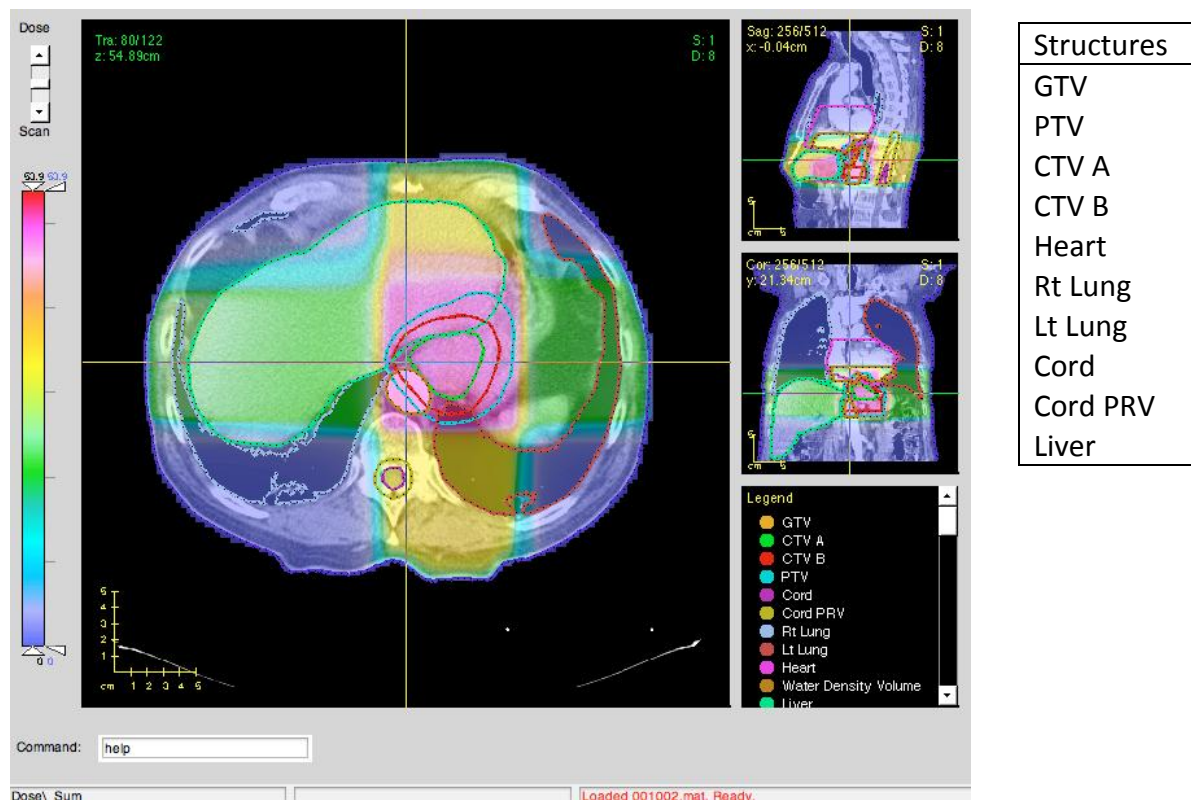


Figure 2.1 – Gold Standard structure naming

It was decided that all patients have their structures named according to the SCOPE 1 protocol. An example is shown in Figure 2.1 showing the treatment plan and structures of a Velindre Cancer Centre patient (this particular patient was used as the 'Gold Standard' in terms of naming structures). Figure 2.2 shows an example of a patient file with the structure names as they were received from another centre participating in the trial. There were 34 separate structures that required identifying and renaming.

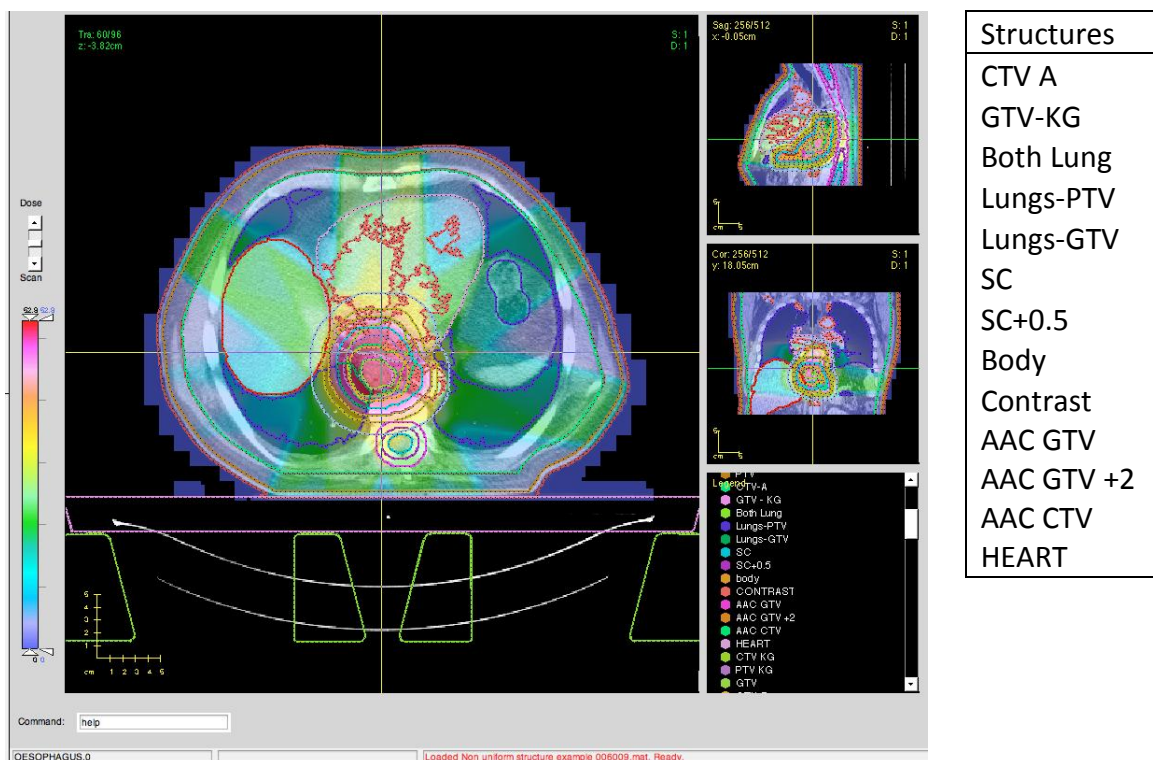


Figure 2.2 – Example of non-uniform naming of patient structures

All 207 patients in the database were uniformed by individually loading each patient into the CERR program and utilising the 'renaming' function to rename all structures as required. In some instances there were multiple version of the same structure with slight variations in name (as shown in figure above). Which version of the

structure to use for analysis was discussed with a member of the original Radiotherapy Trial Quality Assurance (RTTQA) team from the SCOPE 1 trial. In order to ensure that uniformity across the database had been achieved, a Matlab script was written that exported the name of each structure attributed to each patient kept within a specific folder on the computer's hard drive. Viewing this information in an excel spreadsheet allowed all the structures to be analysed simultaneously and any corrections made quickly.

Uniform dose structure

The DICOM format stores dose information in an RTDose file. However, for a complete patient plan, the number of RTDose files included can vary depending on the export method used by the treatment planner on the specific treatment planning system in use at their centre. As a result, there were some patients in the database that had multiple dose files (one for each beam position), and some with one dose file (containing the dose information for all the beam positions combined). Furthermore, the combined dose value for the beams were in some instances the full dose over the course of the treatment (i.e. 50Gy) where as in some patients the combined dose would be normalised to 1Gy per fraction. Using the dose management tools available in CERR it was ensured that the dose values for the entire patient database were uniform in nature. For manipulation of the dose information at a later date it was important that the names of the dose files were uniform, the dose files created for each patient were therefore all named 'Dose_Sum'.

2.2.2 Outcome data preparation

The WCTU is responsible for collating all the data that are generated within the SCOPE 1 trial, and this includes the toxicity and outcome data. These data is collected via Case Report Forms (CRF) that are filled in by the Doctor or Nurse examining the patient at the centre where they are receiving treatment. Baseline assessments include overall length of tumour and stage. The Common Terminology Criteria for Adverse Events (CTCAE) system is used to report toxicities and include pulmonary, gastrointestinal and vascular disease. Recorded grade 3 and 4 toxicity rates in the SCOPE 1 trial were very low. This made any meaningful analysis of this data statistically unsound therefore it is not explored in this thesis.

CRFs were completed at baseline, at end of treatment, and followed up at months 6, 9, 12, 16, 20, 24, 36, 48, and 60. A substantial amount of data were therefore recorded that required cleaning up and formatting. For ease of use it was requested that the data were received from WCTU in Microsoft Excel format, this would also allow easy integration into the EUCLID software for analysis.

An important part of this process was matching the outcome database to the radiotherapy database, i.e. making sure that a patient's radiotherapy plan had the same identification number as that referred to in the outcome dataset.

The survival time was calculated in days from when the patient's treatment finished to their death date using a formula in Excel.

There was also a large amount of data included in the outcome database on which analysis would not take place therefore these were removed.

2.3 Testing the data pathway

With the data uniform and formatted as required, an important next step was testing the data pathway. This consisted of taking the raw DICOM/RTOG data as received from the centres, importing into CERR, creating a test database of information within EUCLID (including dose and outcome data) and producing end results such as Kaplan Meier and Dose Volume Histogram plots. Testing this process on a small test database would minimise problems that may arise when dealing with the full clinical database.

Computational Environment for Radiotherapy Research (CERR)

CERR is a software platform for developing and sharing research results in radiation therapy treatment planning (57). The software package, based in Matlab, addresses four broad needs in treatment planning research

- a. It provides a convenient and powerful software environment to develop and prototype treatment planning concepts
- b. It serves as a software integration environment to combine treatment planning software written in multiple languages (e.g. Matlab, Java etc), together with treatment plan information (CT scans, outlines structures, dose distributions)
- c. It provides the ability to extract and analyse treatment plans from disparate treatment planning systems
- d. It provides a convenient and powerful tool for sharing and reproducing

treatment planning research results

CERR data format: PlanC

All treatment plan information is contained in a Matlab cell-array named planC. The different cells of the planC cell array contain data objects according to the value of the structure indexS. They are as follows:

indexS.header = 1;

indexS.comment = 2;

indexS.scan = 3;

indexS.structures = 4;

indexS.structuresArray = 5;

indexS.beamGeometry = 6;

indexS.dose = 7;

indexS.DVH = 8;

indexS.digital Film = 9;

indexS.CERROptions = 10;

indexS.indexS = 11;

This means that the scan information is all contained in the 3rd element of the scan,

the dose information is all contained in the 7th element, etc.

EUCLID

EUCLID is an outcome analysis tool developed to be used by radiation oncologists and medical physicists (58). The software package, based in Matlab, can provide a fast statistical snapshot of a population and perform univariate, multivariate and dose-volume analysis on a large data set with a large number of physiological, clinical, biological and dosimetric factors. An advantage of EUCLID is its capability of importing clinical information in Excel spreadsheet format. Figure 2.3 shows a spreadsheet that was created in order to test the data pathway and the type of information that can be included. (note - the information contained within the spreadsheet is not clinically accurate and is purely for demonstrating purposes).

	A	B	C	D	E	F	G	H	I	J	K
1	Patient	Max Dose CERR Gy	Sex 0 male 1 female	Age at time of study	Date of therapy start	Death 0 dead 1 alive	Date of death	Today's time	Survival Time	Cetuximab 0 no 1 yes	Pneumonitis grade
2											
3	001002	53.8743	0	74	30/05/2008	1		14/03/2013	4.79	0	2
4	001003	54.9741	1	77						1	4
5	001004	52.7467	0	77	22/08/2008	0	20/02/2012	14/03/2013	3.50	1	3
6	001006	54.4475	0	60	12/08/2008	1		14/03/2013	4.59	0	5
7	001007	53.6161	1	75	10/10/2008	0	27/10/2009	14/03/2013	1.05	1	5
8	001008	53.4567	1	64	04/11/2008	1		14/03/2013	4.36	0	1
9	001009	53.7901	1	68	05/03/2009	0	21/06/2011	14/03/2013	2.30	0	2
10	001010	52.4662	1	59	10/03/2009	1		14/03/2013	4.01	1	1
11	001011	52.6315	1	69	22/04/2009	1		14/03/2013	3.90	1	3
12	001012	54.2387	0	80	24/04/2009	0	09/05/2010	14/03/2013	1.04	1	4
13	001013	53.3559	1	69	05/06/2009	1		14/03/2013	3.78	0	1

Figure 2.3 – Spreadsheet for testing of data pathway

The data contained within the Excel spreadsheet is then saved in a Matlab file format specific to EUCLID, which can be opened to give the options for analysis.

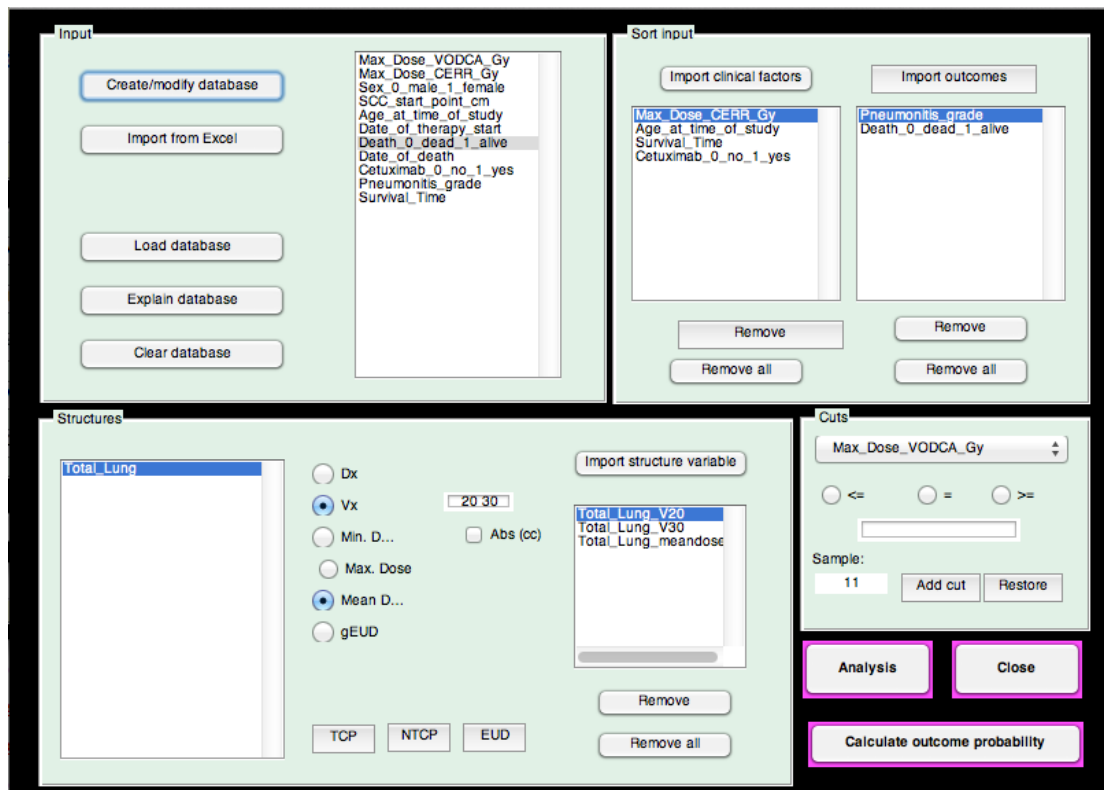


Figure 2.4 – EUCLID interface

It was decided to simulate the analysis of the development of radiation induced pneumonitis as a result of the dose received by the lungs. The appropriate variables were chosen for the input as clinical and outcome factors and the lung dose information imported for each patient, allowing the V20, V30 and mean-dose to be analysed (Figure 2.4). The user is then given the option of the type of statistical analysis to be carried out on the data (Figure 2.5).

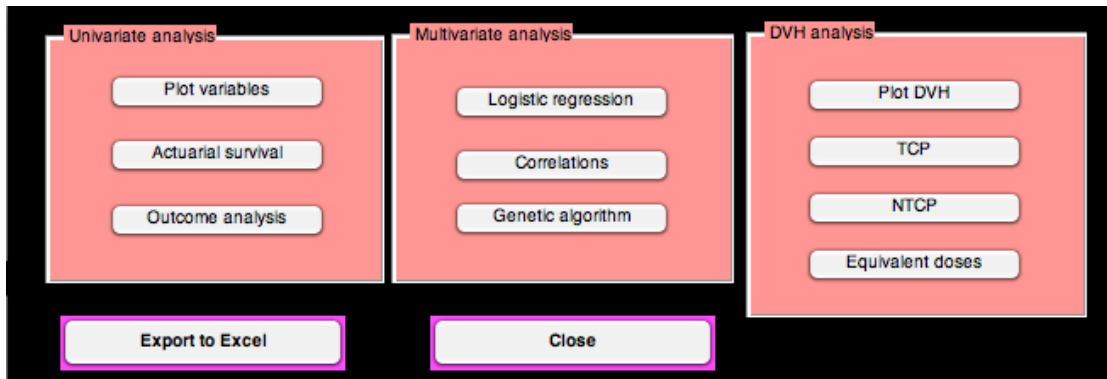


Figure 2.5 – Statistical analysis options in EUCLID

A DVH analysis was generated dependent on pneumonitis grade (Figure 2.6).

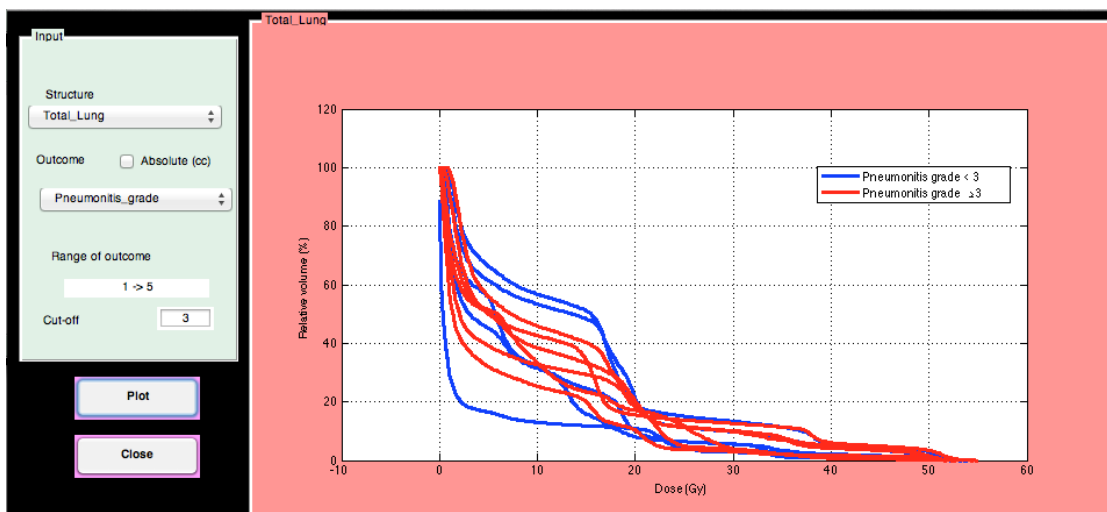


Figure 2.6 – Test DVH analysis with pneumonitis grade

A Kaplan-Meier curve was plotted showing overall survival time and Lung V30 with the best cut off in terms of low p-value (Figure 2.7).

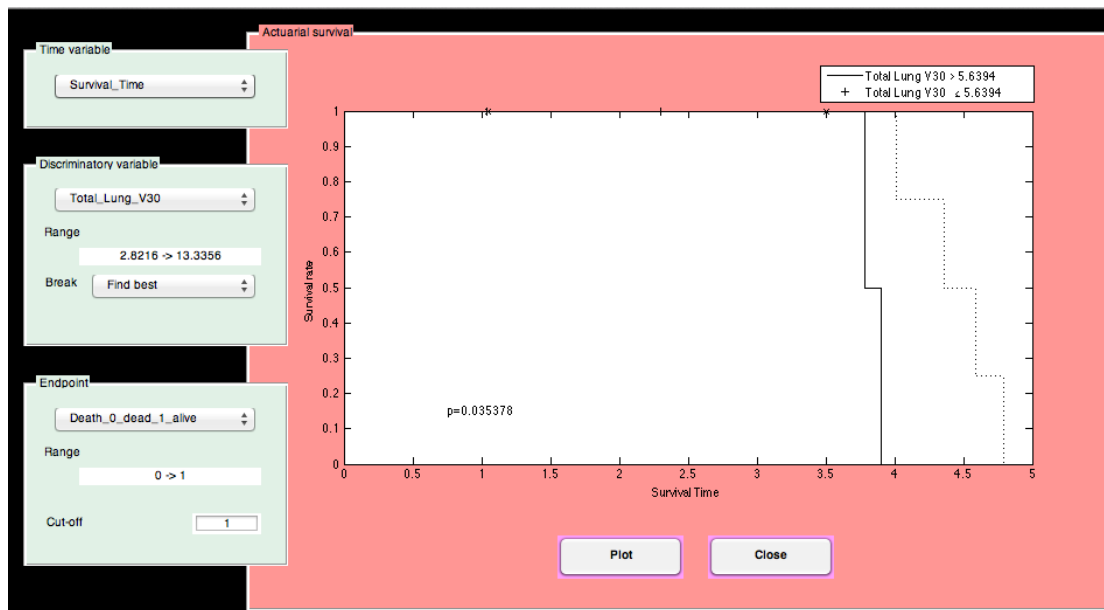


Figure 2.7 – Test Kaplan Meier split by Lung V30 values

Although the data produced here are not clinically relevant, the data pathway was shown to be successful. As a result, the process of importing data from the centres and the analysis of these data could be widened to include the whole SCOPE 1 data set using this method.

2.4 Program and script development

Another aspect of the project is program and script development. The majority of this thesis's data preparation and analysis was undertaken in programs based within the Matlab environment, namely CERR and EUCLID. Although these programs are published in the literature, can be thought of as finished and fully working packages, and in the case of CERR have a strong and wide ranging user community, the fact that they are open source and written in the Matlab environment also allow for a large degree of customisation. The code within these programs, especially CERR, can also be utilised and customised to undertake tasks outside of the program itself.

Along with introducing and explaining Matlab scripts that were written from scratch, this section outlines these customised scripts and their use.

2.4.1 Automatic dose volume histogram calculation

In order to analyse the dose received by each individual patient, and specifically the dose received to each structure and OAR within each patient, it was necessary to calculate the DVH's of the structures and OARs of interest. CERR has the capability of calculating DVHs for structures manually on an individual basis, however for a database as large as that being used in this study, calculating DVHs for all the required structures would be extremely time consuming. As a result, it was decided to write a script in Matlab that would be able to automatically calculate the DVHs required for any investigation within this thesis.

trialInterCalcDVH(filelist, pathname, struct_name, dose_name)

The backbone of this script, the part that actually calculates the DVH of a specific structure within a planC of a patient, was easily available within CERR. Additional scripting was required in order to direct the application of this script in the right place of the patient's planC structure and to carry this out automatically for a list of patients kept within a specific folder.

1. The first part of the script opens the filelist/pathname structure that has to be created for all in house scripts of this nature.
2. The name of the first file within the filelist structure to be opened (i.e. the specific patient) is gathered.

3. The structure number within planC that matches the structure_name input is recorded.
4. The dose number within planC that matches the dose_name input is recorded.
5. The DVH matrix is calculated for the requested structure_name and dose_name using the same script that is used in the CERR manual version.
6. The planC of the patient is updated and saved with the new DVH data.
7. Steps 2-6 are repeated for all patients within the filelist/pathname structure.

trialInterCalcIso(filelist, pathname, dose_name, isodoseLevel, assocScanNum, PrescDose)

In addition to calculating DVHs, there was a requirement in this project to analyse structures that correspond to particular isodose levels. Computing isodoses is easily carried out within CERR itself, together with converting these isodoses to structures saved within planC, however as with the DVHs this has to be done manually for each patient. This script was therefore also automated in a similar fashion to those outlined previously utilising the filelist/pathname structure and was also modified to calculate the isodose level in percentage format dependent on the PrescDose input i.e. the isodose level could be requested as '95% of a prescribed dose of 50Gy' rather than an isodose level expressed in Gy. As isodose levels are clinically usually expressed in percentages this was less likely to cause confusion at a later stage.

2.4.2 DVH import in EUCLID

A significant amount of work was carried out in developing the EUCLID program to be more useful when dealing with large data sets such as those found in nationwide multicentre clinical trials. Originally the program was written for dealing with relatively small databases (<50 patients) therefore the ability to import DVHs of various structures was a manual process. This required that the user manually located each file where the DVHs of the particular patient were kept in order that the program is able to extract this information and include it in the database. This would be an extremely time consuming process when dealing with a database of over 200 patients such as that in this study. A script was therefore written in Matlab that would allow this process to be automated. The goal was to add a function to the EUCLID program that would find the folder in which the patients CERR files were kept, before exporting the DVH data of the structure selected in EUCLID from each specific patient and adding to the EUCLID database. In order for this to be achieved, it required both the modifying of existing scripts already in use by EUCLID in addition to some new scripts being written.

EUCLID database structure

In order to add this functionality it was important to fully understand how the EUCLID database is built up from patient data and information when using the standard program (58).

Microsoft Excel data input

As Matlab converts Excel sheets into arrays, this spreadsheet must be formatted in a particular way for it to be read correctly by EUCLID. Figure 2.8 is an example of how the data must be formatted in Excel.

	A	B	C	D	E	F	G	H	I	J
1	NAME	Sex	Stage	Smoking	Chemo	Delivered_Dose	Age	Survival_time	Death	Pneumonitis
2		1=Male, 2=Female	31-IIIa, 32-IIIb		0=No chemo, 1=Chemo	cGy		Years	0=Alive, 1=Dead	0=No RP, 1=RP
3	Patient1	2	31	0	0	5400	84	1.08	1	0
4	Patient2	2	32	35	0	6000	78	1.75	1	0
5	Patient3	1	31	29	1	6600	79	0.71	0	1
6	Patient4	2	31	60	0	3800	63	1.66	0	1
7	Patient5	1	32	45	1	5400	72	2.53	1	1

Figure 2.8 – Formatting of data in Excel spreadsheet

The first line contains the variable name whilst the second line contains a description of the variable. The first column must contain the patient name with the remaining columns containing clinical factors and outcomes.

Import into EUCLID and database creation

The Excel sheet is imported into EUCLID using the inbuilt xlsread.m function in Matlab. This converts the .xls excel file into a .mat matlab file by creating an array that holds all the required information.

Name ▲	Value
dBBase	<1x200 struct>
patientlist	<1x200 cell>
savename	'O:\rhyscarrington\MATLAB\work\EUCLID\GA\hernando_tob.mat'
structlist	<0x0 cell>
varlist	<1x10 struct>

There are multiple elements in the array created by EUCLID to hold specific information in the database. They are:

dBase: a structure array that is constructed for each patient and holds all the clinical factors and outcomes.

```
>> dBase
dBase =
1x200 struct array with fields:
    Sex
    Race
    KPS
    Rel_weight_loss
    Tobacco_use
    Chemo
    Prescribed_dose
    FEV1_postRT
    V30Gy
    Pneumonitis
```

varlist: a structure array that holds the name and description of each clinical factor or outcome

```
>> varlist
varlist =
1x10 struct array with fields:
    name
    desc
```

patientlist: a cell array that holds all the patient names (not real names)

```
>> patientlist
patientlist =
Columns 1 through 5
    'ALLEN.MARY'    'AVERITT WYNELL'    'AYSCUE.QUINCY'    'BAGGETT JACQUELINE'    'BAINES.JULIA '
Columns 6 through 10
    'BANKS.VELMA'    'BATSON.ELLIS'    'BECKER.WILLIAM'    'BELL..JAMES'    'BEROTH.ELLEN'
```

savename: the name of the file and the directory where the database file is saved in the computer's system

```
>> savename
savename =
O:\ogayou\MATLAB\work\EUCLID\GA\hernando_tob.mat
```

structlist: a cell that holds the names of any structures that are created for DVH analysis.

```
>> structlist
structlist =
    'lung'    'lung_D20'    'lung_V20'    'lung_V30'    'lung_meandose'
```

The elements described above, specifically the structlist cell, are created individually for each patient when the user modifies or adds information to the database. The next section describes what was modified in order to automate the process.

Modifying the EUCLID script

Creating an automatic way of directing the EUCLID script to where the DVHs of each patient are stored was achieved by adding a ‘filepath’ column to the Excel sheet holding the patient’s clinical and outcome information (Figure 2.9).

	Q	R	S	T	U	V	W	X	Y	Z	AA	AB	AC	AD	AE
1	Patient	progression	PTV volume	disl_vpaf	ogtv_vpaf	ctvl_vpaf	ptv_vpaf	Under MDC	Under MDC I	Over MDC	filepath				
3	001002	1477	386.6418	2	2.4	6.6	8.4	-0.031062	0.031062	0.74521	/Users/rhyscarrington/Desktop/SCOPE Data/OnTrial CERR/001002.mat				
4	001003	1106	331.3904	8	7.2	10.8	12.6	-0.015881	0.015881	0.49258	/Users/rhyscarrington/Desktop/SCOPE Data/OnTrial CERR/001003.mat				
5	001006	1563	247.8099	8	6.6	10.2	12	-0.029232	0.029232	0.34761	/Users/rhyscarrington/Desktop/SCOPE Data/OnTrial CERR/001006.mat				
6	001007	390	364.53		8.4	13	14.4	-0.19112	0.19112	0.29489	/Users/rhyscarrington/Desktop/SCOPE Data/OnTrial CERR/001007.mat				
7	001008	1715	214.1744	4	5.4	9.6	11.4	-0.094066	0.094066	0.22691	/Users/rhyscarrington/Desktop/SCOPE Data/OnTrial CERR/001008.mat				
8	001009	845	360.9633	10	10.2	14.4	16.2	-0.020982	0.020982	0.43741	/Users/rhyscarrington/Desktop/SCOPE Data/OnTrial CERR/001009.mat				
9	001010	1638	226.6778	7	7	11	13.1	-0.016797	0.016797	0.29985	/Users/rhyscarrington/Desktop/SCOPE Data/OnTrial CERR/001010.mat				
10	001011	1444	458.5446	13	13.3	18	20	-0.088689	0.088689	0.42558	/Users/rhyscarrington/Desktop/SCOPE Data/OnTrial CERR/001011.mat				
11	001012	264	927.5877	11	11	15	17	-0.1953	0.1953	0.67654	/Users/rhyscarrington/Desktop/SCOPE Data/OnTrial CERR/001012.mat				

Figure 2.9 – Addition of filepath column to Excel spreadsheet

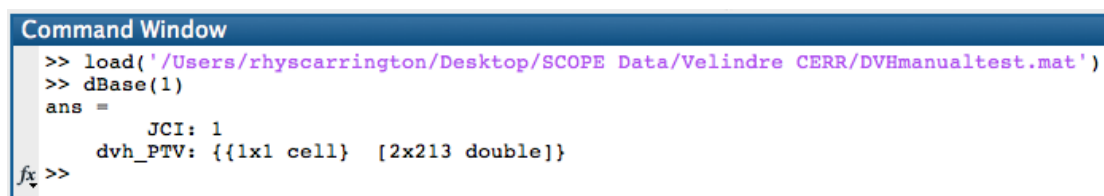
The filepath column holds the individual source path for each patient’s CERR file in which the DVH data is held.

The code was written to work in a loop for the length of the filepath column. There are a number of steps in this loop to extract the correct DVH from each patient and save them in the EUCLID database:

1. The name of the patient and the DVH structure is stored in the form of handles.
2. The EUCLID database created from the Excel spreadsheet is opened.
3. The length of the filepath column is calculated.
4. The planC of the first patient in the list is opened.
5. Structures (and their associated DVHs) are kept in planC using numbers. The number of the same DVH structure may differ from one patient to the next. This step therefore matches the DVH structure requested by EUCLID with the correct structure number within the patient's planC.
6. The DVH matrix is extracted.
7. The matrix is saved in the dBase array in a newly created field for each patient with the prefix '*dvh_structurename*'.
8. The loop goes to the start and steps 1-5 are repeated until the DVHs of the structure requested in EUCLID are extracted and saved in dBase for each patient in the filepath column.

Testing the script

It was important to ensure that the script for extracting and saving DVHs automatically in the format of the EUCLID database Matlab file performed correctly. Fifteen patients from the SCOPE 1 database were used to create a test database by importing the necessary DICOM files into CERR. The `trialBuildFileListGUI.m` and `trialInterCalcDVH.m` scripts were used to calculate and save a DVH of the PTV structure in each patient's CERR file. An excel file was also created to import in to EUCLID and create the `dBase` variable. The filepath column was included for use with the auto DVH feature. Two EUCLID databases were created from the same excel spreadsheet in order to test the feature. One database had the PTV DVH of each patient imported and saved using the original manual method in EUCLID, whilst the other database would have this repeated using the new auto import feature. The first test was to make sure that the DVH data were being stored correctly in the `dBase` structure array. The Figure 2.10 shows how the DVH data is stored when using the manual method. The `1x1` cell holds the name of the DVH, whilst the `2x213` double holds the DVH data stored in absolute format.



```
Command Window
>> load('/Users/rhyscarrington/Desktop/SCOPE Data/Velindre CERR/DVHmanualtest.mat')
>> dBase(1)
ans =
    JCI: 1
    dvh_PTV: {{1x1 cell} [2x213 double]}
fx >>
```

Figure 2.10 – Manual import of DVH data

Figure 2.11 shows the storage of DVH data using the automatic method. It can be seen in this instance that only the absolute DVH data is saved in the array.

```

Command Window
>> load('/Users/rhyscarrington/Desktop/SCOPE Data/Velindre CERR/DVHautotest.mat')
>> dBase(1)
ans =
      JCI: 1
    dvh_PTV: [2x213 double]
fx >> |

```

Figure 2.11 – Automatic import of DVH data

For use in EUCLID this is not a concern as the script in EUCLID is written in a way so as to extract the data from the ‘last’ cell in the series. Therefore if there is only one cell, this is the cell that will be read and the data extracted and saved.

Dose Bin (Gy)	Volume (cc)	
	Automatic Import	Manual Import
50.00	24.11	24.11
50.25	20.52	20.52
50.50	18.85	18.85
50.75	15.48	15.48
51.00	13.50	13.50
51.25	12.47	12.47
51.50	9.23	9.23
51.75	7.38	7.38
52.00	6.62	6.62
52.25	4.70	4.70
52.50	2.51	2.51
52.75	1.01	1.01
53.00	0.06	0.06

Table 2.0 – Dose bins for automatic and manual import of DVH

To ensure that the DVH data stored within the cell is exactly the same, both DVHs were plotted and compared. The dose bins from 50-53Gy and their associated values are in Table 2.0, it can be seen that the values are exactly the same.

The dose volume plots (Figure 2.12) for the PTV were also identical, confirming that the automatic DVH import script worked correctly.

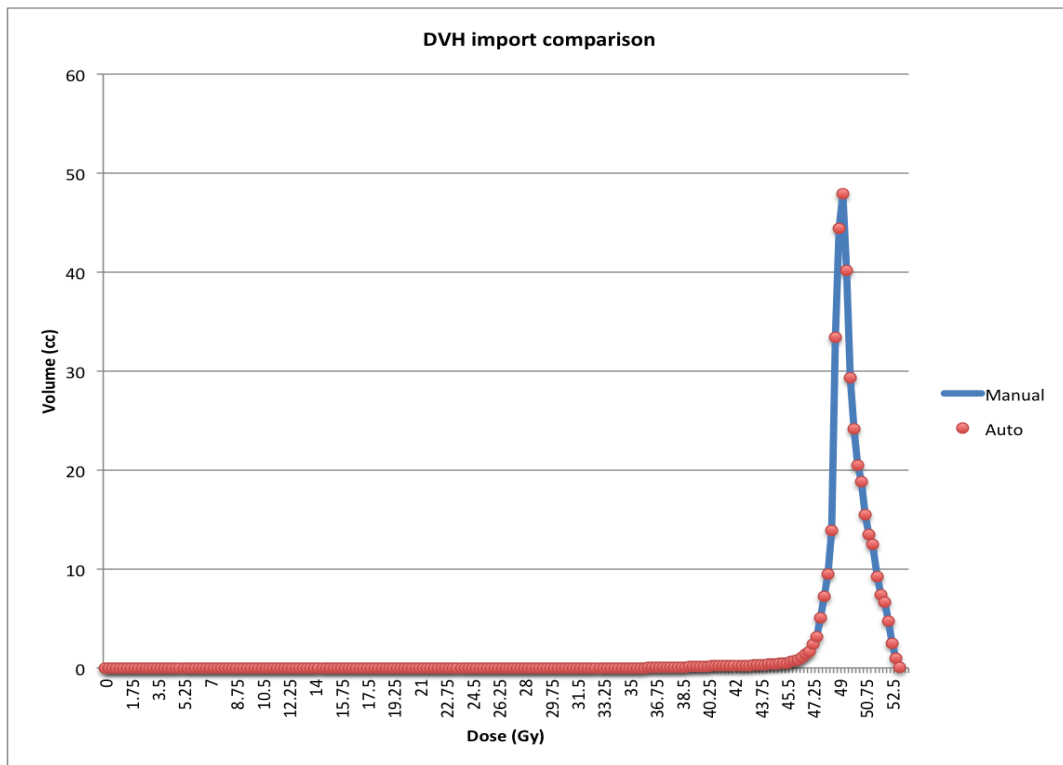


Figure 2.12 – DVH from manual and automatic import

This was also repeated for a DVH of the Total Lung (see Figure 2.13)

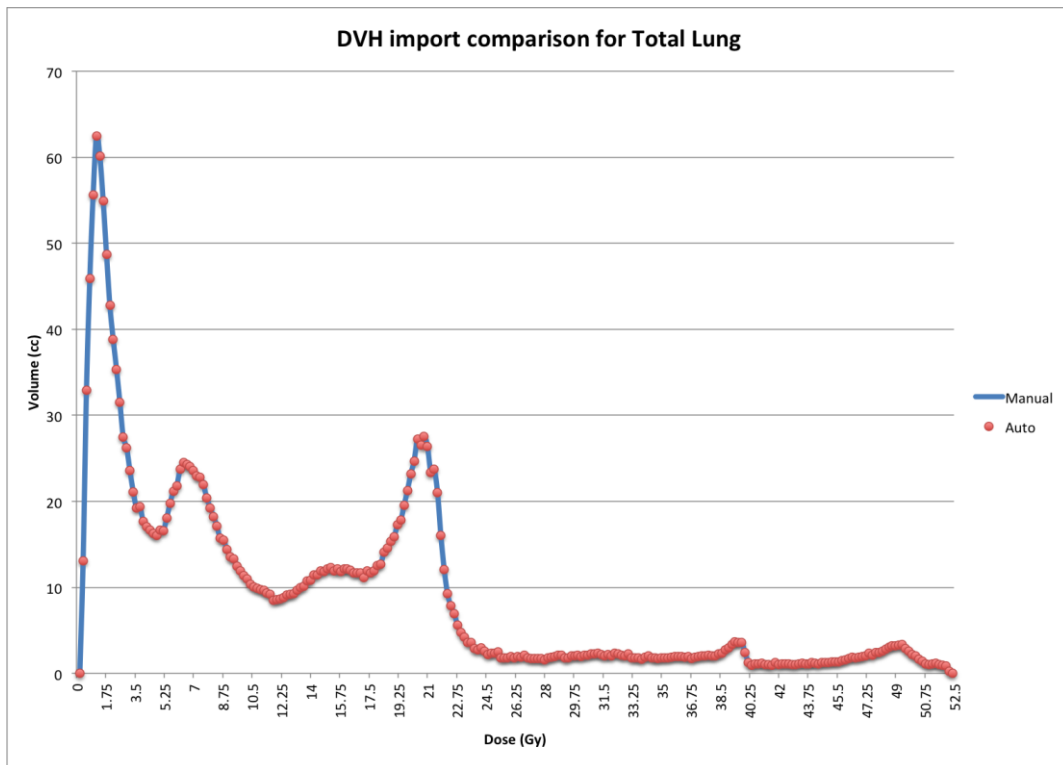


Figure 2.13 – DVH for TotalLung from manual and automatic import

2.4.3 Addition of Hazard Ratio calculation

Although the analysis module of EUCLID is capable of outputting a p value according to the log rank test, an additional test that gives useful information when analysing survival plots is the Cox Proportional hazard test (Section 1.5). The calculation of the Hazard Ratio within EUCLID required the code of the existing Kaplan Meier analysis module to be modified and extended. The Hazard Ratio is calculated on the last line of the script (See Appendix A1 - Computer coding). When undertaking Kaplan Meier analysis within EUCLID this value would then be given as an output. Again, this was tested against the same analysis in SPSS (59), a statistical analysis program, using the same test database as used previously. The hazard ratio calculated using the customised script in EUCLID above was 0.5858 whilst the same analysis in SPSS gave

a hazard ratio of 0.5890. A 0.5% difference would indicate that the script was working correctly.

2.5 Testing the survival analysis module

As the work in this project was going to be utilising the survival analysis module of the EUCLID program it was important that it was tested against a known and reliable external piece of software. Due to its availability and reputation it was decided to use IBM's SPSS software for this purpose.

Using a test database, the survival analysis module was used to analyse the difference in survival between two groups according to the length of the tumour.

The resulting plot is shown in Figure 2.14

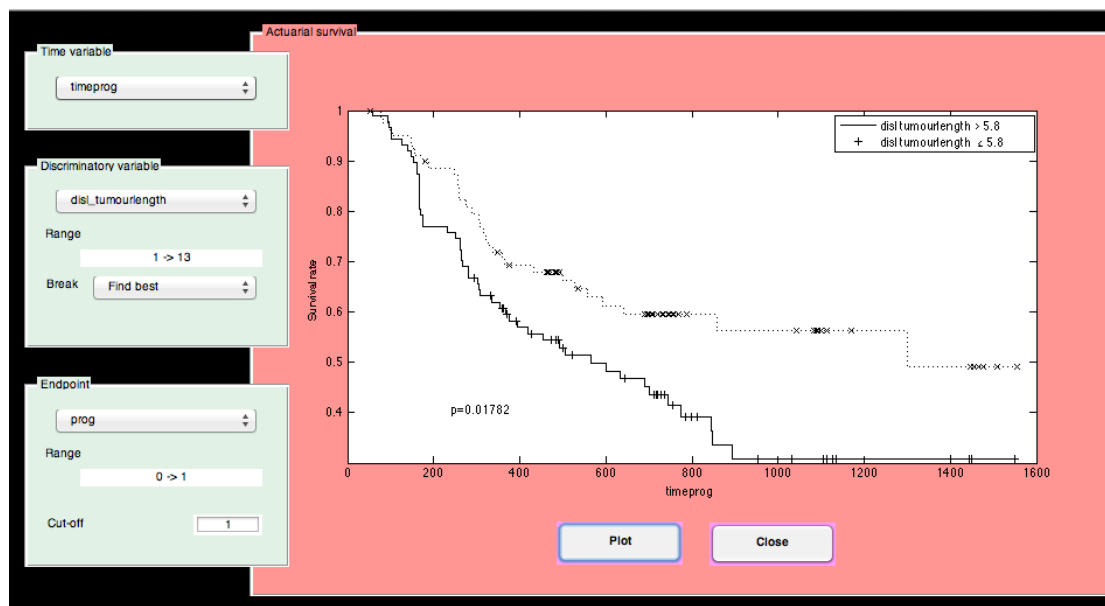


Figure 2.14 – Kaplan Meier plot from EUCLID

The p value obtained for the log rank test conducted between these groups was 0.01782. The same analysis was then undertaken in SPSS (Figure 2.15).

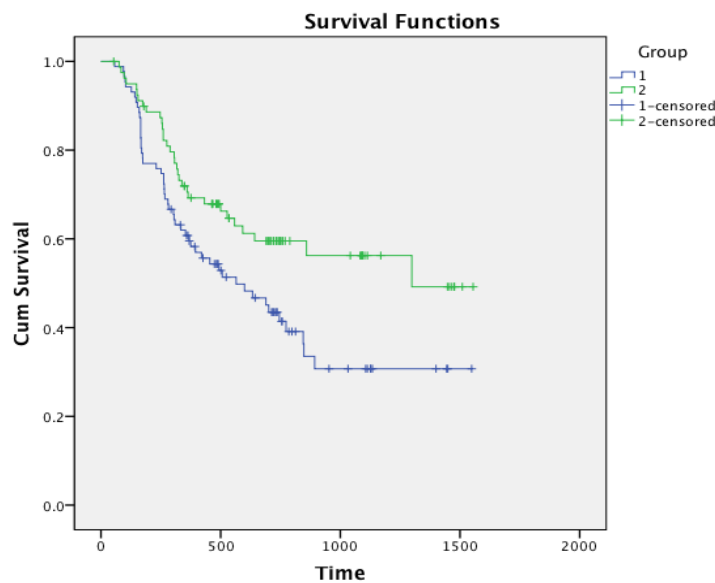


Figure 2.15 – Kaplan Meier plot from SPSS

The p value obtained in SPSS using the log rank test was 0.018.

2.6 Conformity Indices

The investigation of the conformity of the dose distribution surrounding the PTV within this thesis requires the ability to quantify the positional relationship between two structures. A known method for this kind of analysis is the use of a conformity index, able to represent the variation in volume and spatial relationship between two structures in a single metric. A review of these methods was undertaken by L Feuvret et al (60) in which they outline the advantages and disadvantages of a number of conformity indexes in the context of the analysis of dose distribution. It is noted how the improvement in the spatial representation of dose distribution means that obtaining various treatment plans for the same patient is a relatively rapid

process but that choosing which of these plans to use remains difficult. Using a tool such as a conformity index could therefore aid this process as it provides a quantifiable score of the ratio of healthy tissue being irradiated compared to the target volume. A number of conformity indices were proposed and outlined in the RTOG report in 1993 and also included in ICRU Report 62 although their day to day use in a clinical setting remain limited. This may be due to an aspect of using a conformity index that could be seen as both advantageous and disadvantageous, their inherent simplicity. A tool should be simple and quick to understand, implement and use but it also important to remember that the consideration of dose conformity data alone may not be sufficient. The use of conformity indices is widespread in stereotactic radiotherapy (61) (62), (63) both in research and clinical settings, and it is unclear why this is the case in one aspect of radiotherapy whilst being almost unused in the remaining. It is possible that it may be due to the increased complexity of planning in other areas of the body and the proximity of a number of organs at risk due to the target volume.

A conformity index that takes into account critical organs has been proposed by Baltas et al (64). The index was proposed with a view to be implemented in brachytherapy but could equally be used in highly conformal radiotherapy due to the associated high dose gradients. Named the COIN index, it takes into account the quality of tumour irradiation, irradiation of non-critical healthy tissue and irradiation of critical organs and the entire calculation is based on the volume of the reference isodose. It expands the application of another index known as the Van't Riet Conformation Number (CN) (65), first described as a tool to compare RT plans for

prostate cancer using brachytherapy and external beam radiotherapy. A much simpler index has been used by Knoos et al (66) to study the degree of conformity reached in clinical routines of 57 patients treated for breast cancer. The radiation conformity index (RCI) is simply a ratio of the PTV volume and either the treated volume or the volume of the 95% isodose and therefore increases from 0 to 1 with increasing conformity of the two structures. Similarly, the Jaccard Conformity Index (JCI) was used by Mulliez et al to compare the dosimetry of different IMRT techniques (67). It has also been used extensively in the analysis of target volume delineation variation (68) & (69). First described in 1901 by Paul Jaccard as the ‘coefficient de communaute’ as a tool for botanic comparison (68) it is perhaps the most commonly used index in the RT literature. It is a slight variation of the simple RCI index in that it is defined as the size of the intersection of two structures (circles A and B in Figure 2.16) divided by the size of the union of those same two structures.

$$J = \frac{|A \cap B|}{|A \cup B|} \quad (2.0)$$

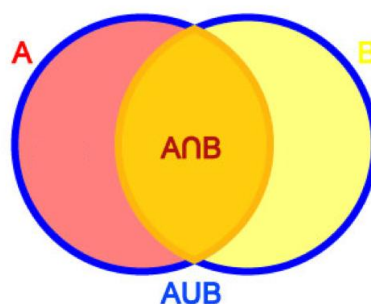


Figure 2.16 – Schematic for Jaccard Conformity Index

Similarly to when using the RCI, a JCI value of zero would be seen if there is no agreement and a value of one if there is complete agreement (overlap). Both of

these indexes have the advantage of being simple to both calculate and understand, however neither of them provide any information about the difference in shape between two volumes. They are also largely confined to the study of spherical shapes, and can fail to function correctly when assessing more complex volumes (70). In addition, the data generated can be difficult to interpret when considering clinical significance of the dose distribution. Considering these drawbacks, Jena et al proposed a new conformity index known as the Mean Distance to Conformity (MDC) (70). The aim of this new index was the following:

1. A single scoring statistic that represents the overall conformity of the two volumes being assessed.
2. Additional statistics that provide information on whether the non-conformity is caused by over or under outlining.
3. A method of display that would facilitate evaluation of the clinical significance of discrepancies.

The MDC metric is a shape-based statistic that measures the mean displacement needed to transpose every voxel in an evaluated volume to a reference volume. It differs from the other indices described so far as it gives a measure of the magnitude of the difference between the two volumes being analysed, giving a value in cm.

For calculating the MDC, Jena et al established a three-dimensional (3D) grid representation for processing the structure contour data. Each node within the grid could then adopt one of four states:

State 0: The node lies outside both reference and evaluation volumes.

State 1: The node lies within the reference volume but not the evaluation volume.

State 2: The node lies within the evaluation volume but not the reference volume.

State 3: The node lies within both volumes.

These states can be visualised in Figure 2.17, which gives a representation of two structures on the grid. The blue contour is the reference contour and the red contour the evaluation contour. The green voxels have been determined to lie within both outlines. The light blue voxels are within the reference volume outline but not within the evaluation volume outline and represent under-coverage errors (under MDC). The dark red voxels are within the evaluation volume outline but not the reference volume outline and represent over-coverage errors (over MDC).

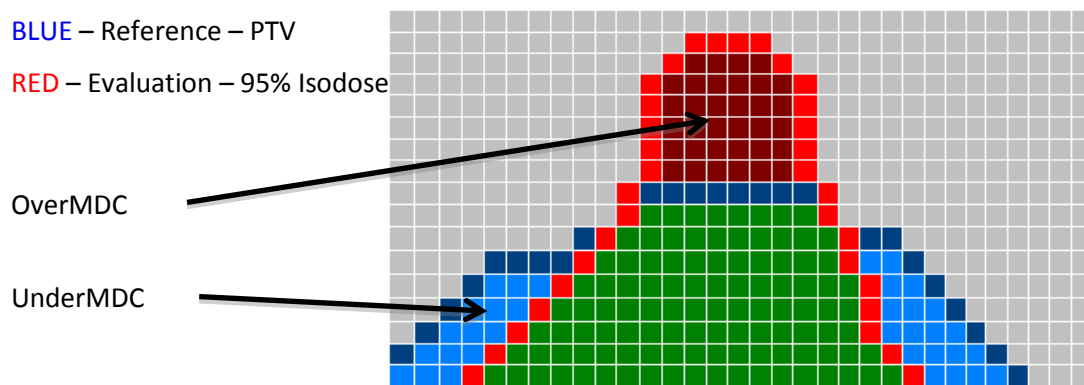


Figure 2.17 – Schematic of MDC showing OverMDC and UnderMDC

Figure 2.18 shows the trendline and near exponential relationship between the MDC and JCI index.

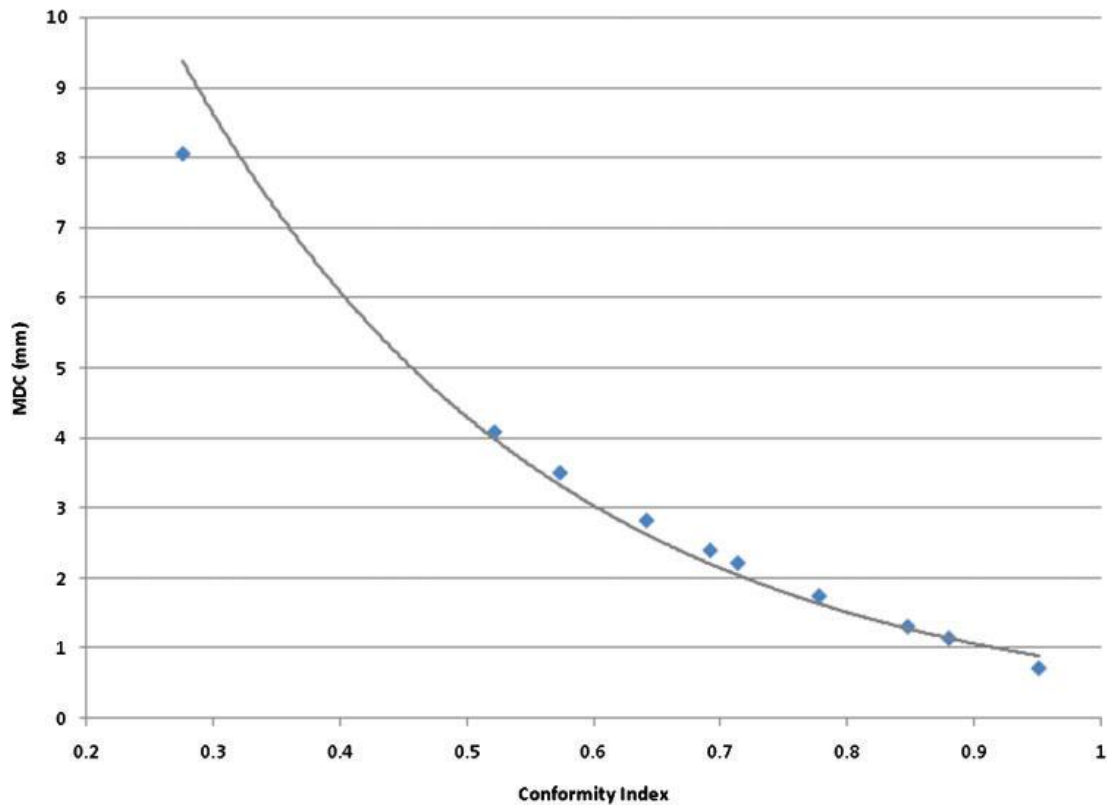


Figure 2.18 - Variation of MDC with change in JCI for two spherical volumes. Reproduced with permission from Jena *et al* A novel algorithm for the morphometric assessment of radiotherapy treatment planning volumes, BJR 83:44-51 (71)

The MDC is simple to both calculate and interpret, yet also provides more clinically useful information than a simple ratio of the overlap of two volumes that is provided by the RCI and JCI. Following the work carried out by Dr Sarah Gwynne for her MD thesis (72) and discussions with her and other colleagues, it was therefore decided to take the JCI and MDC index forward for analysis of conformity in this thesis.

2.7 Type A and Type B algorithms

It is widely appreciated that the choice of dose calculation algorithm for radiotherapy planning affects the accuracy of calculated dose distributions (73). The main disparity between algorithms in routine use is the extent to which they model

scattered dose transport (74), (75) & (76). In heterogeneous situations, the algorithms that provide approximate modelling for the variation of penumbra with density (known as “Type B” according to Knoos et al (74)) provide a more accurate representation of dose than those that do not (known as “Type A”). This is because the Type A algorithms use a one-dimensional density correction which does not accurately model the distribution of secondary electrons in media of different density (77). Type B algorithms meanwhile are corrected for any variation in density along the modelling of a photon ray. Although the limitations of Type A algorithms in calculating dose are well known, the clinical implementation of a Type B algorithm in treatment centres was limited at the start of the SCOPE 1 trial. The commissioning of a new dose calculation algorithm and ensuring patient safety can be time consuming and require significant resources. As a result, in the SCOPE 1 trial it was decided to allow centres to commence recruitment to the trial using their existing algorithms (if Type A) in order to minimize the risks associated with change and ensure that the trial reflected current clinical practice. The dose of radiotherapy plans in the trial data was therefore calculated using these two types of algorithms, dependent on the centre at which they were planned. Wills et al undertook an investigation as a part of the trial design process to assess whether the two types of algorithm needed to be taken into account when applying the radiotherapy protocol to each patient (78). The study took fifteen patient data sets that underwent CRT at Velindre Cancer Centre between 2007 and 2009 for carcinoma of the oesophagus. The patients had been planned according to the SCOPE 1 protocol using a Type A pencil beam algorithm. These plans were then re-calculated in OMP using a Type B collapsed

cone algorithm and the dose volume data for the regions of interest (See Table 2.1) between both sets compared.

Structure	Constraint
PTV	Minimum dose > 93%
PTV	Volume receiving 95% dose (V95%) > 99%
PTV	ICRU maximum dose < 107%
Heart	Volume receiving 40Gy (V40Gy) < 30%
Liver	Volume receiving 30Gy (V30Gy) < 60%
Lung	Volume receiving 20Gy (V20Gy) < 25%
Spinal Cord PRV	Maximum dose < 40Gy

Table 2.1 – Dose Volume constraints for SCOPE 1

It was found that the use of Type B algorithms during optimization results in improved PTV coverage by the 95% isodose. This is especially important when considering the dose in oesophageal cancer, due to the proximity of the treatment volume to the lung. The effect of algorithm type on the calculated dose in lung tissue can be observed in Figure 2.19a & b.

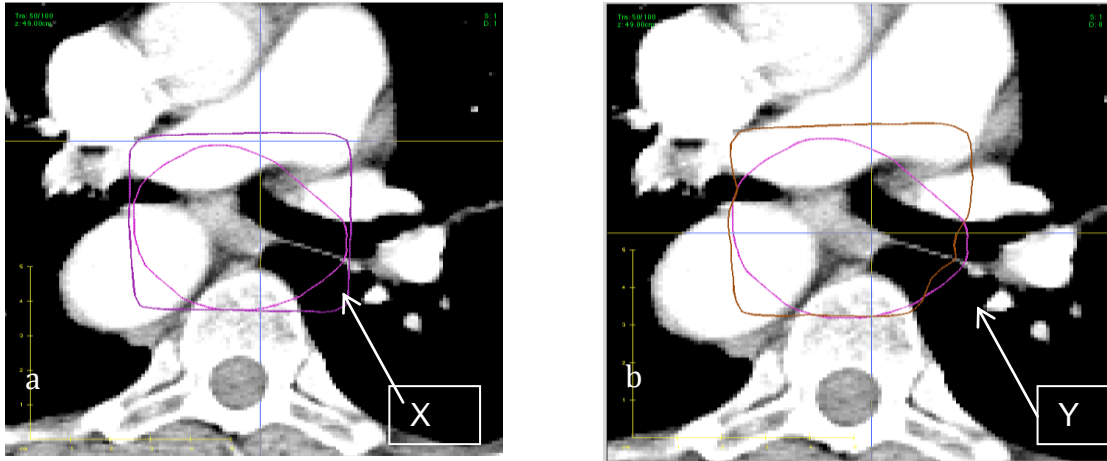


Figure 2.19a Plan using Type A algorithm showing PTV and 95% idodose line, b: plan using Type B algorithm showing PTV and 95% idodose line

Figures 2.19a & b show the same plan calculated with a Type A and Type B algorithm respectively. It can be seen in Figure 2.19b how the 95% isodose line is modelled differently in the lung (marked Y) compared to that in Figure 2.19a (marked X). This is a direct consequence of the lateral electron transport being modelled correctly in Type B algorithms, which will have a large effect at the boundary of relatively dense matter such as the oesophagus with air filled areas such as the lung. As such Type A algorithms can be considered incorrect in the modelling of dose in this area. The analysis by Wills et al was made using only 15 patients from one centre. For completion it was decided to undertake an analysis of the effect of the planning algorithm on the JCI and MDC conformity index value using the complete SCOPE 1 database. This was tested by comparing the JCI and MDC index value between the $V_{95\%}$ and the PTV and comparing the results for patients planned with Type A and Type B algorithms using the Mann Whitney U test in the SPSS package. The JCI (Median = 0.68, Interquartile range = 0.64-0.73) was shown to have a statistically significant dependency with whether the plan was calculated using a Type A (n=94,

Median JCI = 0.67 Interquartile range = 0.63-0.71) or Type B (n=82, Median JCI = 0.71 Interquartile range = 0.67-0.75) algorithm (Mann Whitney U test $p < 0.001$). The test was repeated using the MeanMDC, OverMDC and UnderMDC metrics. The results in mm are shown in Table 2.2:

	Median	Interquartile Range	P value of dependency on algorithm
MeanMDC	2.1	0.9-3.1	<0.001
OverMDC	4.0	3.3-4.7	0.002
UnderMDC	2.1	0.9-2.7	<0.001

Table 2.2 – Mann Whitney U test for MDC metrics between Type A and Type B dose algorithms

These results show how the dose distribution displayed in a radiotherapy plan is dependent on whether the dose was calculated using a Type A or Type B algorithm. As a result of these tests, the prior work in this area and discussions with clinical and technical staff, it was decided that all dosimetric analysis on the database should be carried out with the database split according to those patients planned using a Type A and Type B algorithm. This would ensure that any conclusions reached about the effect of dose distribution could not be influenced by the effect of the planning algorithm. For this project, it was decided to concentrate on the analysis of Type B patients. It was felt that the results would be more relevant to the present clinical situation in the field due to the majority of centres having now moved to using these types of algorithms since the end of the SCOPE 1 trial. Figure 2.20 is a consort diagram showing the patient dropout rate and reasoning. Treatment and tumour

demographics of the final cohorts dependent on planning algorithm are also included.

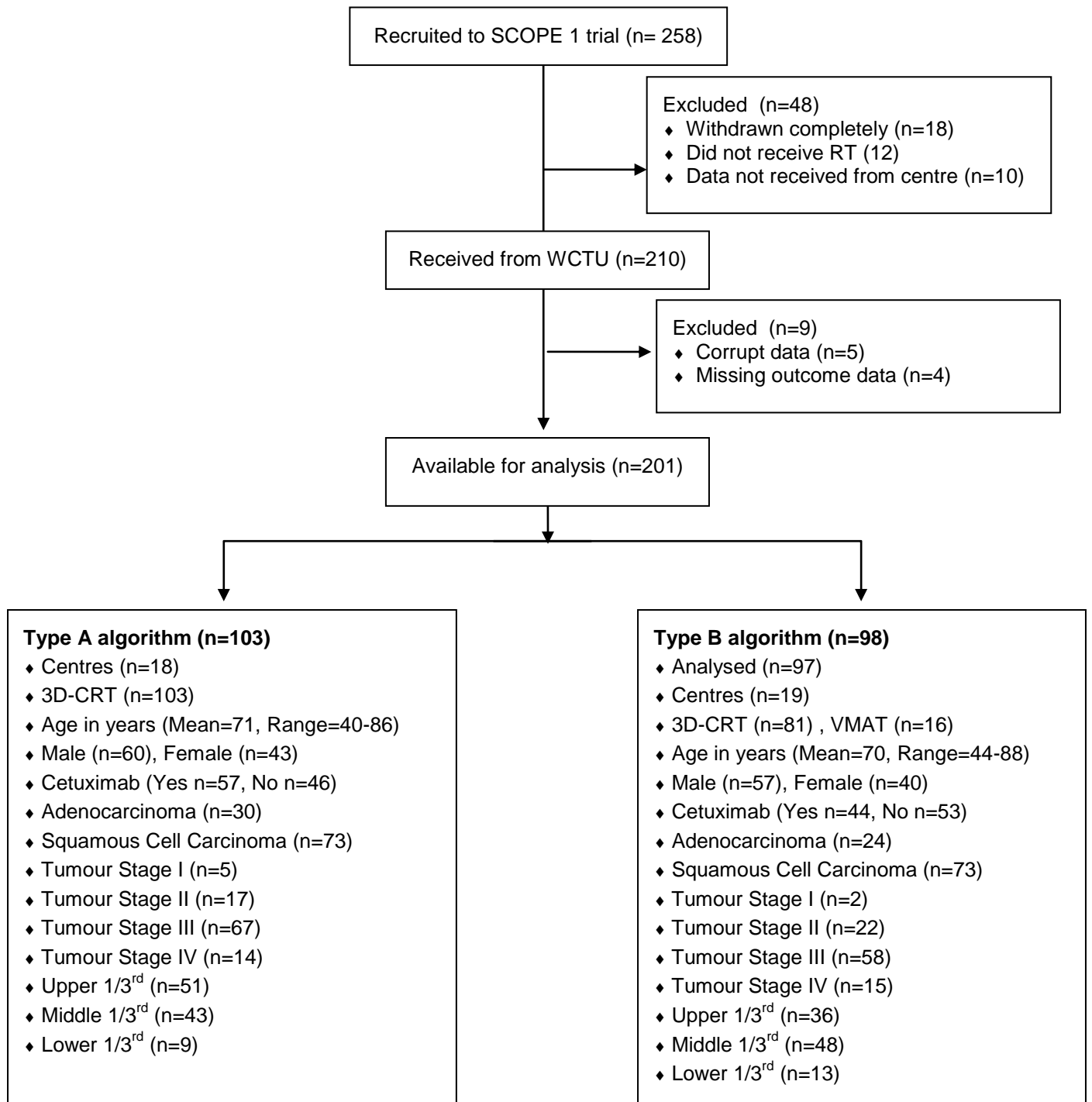


Figure 2.20 – Consort diagram showing patient treatment and tumour demographics

Chapter 3

Dose distribution and patient outcome

3.1 Introduction

It is clear that radiotherapy plays a key role in the treatment of oesophageal tumours, however the formulation and application of optimal radiotherapy protocols to these sites is not well defined (79). There is therefore a clear need to improve the quality and outcome of therapy. It is known that dose distribution is an important factor when evaluating the quality of radiotherapy plans and a plan is considered acceptable if 95% of the prescribed (tumoricidal) dose is delivered to 100% of the PTV (80) & (81). However, although this requirement will be met in the majority of patients undergoing radiotherapy, the quality of the dose distribution may vary according to factors such as PTV volume (82) or by the delivery technique (83). It has been shown that adherence to a site-specific radiotherapy protocol is effective in improving plan quality and patient outcomes (84), and the SCOPE 1 trial provided a detailed radiotherapy study protocol and quality assurance programme (85).

Despite a detailed radiotherapy protocol and planning guidance document, a rigorous RTTQA programme (73) & (86) demonstrated variation in radiotherapy planning practice such as planning technique across the 36 UK centres that participated in this study. These factors may have affected the quality of the dose

distribution achieved for each patient, in addition to those factors already discussed. A recent study by Moore *et al* noted that many plans may still be classed as ‘low quality’ even when adhering to clinical trial protocol (87). The aim of this investigation was two fold; Firstly to assess plan quality using a conformity index and analyse its influence on patient outcome. Secondly, to identify whether clinical and technological factors including GTV length, PTV volume, tumour location and treatment delivery method could be related to the conformity index value.

Number of patients	Reasoning
97	Only Type B algorithm patients analysed (See Figure 2.20 for demographic)

Table 3.0 - Number of patients included in analysis in Chapter 3

3.2 Correlating plan quality with outcome

3.2.1 Quantifying plan quality

Firstly it was hypothesised that plan quality can be objectively assessed by quantifying the relationship between the 95% isodose and the PTV using a conformity index. Secondly, that treatment and patient characteristics may influence plan quality. The use of conformity indices to analyse dose distribution of radiotherapy plans has been carried out previously (66) & (88). However, to the best of my knowledge, this study is the first to explore the relationship of conformity index and patient outcome.

3.2.2 Analysis of conformity index values across the database

The JCI and MDC (See Section 2.6) (UnderMDC and OverMDC) conformity index values were calculated for each patient. Figure 3.1- 3.3 show the resulting distribution of the conformity index values in ascending order.

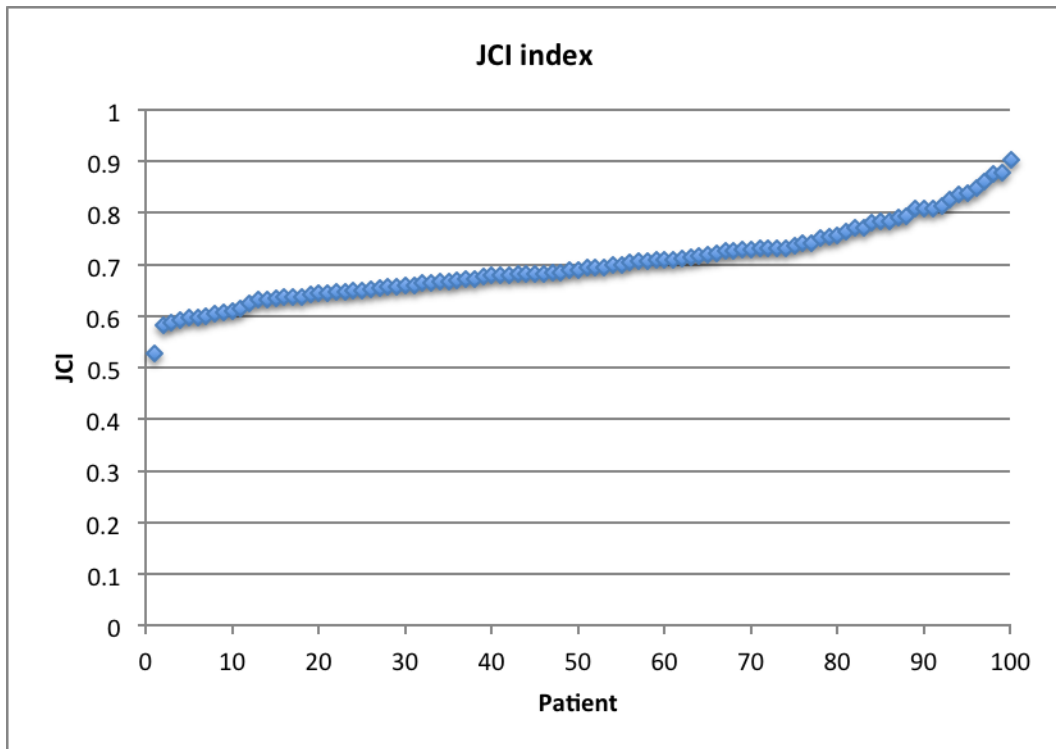


Figure 3.1 – Distribution of JCI values across the database

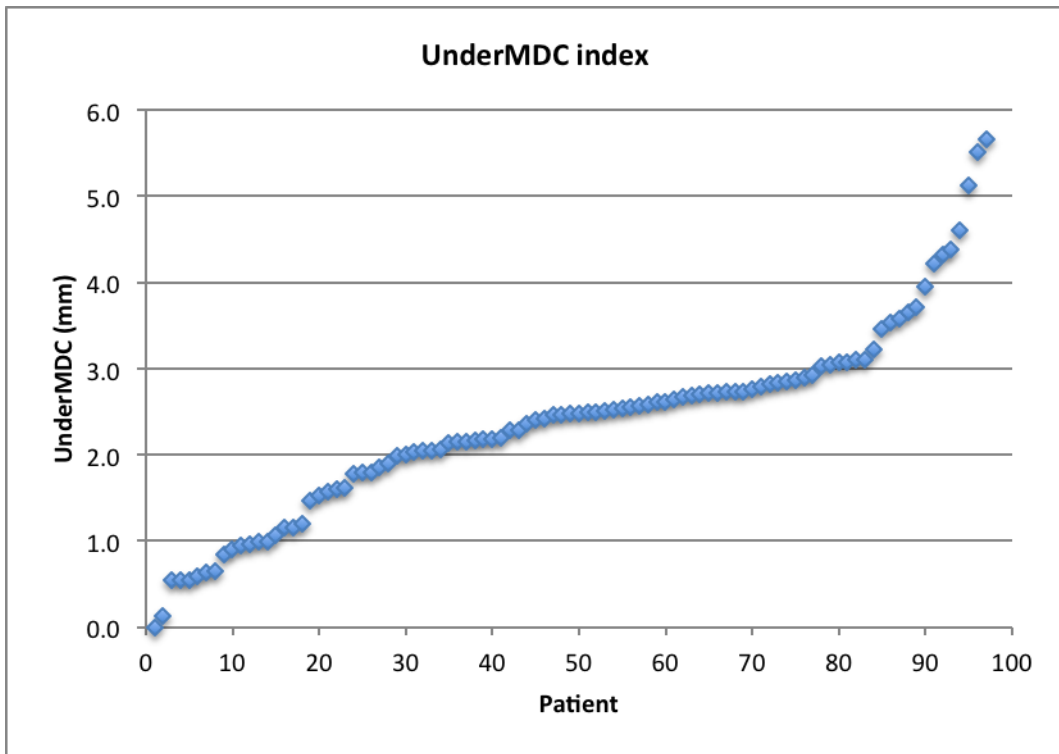


Figure 3.2 – Distribution of UnderMDC values across the database

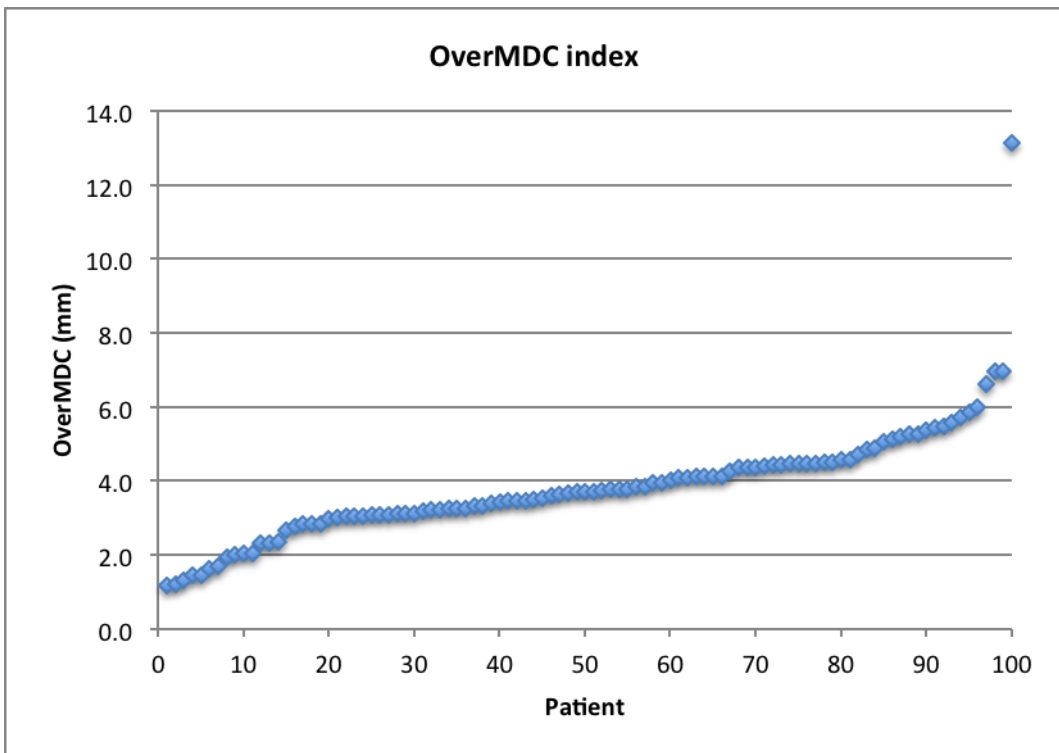


Figure 3.3 – Distribution of OverMDC values across the database

Figure 3.3 clearly shows an outlier in the distribution of OverMDC values. This patient has an over MDC value of 13.1mm, which far exceeds the average of the Type B patient cohort (3.7mm) outlined in Figure 2.20. This value is confirmed by analysing the image from the CERR screen (Figure 3.4).

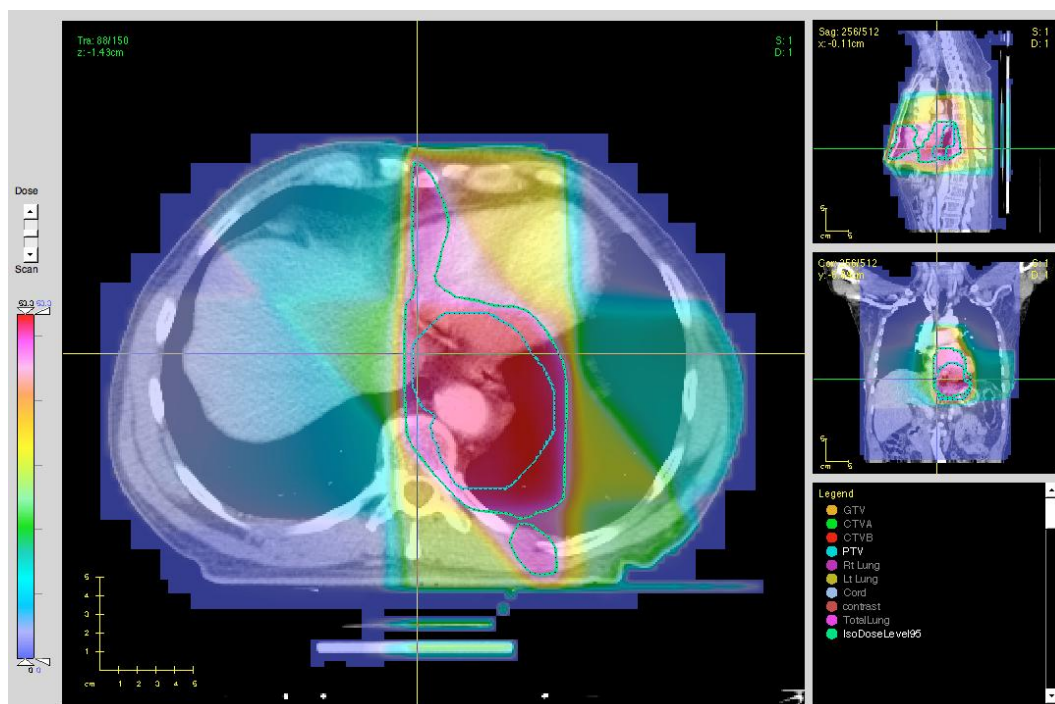


Figure 3.4 – Profile of outlier patient in CERR with dose wash

Figure 3.4 shows that the 95% isodose does indeed have extremely poor conformity with the PTV. There is a significant area of the patient receiving 95% of the prescribed dose anteriorly. The beam arrangement is unusual in the context of the SCOPE 1 trial, and clinical colleagues also noted that the GTV was of an unusual shape. Further discussion with the clinical staff concluded that the beam and dose distribution at least are due to a need to avoid the spinal cord. Due to the highly unusual nature of this plan within the context of the database, I decided to remove this patient from the analysis.

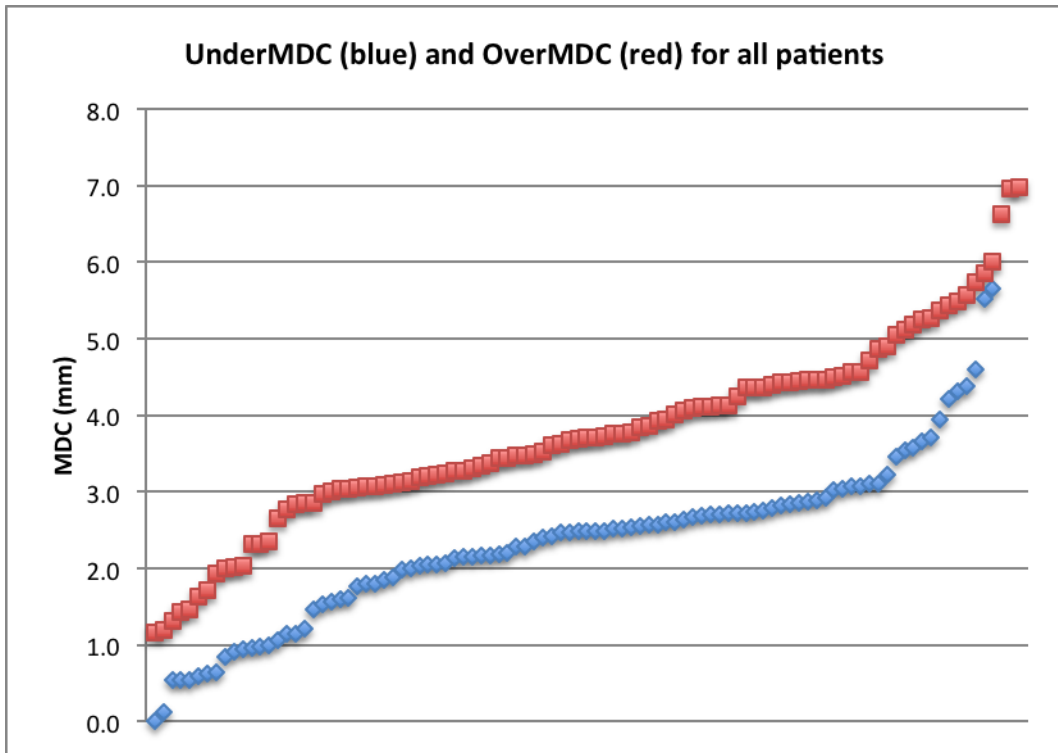


Figure 3.5 – Distribution of UnderMDC and OverMDC values across database

Figure 3.5 shows the distribution of both UnderMDC and OverMDC for the Type B patients with the outlier removed.

3.2.3 Comparing JCI and MDC

In order to gain a further understanding of the relationship between the JCI and MDC indices they were plotted against each other. This would allow the relationship to be visualised and quantified.

OverMDC vs JCI

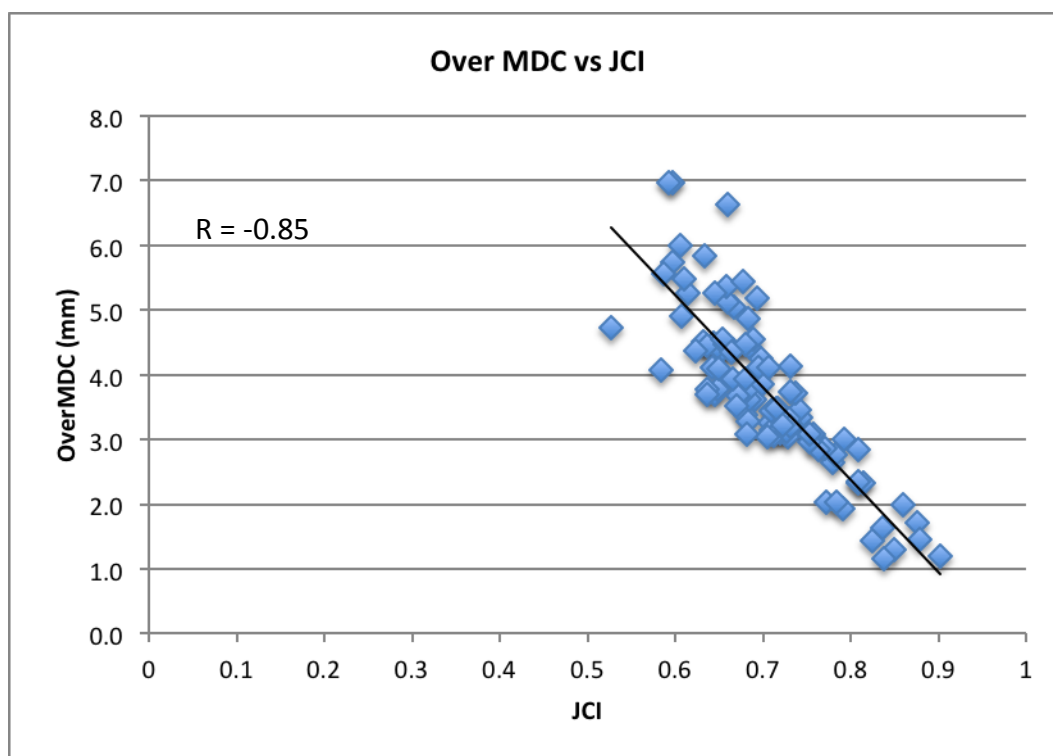


Figure 3.6 – Plot of OverMDC vs JCI

Figure 3.6 shows the correlation of the Over MDC metric with the JCI index. The Pearson coefficient is -0.85 and is highly significant with $p < 0.01$. This correlation is entirely expected due to the nature of both indices. For the JCI index, the conformity of the PTV and 95% Isodose increases as it tends towards 1. It follows therefore that the OverMDC value, which quantifies the extent of over outlining, should decrease as the JCI index increases.

UnderMDC vs JCI

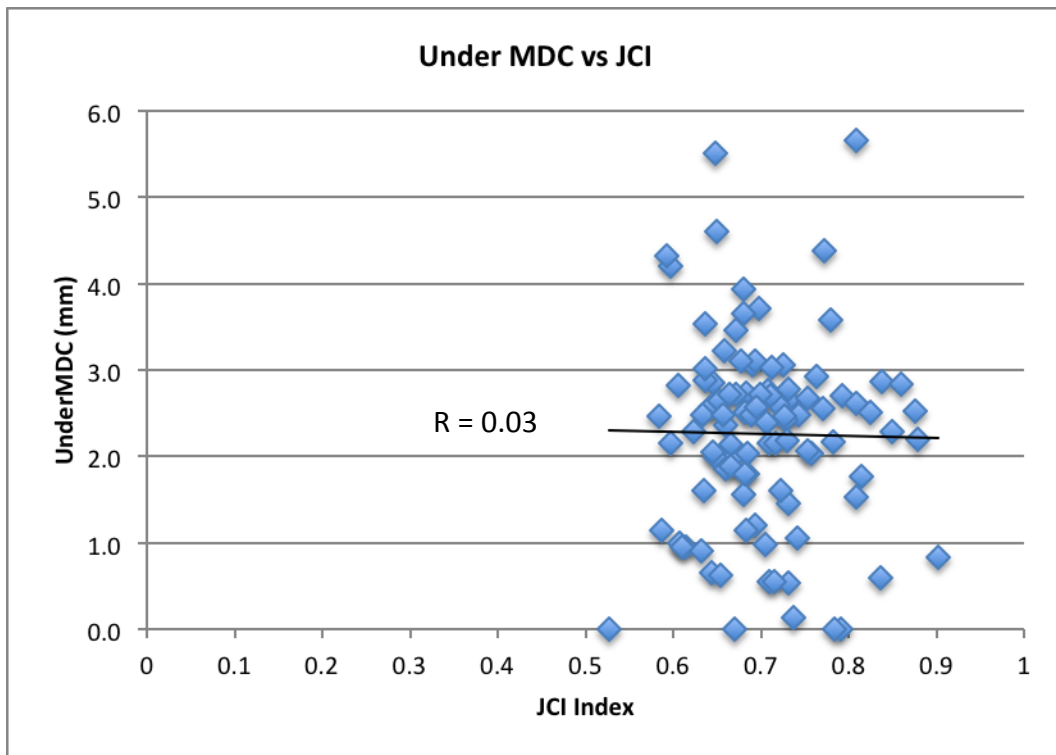


Figure 3.7 – Plot of UnderMDC vs JCI

Figure 3.7 shows the correlation of the Under MDC metric with the JCI index. The Pearson coefficient is 0.03, which confirms the visual lack of correlation on the plot. Exactly why there should be such a lack in correlation remained unclear as it would be expected that similar to the OverMDC vs JCI plot, the UnderMDC metric should reduce as correlation according to JCI increases.

MeanMDC vs JCI

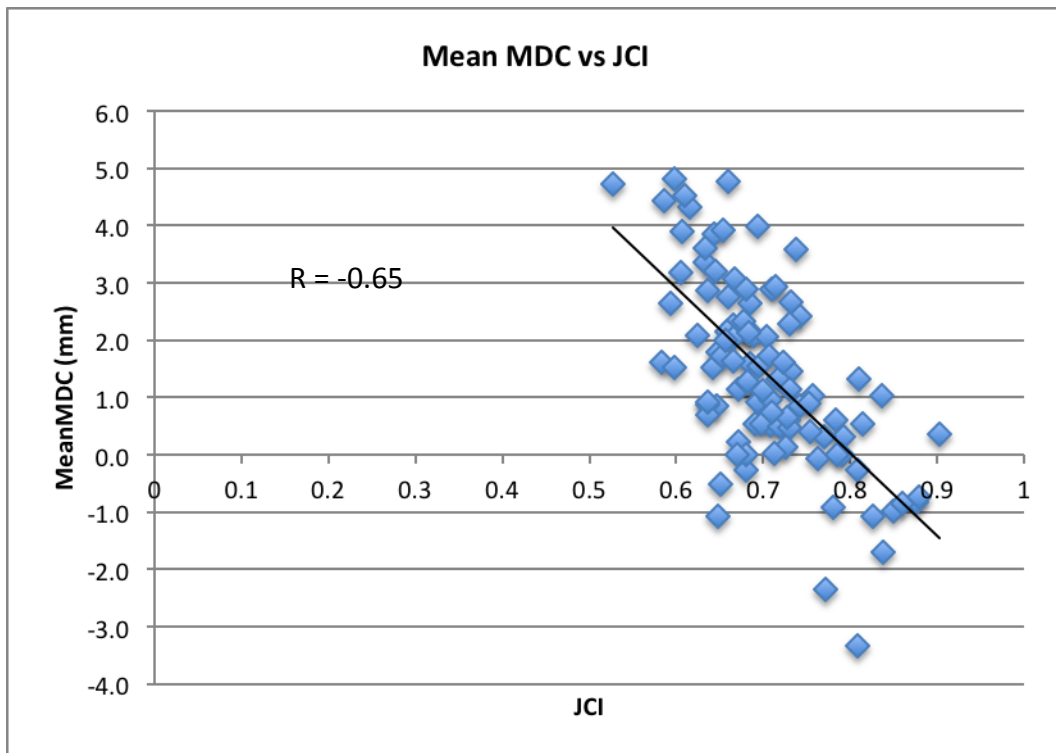


Figure 3.8 – Plot of Mean MDC vs JCI

Figure 3.8 shows the correlation of the Mean MDC metric with the JCI index. The Pearson coefficient is -0.75. It is clear that there is a negative correlation, similar to that observed with the OverMDC vs JCI plot. Again, this is to be expected due to the nature of both indices. As the conformity increases, the JCI index tends towards 1 whilst the Mean MDC tends towards 0.

JCI vs MDC

The JCI and MDC indices are both able to give a quantifiable value of the relationship between two volumes or structures. However as noted previously (see Section 2.6) there are advantages and disadvantages associated to both. To streamline the investigation of the effect of conformity index on patient outcome I decided to

concentrate on only taking the MDC further forward. This was due to the JCI being a composite index and the MDC being able to give a more detailed and clinically meaningful values of the relationship between the two volumes under consideration.

3.2.4 Outcome data

Outcome data for each patient, including overall survival, was collated and prepared by the WCTU. Due to the adverse effect of cetuximab on survival in the SCOPE 1 trial (56), the cetuximab administration data for each patient was also acquired to allow for stratification. Kaplan-Meier plots were generated to observe whether there was a clinically relevant threshold for the CI value in relation to survival. The demographic and prognostic data outlined in Figure 2.20 was also used for multivariate analysis.

3.2.5 Deciding on CI breakpoint

Using the EUCLID package, comparisons of survival for two populations discriminated by a given variable can be performed using a log rank test of the hypothesis that the curves describe the same survival function. This can also be extended to any end point (local control, progression etc) if the time to that endpoint is recorded and available.

A function in EUCLID allows the option to scan the range of the variable (in this case the conformity index) to find the break point value that yields the lowest p-value and therefore best separates the low survival from the high survival population. This is

corrected for multiple comparisons using the Bonferroni adjustment, a method of dealing with multiple testing when finding an optimal break point (89) and has been used elsewhere in literature of other fields with survival data (90) & (91). This function was utilized to find the best cut off in this data set. The EUCLID script code was also modified to allow the data for each group above and below the break-point to be saved, allowing the data to be exported for further analysis in SPSS.

3.4 Results

3.4.1 OverMDC and UnderMDC and overall survival

OverMDC

For the 97 Type B patient plans in this study, the median OverMDC was 3.7mm (Range: 1.2-7.0mm). The break point occurs at an OverMDC value of 4.4mm with $p = 0.02$ (logrank) and results in a 28 above/69 below split in the database. (Figure 3.9)

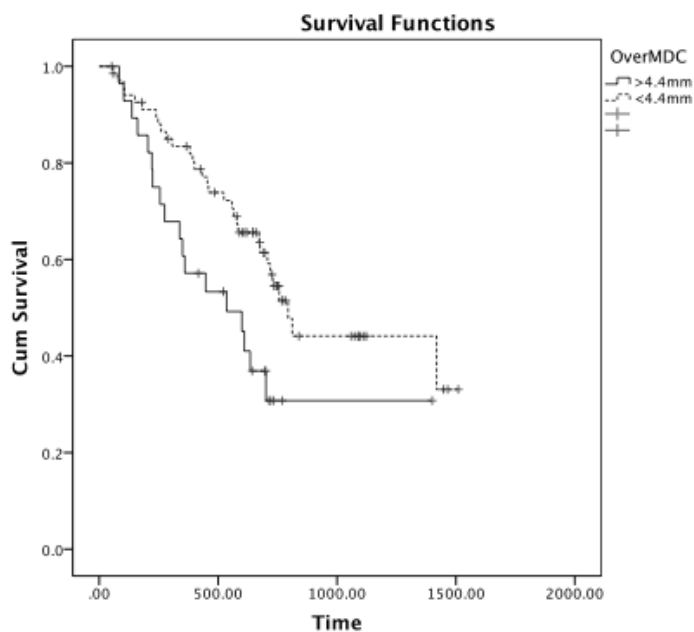


Figure 3.9 – Kaplan Meier according to OverMDC

The Cox Proportional Hazard ratio was calculated in SPSS to be 0.50 (95% CI: 0.28-0.90, $p=0.02$). Stratifying for cetuximab administration, the log rank test between the two groups gave $p=0.04$. Therefore within this cohort, the OverMDC value for the conformity of the 95% isodose line and the PTV for the patient population studied is a predictor for overall survival in univariate analysis, independent of cetuximab administration; a high OverMDC is associated with worse survival.

UnderMDC

The median UnderMDC was 2.5mm (Range: 0-5.7mm). The break point occurs at an UnderMDC value of 2.7mm with a $p = 0.05$ (logrank) and results in a 32 above/62 below split in the database (Figure 3.10).

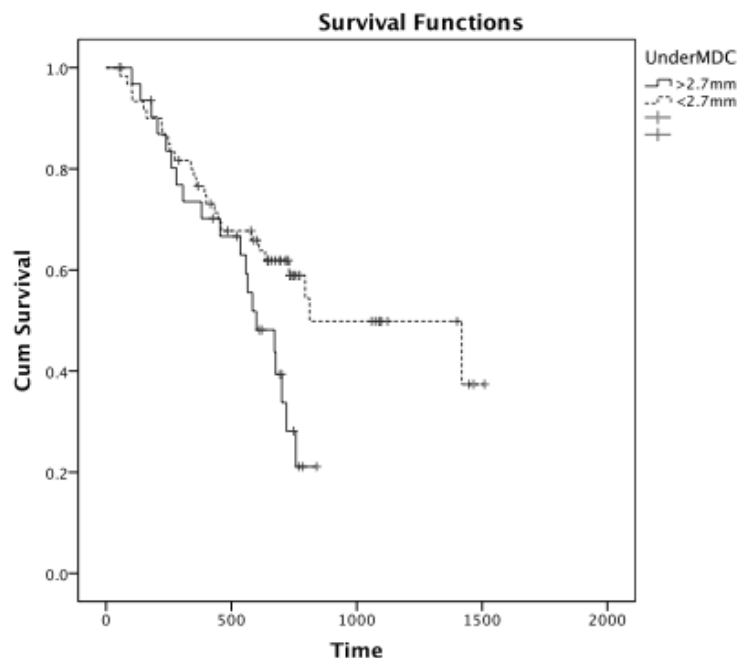


Figure 3.10 – Kaplan Meier according to UnderMDC

The Cox Proportional Hazard ratio was calculated in SPSS to be 0.53 (95% CI: 0.30-0.97, p=0.04). Stratifying for cetuximab administration, the log rank test between the two groups gave p=0.14. Therefore UnderMDC cannot be considered a statistically significant predictor for overall survival when stratifying for cetuximab.

3.5 Analysis of OverMDC values

As only OverMDC remained clinically and statistically significant following stratification for cetuximab, further analysis was limited to this metric.

3.5.1 Clinical factors

Tumour site and OverMDC

Plotting the distribution of upper, middle and lower tumours above and below the break point allowed us to look at the effect of tumour site on OverMDC value. Figures 3.11 and 3.12 show the number of patients in each location and the percentage of the total.

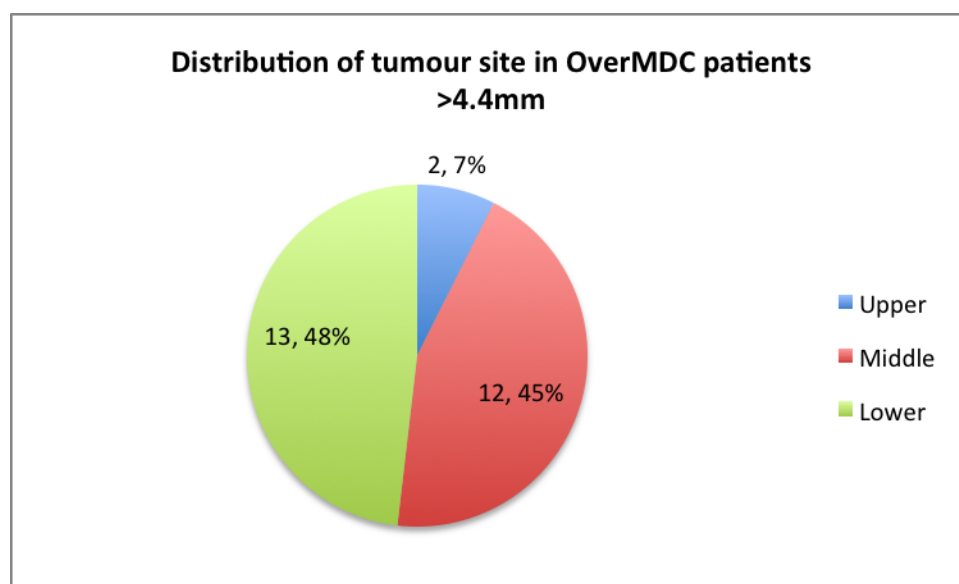


Figure 3.11 – Distribution of tumour site in OverMDC >4.4mm

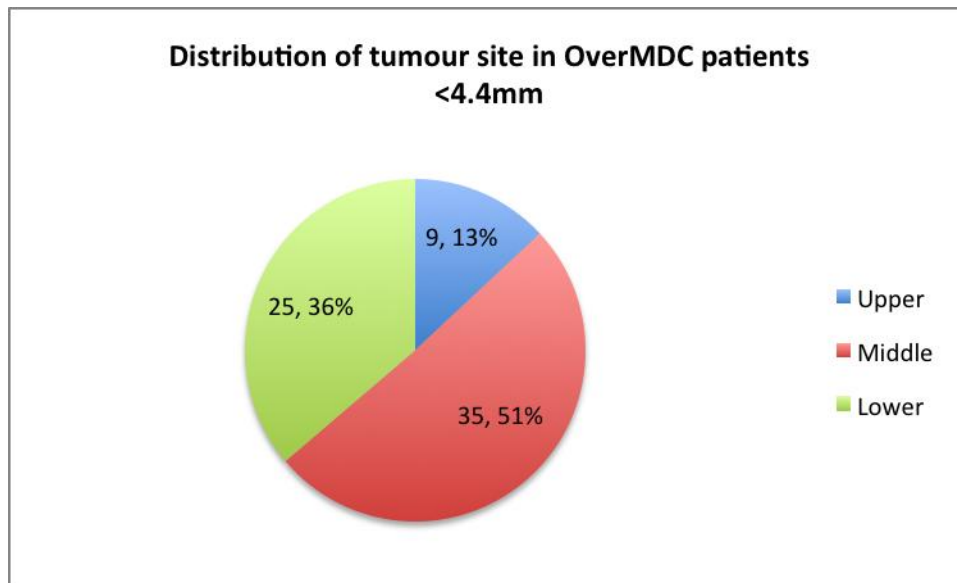


Figure 3.12 – Distribution of tumour site in OverMDC <4.4mm

It can be seen that the proportion of tumours in each site above and below the OverMDC cutoff are similar. This would suggest that tumour site does not impact the OverMDC value.

GTV length and OverMDC

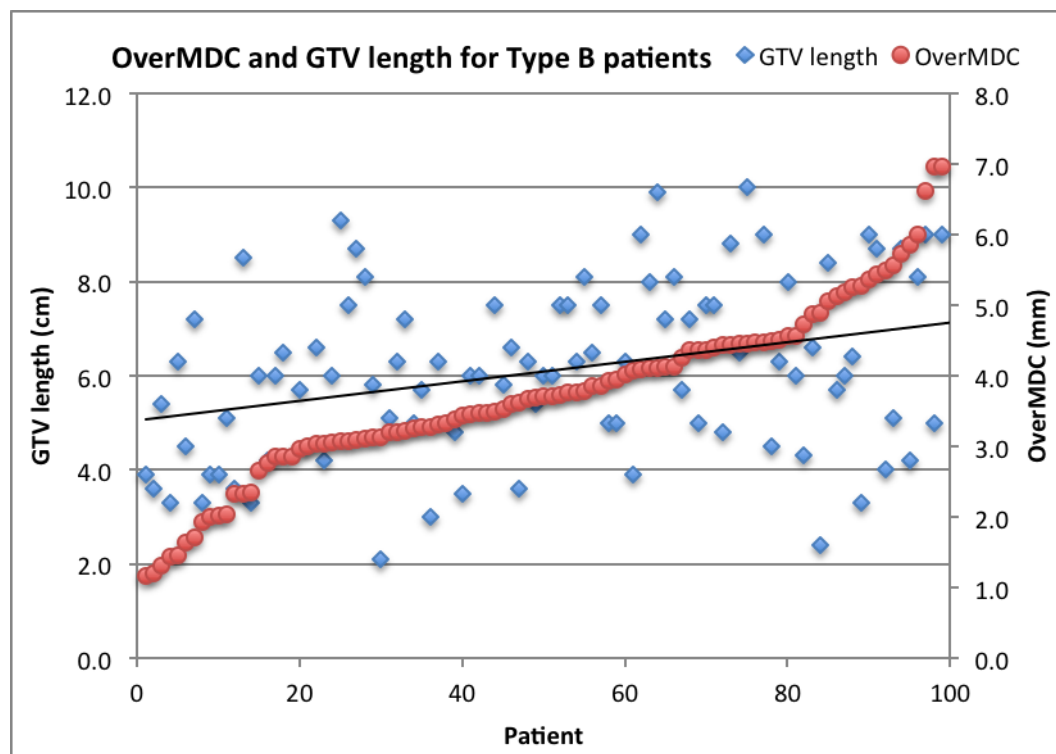


Figure 3.13 – OverMDC and GTV length for patients

Figure 3.13 shows the GTV length for each patient plotted with OverMDC values, ranked by increasing OverMDC value, with the line of best fit for the GTV lengths. There was no significant difference in GTV length either side of the OverMDC breakpoint of 4.4mm (Mann-Whitney $p=0.123$). The Pearson coefficient between the OverMDC metric and GTV length was calculated to be 0.33.

PTV volume and OverMDC

Figure 3.14 shows a similar plot only with PTV volume for each patient plotted with OverMDC values, again ranked by increasing OverMDC value with the line of best fit for the PTV volumes. Here there was a significant difference in PTV volume either

side of the OverMDC breakpoint of 4.4mm (Mann-Whitney $p < 0.001$). The Pearson coefficient between the OverMDC metric and PTV volume was calculated to be 0.47.

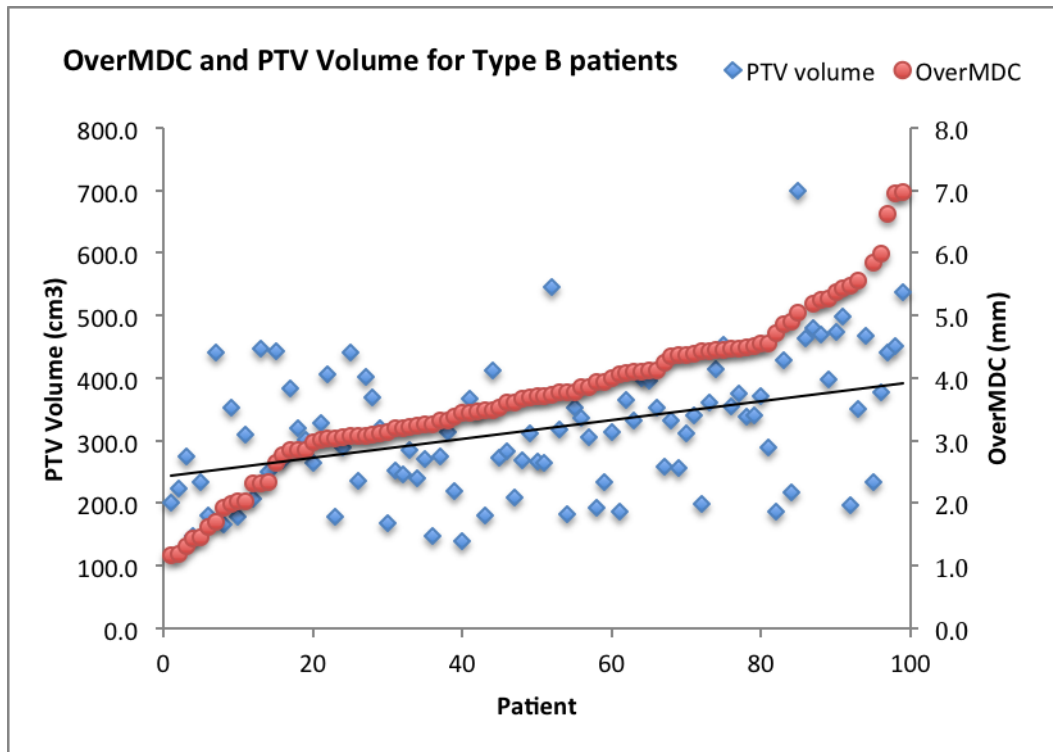


Figure 3.14 – OverMDC and PTV volume for patients

3.5.2 Technological factors

IMRT/VMAT dose delivery

Patients were classified according to whether the dose was delivered via 3D conformal (81 patients) or IMRT/VMAT treatment (16 patients).

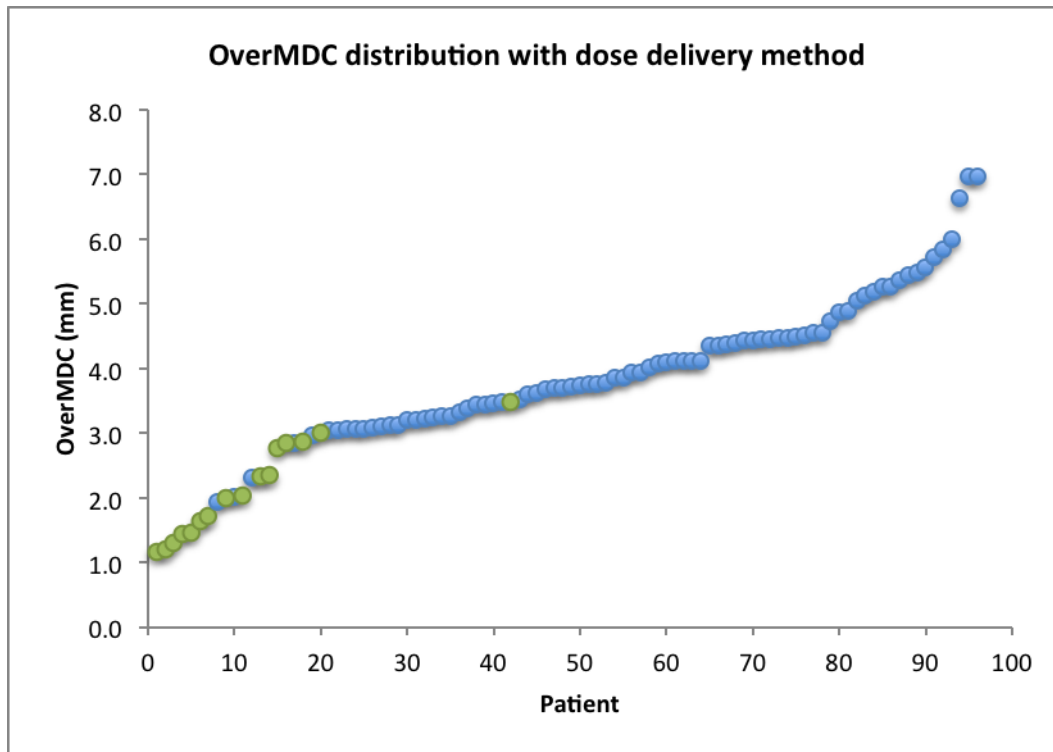


Figure 3.15 – OverMDC and dose delivery method for patients

Figure 3.15 illustrates that IMRT/VMAT (green markers) is associated with a lower OverMDC value than if the patient was treated with 3D-CRT (blue markers) (mean VMAT = 2.1mm, 3D-CRT = 4.1mm; Mann Whitney $p < 0.001$). To eliminate any unintended bias, it was found that there was no significant difference in PTV volume according to the treatment delivery method (Mann Whitney $p = 0.455$). The 16 patients whose dose was delivered using IMRT/VMAT were treated at 3 centres, with 14 at 1 centre and 1 each at the remaining 2 centres.

3.6 Re-Planning of Type B patients in OMP

It has been shown in the previous section that patients treated with IMRT/VMAT type treatments have significantly more conformal dose distributions. However, in order to truly understand the effect of the treatment delivery method on the

conformity of the dose it was decided to re-plan patients who had originally been treated with 3D-CRT using the VMAT method. By having the same target volumes planned using two treatment methods, rather than comparing different treatment methods in different patients, it allows a direct comparison to be made. In addition, this work would allow an assessment to be made of whether the patients with relatively high OverMDC values could be improved by re-planning with VMAT.

3.6.1 Obtaining a VMAT solution in OMP

Patients who receive radiotherapy for oesophageal tumours in Velindre Cancer Centre are currently treated using the 3D-CRT technique. Creating VMAT plans for these patients would therefore require careful consideration and implementation of a new technique in this site. After consultation with the clinical department, it was decided that working towards a planning technique that could be used on all patients, rather than starting afresh with each patient, would be extremely beneficial both for this project and the clinical department. Therefore this work both allowed analysis of my thesis dataset and facilitated development of an advanced clinical service.

3.6.2 Class solutions in Radiotherapy planning

Conventional planning, although successful in obtaining clinically acceptable plans (92), can be a very time consuming process. This is a result of the treatment planner having to obtain a set of unknown relative weighting factors for each individual plan in an iterative manner. Although many manual iterations can be undertaken in designing a plan, time constraints and other factors may still result in a sub-optimal

plan (93) & (94). In addition, a set of factors found to work for one patient may not necessarily work for another. A solution to this problem lies in finding a class solution, where a set of dose weighting factors provides a clinically acceptable plan for the vast majority of patients. If a successful solution is found, the time taken during the planning process is therefore greatly reduced. The user can simply construct the required structures before applying a plan model saved in the database with the associated weighting factors, thereby creating a plan that meets the required dose constraints and objectives and can be safely delivered to the patient. The use of class solutions in a clinical setting has become increasingly prevalent with the implementation of inverse planning, and as a result, IMRT/VMAT dose delivery methods. There is a large amount of literature in which the term 'class solution' is used to describe a method of automating plan generation. Due to the number of different techniques and application of these methods there is also no standard definition of a class solution as applied to radiotherapy planning.

3.6.3 What makes a good treatment plan?

A class solution generated plan that meets all the dose constraint criteria may not necessarily be the best plan for that patient. However, meetings with clinical colleagues made it clear that when approving oesophageal radiotherapy plans for treatment, meeting the dose constraints is the primary criteria for going ahead with treatment. When these are met there is generally not a large amount of time and effort given to improving the plan further. This does not mean that meeting the dose constraints required by plans is easy however, and in some cases this is impossible or may take an unacceptable amount of time to achieve. In these instances, it is up to

the oncologist to decide whether the trade off between dose received by normal tissue compared to the treatment volume is clinically acceptable and can be delivered safely. Although minimising the dose received by every organ at risk whilst maximising the dose received in the treatment volume in each patient is the ideal solution, there will be small trade-offs to be made in most cases. The dose distribution delivered to an organ is unlikely to be uniform; being able to consider trade offs between organs is therefore dependent on being able to describe the dose delivered to each organ. Ideally parameters such as TCP and NTCP (See Section 4.1) would be ideally used to compare one plan to the next as they would model the effect of the dose delivered to the patient to a biological outcome. However the parameters more often used to describe the dose delivered to an organ and make a comparison of plans include mean dose, maximum dose, or the fraction of volume of a structure that receives more or less than a certain specified dose levels. It is managing the trade off between these parameters that will decide what plan is considered better than another. In most treatment planning there will be multiple structures to consider further increasing the time taken to plan each patient using conventional planning techniques.

3.6.4 VMAT optimising volumes

VMAT plans often require the creation of optimising or 'dummy' volumes (95). These are usually simple volumes that are included in a plan in addition to the usual GTV/PTV and OARs to assist the treatment planning system in creating a suitable plan by directing or limiting the dose to specific area. For example, by creating a dummy volume with a particular dose constraint, the TPS will attempt to limit the

dose received by that particular volume. The two additional structures created for the VMAT plan were:

1. DM_PTV – This is simply the original PTV from the 3D-CRT plan grown by 1mm in all directions. This structure is created in order to ensure that the conformity of the 95% isodose to the original PTV grown from the GTV is optimised.
2. DM_Conf_15mm – This is a ring like structure created to achieve the required dose fall off from the planning PTV.

3.6.5 Multicriteria Optimization and creating a Pareto curve

One method for the creation of a class solution is that of Multicriteria Optimisation (MCO) (96). Here each structure is assigned one or several objectives and the end goal is to find a solution that is the best trade off between these objectives. A solution that reaches this end goal is commonly defined as being Pareto optimal. A Pareto optimal solution will therefore be one where no single objective can be improved without deteriorating at least one of the others. The set of solutions that together define the Pareto optimal plan is called the Pareto set. Plotting the image of the Pareto set in objective space gives a 4D Pareto surface, whilst slicing through this surface to focus on two objectives gives a 2D Pareto curve. By analysing the 2D curve it allows the trade-off in coverage between two objectives to be visualised.

When considering the planning of oesophageal cancer treatments, the organs at risk constraints that are most difficult to meet are the lungs and heart. (See Table 3.1 for dose constraints).

Region of interest/Organ at risk	Dose constraint
PTV	V95% (47.5Gy) >99.0%
Heart	V80% (V40Gy) < 30Gy
Combined Lungs	V40% (V20Gy) < 25%

Table 3.1 – Dose constraints for VMAT planning

I therefore wanted to understand the relationship between these two structures when changing the weight of the objective given to achieving a dose constraint on one or the other. It was also important to understand what affect, if any, that changing the relative weighting on achieving dose constraints of these two structures may have on the coverage of the PTV.

The weighting of the Cord, PTV, DM_PTV and DM_Conf_15mm structures were set in the Plan Optimisation Module of OMP as seen in Table 3.2.

Structure	Objective and weight
External (OAR)	Max dose 60.00Gy, weight 1.0
Heart (OAR)	Max average dose 18.00Gy, weight 10.0
Cord PRV (OAR)	Max dose 38.00Gy, weight 1000.0
Combined Lungs (OAR)	Max average dose 11.00Gy, weight 10.0
PTV_RC (Target)	Min dose 47.50Gy, weight 30.0
	Max dose 50.0Gy, weight 300.0
	Min dose 50.0Gy, to 50.0% volume, weight 50.0
DM_PTV_RC (Target)	Min dose 48.50Gy, weight 600.0
	Max dose 50.0Gy, weight 300.0
DM_Conf_15mm (OAR)	Surr dose 50.00 - 47.50Gy, dist 0.5cm, weight 1000.0

Table 3.2 – Objectives and weighting of structures in VMAT plan

From previous work, we know that the dose constraint for the heart is relatively easy to achieve using VMAT (82). Therefore in order to find the optimum lung weighting I set the heart weight to 0 and ran the optimising process with the lung weighting increasing from 5 – 20, in increments of 5.

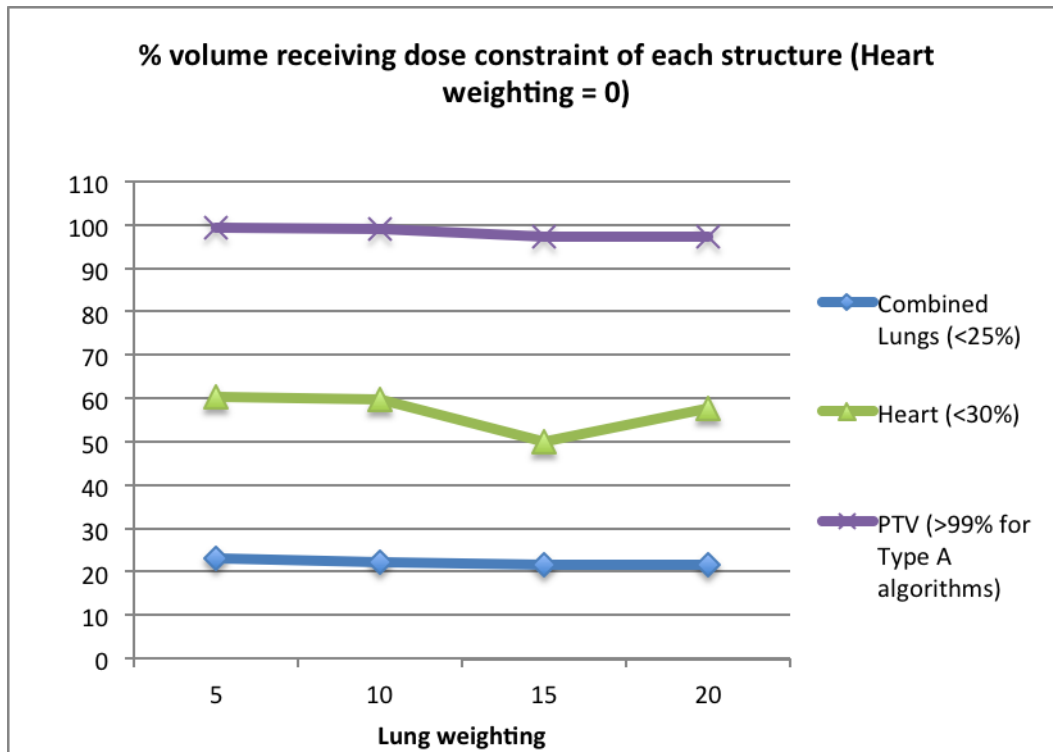


Figure 3.16 - % volume receiving dose constraint of each structure

It can be seen from Figure 3.16 that the lung weighting of 15 gives a favourable (i.e. minimises) dose to the heart. This lung weighting value was therefore initially taken forward to explore the influence of changing the heart weighting on mean heart dose and mean lung dose.

To analyse this aspect of plan weighting and its effect on the dose received by the heart and lung, I created 5 plans with a lung weighting of 15 and heart weightings of 0.5, 5, 10, 15 and 20. The mean heart dose and mean lung dose for each plan created was recorded and is plotted in Figure 3.17

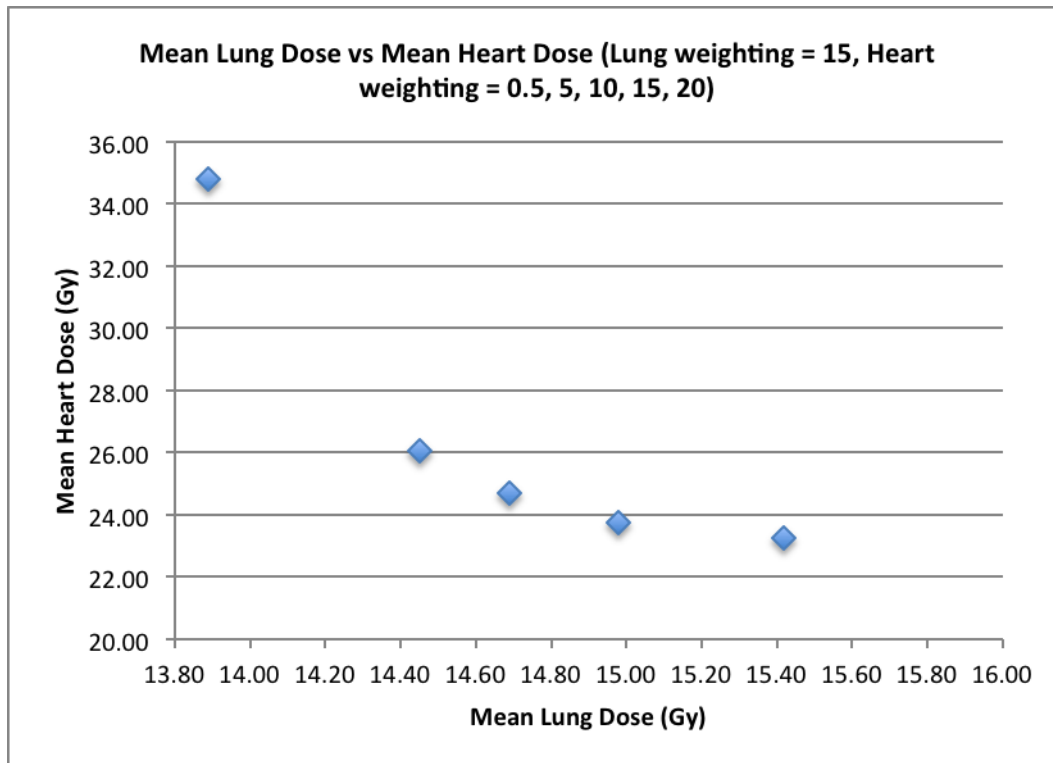


Figure 3.17 – Mean Lung Dose vs Mean Heart Dose

Figure 3.17 shows how an increasing weight on the heart, whilst reducing the mean heart dose also results in an increase in mean lung dose. It can be seen how a pareto curve is being generated, meaning that the plan is pareto optimal.

The effect of changing the weighting on the heart can also be observed in the dose distribution representation images of the plan itself. Figures 3.18 a-e show how as the weighting on the heart increases the dose deposited in the heart decreases. However the dose must be deposited somewhere and this can be observed by the spilling of the dose into the lung tissue as the weighting on the heart increases.

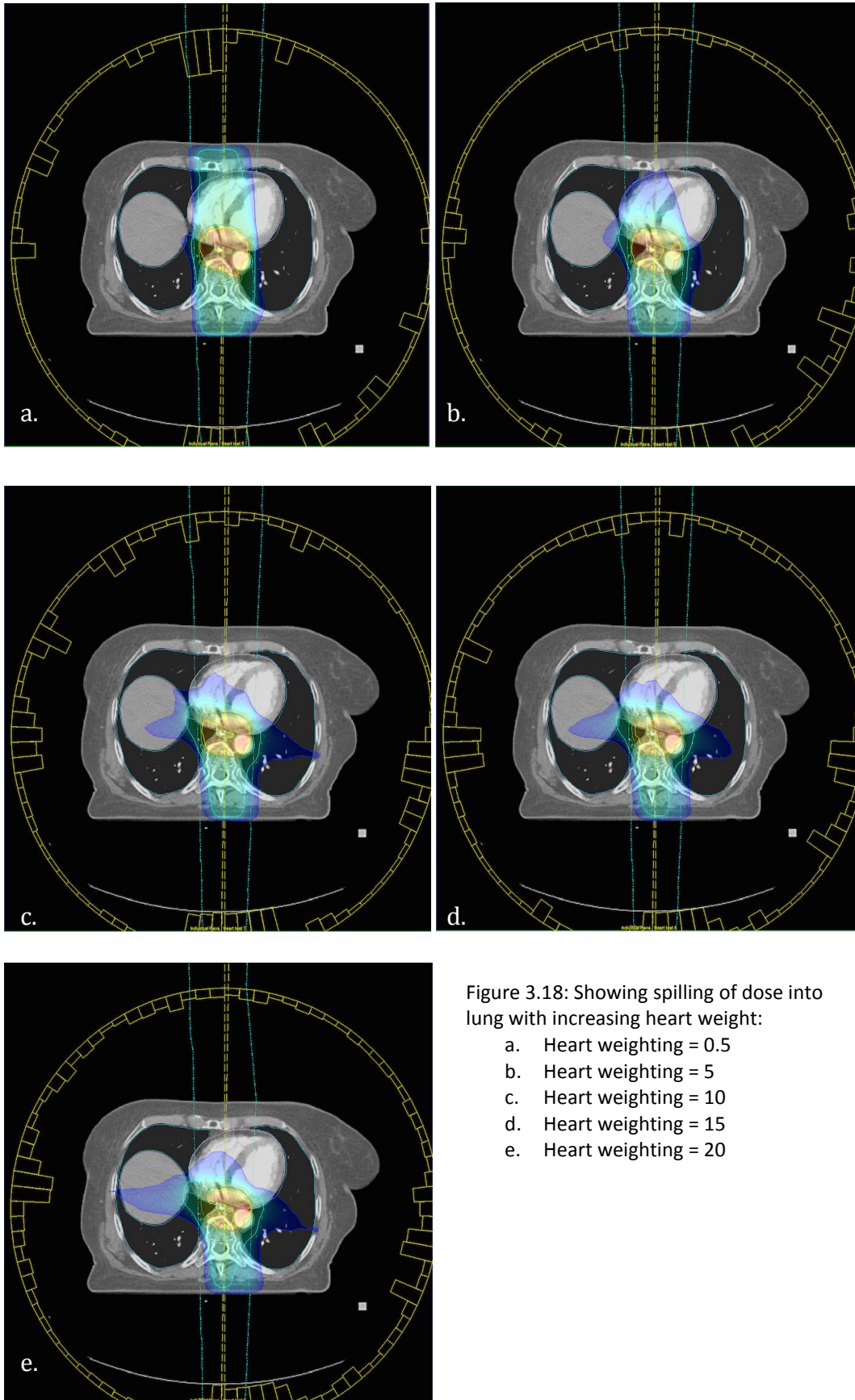


Figure 3.18: Showing spilling of dose into lung with increasing heart weight:

- a. Heart weighting = 0.5
- b. Heart weighting = 5
- c. Heart weighting = 10
- d. Heart weighting = 15
- e. Heart weighting = 20

I then repeated this process with a lung weighting of 10. The mean doses of the heart and lung were again recorded and can be seen in Figure 3.19

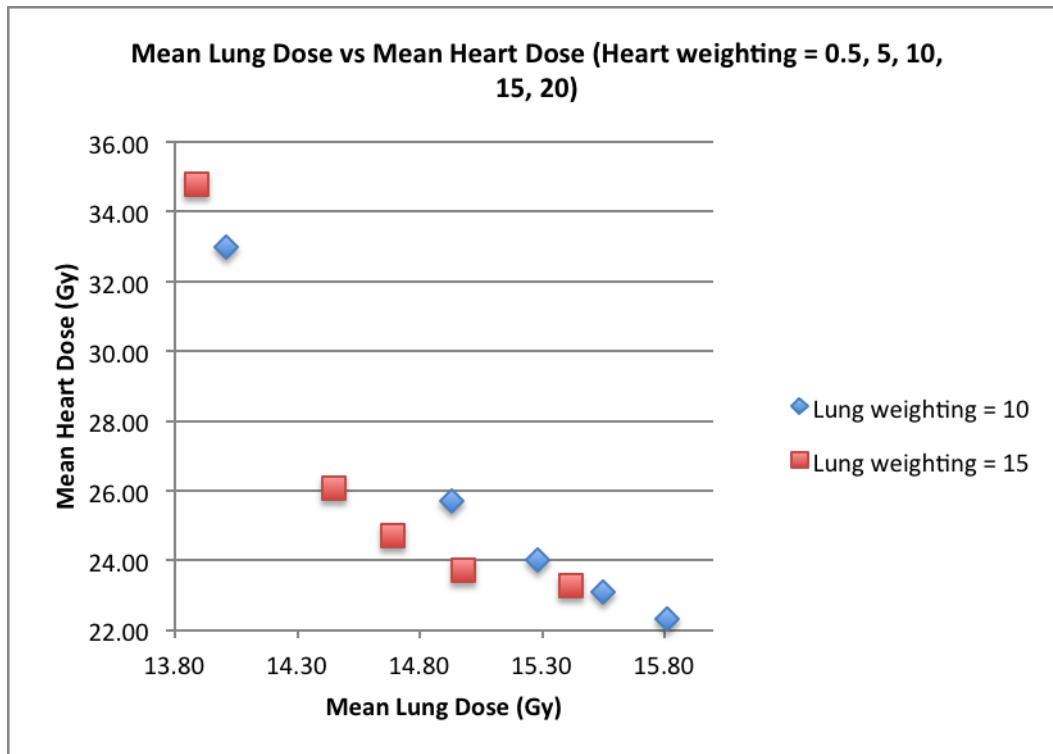


Figure 3.19 –Mean Lung Dose vs Mean Heart Dose for patient 1

Figure 3.20 shows how a reduced lung weighting of 10 results in an increased lung dose when compared to the same plan with a lung weighting of 15.

Repeating with a different patient

It was important to assess whether the weightings used on the OARs would produce a similar plan on another patient. I therefore repeated the previous steps of producing 10 plans with different combinations of weighing on the lung and heart organs. The plot of mean heart dose and mean lung dose can be seen in Figure 3.20.

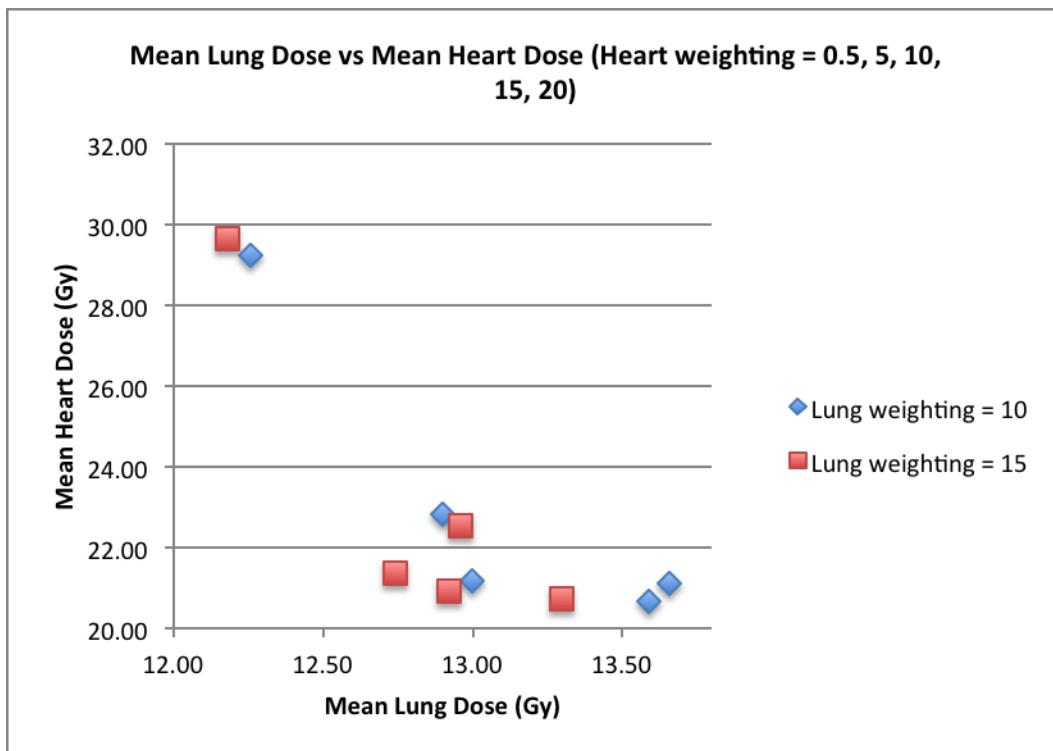


Figure 3.20 – Mean Lung Dose vs Mean Heart Dose for patient 2

The figure shows that in this instance, the curve of mean heart dose vs mean lung dose is not pareto optimal when compared to that in figure 3.19. The weightings are therefore not optimal for this patient.

Patient dependent vs patient independent solution

Although the weightings chosen for the first patient were shown to produce a pareto optimal curve in terms of heart and lung they were not replicated with the second patient. Therefore the solution found for the first patient is not patient independent, meaning that it will not produce a pareto optimal plan for each different patient.

3.6.6 Re-planning worst performing OverMDC patients

The 16 worst performing patient plans according to OverMDC (plotted with square symbols in Figure 3.21) were re-planned from the 3D-CRT to VMAT in OMP using the solution. 11 patients were successfully re-planned using the class solution meeting all dose constraints. The 5 remaining patient plans did not meet the SCOPE 1 protocol dose volumes constraints for the PTV initially, but in all cases acceptable plans were achieved after manual adjustment of the weighting on the PTV objectives.

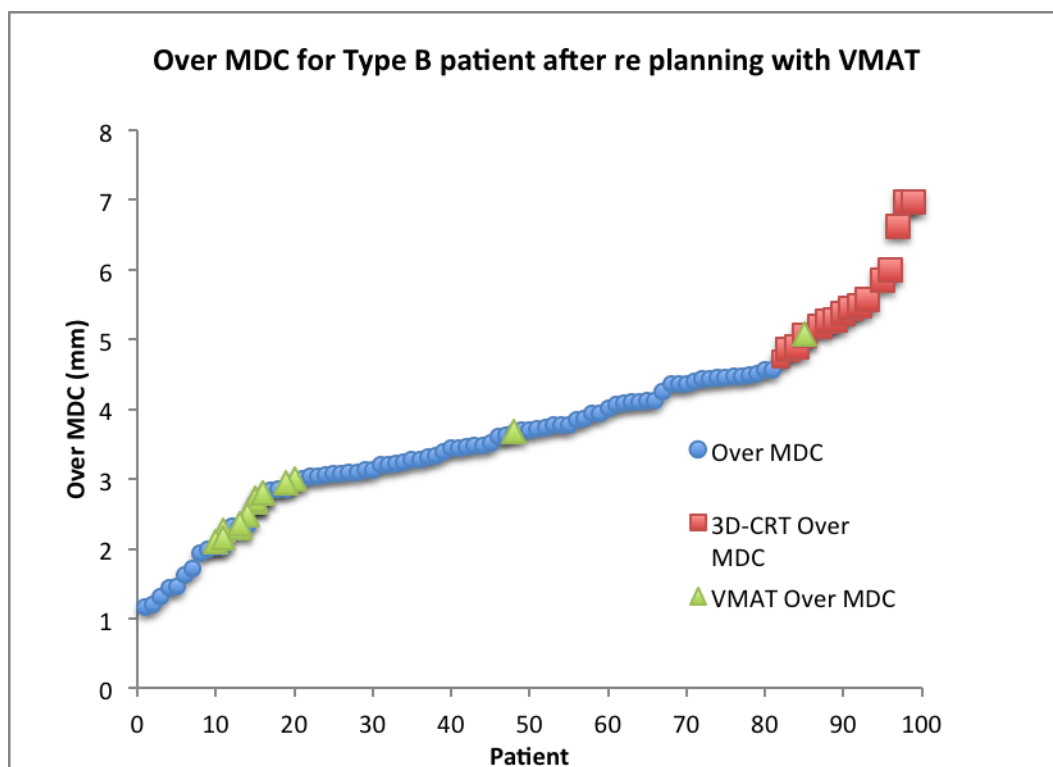


Figure 3.21 – Effect of re-planning from 3D-CRT to VMAT on OverMDC

Table 3.3 gives the OverMDC values before and after re-planning with the VMAT class solution.

Patient ID	3D-CRT OverMDC (mm)	VMAT OverMDC (mm)
101003	4.7	2.7
001023	4.9	2.7
064002	4.9	2.8
007003	5.1	2.3
102009	5.2	2.7
102003	5.3	2.1
007002	5.3	2.7
028003	5.4	2.8
177004	5.4	3.7
069009	5.5	2.3
177003	5.6	2.5
007001	5.8	2.3
002004	6.0	2.2
177005	6.6	5.1
139003	7.0	3.0
028001	7.0	2.9

Table 3.3 – OverMDC after re-planning with VMAT class solution

The OverMDC was reduced for all 16 patients after replanning with VMAT (Figure 3.21 and Table 3.3), with a mean reduction of 2.8mm (Range: 1.6-4.0mm). This confirms that the treatment modality has a large influence on OverMDC value. However there are also two outliers where the OverMDC was not reduced to the same extent. It is known from Figure 3.14 that there is a dependency on OverMDC value on PTV volume and on further review it was found that these two patients had an above average PTV volume (441cm^3 and 498cm^3) when compared to the SCOPE 1 database mean PTV volume (334cm^3). The average PTV volume for the re-planned patients was 393cm^3 .

3.7 Multivariate analysis

OverMDC and UnderMDC were included in a multivariate logistic regression analysis along with other clinical factors. They were, age, sex, tumour type, tumour stage, tumour site, cetuximab administration, PTV volume and disease length.

Variable	Regression Coefficient	Standard Deviation	P-value
Age	0.0686	0.0362	0.0582
Sex	-0.8128	0.5777	0.1594
Tumour Type	0.6688	0.6972	0.3374
Tumour Stage	0.8288	0.4676	0.0763
Tumour Site	-0.1972	0.4755	0.6784
UnderMDC	-0.5292	2.6432	0.8413
OverMDC	1.3680	2.3520	0.5608
Cetuximab	0.5757	0.5263	0.2740
PTV Volume	-0.0009	0.0035	0.7887
Disease Length	-0.0351	0.1641	0.8309

Table 3.4 – Results of multivariate analysis

It was found that none of these factors were statistically significant (Table 3.4). The factors with the lowest p-values were found to be age and tumour staging ($p=0.06$ and $p=0.08$ respectively).

3.8 Discussion

The aim in this piece of work was firstly to quantify plan quality using a CI and its effect on patient outcome. Secondly, to identify whether clinical and technological factors including PTV volume and treatment delivery method could be related to the CI value.

It was found that OverMDC has a statistically significant relationship with overall survival in univariate analysis independent of cetuximab administration, the latter having been shown to adversely effect survival in the SCOPE 1 trial. It was also shown that PTV volume was weakly correlated with the OverMDC value of each patient (Pearson's correlation = 0.47), but the treatment delivery method had a more significant impact with the mean IMRT OverMDC being 51% of the mean 3D-CRT OverMDC value. When OverMDC and UnderMDC were included with other clinical variables in a multivariate logistic regression analysis neither remained significant.

The volume of the PTV may have an influence on dose coverage. Meeting constraints for larger PTVs is more difficult due to the likely increased overlap with organs at risk (OAR). Specifically in the case of oesophageal cancer, OARs such as the heart, lungs and spinal cord are in close proximity to the oesophagus and may limit the ability to optimise the dose distribution. In this study we hypothesized that a larger PTV volume would be associated with an increase in OverMDC and UnderMDC values due to the increased complexity of the resulting RT plan and ability to conform the dose to the PTV due to the need to spare adjacent OARs. Statistical tests showed that there was indeed a significant difference in the PTV volumes of patients either side of the OverMDC break point. No significant difference was found in the case of the UnderMDC metric.

This study also confirmed that using IMRT and VMAT increase dose conformity when compared to 3D-conformal therapy, as shown elsewhere in the literature (97). This is

demonstrated by the significantly smaller OverMDC values between the $V_{95\%}$ and PTV volumes in the IMRT/VMAT patients of the SCOPE 1 trial and furthermore by the re-planning of the worst performing patient plans by OverMDC value from 3D-conformal to VMAT. A study in gastric cancers found similar results when comparing 3D-conformal radiotherapy to IMRT (98), concluding that a better target coverage and therefore significant dose reduction to OARs could be achieved in IMRT plans. It is clear therefore that the more conformal dose delivery techniques should be used to administer RT wherever possible.

The explanation for the improved overall survival in patients treated with a lower OverMDC value and therefore more conformal treatment is not clear. The association with IMRT/VMAT treatment is interesting as only 3 centres treated the 16 patients with IMRT/VMAT in the original trial. In addition Figure 3.21 clearly shows two cases where re-planning with VMAT/IMRT did not reduce the OverMDC value to the same extent, but their PTV volume was higher than the average for the patients included in this study. It is possible that low OverMDC and/or access to IMRT/VMAT reflect other aspects of a high quality RT process that require further investigation in a future study. It is also fully acknowledged that when the OverMDC metric is included in a multivariate analysis it does not remain statistically significant.

Nevertheless, this work suggests that IMRT/VMAT offers a potential tool for safe dose escalation, as the MDC analysis has shown that unnecessary irradiation of normal tissue can be significantly reduced without affecting PTV coverage. This is consistent with the findings of Freilich et al (99) who concluded that although the

use of IMRT did not impact on survival, it was associated with significantly less toxicity, and Warren et al who have shown that IMRT allows dose escalation to 60Gy with the same level of normal tissue irradiation as 3D-CRT to 50Gy (82). This is being taken forward in the recently funded SCOPE 2 trial. Unfortunately there were an insufficient number of patients treated with IMRT/VMAT in this study to detect any impact on survival. In addition, patients treated with IMRT/VMAT may have been expected to have a lower rate of toxicity, however the rates were so low within the SCOPE 1 trial that this could not be studied.

In a clinical setting, this work suggests that careful attention to the quality of RT planning, expressed in terms of conformity of the dose distribution to the target volume, may impact on overall survival. IMRT/VMAT should be considered for all patients when conforming the 95% isodose to the PTV is difficult.

3.9 Conclusion

I have shown using the MDC index that in univariate analysis the quality of a plan with respect to PTV coverage has a significant correlation with patient outcome in terms of overall survival, thereby meeting an initial aim of the project as set out in Section 1.9. It has also been shown that plan quality is also strongly related to the use of advanced radiotherapy delivery techniques, allowing the possibility of dose escalation to the tumour whilst minimising dose to OARs. This is explored further in Chapter 4.

Chapter 4

The effect of dose escalation on gastric toxicity.

4.1 Introduction

The end point of true clinical interest in radiotherapy is controlling the tumour (100). We therefore want to convert a dose distribution in the tumour to a quantifiable value of tumour control. Radiobiological modelling is a method of approximating the clinical outcome of radiotherapy treatment in terms of TCP and NTCP. The modelling of TCP and NTCP will therefore be used in this chapter to study the potential of VMAT dose delivery to safely dose escalate lower oesophageal tumours with a focus on gastric toxicity.

4.1.1 Tumour control probability

The TCP is the probability of killing all tumour cells in the defined tumour volume following irradiation with a certain dose distribution. Using data in the form of survival fraction curves (which carry information of the proportion of cells that survive a specified dose of radiation), as a probability model for radiation-induced individual clonogenic cell death, the TCP computes the probability of tumour eradication by taking into account factors such as cell proliferation between radiation treatment fractions, and natural cell death rates (101).

Several models have been developed to study TCP (See Zaider and Hanin et al for a review (102)). However modelling TCP can be split into four main methods:

1. Binomial statistics: This is the simplest model and does not take into account cell proliferation between fractions or stochastic effects. Success is simply defined as cell death, and the TCP is defined as the probability that there are n_0 successes where n_0 is the total clonogenic cell population.
2. Poisson statistics: The model also takes into account the stochastic process of radiation-induced cell killing. Here, deterministic differential equations are used that account for cell death both naturally and due to radiation. TCP is then given by a poisson distribution with a mean is the solution of the differential equations.
3. Zaider-Minerbo model: This model also describes the stochastic effects of cell birth and death but with greater accuracy. A master equation that takes into account these effects is transformed into a partial differential equation that in turn can be solved to give a value for TCP.
4. Monte-Carlo model: As with all Monte-Carlo methods, this method is capable of simulating a very large number of cells. To date, Monte-Carlo methods are the most accurate methods of modelling but require specialist software packages and computing hardware.

The method most commonly used for quantitative predictions of dose/fractionation dependencies is the linear-quadratic (LQ) formalism (103) that utilises poisson statistics. Here the number of surviving cells following radiation is given by

$$S(D) = e^{-(\alpha D + \beta D^2)} \quad (4.0)$$

Where S is the number of surviving cells following a dose of D, and α and β describe the linear and quadratic parts of the survival curve respectively. The α and β constants vary between different tissues and tumours. A useful and widely used term is the α/β ratio, which describes the dose in Gy when the number of cells killed by the linear component is equal to the cell kill from the quadratic component.

For the calculation of TCP from DVH data, the tumour volume is considered to be constructed from independent sub-volumes. If each sub-volume (denoted by i in formula 4.1) is considered small enough to receive a uniform dose then the TCP for the tumour is the product of the TCP values calculated in each of the sub-volumes, given by TCP_i .

$$TCP = \prod_{i=1}^m TCP_i \quad (4.1)$$

4.1.2 Normal tissue complication probability

The NTCP can be defined as the probability that otherwise normal tissue (i.e. non cancerous) will develop adverse late effects as a result of being irradiated. In the past, knowledge of the tolerance of normal tissue to irradiation was severely lacking. However the seminal Emami paper (104) and consequent Quantitative Analyses of Normal Tissue Effects in the Clinic (QUANTEC) (105) working group report have since vastly improved the knowledge base within this area, to the extent that NTCP

modelling is now a recognised and well regarded method of approximating the expected normal tissue toxicity resulting from irradiation. Initially, Burman et al (106) fitted a Lyman model (107) to the Emami data, allowing the ability to use Emami's constraints for an arbitrary fraction of a whole organ uniformly irradiated. Kutcher et al (108) then expanded on this work to allow the analysis of NTCP via DVH data. This Lyman-Kutcher-Burman model is now the most widely used method of estimating NTCP.

The specific symptom that results from the exposure to radiation is known as a clinical endpoint. The endpoints can be grouped into two categories; those that are binary and relate to functional changes (paralysis or death) and those that are scalar, describe physiological changes and are usually graded by increasing severity.

4.1.3 Clinical derivation and use of TCP and NTCP

Most of the models that have been developed to describe the dose response of different normal tissues and tumours have the following common features:

- Cell survival after irradiation is binomial and obeys binomial or Poisson statistics
- Response of an organ is determined by the death or survival of its target cells
- All the target cells respond identically
- Equal effects are obtained from equal dose fractions if sufficiently separated in time

The modelling of both TCP and NTCP requires reliable data from specific clinical studies. As the setting up of a suitable study for the sole benefit of producing reliable TCP and NTCP data is unlikely to be justified, most data used in the generation of models is gathered from retrospective analysis of suitable cohort studies and clinical trials. In order to accurately model TCP and NTCP, there must be detailed information on the radiation exposure and treatment outcome available for assessment. However, radiobiological modelling is a complicated process even with the use of accurate data. In general, the information available only covers a small part of the dose-response curve required for the model as the treatment administered during radiotherapy is usually at a very specific dose. As a result, the part of the dose-response outside the region of the clinical data is based on the model only and can be difficult to verify. However radiobiological modelling is an established field with a large body of published work. Indeed there is an increasing call for radiobiological modelling to be utilised in the routine treatment planning process (109) & (47).

4.2 The need for dose escalation

The incidence of lower third oesophagus tumours are increasing in most Western populations (110) and it is becoming increasingly clear that chemo-radiotherapy (CRT) is now a valid alternative to surgical resection in the treatment of gastroesophageal junction (GEJ) cancer (111). However, local in-field recurrence is still the main reason of treatment failure (112) following definitive CRT, with >75% of these occurring within the GTV when the standard radiation dose of $\approx 50\text{Gy}$ is

delivered. Indeed, local recurrence also contributes towards a worse prognosis in GEJ carcinoma (111).

In theory, a higher radiation dose delivered to the tumour should result in higher local control rate. However it is only with the recent technological advances in RT planning and delivery that the ability to deliver increased dose to the tumour whilst minimising dose to normal, healthy tissue and OARs is becoming possible (113). Increased TCP should therefore be achievable by increasing the standard dose prescription beyond $\approx 50\text{Gy}$. A retrospective study by Zhang et al (114) found that there was significantly higher overall survival in their patient cohort if the patient was treated in a high dose group ($>51\text{Gy}$) compared to the low dose group ($<51\text{Gy}$), whilst Geh et al found there was a dose-response relationship between increasing prescribed radiotherapy dose and pathological complete response in the neoadjuvant setting(115). Bedford et al (116) also found via radiobiological modelling that conformal techniques offered the potential of a 5-10Gy increase in dose delivered to the GTV up to 60Gy with acceptable increases in toxicity.

The organs most at risk when planning oesophageal radiotherapy treatment, and for which the most stringent dose constraints are usually applied are the heart, lungs and spinal cord. Oesophageal cancer cases are therefore planned according to a combination of the achievable dose coverage of the PTV and the meeting of dose constraints for these organs. Work I undertook in collaboration with Oxford University in preparation for the forthcoming SCOPE 2 trial (82) has shown that dose escalation to 62.5Gy in mid oesophageal patients is feasible, with the additional dose able to be delivered without exceeding the OAR dose constraints in 75% of patients. However, dose escalation has not yet been studied in lower oesophageal cancers,

when the added proximity of the relatively radiosensitive stomach provides an added planning challenge (117). With the role of radiotherapy dose escalation identified as a research priority (118) for improving outcomes and the likely increase in individualised RT dose prescription in the future, it is important to quantify the increased risk that this may pose in sites such as the lower oesophagus where clinical evidence for dose-toxicity correlation for adjacent organs (such as stomach) is lacking. This planning study therefore aims to investigate the feasibility of lower oesophageal dose escalation with a focus on toxicity to the stomach.

4.3 Modelling the impact of dose escalation

4.3.1 Study dataset

Ten patients with tumours in the lower third region (centre of tumour at 32-40cm from back of teeth measured via Endoscopic ultrasound (EUS)) were selected at random from both arms of the SCOPE 1 database and their classification in the documentation as lower third tumours confirmed visually. The subset had a range of planning target volumes (PTV1) from 219 to 484cm³ and a mean volume of 348cm³, similar to that of the entire SCOPE 1 cohort (mean 327cm³). These 10 patients were therefore judged to give a good representation of the whole patient cohort. The GTVs and OARs outlined as per the SCOPE 1 protocol were re-used.

Number of patients	Reasoning
10	<p data-bbox="632 280 1241 353">Lower oesophageal patients with PTV volumes representative of SCOPE 1 cohort</p> <p data-bbox="858 398 1011 427">Centres = 7</p> <p data-bbox="679 436 1193 472">Age in years (Mean = 72, Range: 61-81)</p> <p data-bbox="770 477 1102 512">Male (n=4), Female (n=6)</p> <p data-bbox="735 517 1137 553">Cetuximab (Yes(n=4), No(n=6))</p> <p data-bbox="799 557 1074 593">Adenocarcinoma (n=2)</p> <p data-bbox="740 598 1133 633">Squamous Cell Carcinoma (n=8)</p> <p data-bbox="783 638 1090 674">Tumour Stage III (n=10)</p>

Table 4.0 – Number of patients included in analysis in Chapter 4

4.3.2 Treatment planning

PTV1 was grown by adding 1cm isotropically to the CTV, itself grown by adding 1cm radially and 2cm superiorly and inferiorly (along axis of oesophagus) to the GTV and may include the stomach mucosa at the inferior limit. For the purpose of this specific study and the use of the simultaneous integrated boost (SIB) technique for dose escalation, additional structures were also created. A PTV2 (boost volume) was created for the dose escalated plans by adding an isotropic 0.5cm margin to the GTV, supported by a study by Hawkins et al (119) and reflecting the technique in the SCOPE 2 trial where margins will not be adjusted dependent on tumour position (82). The protocol did not address stomach filling or any dose constraints for that organ specifically; there were no constraints or protocol concerning the filling state of the stomach in the SCOPE 1 trial and therefore for the patients in this study. The stomach was contoured as (a) whole organ and (b) stomach wall. The stomach wall volume was generated by creating a ring like structure encompassing the outer 5mm of the whole stomach outline. This has been shown to provide a satisfactory approximation of stomach wall thickness (120) & (121). In addition, the stomach and

stomach wall structures were divided into the volume that was within PTV1 (Stomach-In and StomachWall-In) and outside PTV1 (Stomach-Out and StomachWall-Out) (See Figure 4.1).

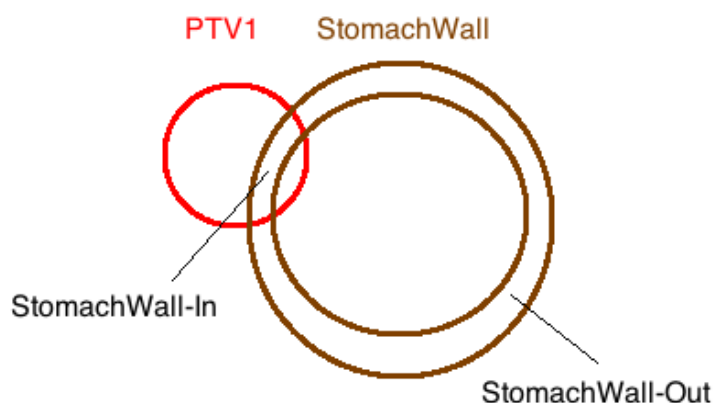


Figure 4.1 – Schematic of StomachWall-In and StomachWall-Out volumes

Specific dose constraints were given for each for the SIB plans (Table 4.0) based on the recommendations of the QUANTEC paper for dose volume effects in the stomach and small bowel (122). An SIB dose of 60Gy in 25 fractions was considered to be clinically meaningful and is being taken forward within an on going prospective dose escalation trial (SCOPE 2).

All treatment planning was undertaken in Eclipse (Version 10). The original 3D conformal plans were imported in DICOM format and the doses recalculated using the AAA algorithm with a 2.5mm grid. RapidArc (RA) plans were generated using 2 arcs of 360⁰, clockwise and counter-clockwise with a collimator rotation of 10⁰. The 50Gy 3D conformal plans (50Gy_{3D}) were then compared to 50Gy RapidArc plans (50Gy_{RA}) and to plans with an additional simultaneously integrated boost of 60Gy to PTV2 (60Gy_{RA}) (See Figure 4.2).

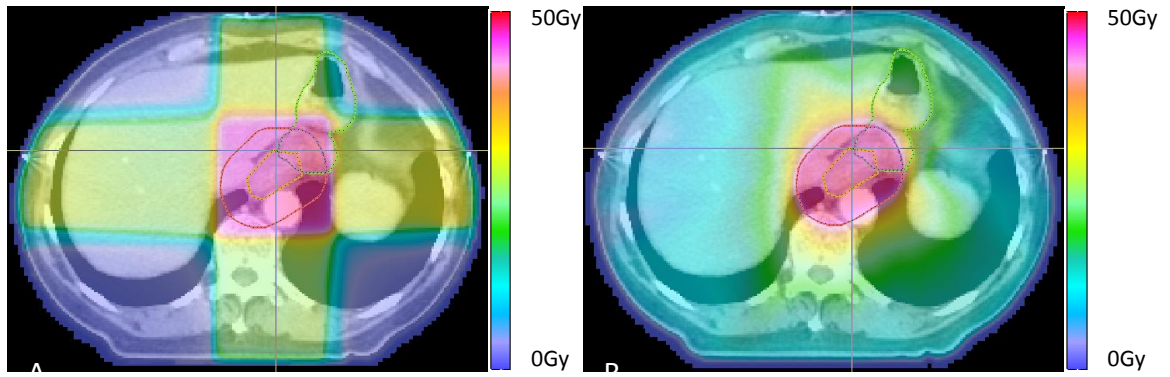


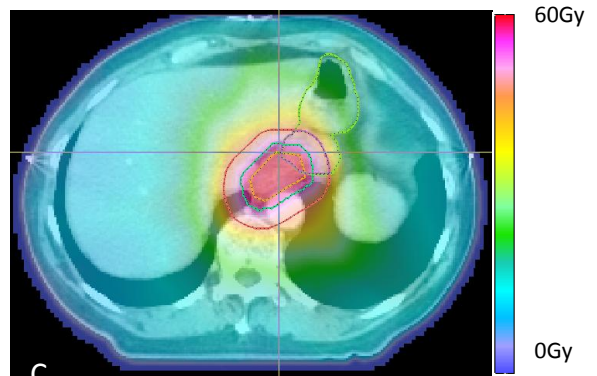
Figure 4.2

A: 50Gy_{3D} plan with GTV, PTV and stomach outline

B: 50Gy_{RA} plan with GTV, PTV and stomach outline

C: 60Gy_{RA} plan with GTV, PTV2, PTV and stomach outline

Outlines: GTV – dashed orange
 PTV – dashed red
 PTV2 – dashed blue



Dose constraints for all the structures are listed in Table 4.1.

Dose-volume constraints	
PTV1 (50 Gy)	V _{95%} (47.5 Gy) > 95% D _{max} (0.1cc) < 107% (53.5 Gy)
PTV2 (60 Gy)	V _{95%} (57 Gy) > 95% D _{max} (0.1cc) < 107% (64.2 Gy)
Lung	Mean dose < 20 Gy V _{20Gy} < 25 %
Heart	Mean dose < 25 Gy V _{30Gy} < 45%* V _{40Gy} < 30%**
CordPRV	D _{max} (0.1cc) < 40 Gy (45 Gy permitted)
Liver	V _{30Gy} < 60%
Individual Kidneys	V _{20Gy} < 25%
StomachIn***	Max dose < 60Gy
StomachOut***	Max dose < 45Gy

Table 4.1 – Dose constraints for dose escalated radiotherapy plans. *Applies only to 50Gy_{RA} and 60Gy_{RA} plans. **Applies only to 50Gy_{3D} plans. ***Applies only to 60Gy_{RA} plans

Patient 6 was originally planned using 50Gy_{RA} therefore a 50Gy_{3D} plan was not created in this case.

4.3.3 Radiobiological modelling

Radiobiological modelling of TCP was undertaken using the parameters derived by Geh et al (115). This multivariate logistics regression model was constructed using data from 26 pre-operative CRT trials in oesophageal cancer and was considered a good representative of the SCOPE 1 patient cohort. The TCP modelling was undertaken bin-wise in Microsoft Excel using parameters by Geh et al found in their original paper (115). Differential dose-volume histograms (DVH) for each structure were calculated in CERR utilising Matlab scripts developed in-house (86) before being converted to relative DVHs in Microsoft Excel. TCP was calculated as:

$$TCP(z) = \frac{\exp(z)}{1 + \exp(z)} \quad (4.2)$$

where $z = a_0 + a_1$ total RT dose + a_2 total RT dose \times dose per fraction + a_3 duration + a_4 age + a_5 5FU dose + a_6 cisplatin dose. The α/β was 4.9Gy.

NTCP modelling was carried out in Eclipse Biological Evaluation module using the whole heart volume model of Gagliardi et al (123) with an endpoint of cardiac mortality, and for the lung using the model parameters from De Jaeger et al (124), which predicts a radiation pneumonitis (RP) of grade 2 or higher. NTCP models for the stomach are limited therefore modelling was carried out using those judged to

be most relevant. The whole stomach was modelled using parameters derived by Burman et al (106) with the endpoint being ulceration, whilst the stomach wall parameters were derived by Feng et al (125), modelling the probability of ≥ 3 grade gastric bleeding.

Data were analysed using the SPSS statistics package version 20.0.0 (IBM), and results are reported as median (range) values. Both the Z-score and the P-Values were calculated.

4.4 Results

Table 4.1 (Page 138) reports the dose-volume metrics and the results of the Wilcoxon signed rank test for all radiotherapy plans. Adequate target dose coverage was possible for all patients in all treatment modalities when considering the coverage of PTV1 (Table 4.1). Four patients failed to meet the minimum coverage of PTV2 with the minimum coverage being 92.4%. All OAR dose constraints for the heart and lung were met for all patients for all treatment plans. 6 patients failed to meet the Stomach-In constraint and 1 failed to meet the Stomach-Out constraint for the 60Gy_{RA} plans. All other dose constraints in Table 4.0 were met.

There was a mean decrease 1.0% (Range: -3.0%, 0.6%) in TCP from the 50Gy_{3D} to the 50Gy_{RA} plans, a mean increase of 12.0% (9.9%, 13.6%) in TCP from the 50Gy_{3D} plans to the 60Gy_{RA} plans and a mean increase of 13.0% (12.4%, 13.4%) in TCP from the 50Gy_{RA} plans to the 60Gy_{RA} plans (Figure 4.3).

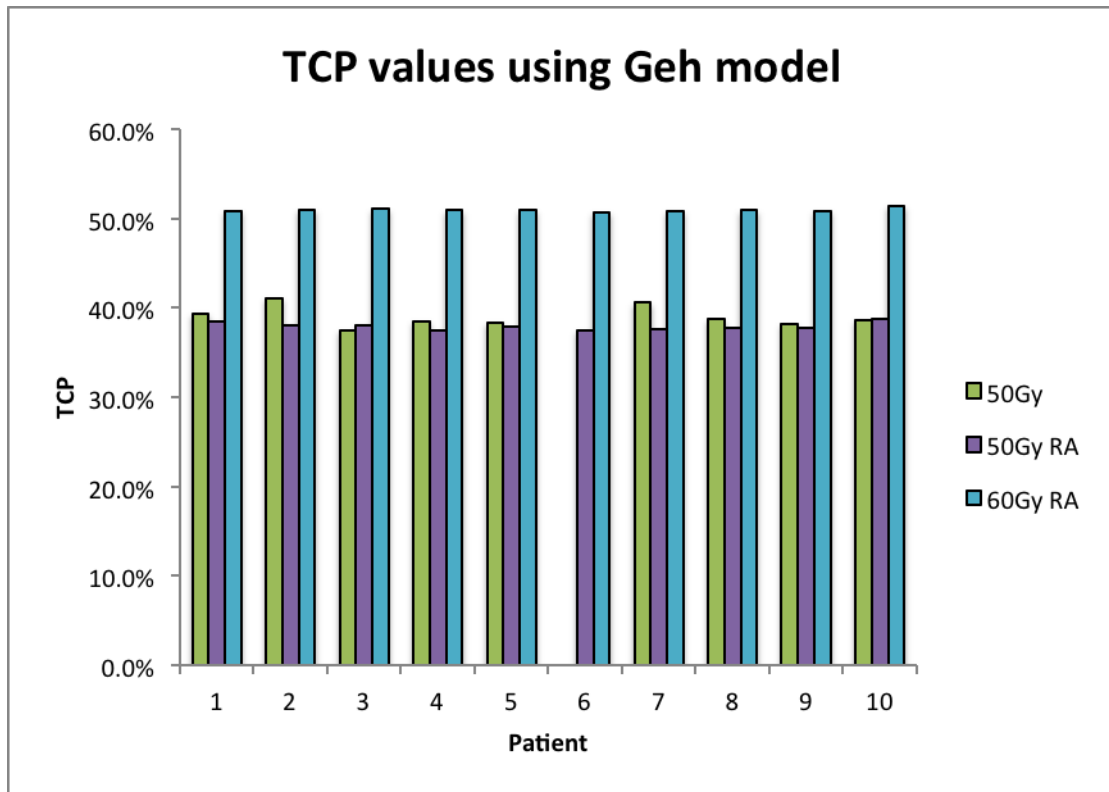


Figure 4.3 – TCP values of 50Gy_{3D}, 50Gy_{RA} and 60Gy_{RA} radiotherapy plans

For NTCP there was a mean decrease of 3.4% (-6.3%, 0%) for the heart from the 50Gy_{3D} to the 50Gy_{RA} plans, a mean decrease of 2.2% (-4.9%, 2.0%) from the 50Gy_{3D} to the 60Gy_{RA} plans and a mean increase of 1.2% (0.5%, 2.0%) in NTCP for the heart from the 50Gy_{RA} to the 60Gy_{RA} plans (Figure 4.4).

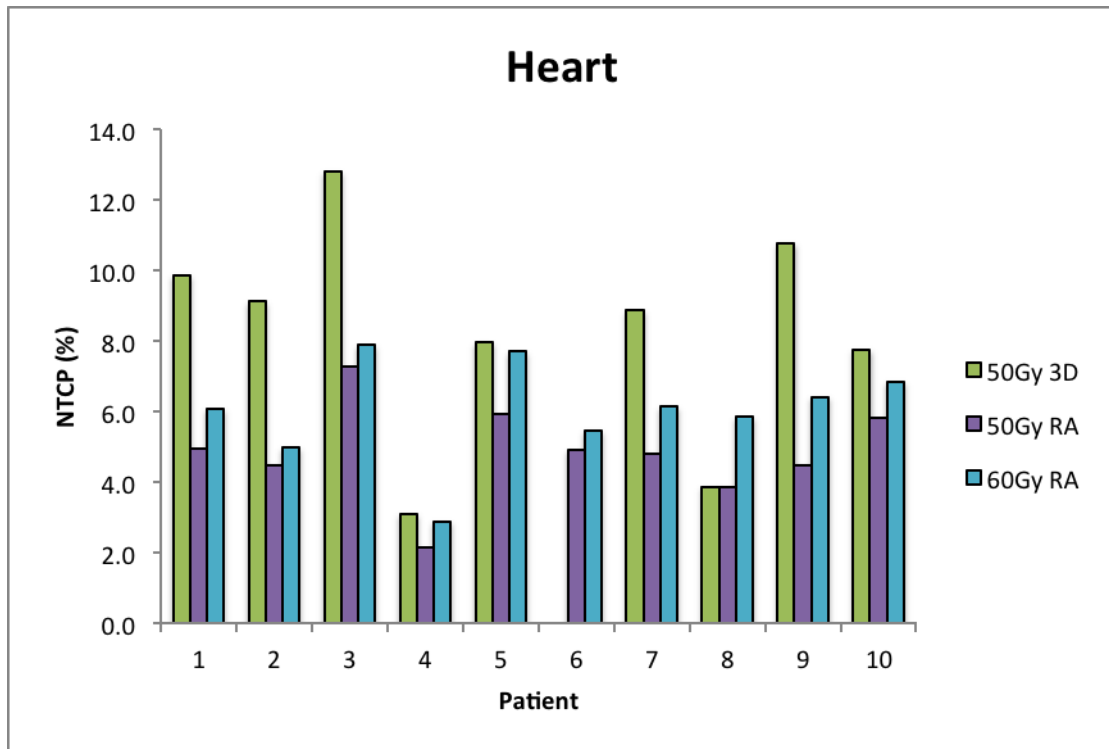


Figure 4.4 – NTCP for heart for 50Gy_{3D}, 50Gy_{RA} and 60Gy_{RA} radiotherapy plans

For lung there was a mean increase of 0.4% (-0.8%, 2.2%) in NTCP from the 50Gy_{3D} to the 50Gy_{RA} plans, a mean increase of 1.0% (-0.6%, 3.2%) from 50Gy_{3D} to 60Gy_{RA}, and a mean increase of 0.6% (0.1%, 1.2%) from the 50Gy_{RA} to the 60Gy_{RA} plans (Figure 4.5).

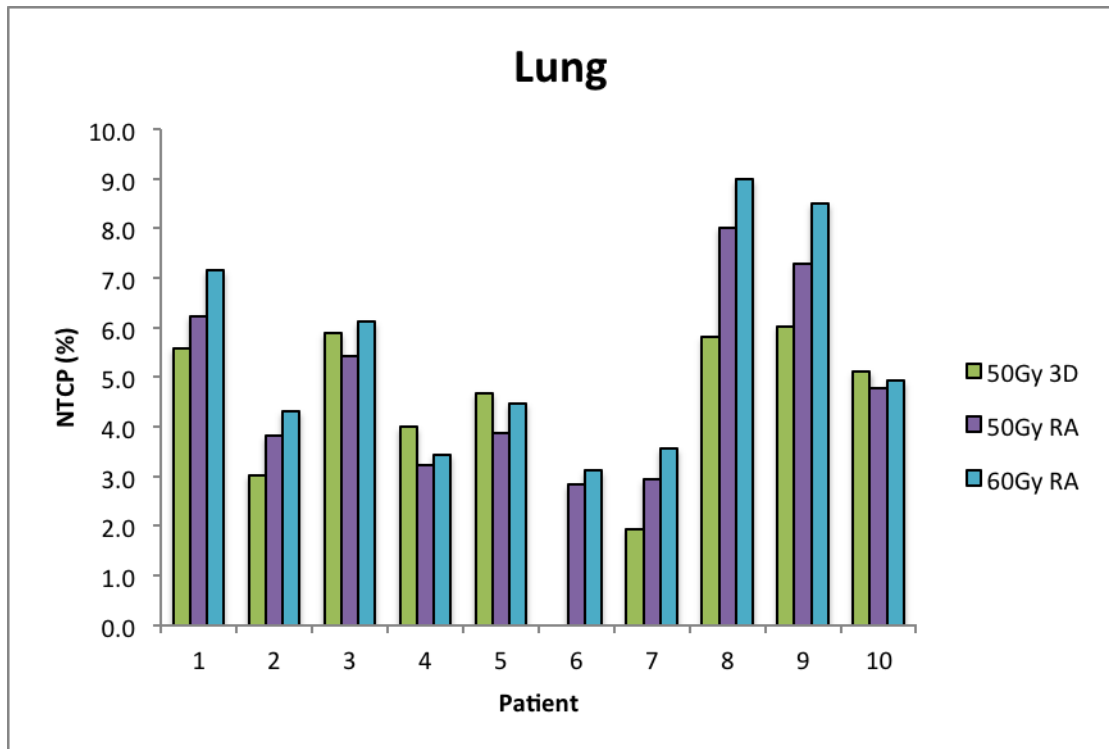


Figure 4.5 – NTCP for lung for 50Gy_{3D}, 50Gy_{RA} and 60Gy_{RA} radiotherapy plans

For the stomach and stomach wall the variation in NTCP between patients was considerable. Patients 1, 2, 6 & 8 all had stomach NTCP values <0.03% for all treatment plans whilst the largest value was 3.4% for a patient planned using the 60Gy_{RA} technique (Figure 4.6).

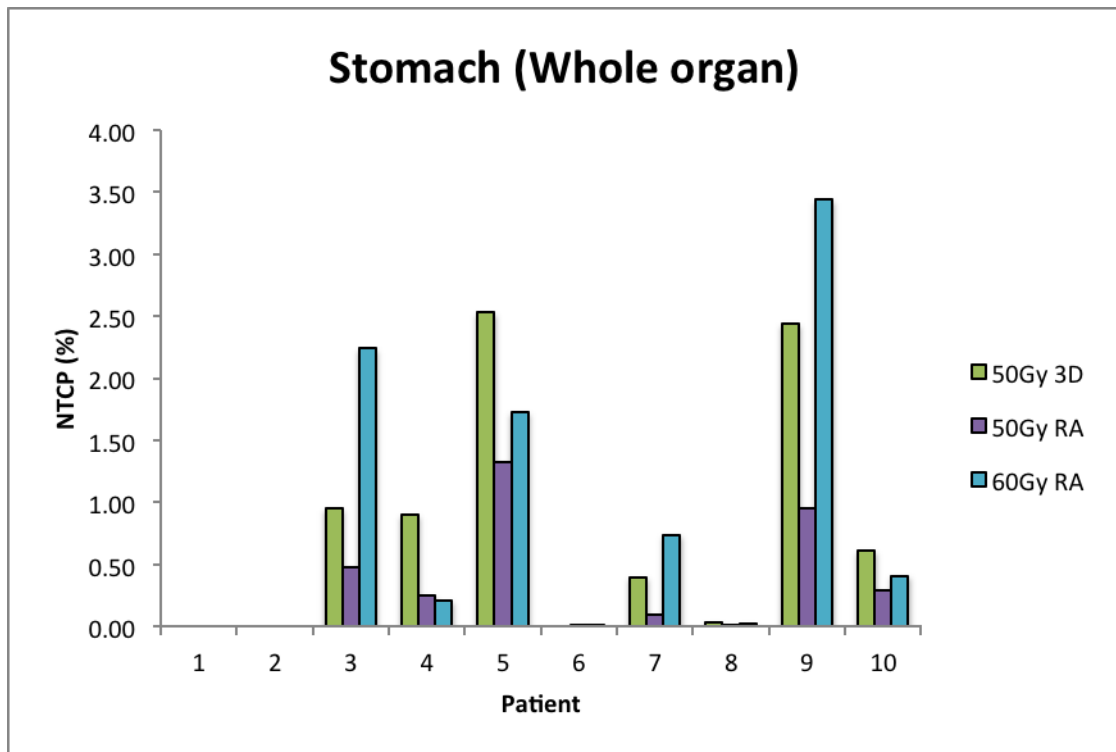


Figure 4.6 – NTCP for stomach for 50Gy_{3D}, 50Gy_{RA} and 60Gy_{RA} radiotherapy plans

The stomach wall model, which models gastric bleeding, showed considerably larger absolute values of NTCP, the largest being 39.4% for a patient planned with the 60Gy_{RA} plan. Across the whole study, there was a mean decrease in stomach wall NTCP of 3.1% (-6.5, 0%) from the 50Gy_{3D} plans to the 50Gy_{RA} plans, a mean increase of 5.9% (-4.7, 18.7%) in NTCP from the 50Gy_{3D} to the 60Gy_{RA} plans and a mean increase of 8.2% (-0.4, 21.3%) in NTCP from the 50Gy_{RA} to the 60Gy_{RA} plans (Figure 4.7).

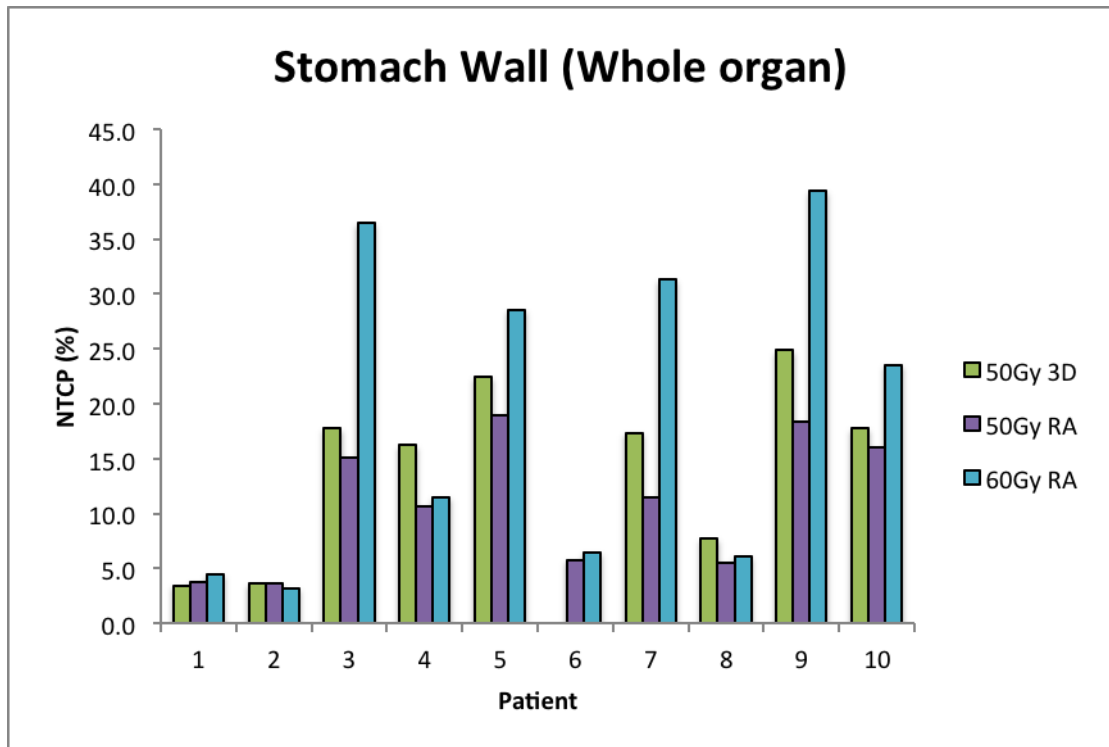


Figure 4.7 – NTCP for whole stomach wall for 50Gy_{3D}, 50Gy_{3D} and 60Gy_{RA} radiotherapy plans

To address the fact that both part of the stomach and stomach wall are within the PTVs, particularly the dose escalated PTV2, I restricted the NTCP modelling to the volume outside the boost volume (PTV2). There was in general a smaller difference between the NTCP values between plans. In this case there was a mean decrease of 3.4% (-7.4%, 0.3%) from the 50Gy_{3D} to the 50Gy_{RA} plans, a mean decrease of 0.9% (-4.7%, 1.0%) in NTCP from the 50Gy_{3D} to the 60Gy_{RA} plans, and a mean increase of 2.3% (-0.4%, 6.9%) in NTCP from the 50Gy_{RA} to the 60Gy_{RA} plans (Figure 4.8).

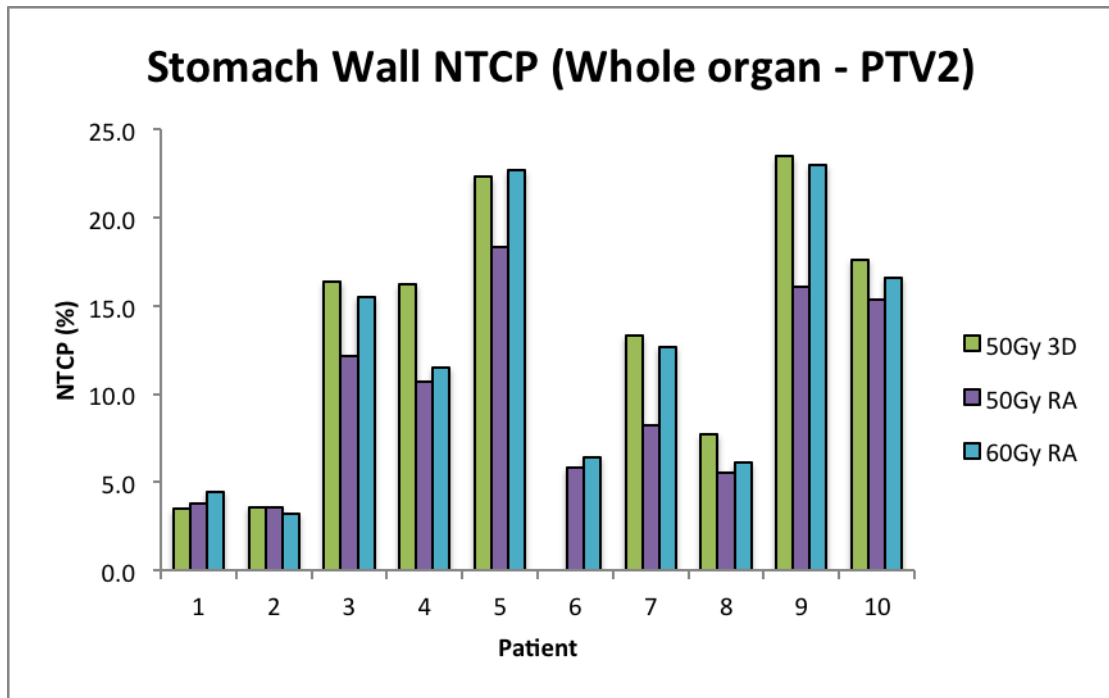


Figure 4.8 – NTCP for stomach wall minus PTV2 for 50Gy_{3D}, 50Gy_{3D} and 60Gy_{RA} radiotherapy plans

Table 4.3 shows the Pearson correlation coefficients between the Stomach and Stomach Wall volumes and associated dose metrics.

Volumes:	Pearson Coefficient		
	50Gy3D	50GyRA	60GyRA
Stomach Volume - Stomach Mean Dose	0.35	0.60	0.61
Stomach Volume - Stomach Max Dose	-0.19	0.12	0.55
Stomach Volume - Stomach V45	0.16	0.08	-0.02
Stomach Volume - Stomach V50	0.11	0.05	-0.04
Stomach Wall Volume - Stomach Wall Mean Dose	0.63	0.66	0.66
Stomach Wall Volume - Stomach Wall Max Dose	-0.12	0.32	0.68
Stomach Wall Volume - Stomach Wall V45	0.23	0.21	0.12
Stomach Wall Volume - Stomach Wall V50	0.38	0.22	0.04

Table 4.3 – Pearson correlation coefficients between stomach, stomach wall volumes and dose metrics

It can be seen how the strongest correlations are between the stomach wall volumes in each plan and the mean dose received by those volumes (0.63, 0.66 and 0.66 for the 50Gy_{3D}, 50Gy_{RA} and 60Gy_{RA} respectively).

Six patients had an overlap between the GTV and PTV2 and Stomach Wall structure whilst all patients had an overlap between the PTV1 and Stomach Wall structures. There was a strong correlation between the NTCP value and the Stomach Wall structure/PTV1 overlap structure volume for all treatment plans (Pearson's R=0.80, 0.77 and 0.77 for the 60Gy_{RA}, 50Gy_{RA} and 50Gy_{3D} plans respectively). Figure 4.9 shows the correlation between NTCP and the Stomach Wall/PTV1 overlap structure volume for the 60Gy_{RA} plans.

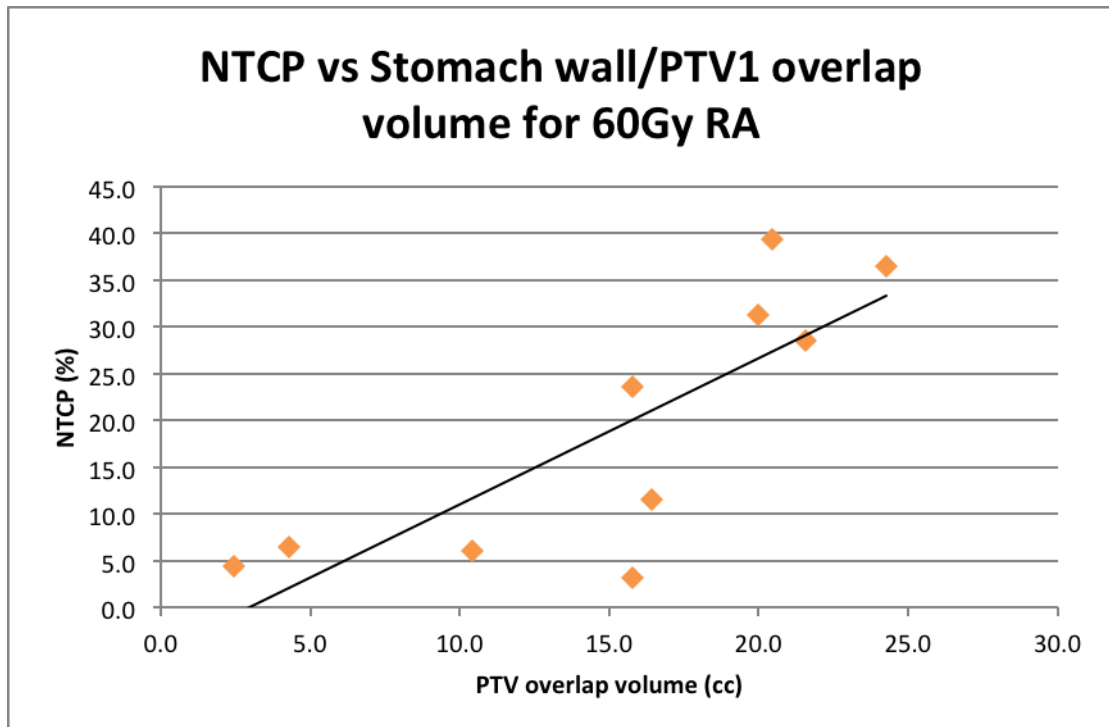


Figure 4.9 – NTCP vs whole stomach wall/PTV1 overlap structure volume for 60Gy_{RA} radiotherapy plans

There was also a strong correlation between the NTCP value and the Stomach Wall/PTV2 overlap structure volume for the 60Gy_{RA} plan (R= 0.82) (Figure 4.10).

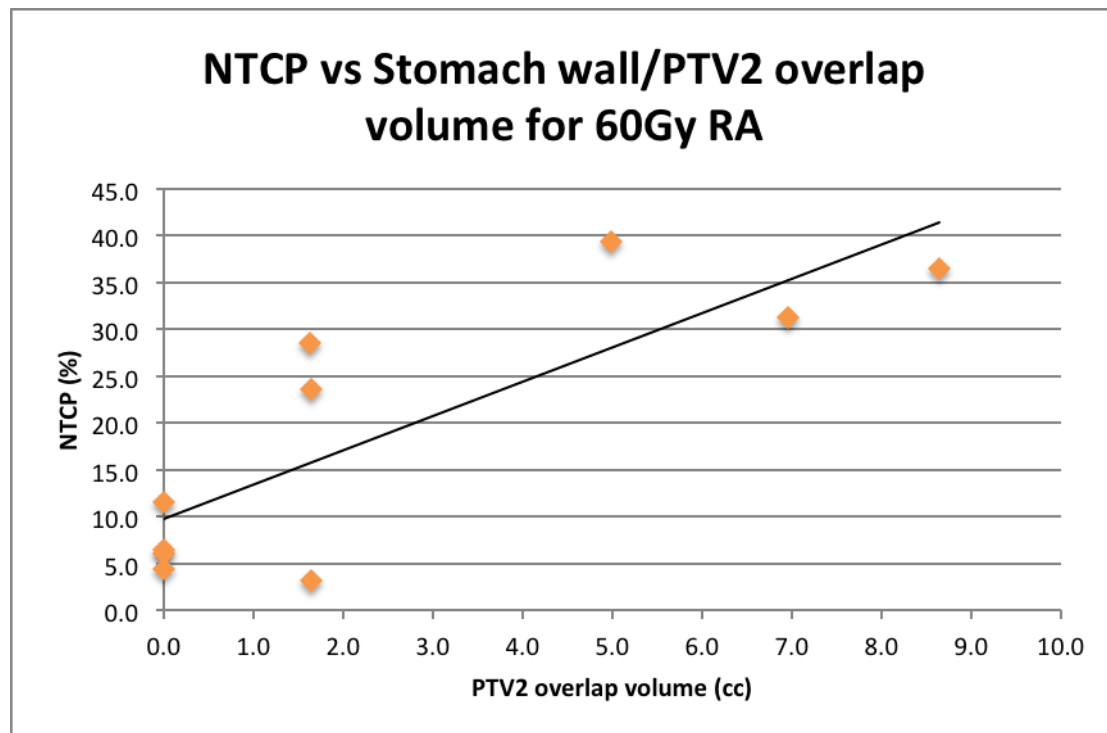


Figure 4.10 – NTCP vs whole stomach wall/PTV2 overlap structure volume for 60Gy_{RA} radiotherapy plans

4.5 Discussion

This study has shown that using a VMAT delivered SIB technique it is possible to deliver a dose of 60Gy to the tumour whilst adhering to all standard OAR dose constraints for lower oesophagus tumours. In addition, this study, to my knowledge, is the first to specifically investigate the effect of dose escalation in lower oesophageal tumours on the stomach using radiobiological modelling.

When comparing the 50Gy_{RA} to the 60Gy_{RA} plans there was a significant increase in TCP but also an increase in the mean dose parameter for the lung (See Table 4.2).

There was also a significant increase in mean TCP (≈ 12) going from the 50Gy_{3D} to the 60Gy_{RA} plan. Comparing 50Gy_{3D} and 50Gy_{RA}, there was a statistically significant increase in lung V13Gy, which can be explained by the low dose wash associated with RapidArc type treatment plans, however V20Gy reduced and mean lung NTCP was reduced from 5.1% to 4.3%. There was a significant decrease in the heart V30/40Gy values. Although this did not result in a significant decrease in NTCP between the two planning methods in this study, this agrees with results from previous work I was involved in on mid-oesophageal cancer patients (82). For the 60Gy_{RA} plans as a whole, the NTCP values for the heart and lung were lower than those found in the previous study on mid oesophageal cancer patients as would be expected due to the more inferior location of the tumour. However, there was still a similar modest increase in heart and lung toxicities when using the boost technique (82). This also agrees with the recently published study by Roeder et al who delivered 60Gy to patients with oesophageal cancer using a SIB technique and found acceptable acute and late overall toxicity to the lung and heart (126).

However, when treating lower oesophageal tumours there is the added complication of having the stomach adjacent to the treatment volume. Here I used two models for the stomach and applied them to both the structure as a whole and inside and outside the PTV. The model for the stomach wall by Feng et al (125) was found to predict a higher rate of toxicity than that for the whole stomach, most likely the result of the different endpoints of gastric bleeding and ulceration being modelled respectively. Max dose constraints of 45Gy and 60Gy were applied to the stomach outside (Stomach-Out) and inside (Stomach-In) the PTV respectively for the 60Gy_{RA} plans. The NTCP results for the 60Gy_{RA} when modelling the volume outside the PTV

were similar to those of the 50Gy_{RA} and 50Gy_{3D} plans (Max NTCP of 23.0% and 23.4% for the 60Gy_{RA} and 50Gy_{3D} plans respectively), suggesting that dose escalation may not pose any more risk to normal stomach than 3D conformal radiotherapy (Figure 4.8). However, when considering the stomach wall structure as a whole it was found that there was up to 20% increase in NTCP when using the dose escalation plan compared to the 50Gy_{RA} plan. This value however could be considered as being the worst case scenario, as it is acknowledged that stomach movement and filling over the course of treatment may blur out any dose hot spots. Any NTCP value is also by nature calculated from a model that is open to interpretation therefore should only be used to give an approximate risk. It is fully acknowledged that radiobiological modelling inherently has limitations that limit its accuracy. Specifically in the case of this study, there is a lack of both clinical outcome data and radiobiological models for stomach toxicity when prescribing a dose >50Gy. However the model used was deemed to be the most suitable in this instance. The application of radiobiological modelling to partial organ irradiation is also a contentious one that may affect the results. However the purpose of this study was not to give definitive values of stomach toxicity, but to investigate and inform of the potential relative risks involved in dose escalation of lower oesophagus tumours both in a forthcoming trial and in clinical practice.

I have shown that there is a strong correlation in NTCP with the volume of overlap between the stomach wall with both PTV1 and the high dose region PTV2. When more clinical data are available it may become apparent that safe delivery of the 60Gy SIB is dependent on this volume of the overlap, which could potentially be

reduced by reducing the treatment margins for individual patients using techniques such as 4DCT, gating and breath hold protocols. However it has been reported that the inter-patient motion of oesophageal tumours is highly variable (127) and that even the use of 4DCT may not even fully account for organ motion in between fractions (128). A move to reduce population-based margins from those used in the SCOPE 1 and SCOPE 2 trials, rather than on an individual basis, may therefore increase the risk of failure to control the disease. The margins used in this investigation were taken from the SCOPE 2 protocol and therefore give an approximation of results from a forthcoming nationwide trial, taking into account the inherent errors in radiobiological modelling.

An inclusion criteria for the SCOPE 1 trial was that patients were to have histologically confirmed carcinoma of the oesophagus with no more than 2cm of mucosal tumour extension into the stomach. As this patient group is also likely to be included in the SCOPE 2 trial, this study's findings mean I would recommend that in the radiotherapy protocol that these patients be treated with caution until the safety of this dose escalation method is clearly defined within the SCOPE 2 trial.

The results also suggest that the maximum prescribed dose achievable for each patient may be dependent on the volume of the stomach overlap with the treatment volume.

	50Gy _{3D}	50Gy _{RA}	60Gy _{RA}	Wilcoxon signed-rank test		
	Median (range)	Median (range)	Median (range)	50Gy _{3D} - 50Gy _{RA}	50Gy _{3D} - 60Gy _{RA}	50Gy _{RA} - 60Gy _{RA}
PTV1						
V95%	98.2 (96.0-100)	99.1 (95.2-100)	97.0 (95.0-98.2)	Z=0.53 (p=.57)	Z=1.07 (p=.28)	Z=1.36 (p=.17)
PTV2 (GTV+0.5cm)						
V95%			95.1 (92.4-97.4)			
TCP (%) Geh	38.7 (37.5-41.1)	37.8 (37.5-38.7)	50.9 (50.7-51.4)	Z=2.11 (p=.04)	Z=2.67 (p=.01)	Z=2.81 (p=.01)
Lung						
Mean dose (Gy)	9.8 (6.0-11.1)	10.2 (5.8-14.3)	10.7 (6.4-15.2)	Z=1.78 (p=.07)	Z=2.40 (p=.02)	Z=2.80 (p=.01)
V13Gy (%)	26.8 (20.0-35.9)	32.8 (15.1-51.6)	34.4 (18.0-54.2)	Z=2.19 (p=.03)	Z=2.55 (p=.01)	Z=2.09 (p=.04)
V20Gy (%)	19.7 (12.3-24.3)	11.3 (4.6-17.4)	15.6 (6.5-23.4)	Z=2.55 (p=.01)	Z=1.72 (p=.09)	Z=2.81 (p=.01)
NTCP (%) De Jaeger	5.1 (1.9-6.0)	4.3 (2.8-8.0)	4.7 (3.1-9.0)	Z=1.49 (p=.14)	Z=2.09 (p=.04)	Z=2.80 (p=.01)
Heart						
Mean dose (Gy)	26.8 (13.9-31.2)	21.2 (14.6-23.6)	20.2 (16.4-23.2)	Z=1.68 (p=.09)	Z=1.58 (p=.11)	Z=0.15 (p=.88)
V30Gy (%)	55.1 (9.7-67.9)	17.2 (8.2-25.3)	18.7 (10.3-22.6)	Z=2.67 (p=.01)	Z=2.55 (p=.01)	Z=0.87 (p=.39)
V40Gy (%)	16.2 (5.9-24.5)	10.1 (4.5-14.8)	10.6 (5.6-13.6)	Z=2.67 (p=.01)	Z=2.67 (p=.01)	Z=1.58 (p=.11)
NTCP (%) Gagliardi	8.9 (3.1-12.8)	4.9 (2.2-7.3)	6.1 (2.9-7.9)	Z=1.90 (p=.06)	Z=1.38 (p=.17)	Z=2.80 (p=.01)
Stomach						
Mean dose (Gy)	29.8 (5.5-44.2)	24.1 (5.4-40.4)	23 (6.5-36.1)	Z=1.17 (p=.24)	Z=0.97 (p=.33)	Z=1.60 (p=.11)
Max dose (Gy)	52.6 (49.6-53.4)	51.9 (42.4-52.9)	60.9 (51.6-61.6)	Z=0.83 (p=.41)	Z=2.61 (p=.01)	Z=2.81 (p=.01)
V45 (cc)	47.3 (7.3-80.4)	32.8 (0-49.8)	34.3 (5.4-25.4)	Z=2.60 (p=.01)	Z=2.50 (p=.01)	Z=0.36 (p=.72)
V50 (cc)	31.5 (0-23.4)	17.7 (0-14.8)	21.4 (2.2-19.2)	Z=2.31 (p=.02)	Z=1.78 (p=.07)	Z=1.27 (p=.20)
StomachIn max dose (Gy)	52.6 (49.6-53.4)	51.9 (42.4-52.9)	60.9 (51.6-61.6)	Z=0.77 (p=.44)	Z=2.61 (p=.01)	Z=2.81 (p=.01)
StomachOut max dose (Gy)	51.4 (49.4-53.1)	44.4 (36.6-43.6)	44.8 (42.3-46.1)	Z=1.76 (p=.07)	Z=1.79 (p=.07)	Z=0.14 (p=.88)

NTCP (%) Burman	0.6 (0-2.5)	0.2 (0-1.3)	0.3 (0-3.4)	Z=2.38 (p=.02)	Z=0.35 (p=.73)	Z=2.03 (p=.04)
Stomach wall						
Mean dose (Gy)	29.5 (8.2-42.6)	22.9 (7.9-38.7)	22.4 (9.1-35.0)	Z=0.97 (p=.33)	Z=0.76 (p=.45)	Z=0.87 (p=.39)
Max dose (Gy)	52.6 (49.6-53.4)	51.9 (43.4-52.9)	61 (51.6-61.6)	Z=0.77 (p=.44)	Z=2.55 (p=.01)	Z=2.81 (p=.01)
V45 (cc)	28 (6.2-39.9)	17.9 (0-26.9)	17.9 (5.4-25.4)	Z=2.19 (p=.03)	Z=2.19 (p=.03)	Z=0.46 (p=.65)
V50 (cc)	15.8 (0-23.4)	9.1 (0-14.8)	9.2 (2.2-19.2)	Z=2.31 (p=.02)	Z=1.48 (p=.14)	Z=1.28 (p=.20)
NTCP (%) Feng	17.4 (3.5-24.9)	11.1 (3.6-18.9)	17.5 (3.2-39.4)	Z=1.72 (p=.09)	Z=1.99 (p=.05)	Z=2.70 (p=.01)
Cord PRV						
Dmax 0.1cc (Gy)	36.9 (16.1-41.3)	31.1 (26.2-44.1)	34.9 (28.4-39.6)	Z=0.47 (p=.64)	Z=0.18 (p=.86)	Z=1.67 (p=.10)

Table 4.2 – Comparison of dose volume metrics and TCP and NTCP values for all radiotherapy plans

4.6 Quantification of stomach movement

The work in the previous section on approximating stomach toxicity when escalating the dose of lower oesophageal tumours to 60Gy was undertaken by modelling NTCP from RT plans constructed using the patients planning CTs.

Although the majority of radiotherapy is delivered based on the plan from a single CT scan such as this, the anatomy of a patient may change over the course of treatment. This is mainly due to patient movement, inaccurate patient positioning, and organ motion (129). The first two of these factors can be minimised by patient and staff training and the third to a lesser extent by the use of protocols and specialist equipment. However there is still likely to be internal organ motion that cannot be accounted for without using advanced techniques such as Image Guided Radiotherapy (IGRT) where on set CT images are used to position the patient correctly and track their movement during the fraction. Nakamura et al discuss how large variations in stomach volume may have a detrimental effect on dose escalation when treating pancreatic cancer, despite using a breath hold technique (130). As a result, the dose distribution received by the patient during treatment will most likely differ slightly to what was planned. This will therefore affect the dose distribution around the tumour volume and also any adjacent organs at risk and in turn any TCP or NTCP modelling. The impact of variation in gas in the stomach on dose distribution should also be considered. For example, Kumagai et al found that dose conformation to the CTV was degraded due to bowel gas movement when treating pancreatic cancer using carbon ion beams (131) and consequently may also be applicable when using photon beams. Bouchard et al also found that changes in

stomach filling resulted in the boost target being missed when treating GEJ tumours with IMRT-SIB (132).

Motion of the tumour volume is accounted for by the use of margins that encompass the tumour volume as set out in ICRU Reports 50 and 62 (80) & (81), and there are several methods reported in the literature to minimise the uncertainty of target localisation and reproducibility during RT for lung, liver and intrapelvic tumours. However there are usually no such margins added to the outline of organs at risk. Some trial protocols specify methods to decrease uncertainty in OAR position such as drinking a specific amount of water to fill bladder or stomach. According to Urie et al, the problem of internal organ motion is most pronounced and severe in the abdominal region (133), where organ motion may arise from differences in filling states in addition to respiratory motion. As there was no stomach filling protocol for the SCOPE 1 trial, a study to investigate and quantify stomach filling between fractions may give an indication towards what impact, if any, the inclusion of a stomach filling or breath hold protocol would have on stomach toxicity and dose distribution when treating lower oesophageal tumours. The objective of the following study was therefore to investigate the inter fraction movement of the stomach by analysing the cone beam computed tomography (CBCT) images for patients being treated for lower oesophageal tumours. This may then give an indication of how stomach movement could affect the dose distribution and consequent TCP and NTCP modelling when dose escalating patients.

4.7 Cone Beam Computed Tomography

Compared to the now widespread multi-slice CT scanners, cone beam computed tomography is a relatively recent technology (134). A divergent pyramidal or cone shaped source of ionizing radiation is directed through the middle of the area of interest on to an x-ray detector on the opposite side (Figure 4.11).

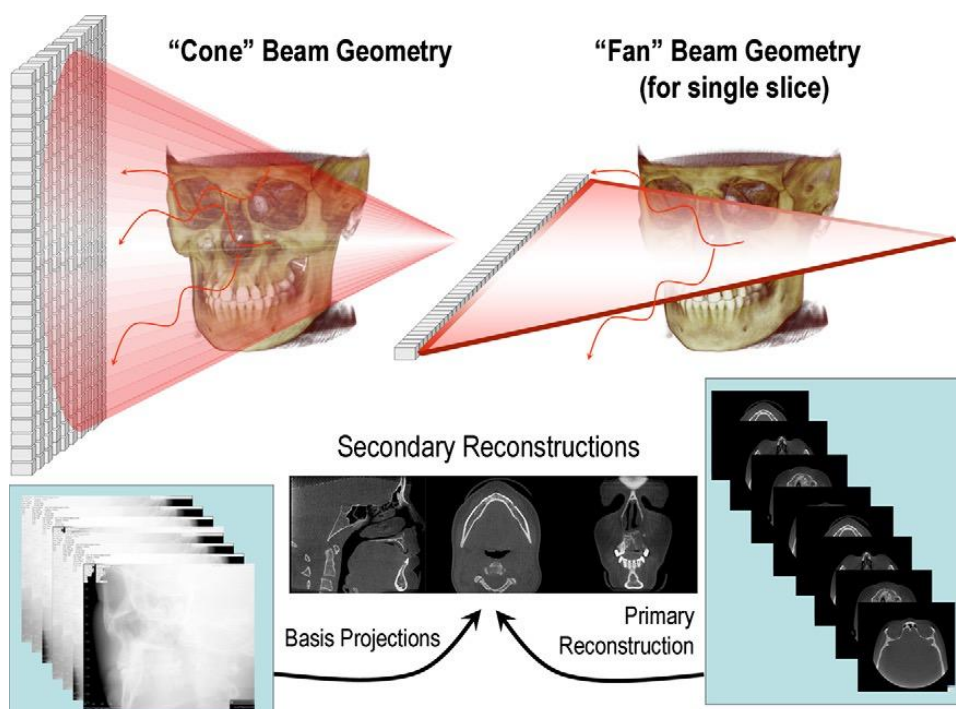


Figure 4.11 – Schematic of CBCT and conventional 'fan' CT. (135)

Figure 4.11 shows the difference between CBCT and conventional 'fan' CT. In CBCT, multiple basis projections for the projection data from which orthogonal planar images are secondarily reconstructed. In fan beam geometry, primary reconstruction of data produces axial slices from which secondary reconstruction generates orthogonal images. The amount of scatter generated and recorded by cone beam acquisition is substantially higher, therefore reducing image contrast and increasing

image noise.

4.8 Preparing for analysis

Patients undergoing treatment for lower oesophageal cancer at Velindre Cancer Centre receive a cone beam scan on the first three fractions of their radiotherapy treatment, and then once weekly. This follows the guidance of the National Cancer Action Team report published in August 2012 (136). By utilising and analysing these images together with the planning CT, a clearer picture of the inter-fraction movement of the stomach could be gained. The planning CT image and CBCTs images for 4 patients treated at Velindre Cancer Centre were chosen for analysis. Although there were a greater number of patients with CBCT images available, there was a large variation in image quality of the CBCT images. As a result, I was only confident in being able to correctly identify the stomach on these 4 patients.

4.8.1 Outlining the stomach volume

The stomach organ volumes were outlined on both the planning CT and the cone beam CT for each patient on the OMP treatment planning system. These were checked and confirmed for accuracy by an oncologist before commencing with the study.

4.8.2 Image registration

To assess the movement of the stomach, it was important to assign one reference stomach volume from which the movement over the other fractions could be quantified. For the purpose of this study, the volume outlined on the planning CT

scan was assigned as the reference volume. Another requirement was the position matching of the bony anatomy of the patient from one CT image to the next, this would ensure that any change in the stomach's position within the patient would be relative. This process of matching the 3D position of the patient between images is known as image registration and I carried this out between the planning CT image and the 4 CBCT images on the Velocity (Varian Medical Systems Palo Alto) software package. This was largely an automatic process using specific tools within the software, however on some occasions some manual adjustments were required. Figures 4.12 and 4.13 show the before and after of the process.

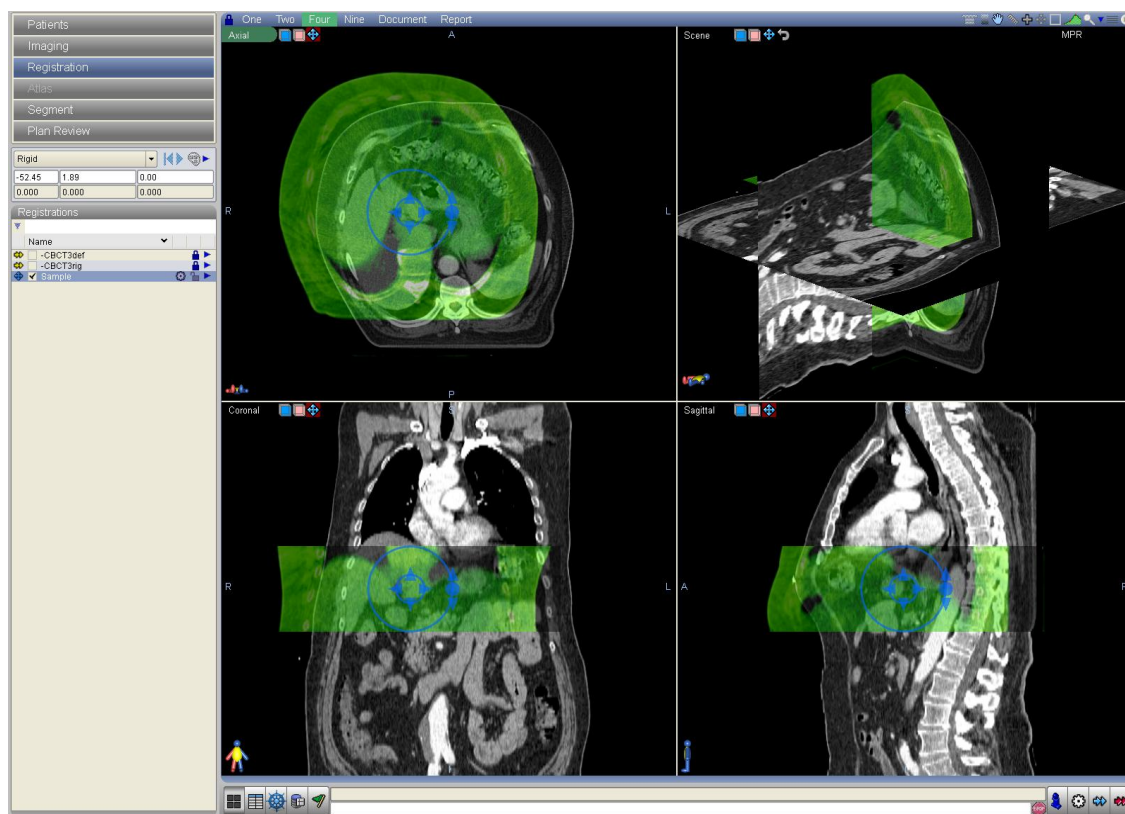


Figure 4.12 – Pre registration of planning CT and CBCT images

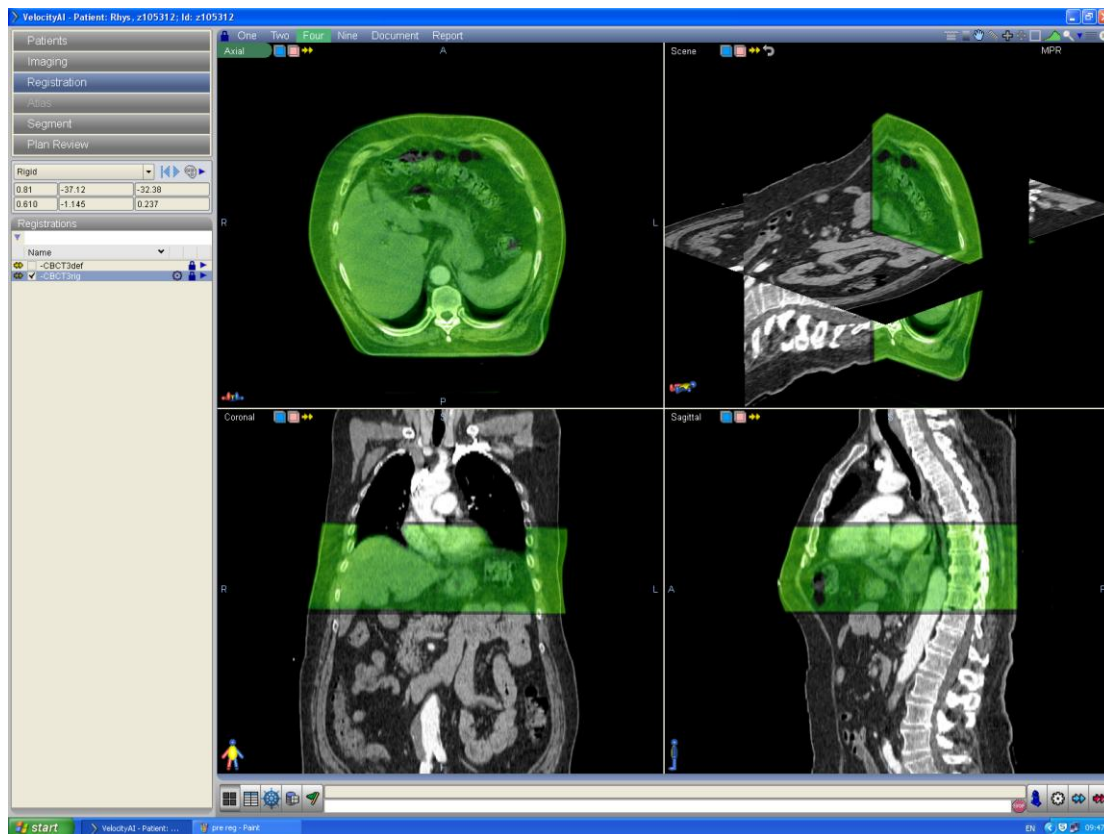


Figure 4.13 – Post registration of planning CT and CBCT images

Once the CBCT image was matched to the planning CT the associated stomach structures were imported and all the separate registrations (CT:CBCT1, CT:CBCT2, CT:CBCT3 and CT:CBCT4) fused into one image set. This created one planning CT image set with the associated stomach volume from each registered CT:CBCT combination. This image set was then exported in DICOM format for analysis.

4.8.3 Quantifying the stomach position

The quantification of the change in the stomach's position was carried out in CERR. The DICOM file containing all the stomach volumes was imported and a CERR .mat file created. A screen shot of the resulting file can be seen in Figure 4.14. It can be

seen how all the stomach volumes from the planning CT, CBCT1, CBCT2, CBCT3 and CBCT4 are all present as separate structures.

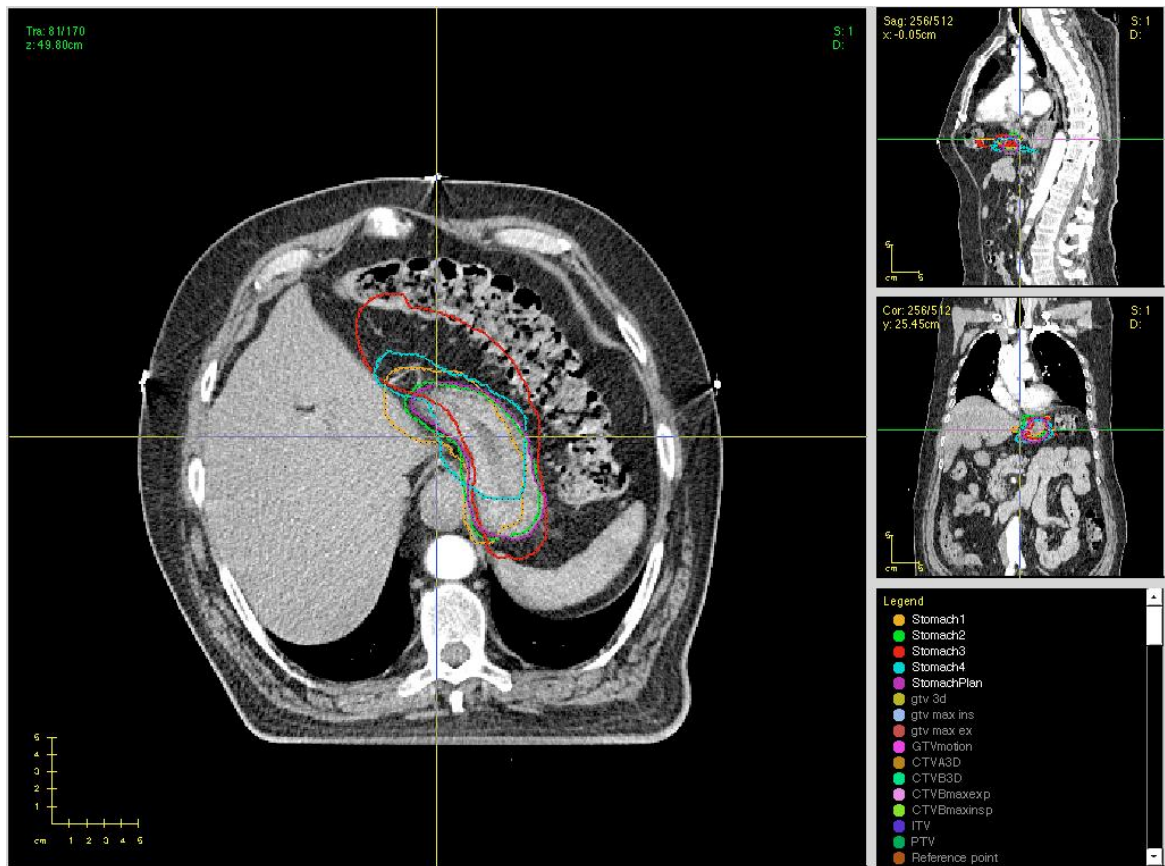


Figure 4.14 – Screen grab from CERR showing all stomach volumes

The position of each stomach structure was quantified by recording the maximum and minimum x, y and z coordinates of the structure using a script in Matlab. The coordinates for the centre of mass (COM) of each stomach structure were also recorded and the total volume of each stomach structure and the overlap volumes between the stomach and PTV and PTV2 calculated.

4.9 Results

4.9.1 Difference in maximum and minimum XYZ coordinates and COM

Patient 1

The differences between the minimum, maximum and COM xyz coordinates and COM were calculated in mm. Table 4.4 shows the results for Patient 1.

Difference	Plan - CBCT1	Plan - CBCT2	Plan - CBCT3	Plan - CBCT4
Min X	-11.7	0	-6.8	2
Min Y	2.9	2	13.7	8.8
Min Z	0	3	0	-6
Max X	-1	3.9	-3.9	-4.9
Max Y	4.9	3.9	-36.1	-19.5
Max Z	9	6	18	9
COM X	-1.4	-1.2	-12.1	5.5
COM Y	-3.2	2.4	-5.7	-11.7
COM Z	11.3	6.8	8.2	-0.1

Table 4.4 – Difference in minimum, maximum and COM xyz coordinates (mm) for stomach structures (Patient 1)

It can be seen that there is a displacement of up to 36.1mm in the maximum Y coordinate.

Patient 2

Difference	Plan - CBCT1	Plan - CBCT2	Plan - CBCT3	Plan - CBCT4
Min X	4.9	-1	-1	5.9
Min Y	-3.9	-3.9	-4.9	-9.8
Min Z	-6	18	-3	18
Max X	6.8	4.9	4.9	7.8
Max Y	3.9	2	2	-1
Max Z	6	42	12	30
COM X	2.5	-6.7	-2.8	3.7
COM Y	0.1	2	-0.8	-3.2
COM Z	2.4	31.4	6.6	26.6

Table 4.5 – Difference in minimum, maximum and COM xyz coordinates (mm) for stomach structures (Patient 2)

The maximum displacement for patient 2 was 42mm in the Z direction.

Patient 3

Difference	Plan - CBCT1	Plan - CBCT2	Plan - CBCT3	Plan - CBCT4
Min X	8.8	4.9	2	2
Min Y	3.9	5.9	2.9	5.9
Min Z	-3	0	-15	0
Max X	-8.8	0	-4.9	-3.9
Max Y	-10.7	6.8	2.9	2
Max Z	-12	-3	-12	0
COM X	0.7	1.6	-1.6	0.7
COM Y	-6.3	6.4	1.5	0.8
COM Z	-7.3	0.4	-10.4	-0.8

Table 4.6 – Difference in minimum, maximum and COM xyz coordinates (mm) for stomach structures (Patient 3)

The maximum displacement for patient 3 was 15mm in the Z direction.

Patient 4

Difference	Plan - CBCT1	Plan - CBCT2	Plan - CBCT3	Plan - CBCT4
Min X	-3.9	-3.9	6.8	-2
Min Y	-1.27	0	0.2	-1.37
Min Z	-1.5	0	-0.3	-1.8
Max X	-2.9	-12.7	-9.8	23.4
Max Y	2	-2	0	19.5
Max Z	18	9	15	27
COM X	1.3	-4.1	2.9	14.6
COM Y	-3.2	-2.5	2.1	-1.1
COM Z	6.1	4.1	6.6	9.3

Table 4.7 – Difference in minimum, maximum and COM xyz coordinates for stomach structures (Patient 4)

The maximum displacement for patient 4 was 27mm in the Z direction.

4.9.2 Average displacement of XYZ and COM coordinates

The average displacement, regardless of direction, across all patients is shown in

Table 4.8

Average	Plan - CBCT1	Plan - CBCT2	Plan - CBCT3	Plan - CBCT4
Min X	7.3	2.4	4.2	2.9
Min Y	5.9	2.9	5.9	9.5
Min Z	6	5.3	5.3	10.5
Max X	4.9	5.4	5.9	10
Max Y	5.4	3.7	10.3	10.5
Max Z	11.3	15	14.3	16.5
COM X	1.5	3.4	4.9	6.1
COM Y	3.2	3.3	2.5	4.2
COM Z	6.8	10.7	8	9.2

Table 4.8 – Average displacement of minimum, maximum and COM xyz coordinates

The average and range of displacement across all image sets, for both the maximum and minimum xyz coordinates of the structures are shown in Table 4.9:

Average XYZ	
X	5.4 (0.0-23.4)
Y	6.7 (0.0-36.1)
Z	10.5 (0.0-42.0)

Table 4.9 – Average xyz coordinates across all image sets

The average and range of displacement for the COM coordinates across all image sets are shown in Table 4.10:

Average COM	
X	4.0 (7.0-14.6)
Y	3.3 (1.0-11.7)
Z	8.7 (1.0-31.4)

Table 4.10 – Average COM coordinates across all images

4.9.3 Difference in total volume

I also calculated the total volume of the stomach for each patient in each image. This would allow a clearer picture of the change in the stomach structure. Figure 4.15 shows the change in absolute stomach volume for each CT scan. Table 4.11 shows the percentage difference in volume recorded with the CBCT scan compared to the planning scan.

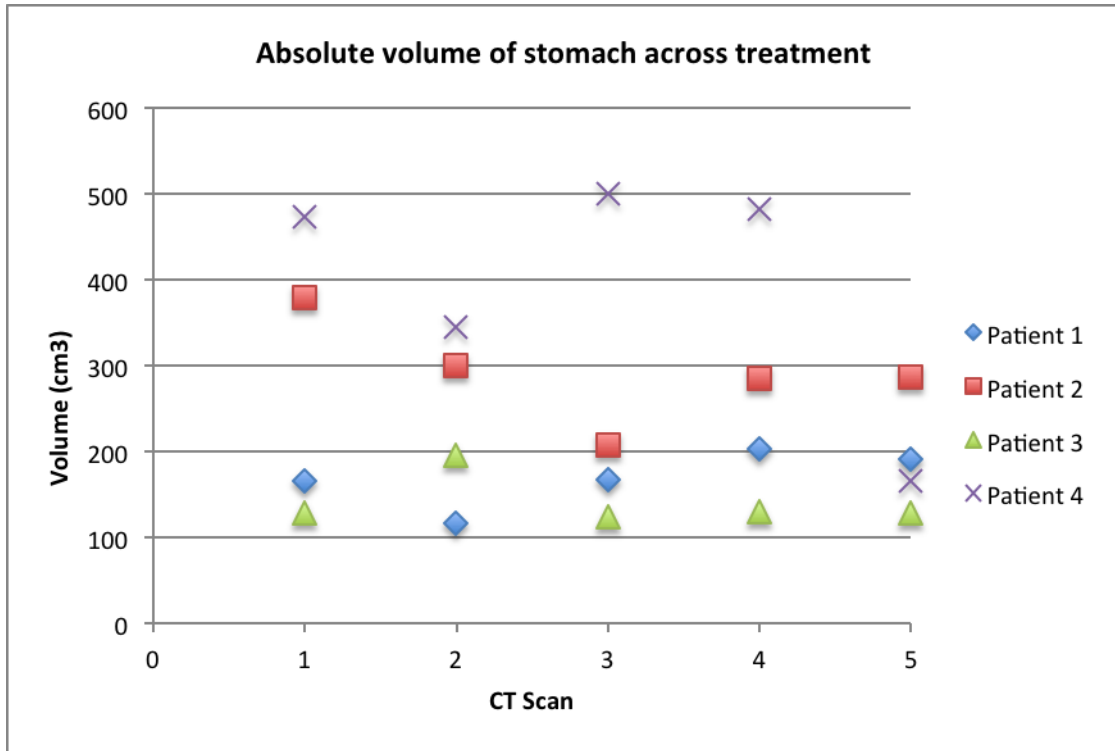


Figure 4.15 – Absolute volume of stomach across treatment

	Plan Volume	CBCT1	CBCT2	CBCT3	CBCT4
Patient 1	166.30	-29.47	+0.43	+22.48	+14.69
Patient 2	379.45	-20.94	-45.38	-24.65	-24.27
Patient 3	128.78	+52.19	-3.34	+1.59	+0.38
Patient 4	473.88	-27.06	5.57	+1.86	-64.86

Table 4.11 – Percentage difference in stomach volume between CBCT and planning image

4.9.4 Difference in overlap volumes

The change in overlap volume between the stomach and PTV is shown in Figure 4.16. Table 4.12 shows the percentage difference in volume recorded with the CBCT scan compared to the planning scan.

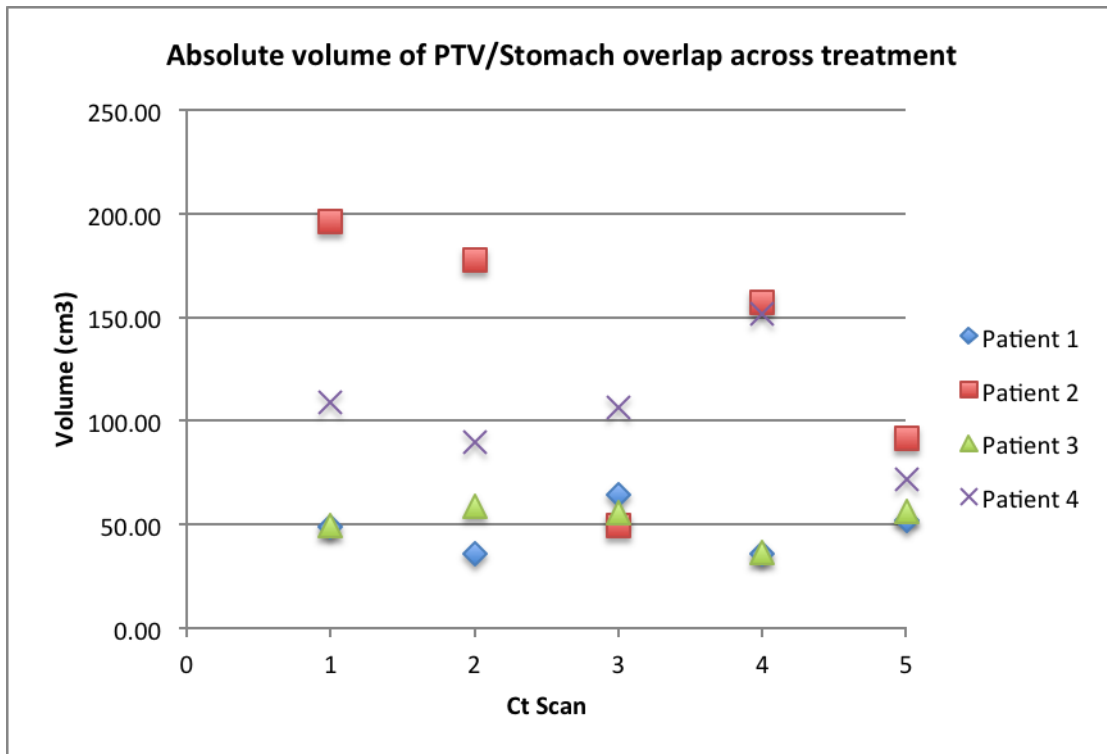


Figure 4.16 – Absolute volume of PTV/Stomach overlap across treatment

	Plan Volume	CBCT1	CBCT2	CBCT3	CBCT4
Patient 1	48.77	-26.51	+32.17	-26.58	+6.03
Patient 2	195.92	-9.38	-74.87	-19.63	-53.26
Patient 3	49.40	+18.93	+12.53	-26.30	+13.68
Patient 4	108.94	-17.84	-2.08	+38.99	-33.85

Table 4.12 - Percentage difference in PTV/stomach overlap volume between CBCT and planning image

The change in overlap volume between the stomach and PTV2 is shown in Figure 4.17. Table 4.13 shows the percentage difference in volume recorded with the CBCT scan compared to the planning scan.

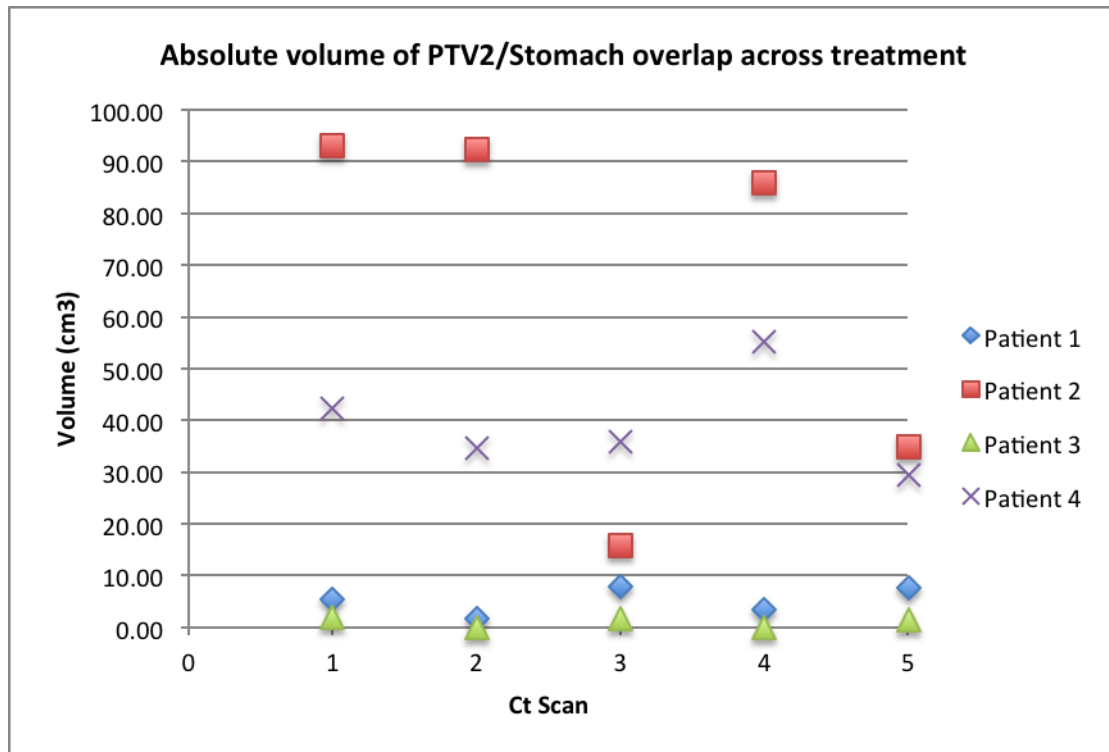


Figure 4.17 – Absolute volume of PTV2/Stomach overlap across treatment

	Plan Volume	CBCT1	CBCT2	CBCT3	CBCT4
Patient 1	5.32	-70.45	48.52	-37.72	42.77
Patient 2	93.12	-0.90	-83.13	-7.83	-62.64
Patient 3	1.84	-99.38	-4.05	-100.00	-16.67
Patient 4	42.23	-18.04	-15.27	30.86	-30.50

Table 4.13 - Percentage difference in PTV2/stomach overlap volume between CBCT and planning image

4.10 Discussion

This study quantified the inter-fraction movement of the stomach by utilising the planning CT and CBCT images. It is well recognised that the stomach continually changes volume and position during radiotherapy (137). Previous work has used endoscopically placed clips to try to quantify gastric movement, however these proved problematic by displacement during the course of RT (138). Fluoroscopy has also been used to identify the most superior, inferior, anterior, posterior and lateral

site of mucosal surface on film (139). In this study however I outlined the stomach on a treatment planning system and used a Matlab script to record the maximum and minimum xyz coordinates of the stomach structure in CT images taken across the course of radiotherapy treatment. It is clear that stomach movement is a combination of translations, rotations and changes in morphology (size and shape) therefore the difference in the maximum and minimum xyz coordinates of the outer limit of the structure together with the difference in COM coordinates gives a good indication of any change. The change in total volume of the stomach in each patient was also recorded. It was found that there was on average a 5.4mm, 6.7mm and 10.5mm displacement in the outer border (maximum) of the stomach for the x y and z coordinates respectively. For the COM there was a 4.0mm, 3.3mm and 8.7mm displacement in the x y and z coordinates respectively. In their study of six patients, Watanabe et al also found that there was increased movement in the z direction, recording an average inter fractional movement of 1.9mm, 1.5mm and 4.1mm in the x y z directions respectively for the COM. It is unclear why the movement recorded in their study should be larger than in this thesis, however a possible reason is the differing techniques in outlining the stomach. It is unclear from their publication how the COM was calculated for instance, and they also make assumptions that the stomach was rectangular parallel piped in shape.

In order to further ascertain the influence any change in stomach volume may have on the dose it receives and the plan in general, the change in total volume and overlap volumes between the stomach and PTV and PTV2 (high dose 60Gy) regions was calculated. For the total volume there was an average percentage change of 21.20% (0.38-64.86) between the volume of the stomach on the planning CT and

over the course of the CBCT images. The same average change was 29.38% (2.08-74.87) for the PTV/Stomach overlap volume and 41.80% (0.90-100) for the PTV2/Stomach overlap volume. Although the change in absolute volume for the overlap volumes may be small, Figures 4.8 & 4.9 show how a small change in volume can have an effect on NTCP value. This would indicate that the risk of toxicity to the patient is highly variable from one fraction to the next for the same patient dependent on the filling state of the stomach. In order to minimise the risk of toxicity to the patient it would be beneficial to reduce the volume of the stomach receiving a high dose and to keep this condition constant over the course of treatment. A stomach filling protocol could therefore aid the minimisation of risk of toxicity to the patient.

4.11 Conclusion

One aim of the overall project was to investigate the role of radiotherapy dose escalation in improving patient outcome. In this chapter, radiobiological modeling suggests that although increasing the prescribed dose to 60Gy is likely to improve tumour control, it may also be associated with a significantly increased risk of toxicity to the stomach within the boost volume. Results also suggest that the maximum prescribed dose safely achievable for each patient in the future may be dependent on the volume of the stomach within the treatment volume. This implies that the volume of the stomach is a clinical parameter that may affect patient outcome by increasing the risk of toxicity. By analysing the position of the stomach on CBCT images during treatment and comparing to that on the planning CT image the study was therefore extended to show that the position and volume of the

stomach of a patient is also highly variable. In order to minimise the risk of toxicity of the stomach during treatment using high dose regimes (>50Gy), and thereby improve treatment outcome a stomach filling protocol is recommended before each fraction. This has been taken forward in the SCOPE 2 trial, with the patient being required to fast for 2 hours and the drink 200mls of liquid prior to CT planning and treatment in an attempt to reproduce the same anatomical position of the stomach. As radiotherapy becomes more individualised, dose escalation may be more likely to be administered to a high-risk patient group, therefore any information that may aid the identification of a patient as having high or low risk of recurrence or spread will be beneficial. In the next chapter, an investigation in the emerging field of CT image texture analysis aims to contribute to this aspect of radiotherapy.

Chapter 5

Exploring the link between tumour heterogeneity and patient outcome

5.1 Introduction

Heterogeneity is a well recognised feature associated with adverse tumour biology (140). It has also been shown how heterogeneity is associated with variations in genomic subtypes, expression of growth and angiogenic factors and the tumoral microenvironment, which also result in regional variations within individual tumours in proliferation, cell death, metabolic activity and vascularity (141). Combining this information, tumour heterogeneity has also been associated with tumour grades (142).

Tumour heterogeneity can be assessed by imaging or biopsy, however the latter is invasive and can be difficult to obtain, while the former being until recently was limited to qualitative rather than quantitative analysis. However advances in image processing methods and computing software have allowed heterogeneity information to be extracted from medical images that may not be visible to the naked eye. Because of its availability and ease of use, the analysis of CT images is one relatively easy method of gaining heterogeneity information. In addition, as CT images are routinely taken as part of radiotherapy treatment, there should also not

be any further burden on the patient in acquiring this information. Other advantages include the relatively high levels of spatial resolution and reproducibility as well as the important consideration that the individual pixel intensity within a CT image directly reflects the physical density of the organs. Heterogeneity on CT can be assessed using texture analysis (TA), which quantifies the distribution of pixel values within a lesion. Using different filters, the two most important CT texture features that may be extracted are entropy and uniformity (143). Entropy is a measure of texture irregularity, whilst the uniformity is a measure of the gray level distribution within the tumour. A heterogeneous lesion would therefore be expected to show high entropy and low uniformity. According to a review paper by Alobaidli et al, the initial implementation of TA to predict patient survival was suggested by Ganeshan et al in 2007 (144). The method proposed has since resulted in a number of published studies from single centres investigating the role of TA in a range of tumour sites including non-small cell lung cancer and colorectal cancer ((145) & (146)).

Clinically, the ability to identify high-risk patients according to the heterogeneity of their planning CT images could be extremely beneficial. For example it could result in alternative treatment such as individualised radiotherapy dose escalation. The purpose of this study was therefore to analyse the CT heterogeneity of the planning CT images from the SCOPE 1 trial, and using the available outcome data, identify which heterogeneity parameters if any could be used to determine whether a patient was in a high or low risk group in terms of overall survival. To the author's knowledge this is the first investigation of its type to analyse data from a nationwide

multicentre clinical trial, rather than from a single centre.

Number of patients	Reasoning
179	Contrast administration data not available for 22 patients Centres = 34 Age in years (Mean = 70, Range: 40-88) Male (n=93), Female (n=86) Cetuximab (Yes(n=83), No(n=96)) Adenocarcinoma (n=46) Squamous Cell Carcinoma (n=133) Tumour Stage 1 (n=6) Tumour Stage II (n=37) Tumour Stage III (n=117) Tumour Stage IV (n=19)

Table 5.0 – Number of patients included in analysis in Chapter 5

5.2 Texture analysis of the SCOPE 1 data

The planning CT images of 179 patients from the SCOPE 1 database were analysed using a software package named TexRAD (TexRAD Ltd, Somerset, England, United Kingdom). This package was chosen due to it being the only commercially available software able to conduct the work required and work using the programme that had been published previously.

5.2.1 TexRAD software package

TexRAD is a sophisticated imaging risk stratification research tool that analyses the textures in existing radiological scans. Using a novel algorithm, it allows the user to analyse a region of interest (ROI) on a CT image, generating a number of parameters from that particular slice that may be associated with any aspect of patient outcome.

In addition to entropy, these parameters are shown in Table 5.1:

Parameter	Definition
Mean	The average value of all the pixels within the region of interest
Mean Positive Pixel (MPP)	The average value of all the positive pixels within the region of interest
SD	A measure of how much variation or "dispersion" exists from the average (mean value). A low standard deviation indicates that the data points tend to be very close to the mean; high standard deviation indicates that the data points are spread out over a large range of values.
Skewness	A measure of the asymmetry of the histogram. The skewness value can be positive or negative. A negative skew indicates that the tail on the left side of the histogram is longer than the right side. A positive skew indicates that the tail on the right side is longer than the left side. A zero value indicates that the values are evenly distributed on both sides of the mean.
Kurtosis	A measure of the "peakedness" of the histogram. The kurtosis value can be positive or negative. A positive kurtosis indicates a histogram that is more peaked than a Gaussian (normal) distribution. A negative kurtosis indicates that histogram is flatter than a Gaussian (normal) distribution.

Table 5.1 - TexRAD image analysis parameters

All the parameters shown in Table 5.1 can be acquired on a range of filters that are classified by the Spatial Scaling Factor (SSF). This approach uses the Laplacian of Gaussian band pass filters to highlight and enhance different spatial scales between fine and coarse textures (147) in a CT image, therefore providing a means of highlighting different aspects of tumour biology if required. In the TexRAD package the SSF range is from fine (2.0mm) to coarse (6.0mm). A lower SSF value (*e.g.* 2 mm) extracts and enhances features of a “finer” texture scale, whereas an SSF value of 3, 4 or 5 mm extracts and enhances features of a “medium” texture scale and a higher SSF value (*e.g.* 6 mm) extracts and enhances features of a “coarser” texture scale (148).

In addition to the texture analysis module, TexRAD has a separate ‘data miner’ module that allows the user to find and quantify relationships between the acquired heterogeneity parameters and patient outcome. There are a range of statistical analyses that can be undertaken on the data including correlations (Pearson) and Kaplan-Meier survival curve plotting.

The Kaplan-Meier plotting module has a function that finds the lowest p-value in the log rank test between two groups. This function was used in the analysis of heterogeneity parameters with survival data.

5.2.2 Considering contrast and cetuximab

An important consideration when analysing CT images is whether the image is acquired using a contrast-enhancing agent. Radio contrast agents, such as iodine or

barium, are a type of medical contrast medium used to improve the visibility of internal bodily structures. The SCOPE 1 radiotherapy protocol suggests that using an intravenous contrast agent may be useful in distinguishing the GTV from the surrounding structures. Typically between 75cc and 150cc of contrast is used depending on the patient's age, weight, cardiovascular health and the area being imaged. Once the agent has been injected it circulates through the blood stream and increases the attenuation of the x-rays creating the image, thereby making the areas in which contrast is present show up better on the recorded image. However, the resulting image will have different pixel gray values and therefore heterogeneity when compared to the same scan acquired without contrast. This would therefore have an impact on the values of the parameters being recorded. When analysing the SCOPE 1 database it was important therefore to take the administration of contrast into account. As the data miner in the TexRAD software package is unable to stratify any survival data analysis according to a particular variable, the only way to compensate for contrast was to split the database into patients with and without contrast.

In addition, as with previous analysis involving survival data in Chapter 3, the administration of cetuximab to each patient must be considered due to its effect on a patient's outcome.

5.2.3 Importing GTV outlines

The TexRAD package allows a user to either manually outline a ROI or import from

an external source as an extensible markup language (XML) file. This study was an analysis of the SCOPE 1 database where a suitable ROI, the GTV, had already been outlined by the clinicians treating the patients. A workflow was therefore required to convert the GTV outline structure from the DICOM files received by the centres to an XML file suitable for import into TexRAD.

The key to this process was identifying a suitable program that allowed the user to export a single ROI slice as an XML file for import into TexRAD. Discussions with colleagues resulted in the OsiriX software package being used for this purpose, however there was still a substantial amount of preparation work required.

The resulting workflow for creating a single ROI slice and importing to TexRAD was as follows:

1. Import raw DICOM files into CERR
2. Delete all structures other than GTV
3. Identify central slice of GTV and delete all other slices
4. Save and export as new DICOM file
5. Delete RTDose file
6. Import and load new DICOM file into OsiriX (CT and RTStruct only)
7. Export single GTV slice as XML file
8. Manually alter XML file from OsiriX format to TexRAD format in XMLSpear
9. Find correct image slice of patient on TexRAD
10. Import and check position of GTV on image slice

Manually altering the XML file

Step 8 was crucial in getting the above workflow to work. This section shows this process in more detail. Testing was carried out on the PTV structure.

Figure 5.1 shows the PTV structure of a patient as imported into the Osirix program.

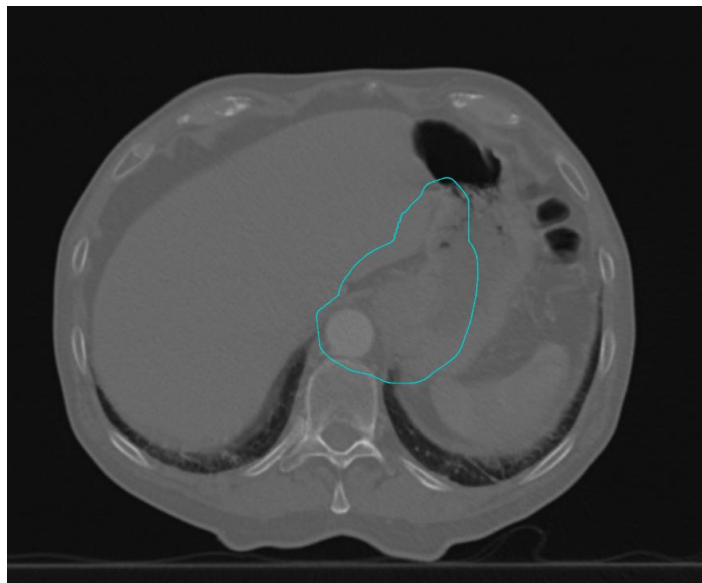


Figure 5.1 – PTV outline in OsiriX

Exporting the PTV structure as an XML file results in the following XML file (Figure 5.2)

```

1 <?xml version="1.0" encoding="UTF-8"?>
2 <!DOCTYPE plist PUBLIC "-//Apple//DTD PLIST 1.0//EN" "http://www.apple.com/DTDs/PropertyList-1.0.dtd">
3 <plist version="1.0">
4   <dict>
5     <key>Images</key>
6     <array>
7       <dict>
8         <key>ImageIndex</key>
9         <integer>79</integer>
10        <key>NumberOfROIs</key>
11        <integer>1</integer>
12        <key>ROIs</key>
13        <array>
14          <dict>
15            <key>Area</key>
16            <real>13.04776668548584</real>
17            <key>Center</key>
18            <string>(26.412821, -214.208466, -548.000000)</string>
19            <key>Dev</key>
20            <real>41.335281372070312</real>
21            <key>IndexInImage</key>
22            <integer>0</integer>
23            <key>Length</key>
24            <real>13.516459465026855</real>
25            <key>Max</key>
26            <real>138</real>
27            <key>Mean</key>
28            <real>40.330146789550781</real>
29            <key>Min</key>
30            <real>-117</real>
31            <key>Name</key>
32            <string>CTV</string>
33            <key>NumberOfPoints</key>
34            <integer>13</integer>
35            <key>Point_mm</key>
36            <array>
37              <string>(35.517075, -232.447800, -548.000000)</string>
38              <string>(44.343567, -230.040573, -548.000000)</string>
39              <string>(47.553207, -222.016510, -548.000000)</string>
40              <string>(45.145966, -212.788834, -548.000000)</string>
41              <string>(40.732742, -201.956329, -548.000000)</string>
42              <string>(34.313488, -192.327438, -548.000000)</string>
43              <string>(27.091812, -191.525024, -548.000000)</string>
44              <string>(18.666553, -194.333450, -548.000000)</string>
45              <string>(6.630421, -208.776779, -548.000000)</string>
46              <string>(1.013565, -215.998444, -548.000000)</string>
47              <string>(4.624414, -222.417709, -548.000000)</string>
48              <string>(15.858126, -229.238174, -548.000000)</string>
49              <string>(21.876167, -230.843002, -548.000000)</string>
50            </array>
51            <key>Point_px</key>
52            <array>
53              <string>(301.461853, 231.106812)</string>
54              <string>(312.759766, 234.188065)</string>
55              <string>(316.868103, 244.458862)</string>
56              <string>(313.786835, 256.270294)</string>
57              <string>(308.137909, 270.135895)</string>
58              <string>(299.921265, 282.460876)</string>

```

Figure 5.2 – XML output from OsiriX

Initially it was thought that the first set of x y z coordinates (e.g. 35.517075, -232.447800, -548) were required for translation to the TexRAD environment. However using those coordinates resulted in the following orientation of the structure when imported into TexRAD (Figure 5.3)

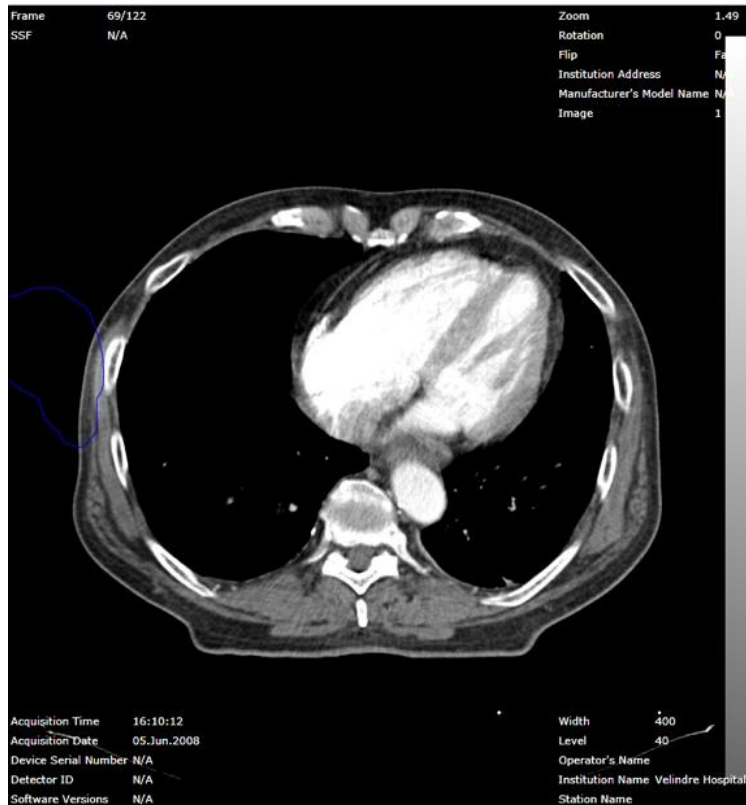


Figure 5.3 – In correct orientation of structure in TexRAD

Figure 5.3 shows how the structure is not orientated correctly when compared to the original structure in OsiriX. The structure is flipped and is also smaller relative to the original.

Using the 'Point_px' coordinates (e.g. 301.461853, 231.16812) however resulted in the correct orientation of the structure in TexRAD. By using these coordinates and arranging them in the XML format required by TexRAD (Figure 5.4), it can be seen in Figure 5.5 how the structure is imported correctly on to the appropriate slice. No Z coordinate is needed as the structure is imported manually on to the appropriate slice.

```

1 <?xml version="1.0" encoding="utf-8"?>
2 <ANNOTATION IsAccuracyLimited="True" AccuracyFormat="0.##">
3   <OBJECT Id="0" Name="ROI_0" Guid="dd961e39-cb03-40cc-907f-776828247fb6"
4     ImageUID="1.3.12.2.1107.5.1.4.49304.3000008060509025976500001615"
5     StudyUID="1.3.12.2.1107.5.1.4.49304.3000008060508534418700000037"
6     IsTexRADRegion="True" Type="ROI" Shape="polygon" IsPixelRatioDefault="True">
7     <GEOM>
8       <FIGURES>
9         <FIGURE>
10          <SEGMENTS>
11            <SEGMENT Type="PLine">
12              <POINTS>
13                <P>
14                  <X>301.461853</X>
15                  <Y>231.106812</Y>
16                </P>
17                <P>
18                  <X>312.759766</X>
19                  <Y>234.188065</Y>
20                </P>
21                <P>
22                  <X>316.868103</X>
23                  <Y>244.458862</Y>
24                </P>
25                <P>
26                  <X>313.786835</X>
27                  <Y>256.270294</Y>
28                </P>
29                <P>
30                  <X>308.137909</X>
31                  <Y>270.135895</Y>
32                </P>
33                <P>
34                  <X>299.921265</X>
35                  <Y>282.460876</Y>
36                </P>
37                <P>
38                  <X>290.677521</X>
39                </P>
40                <P>
41                  <X>276.298401</X>
42                  <Y>235.215134</Y>
43                </P>
44                <P>
45                  <X>284.001495</X>
46                  <Y>233.160965</Y>
47                </P>
48              </POINTS>
49            </SEGMENT>
50          </SEGMENTS>
51        </FIGURE>
52      </FIGURES>
53    </GEOM>
54  </OBJECT>
55 </ANNOTATION>

```

Figure 5.4 – TexRAD XML format

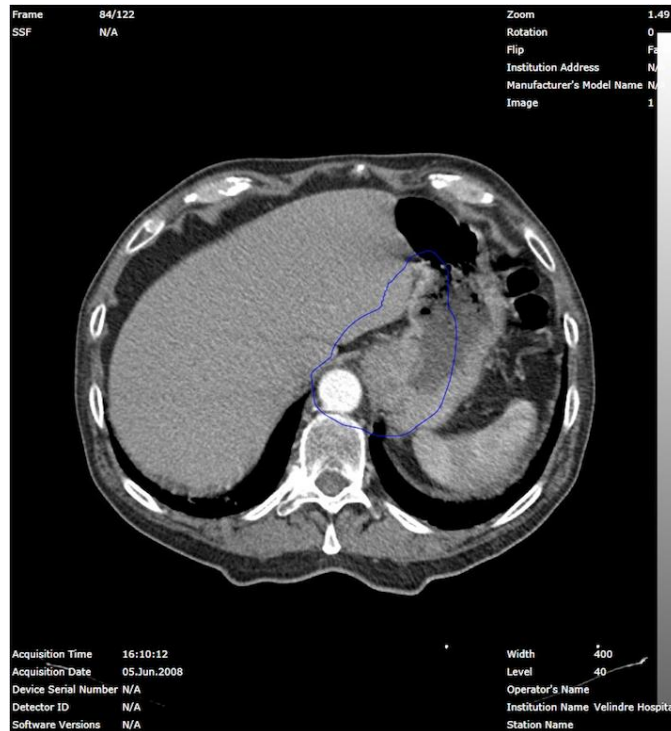


Figure 5.5 – Correct import of structure into TexRAD

The manual manipulation of each separate XML file for a large database of patients such as the SCOPE 1 trial would be extremely time consuming. Therefore, once the correct format of the XML file required was known the process of creating the files was automated in MatLab. The automated version works slightly differently by creating the XML files directly from the CERR file for each patient. The script writes an XML files for each slice of the required structure (in this case the GTV) and saves them in a folder on the user's computer. The user can then select which slice to upload into the TexRAD software. For this study, the central slice of the GTV was selected however where a central slice was not possible, for consistency the most superior slice from the centre of the GTV was always chosen.

5.2.4 Texture analysis algorithm settings for oesophageal cancer

TexRAD allows the user to specify the algorithm to analyse the ROI. The pre-set algorithms are as follows:

- ‘Liver’ - Includes only pixels between 0-300 HU within ROI after erosion for reducing edge artefacts in the case of large organ - Liver
- ‘Lung’ - Includes only pixels above -50HU within ROI after erosion for reducing edge artefacts in the case of lung tumours
- ‘Small Tumour’ - Includes only pixels above -50HU within ROI after erosion for reducing edge artefacts in the case of small tumours
- ‘Phantom’ - Includes all pixels (no thresholds) within ROI after erosion for reducing edge artefacts in the case of CT phantom studies

However there was no pre-set algorithm for the analysis of oesophageal tumours therefore this required the creation of a ‘custom’ setting. After consultation with the developers of TexRAD it was decided to use the settings of analyzing Hounsfield Units from -50 to infinity. Setting from -50 to 200 HU may exclude calcification of the oesophagus but discussions with the Chief Investigator of the SCOPE 1 trial stated that this would not be an issue with this dataset as calcification had not be observed.

5.2.5 Analysed sample size

179 patients’ DICOM images were imported into the TexRAD database. 22 patients were excluded from the whole SCOPE database of 201 patients due to their contrast

administration data being unavailable.

Initially, analysis was carried out on two groups; those patients who were imaged using contrast and those who were not. To take into account both the use of contrast and the administration of cetuximab, the database was then split into 4 sub groups (Table 5.2).

	Cetuximab	Contrast	Number of patients
Group 1	0	1	64
Group 2	1	1	57
Group 3	0	0	29
Group 4	1	0	29

Table 5.2 – Sub Groups of patients

5.3 Results

5.3.1 Texture analysis in TexRAD

All parameters in Table 5.3 including entropy were analysed for their impact on overall survival using SSF values of 2-6mm. Results for patients imaged with contrast (121 patients):

SSF2	Cut Off	P-value	Log-Rank	Upper	Lower
Entropy	>5.355	0.0098	6.6801	77	44
MPP	<93.485	0.0236	5.1264	95	26
Skewness	>2.63	0.0017	9.8669	12	109
Kurtosis	>10.89	0.0044	8.1287	11	110
SSF3	Cut off	P-value	Log-Rank	Upper	Lower
Entropy	>5.445	0.0081	7.0032	78	44
SSF4	Cut off	P-value	Log-Rank	Upper	Lower
Entropy	>5.565	0.0028	8.9124	75	47
MPP	<169.87	0.0306	4.68	94	28
SSF5	Cut off	P-value	Log-Rank	Upper	Lower
Entropy	>5.61	0.0142	6.0089	73	49
Kurtosis	>-0.825	0.0484	3.9003	109	13
SSF6	Cut off	P-value	Log-Rank	Upper	Lower
Entropy	>5.195	0.0187	5.5293	100	22
Kurtosis	>-0.71	0.0097	6.6847	102	20

Table 5.3 – Statistically significant results for all patients imaged with contrast

Table 5.3 shows the statistically significant parameters for all patients imaged using contrast. The cut off indicates the patient group with worse survival. For example using the SSF2 filter, patients with an entropy value higher than 5.355 had worse survival than those with a value lower than 5.355. The upper and lower columns refer to the number of patients either side of the cut off point. The results show how entropy (highlighted in blue) is significant using all SSF filters.

Results for patient not imaged with contrast (58 patients):

SSF2	Cut off	P-value	Log-Rank	Upper	Lower
SD	<277.86501	0.0309	4.6625	15	43
Skewness	>2.3	0.0003	12.8114	22	36
Kurtosis	>17.85500	0.0037	8.4059	4	54
SSF3	Cut off	P-value	Log-Rank	Upper	Lower
Mean	>30.03	0.042	4.139	47	10
SD	>386.045	0.0233	5.1516	12	45
Skewness	>1.395	0.0057	7.6476	32	25
Kurtosis	>7.7	0.0018	9.7945	9	48
SSF4	Cut off	P-value	Log-Rank	Upper	Lower
Mean	>42.875	0.0258	4.9737	45	12
Skewness	>1.115	0.016	5.8027	28	29
Kurtosis	>5.475	0.0023	9.2726	5	52
SSF5	Cut off	P-value	Log-Rank	Upper	Lower
Kurtosis	>3.915	0.0269	4.9018	4	53
SSF6	Cut off	P-value	Log-Rank	Upper	Lower
Mean	<576.39499	0.0382	4.3019	9	48
SD	<459.36	0.0459	3.9899	6	51

Table 5.4 – Statistically significant results for all patients not imaged with contrast

Table 5.4 shows the statistically significant result for all patients not imaged with contrast. The key result in this table is that Kurtosis (highlighted in green) is statistically significant for SSF2-5 whilst Skewness (highlighted in cyan) is significant for SSF2-4.

Group 1

SSF2	Cut Off	P-value	Log-Rank	Upper	Lower
Entropy	>5.225	0.02	5.41	49	15
MPP	<93.485	0.04	4.07	49	15
Skewness	>2.61	0.01	5.93	8	56
Kurtosis	>10.85	0.02	5.68	6	58
SSF3	Cut off	P-value	Log-Rank	Upper	Lower
Mean	<157.01	0.03	4.53	18	47
Entropy	>5.39	0.02	5.79	46	19
SSF4	Cut off	P-value	Log-Rank	Upper	Lower
Mean	<145.445	0.03	4.75	25	40
Entropy	>5.575	0.02	5.49	41	24
SSF5	Cut off	P-value	Log-Rank	Upper	Lower
Mean	<320.505	0.03	4.57	14	51
Kurtosis	>0.195	0.02	5.89	45	20
SSF6	Cut off	P-value	Log-Rank	Upper	Lower
Mean	<347.1299	0.02	5.10	15	50
MPP	<387.58	0.02	5.19	27	38
Kurtosis	>-0.66	0.03	4.84	55	10

Table 5.5 – Statistically significant results for patients imaged with contrast and not administered cetuximab

Table 5.5 shows that entropy (highlighted in blue) is a significant predictor for SSF2-4 for contrast enhanced patients not administered with cetuximab.

Group 2

SSF2	Cut off	P-value	Log-Rank	Upper	Lower
Entropy	>5.695	0.01	6.14	12	45
Skewness	>2.26	0.04	4.43	8	49
SSF3	Cut off	P-value	Log-Rank	Upper	Lower
Entropy	>5.955	0.00	9.54	7	50
SSF4	Cut off	P-value	Log-Rank	Upper	Lower
Mean	>260.965	0.05	3.98	16	41
Entropy	>6.095	0.00	12.04	8	49
SSF5	Cut off	P-value	Log-Rank	Upper	Lower
Mean	>166.22	0.04	4.34	30	27
SD	>351.535	0.04	4.27	30	27
Entropy	>6.11	0.00	8.75	9	48
SSF6	Cut off	P-value	Log-Rank	Upper	Lower
Mean	>266.73999	0.02	5.22	20	37
SD	>355.0551	0.01	6.22	29	28
Entropy	>5.91	0.00	8.65	18	39

Table 5.6 – Statistically significant results for patients imaged with contrast and administered cetuximab

Table 5.6 shows that entropy (highlighted in blue) is a significant predictor for all SSF filters for contrast enhanced patients who were administered with cetuximab.

Group 3

SSF2	Cut off	P-value	Log-Rank	Upper	Lower
Skewness	>2.3	0.00	9.42	11	18
Kurtosis	>5.61	0.03	4.66	17	12
SSF3	Cut off	P-value	Log-Rank	Upper	Lower
Skewness	>1.92	0.01	6.10	9	20
Kurtosis	>7.945	0.02	5.67	5	24
SSF4	Cut off	P-value	Log-Rank	Upper	Lower
Skewness	>1.115	0.01	7.80	16	13
Kurtosis	>5.475	0.00	8.40	4	25
SSF5	Cut off	P-value	Log-Rank	Upper	Lower
Skewness	>0.67	0.02	5.31	18	11
Kurtosis	>3.25	0.05	3.95	5	24

Table 5.7 – Statistically significant results for patients not imaged with contrast and not administered cetuximab

Table 5.7 shows that skewness and kurtosis (highlighted in cyan and green

respectively) are significant predictors for all SSF filters for non-contrast enhanced patients who were not administered with cetuximab.

Group 4

SSF2	Cut off	P-value	Log-Rank	Upper	Lower
Skewness	>2.535	0.03	4.62	9	20
Kurtosis	>13.38	0.02	5.05	5	24
SSF3	Cut off	P-value	Log-Rank	Upper	Lower
Mean	>56.385	0.04	4.18	20	8
SSF4	Cut off	P-value	Log-Rank	Upper	Lower
Mean	>51.735	0.04	4.18	20	8
SSF5	Cut off	P-value	Log-Rank	Upper	Lower
Mean	>39.45	0.04	4.18	20	8

Table 5.8 – Statistically significant results for patients not imaged with contrast and administered cetuximab

Table 5.8 shows that skewness and kurtosis (highlighted in cyan and green respectively) are a significant predictor for only SSF2 for non-contrast enhanced patients who were administered with cetuximab.

5.3.2 Multivariate analysis

The entropy values calculated for each patient from group 1 were included with the clinical factors of age and tumour staging (the most statistically significant factors identified in Section 3.7) in a multivariate logistic regression analysis in SPSS. The results are shown in Table 5.9

Variable	Regression Coefficient	Standard Deviation	P-value
Stage	1.952	0.125	<0.001
Age	1.032	0.01	0.002
Entropy	0.832	0.159	0.248

Table 5.9 – Multivariate analysis

The results show how entropy does not remain statistically significant when included with tumour staging and patient age.

5.4 Discussion

The hypothesis of this study was that CT image heterogeneity parameters from a clinical trial based patient cohort can be used as prognostic factors for patient outcome. The SCOPE 1 database was therefore uploaded to a specific texture analysis software package that would allow the relationship between CT heterogeneity parameters and patient outcome to be explored. The original GTV outlines were imported and the CT image heterogeneity within these structures analysed using a number of parameters. The use of contrast for imaging was taken into account by splitting the database according to whether contrast was used or not. It is clear from the results that contrast has an effect on the heterogeneity, as the statistically significant parameters are dependent on whether contrast was administered prior to acquiring the CT images. For patients scanned using contrast, entropy was statistically significant using all SSF filters (Table 5.3), whilst for patients scanned with no contrast, entropy was not significant using any filters, although kurtosis was significant for SSF levels 2, 3, 4 and 5 (Table 5.4). Skewness was also statistically significant for SSF 2, 3 and 4. However as with the other studies in this

thesis that included survival data, it was vital to take into account the administration of cetuximab when undertaking the analysis. The database was therefore further stratified according to cetuximab administration. The results in tables 5.5-5.8 show that the administration of cetuximab also had an influence on the statistically significant heterogeneity parameters that were found. For example in the contrast group, entropy remained significant using all SSF filters for patients who were administered cetuximab but was only significant for SSF 2, 3 and 4 when cetuximab was not administered. Similarly for patients not imaged with contrast, skewness and kurtosis remained significant for all SSF levels when no cetuximab was administered, but was only significant for SSF 2 when cetuximab was administered. Although it is interesting that the administration of cetuximab has an influence on CT heterogeneity parameters, and may confirm its effect on the biology of the tumour volume, it does not appear to have a clinically meaningful beneficial effect. The conclusion of the SCOPE 1 trial was that cetuximab is not recommended for use in patients with oesophageal cancer (56), therefore it is unlikely to be used again in the future. It is only the results of the patients not administered cetuximab that are therefore relevant for further discussion. In addition, there were considerably more patients scanned using contrast than without (121 compared to 58). This would suggest that the most clinically relevant group in this analysis is Group 1, where contrast is used but no cetuximab is administered. The key result of this group was that the entropy value of a patient's planning CT image was a statistically significant predictor of the patient's overall survival. The most statistically significant result for entropy was using SSF4, with a cut off value of 5.575 and $p=0.0191$. Yip et al also found entropy to be a statistically significant predictor of survival in a similar study of

patients with oesophageal cancer. Their retrospective study consisted of 36 patients from a single centre, all of whom were imaged with a contrast enhanced CT scan before and after CRT treatment. The chemotherapy regime differed in that patients received Cisplatin and 5-Fluorouracil (5-FU) compared to Cisplatin and Capecitabine in the SCOPE 1 trial. These differences in CRT regime, and the number of patients and centres may explain why the significant entropy cut off values found in their study of 7.356 and 7.116 for the medium and coarse filters respectively were higher than those found using the larger multicentre database here. Ganeshan et al also found a link between CT heterogeneity parameters and patient survival, albeit only with uniformity (149). Again, this was a relatively small database of 21 patients and patients were not scanned using contrast enhanced CT.

When included in a multivariate cox regression analysis with age and tumour staging data, entropy did not remain significant. This may indicate that there is a strong correlation between the entropy parameter and tumour staging and age. In a clinical setting however, TA derived heterogeneity parameters are unlikely to be used as singular prognostic factors of outcome. Therefore although entropy is not significant in a multivariate model, it may still be useful in improving the depth of information on which a clinical decision is made.

A strong point of this study is that the analysed database is from a national multi-centre clinical trial, with some standardization of the radiotherapy planning scan parameters. However, it should be noted that this may also have a detrimental effect on the results due to the number of individual CT scanners (30 centres) used to collect the images for the patients. It has been shown previously that there is a

variation in image settings between the same model of CT scanner in different centres (150). This may be exacerbated in this study due to the nationwide nature of the database and that a variety of CT scanner models will have been used across the centres. The study is also limited by the fact that analysis using the TexRAD package is limited to that of a single slice of the GTV rather than the whole volume. Discussions with clinical colleagues concluded that the heterogeneity of a tumour is likely to not be uniform across its whole volume. As such the TA parameters will also likely be different depending on which section of the tumour is analysed. It is essential that this aspect be investigated further and the influence of single slice vs whole volume analysis confirmed.

The field of TA of diagnostic images is however relatively young; for example at the time of writing, a PubMed search of the combined words 'CT', 'Texture', 'Analysis' and 'Outcome' returned 23 documents. A considerable amount of work still needs to be carried out in order to establish the exact relationship between TA parameters and patient outcome. The review article by Chalkidou et al concludes that there is currently insufficient evidence to fully support a relationship between texture features and patient survival (151). In the case of the work presented in this thesis, the statistically significant parameters would need validating on a similar data set if one were to come available. The forthcoming SCOPE 2 trial may provide an opportunity for this work.

5.5 Conclusion

Although the exact value of the cut off in entropy value may differ between studies, these results show the potential of texture analysis to provide clinically meaningful information. The results of the multivariate analysis also suggest that heterogeneity parameters may not be suitable as individual predictors of outcome. The application and use of texture analysis in clinical practice is still exploratory in nature, but the clinical trial nature of the database in this study adds significant weight to the evidence that CT heterogeneity parameters can be useful as potential predictors of patient outcome. This work differs slightly from those in previous chapters by establishing a relationship between a diagnostic element of radiotherapy and outcome rather than the dose delivery aspect of treatment. In the future, this may allow high-risk patients to be identified and their treatment modified or individualized.

Chapter 6

Conclusions and further work

6.1 Conclusions

The work contained within this thesis has concentrated on relating quantifiable parameters associated with the treatment of oesophageal cancer with patient outcome. In all, three main original contributions to research were made that together succeeded in meeting the aims and objectives of the study as set out in Section 1.9. In Chapter 3 a conformity index was used as a quality metric of the planned dose distribution for each individual patient. It was shown in a univariate analysis that the relationship between the 95% isodose and the PTV was significantly associated with patient survival. In addition, it was shown how the quality of the dose distribution could be improved by delivering the radiotherapy dose using the VMAT technique rather than the 3D-CRT technique that most patients in the trial received. Although the relationship between dose distribution and outcome did not remain significant when included in a multivariate analysis with other biological and clinical factors, the study suggests that the quality of the dose distribution may have a greater impact on patient outcome than thought previously. The work also suggests that using the VMAT technique offers a safer tool for dose escalation, therefore this aspect of the study was carried forward to Chapter 4. Here, as part of

important preparatory work for a forthcoming clinical trial, TCP and NTCP modelling was used to quantify the relationship between the dose received by the tumour and its effect on treatment outcome in terms of both tumour control and normal tissue toxicity. The study was centred on dose escalation for patients suffering from lower oesophageal cancer as the possible increased risk to the stomach in these patients was unknown. By comparing three different planning methods, the results show that the probability of tumour control is increased with higher doses. However, depending on the volume of the overlap of the stomach with the high dose region of the plan there may also be considerable increased risk of stomach toxicity for patients when the prescription dose to the tumour is escalated. Although further work showed that the change in volume of the overlap over the course of treatment was small, any variation could still impact on the risk of toxicity. Including a protocol to minimise stomach volume during treatment may therefore improve patient outcome. A similar conclusion was found in the dose escalation study on mid oesophageal patients, where it was reported that dose escalation was feasible depending on the amount of overlap between the lung and the PTV. Both of these studies suggest that as radiotherapy moves towards dose escalation, there may be additional differential issues such as these to consider compared to previous planning techniques and dosing regimes. However in both instances, the increased likelihood of toxicity is almost certainly justified if the increased tumour control is achieved. Finally, a software package was utilised that allowed the relatively new found relationship between heterogeneity parameters of CT images and patient outcome to be explored. Previous work in the literature has shown this relationship to be statistically significant however these studies were confined to single centres.

The study undertaken in Chapter 5 is therefore the first to expand this type of analysis to data from a nationwide clinical trial. By analysing the area of interest originally outlined for treatment during RT the results confirm and strengthen those found previously in the literature. Although CT heterogeneity parameters are unlikely to be used as independent identifiers of patient outcome in a clinical setting, they can be generated from images already acquired as part of routine RT treatment. This means they are a relatively easy method of improving the depth of information on which a clinical treatment decision is based and its effect on treatment outcome. This type of analysis is comparatively new in nature and confidence and certainty in the results and how to best use them will grow as the field matures.

As the treatment of cancer becomes increasingly personalised, the ability to identify both clinical and technological parameters that affect an individual patient's outcome will become progressively more important. The author hopes that the work contained within this thesis goes some way to contributing in this regard.

6.2 Further work

There are several areas investigated within this study that open up the possibility of further work. In Chapter 3, the investigation was carried out on patients whose radiotherapy dose was planned using Type B algorithm. This was due to the increased accuracy of the dose calculation in and around areas of low density tissue such as the lung when compared to those planned using Type A algorithms. It could be possible to increase the power of this study, or alternatively provide a validation dataset, by re-calculating the RT plans of the 109 Type A patients with a Type B

algorithm. However this would mean that half the resulting database of plans was calculated using only the specific algorithm and TPS available at the author's centre. More importantly, as the treatment planning system of each centre that participated in the SCOPE 1 trial is dosimetrically matched to their local linear accelerators, a re-calculated plan at the author's centre would not give a correct representation of the actual dose received by the patient. This would mean that the outcome data did not match the dose distribution being analysed and might skew the results and eliminate any confidence in the conclusions. A possible solution would be to contact the centres at which the patients were planned in order to gain the required information or to ask the centre themselves to re-calculate using a Type B algorithm and send the DICOM data for analysis. The work on dose escalation in Chapter 4 is being taken forward in the SCOPE 2 clinical trial and will go some way towards addressing the role of dose escalation for oesophageal cancers. As a result of the work on gastric movement, a stomach filling protocol is being added to the SCOPE 2 trial protocol. It would be beneficial to therefore explore the same movement parameters after the inclusion of this protocol to confirm its effect on gastric movement and positional consistency. The modeling work could be expanded to include an analysis of spot scanning proton planning similar to the work carried out by Warren et al on mid-oesophageal patients (152). It is possible that the use of proton planning in treating lower oesophageal cancer patients could reduce the risk of toxicity to the stomach due to the nature of the Bragg peak absorption curve in the body. However the main limiting factor is the volume of stomach within the high dose region, therefore identifying or designing a suitable pre-treatment planning protocol to reduce this should be the priority. Finally, the work in Chapter 5 was conducted on a single slice

of the GTV. The work will therefore be expanded to investigate how the TA parameters may change over the length of the tumour. It would also be extremely interesting to apply the CT heterogeneity analysis software used in Chapter 5 to CBCT images acquired during the course of RT treatment. It may be possible to observe a change in the biology of the tumour during treatment, which could result in treatment being adjusted to improve the outcome of the patient. Although the inferior image quality of CBCT compared to RT planning CT scans will likely need overcoming in a clinical setting, initial results by Fave et al and van Timmeren et al on lung cancer have been promising (153) & (153). This could therefore be further explored in oesophageal cancer using the SCOPE 1 database. The results of this chapter should also be validated on a similar dataset. The forthcoming SCOPE 2 trial may therefore provide an opportunity for this work. Other oesophageal trials such as NeoScope would also be suitable. However with both of these datasets, as was the case with the SCOPE 1 trial in this thesis, the patient cohort would have to be split according to the treatment parameter that affects overall patient survival reducing the overall power of the analysis.

Dissemination of work and attended courses, seminars and conferences

7.1 Publications

Journal Papers

Relating CT heterogeneity parameters and patient outcome in the SCOPE 1 oesophageal cancer trial

Rhys Carrington, Emiliano Spezi, Sarah Gwynne, John Staffurth, Thomas Crosby
(In preparation)

The influence of dose distribution on treatment outcome in the SCOPE 1 oesophageal cancer trial

Rhys Carrington, Emiliano Spezi, Sarah Gwynne, Peter Dutton, Chris Hurt, John Staffurth, Thomas Crosby
January 2016 · *Radiation Oncology* 1/2016; 11(1).

The effect of dose escalation on gastric toxicity when treating lower oesophageal tumours: a radiobiological investigation

Rhys Carrington, John Staffurth, Samantha Warren, Mike Partridge, Chris Hurt, Emiliano Spezi, Sarah Gwynne, Maria A. Hawkins, Thomas Crosby
December 2015 · *Radiation Oncology* 12/2015; 10(1).

Radiobiological determination of dose escalation and normal tissue toxicity in definitive chemoradiation therapy for esophageal cancer

Samantha Warren, Mike Partridge, Rhys Carrington, Chris Hurt, Thomas Crosby, Maria A. Hawkins

International journal of radiation oncology, biology, physics 10/2014; 90(2):423-429.

Conference abstracts

EP-1632: Should dose escalation in oesophageal cancer be re-visited? A radiobiological analysis

S.Warren, M.Partridge, M.Hawkins, R.Carrington, T.Crosby, C.N.Hurt

Radiotherapy and Oncology 12/2014; 111:S218.

EP-1583: An analysis of the dose distribution in the SCOPE 1 oesophageal cancer trial data

R.Carrington, E.Spezi, S.Gwynne, P.Dutton, C.Hurt, J.Staffurth, T.Crosby

Radiotherapy and Oncology 12/2014: 111:S196-S197.

EP-1470: Does gastric toxicity influence dose escalation in lower oesophageal tumours? A radiobiological investigation

J.Staffurth, R.Carrington, S.Warren, M.Partridge, C.Hurt, E.Spezi, S.Gwynne,

M.Hawkins, T.Crosby

Radiotherapy and Oncology 04/2015; 115:S797-S798.

PO-0986: Can radiotherapy dose distribution be related to outcome? An analysis of the SCOPE 1 oesophageal cancer trial data

R.Carrington, E.Spezi, S.Gwynne, P.Dutton, C.Hurt, T.Crosby, J.Staffurth

Radiotherapy and Oncology 04/2015; 115:S526-S527.

TH-AB-304-11: The influence of radiotherapy treatment method on dose distribution and its relation to patient outcome in the SCOPE 1 oesophageal cancer trial using Type B algorithms.

R.Carrington, E.Spezi, S.Gwynne, P.Dutton, C.Hurt, T.Crosby, J.Staffurth

Medical Physics (Impact Factor: 2.64). 06/2015; 42(6):3703.

SU-E-T-69: A radiobiological investigation of dose escalation in lower oesophageal tumours with a focus on gastric toxicity

R.Carrington, J.Staffurth, S.Warren, M.Partridge, E.Spezi, S.Gwynne, M.Hawkins,

T.Crosby

Medical Physics 06/2015; 42(6):3346.

7.2 Attended courses, seminars and conferences

Courses attended at Cardiff University

- Biomedical Research Techniques (October – December 2012)
- How to write a literature review (January 2013)
- Endnote: An introduction (March 2013)
- Matlab: An introduction (June 2013)

- Effective Researcher: Effective Progress – The Second Year

Courses attended elsewhere

- ESTRO course in Quantitative Methods in Radiation Oncology, Cambridge, UK (September 2013)

Conferences and seminars attended

- CRW symposium, Swalec Stadium, Cardiff, March 2013, (Poster presentation)
- Departmental Seminar, Velindre Cancer Centre, Cardiff, May 2013 (Oral presentation)
- UKRO, Nottingham, October 2013 (Poster presentation)
- ESTRO, Vienna, April 2014 (Poster presentation)
- MPCE, Cardiff, June 2014 (Oral presentation)
- NCRI, Liverpool, November 2014 (Poster presentation)
- ESTRO, Barcelona, April 2015 (Poster presentation)
- UKRO, Coventry, June 2015 (Oral and poster presentation)
- AAPM, Anaheim, Los Angeles, July 2015 (Oral and poster presentation)
- ESTRO, Turin, May 2016 (Poster presentation)

Appendix

A1 Computer Coding

```
function p=logranktest(tA,cA,tB,cB)
% log rank risk for survival (two variables only)
% written by Issam ElNaqa, 02/03
tt=[tA,tB];
ct=[cA',cB'];
lA=length(tA); lB=length(tB);
nt = length(tt);
[tt,ind] = sort(tt); % should in ascending order
ct = ct(ind);
ft = ones(1,nt);
totcumfreq = nt-cumsum(ft)+1;
qt=ct./totcumfreq;
nAc=lA;
nBc=lB;
for i=1:nt
    nA(i)=nAc;
    nB(i)=nBc;
    if (ind(i)<=lA)
        nAc=nAc-1;
    else
        nBc=nBc-1;
    end
end
EA=sum(nA.*qt);
EB=sum(nB.*qt);
OA=sum(cA);
OB=sum(cB);
testA=(OA-EA)^2/EA;
testB=(OB-EB)^2/EB;
logtest=testA+testB;
p=1-max(min(gammainc(logtest/2,1/2),1),0); % chi2 by integrating
gamma.
HazardRatio=((OA/EA)/(OB/EB))/2;
```

Figure A1 – Script for computing Hazard Ratio

A2 SCOPE 1 Radiotherapy Protocol

SCOPE 1

Radiotherapy Treatment Planning and Delivery

SCOPE 1: Study of Chemoradiotherapy in Oesophageal Cancer Plus or Minus Erbitux

A randomised phase II/III multi-centre clinical trial of definitive chemo-radiation, with or without Cetuximab, in carcinoma of the oesophagus

RADIOTHERAPY GUIDANCE and PROCEDURES

Version 4.0, 12th February 2010

This document should be read in conjunction with the SCOPE 1 protocol (EUDRACT No. 2006-002241-37, ISRCTN: 47718479)

Authorised by:

Name: Dr Tom Crosby

Role: Chief Investigator

Signature: _____

Date: _____

Name: Gareth Griffiths

Role: Scientific Director WCTU

Signature: _____

Date: _____

SPONSOR: Velindre NHS Trust

SCOPE 1 Radiotherapy Guidance and Procedures

Radiotherapy Treatment Planning and Delivery

Abbreviations and Glossary

CT	Computerised tomography
CTV	Clinical Treatment Volume
DVH	Dose Volume Histogram
EUS	Endoscopic ultrasound
FSD	Focus to surface distance
GOJ	Gastro-oesophageal junction
GTV	Gross Tumour Volume
ICRU	International Commission on Radiation Units and Measurements
IRMER	The Ionising Radiation (Medical Exposure) Regulations
OAR	Organs at Risk
PET	Positron Emission Tomography
PRV	Planning Risk Volume
PTV	Planning Treatment Volume
RCR	The Royal College of Radiologists
TMG	Trial Management Group
WCTU	Wales Cancer Trials Unit

Introduction

This document describes the process for radiotherapy treatment planning of oesophageal cancer and has been developed for the purpose of the SCOPE 1 trial. The aim is to aid the delivery of high quality radiotherapy and to allow quality assurance procedures to be applied to ensure this is achieved. However, some aspects of the process are not explicitly defined and will vary according to the capabilities and characteristics of each centre and to some extent their local practice and experience. Guidelines for the delivery of concurrent chemotherapy are described elsewhere.

1.1 General Requirements

Conformal radiotherapy with a pixel based inhomogeneity correction is essential. The type of dose calculation algorithm to be used is not specified; the guidelines for Planning Treatment Volume (PTV) coverage are given later in section 5.1 and are based on use of a pencil beam algorithm. It is recognised however that these guidelines may not be realistic for other algorithms. Centres should assess dose coverage to PTV according to local experience in this case. Photon energy should be between 6MV and 10MV (but energies in excess of 10MV should only be used in exceptional cases due to secondary build-up depth). A combination of energies is permissible. Final calculation grid spacing of no greater than 0.3cm is recommended.

1 Patient Positioning and Computerised Tomography (CT) Planning Scan Acquisition

2.1 Timing of the Planning Scan

The planning scan should be performed within 2 weeks of starting the neo-adjuvant phase of chemotherapy AND within 6 weeks of the staging CT scan.

2.2 Treatment Position

Patients should be planned and treated in the supine position with both arms above their heads. Immobilisation of the patient using a 'chest board' which fixes the arm positions above the head is recommended and immobilisation of the legs with a device similar to a 'knee-fix' is also encouraged.

2.3 System of Reference

For the CT planning scan a suitable system of reference must be used. Three transversely aligned tattoos marked at the right, anterior and left surfaces of the patient (tattoos correspond to radio-opaque markers held in place for the duration of the CT planning scan) enable the patient to be correctly aligned for treatment. A single reference mark (for example the anterior mark) may be used to reference the isocentre of the external beam plan.

2.4 Use of IV Contrast

Use of IV contrast is recommended in line with RCR Recommendations¹. Where contrast-enhanced CT planning scans are to be used for the dose calculation there may be an effect on the monitor unit calculation, which will not be representative of the treatment situation. The magnitude of this effect will vary between individual patients, scanning protocols and centres. There are three acceptable solutions:

1. Use of single contrast-enhanced scan only. This can be used if the centre is satisfied that there are no implications of using contrast, for example if it has performed a study to assess the dosimetric effects of using contrast.
2. Use of both contrasted-enhanced and non-contrast CT scans. The contrast-enhanced scan is used for target volume definition and fused with the non-contrast scan which is used for dose calculation.
3. Use of single contrast-enhanced scan and assignation of unit density to heavily contrasted areas.

2.4.1 Additional issues to consider with the use of IV contrast enhanced radiotherapy planning scans

1. Safety: It is strongly recommended that each centre develops its own working instructions for the delivery of IV contrast for radiotherapy planning scans. It is also recommended that the RCR document 'Standards For Iodinated Intravascular Contrast Agent Administration To Adult Patients' is read and followed. The following should be considered:

- a. Patient identification:
 - i. Ensure that the correct patient is scanned following the correct protocol.
 - ii. Ensure consent form for this procedure is completed
- b. Allergic reaction to contrast:
 - i. Awareness of features associated with increased risk of reaction: history of allergy or asthma. Ask if patient has had previous contrast-enhanced imaging
 - ii. Awareness of medical support: a member of the medical team should be contactable throughout the duration of the scan and the emergency drugs trolley should be brought round to the scanner or be easily accessible.
- c. Effects of contrast in renal insufficiency; ensure recent creatinine is available and that patient is not dehydrated. Note that risks are increased in elderly patients, patients with cardiac failure, and diabetics (especially if taking oral metformin)
 - i. If serum creatinine level is above 120 μ mol/l but less than 150micromol/l, a member of the medical team should be informed and contrast administered at their discretion.
 - ii. If serum creatinine level is above 150 μ mol/l, a member of the medical team should be informed and contrast should not be administered, unless patient is on dialysis that will take place within 24hrs.

If in doubt, the decision should be made by a member of the medical team and if necessary discussed with a member of the TMG. Any reactions should be included in the patient's notes, and reported to the WCTU.

2. Practical procedure for IV contrast:

- a. Insert cannula
- b. Position patient in radiotherapy position
- c. Select correct imaging protocol; consider requirement for pre and post- contrast image acquisition
- d. **Optimise image quality with IV contrast:** These are recommendations based on experience from three centres, who have kindly allowed us to review their clinical protocols: Mount Vernon Hospital, Royal Marsden NHS Trust, and Velindre NHS Trust. Centres need to be aware that these recommendations are from clinical experience with their own hardware and

software, and that some degree of local development may be required.

- i. Type: Either Omnipaque or Visipaque can be used
 - ii. Temperature: ensure contrast is brought to room temperature by placing in warm water
 - iii. Volume: 100ml
 - iv. Infusion rate: 2.5-3mls per sec. This may be reduced to as low as 1ml per sec, depending on cannula size
 - v. Time between injection and CT: 35-40s
- e. Remove cannula at completion of scan

2.5 Extent of the Scan

To enable accurate assessment of the dose to organs at risk the scan should extend superiorly to at least one CT slice above the apices of the lungs and inferiorly to the iliac crest (L2). Scans for upper third tumours may need to extend superiorly to the tragus. Slice thickness should be no greater than 0.5cm.

2 Organs at risk (OAR)

3.1 Lungs

The full extent of the right and left lungs are to be outlined, this should be done in such a way that the planning system will be able to calculate a combined lung Dose Volume Histogram (DVH).

3.2 Spinal Cord

The spinal cord should be outlined on slices which include or are within 2cm of the PTV in the superior and inferior directions. A Planning Risk Volume (PRV) for the cord is created to account for positioning error. The size of the margin added to the cord being commensurate with the accuracy of treatment delivery expected and as such, the tolerance level allowed in portal image verification on treatment. For example, Velindre Hospital applies a margin of 0.5cm isotropically to generate the spinal cord PRV and allows no more than 0.5cm movement of the isocentre on treatment before corrective action is taken. See section 7.1

3.3 Heart

The whole heart should be outlined to the extent of the pericardial sac (if visible). The major blood vessels (superior to the organ) and the inferior vena cava (towards the inferior extent of the heart) are excluded. Appendix 1 contains an example.

3.4 Liver

The whole liver should be outlined if the level of its superior edge overlaps with the level of the inferior extent of the PTV.

3.5 Kidneys

Each kidney should be outlined separately if the level of its superior edge overlaps with the level of the inferior extent of the PTV.

3 Definition of Treatment Volumes

Targets are defined following the principles of ICRU 50 and 62. The spinal cord and spinal cord PRV (section 3.2) should be outlined prior to definition of the treatment volumes. Dialogue with a specialist Upper GI radiologist regarding the target volume definition is encouraged.

4.1 GTV Definition

The Gross Tumour Volume (GTV) is the gross primary and nodal disease as defined on the planning CT scan with all available diagnostic information. This should include as a minimum: Endoscopic ultrasound (EUS) and contrast-enhanced CT. Some centres may have access to Positron Emission Tomography (PET) scans and their use is encouraged. In some cases the EUS will not define the full extent of the disease because the scope has failed to pass through the stricture, in such cases information is used from the original endoscopy and the diagnostic CT scan.

The GTV is localised on axial slices of the planning CT scan using the EUS to define a reference point (tracheal carina or the arch of the aorta) as well as the superior and inferior extent of the GTV. In principle the GTV should encompass the disease as defined on any of the above imaging modalities used (i.e. CT, EUS and/or PET), even if it's only apparent on a single modality.

4.2 CTV Definition

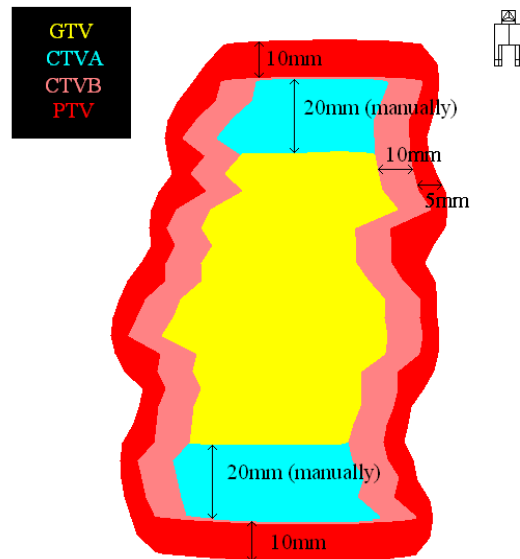
The Clinical Treatment Volume (CTV) is defined differently in two clinical situations depending on the proximity of the GTV to the gastro-oesophageal junction (GOJ). Tumours that have a high risk of disease within the stomach have the potential to metastasise to lymph nodes that will only be included within the CTV if specifically outlined. Thus, two CTV definition protocols are defined below.

4.2.1 CTV Definition for a GTV which does not extend to within 2cm of the gastro-oesophageal junction.

The CTV will comprise the GTV plus a margin of up to 1cm laterally and 2cm superiorly and inferiorly (along the line of the oesophagus). It is created in three steps:

- Step 1: The GTV is copied and labelled 'CTVA' (so that the GTV is preserved as a separate structure) and extended by 2cm superiorly and inferiorly by manually drawing along the line of the oesophagus.

- Step 2: CTVA is copied and labelled 'CTVB'. It is grown by a margin of 1cm in the right, left, anterior and posterior directions.
- Step 3: CTVB may then be adjusted as follows. Assessment of CTVB's proximity to the spinal cord PRV is made and where it is deemed that the spinal cord dose volume constraints will not be met, the posterior margin may be reduced. This reduction should be performed on a slice-by-slice basis and should be subject to a minimum CTVA to CTVB margin of 0.5cm. This is discussed in more detail in Appendix 2.

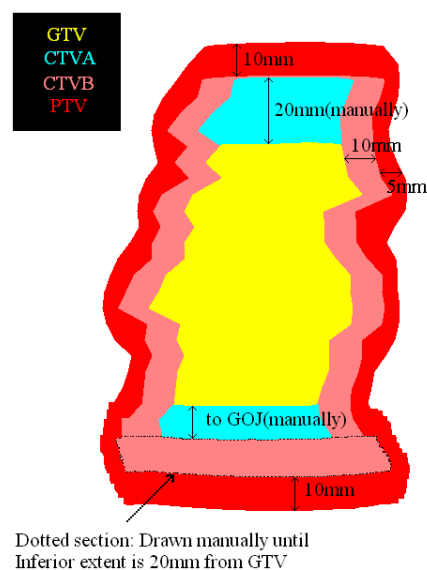


4.2.2 CTV Definition for a GTV which involves or comes within 2cm of the gastro-oesophageal junction.

The CTV will comprise the GTV plus a margin of up to 1cm laterally, 2cm superiorly (along the line of the oesophagus) and 2 cm inferiorly (this will include the mucosa of the stomach in the direction of the lymph node stations along the lesser curve including the para-cardial and left gastric lymph nodes). It is created in five steps:

- Step 1: The GTV is copied and labelled 'CTVA' (so that the GTV is preserved as a separate structure) and extended by 2cm superiorly by manual drawing along the line of the oesophagus.
- Step 2: CTVA is extended inferiorly as far as the GOJ making note of the length of extension from the GTV to this point. This step is not necessary if the GTV already extends to the level of the GOJ.
- Step 3: CTVA is copied and labelled 'CTVB'. This is grown with a margin of 1cm in the right, left, anterior and posterior directions.

- Step 4: CTVB is manually extended inferiorly such that the total inferior extension from GTV to CTVB is 2cm. This extension should aim to include the mucosa of the stomach, in the direction of the lymph node stations along the lesser curve including the para-cardial and left gastric lymph nodes.
- Step 5: CTVB may then be adjusted as follows. Assessment of CTVB's proximity to the spinal cord PRV is made and where it is deemed that the spinal cord dose volume constraints will not be met, the posterior margin may be reduced. This reduction should be performed on a slice-by-slice basis and should be subject to a minimum CTVA – CTVB margin of 0.5cm. This is discussed in more detail in Appendix 2.



4.3 PTV Definition

CTVB is copied and labelled 'PTV'. It is created by the addition of the following margins:

Superiorly and inferiorly: 1.0cm
Laterally, anteriorly and posteriorly: 0.5cm (this margin is applied in all circumstances regardless of the proximity of the target to the spinal cord)

The maximum treatment field length is 17cm, i.e. maximum EUS disease length of primary tumour and lymph nodes is 10cm (assumes approximate 1cm extension from PTV to field length).

4 Dose Volume Guidelines

There follows a set of 'dose volume guidelines.' The guidelines for the PTV (section 5.1) should be taken as definitive (subject to the type of dose calculation algorithm used), however the aim of the remaining guidelines (sections 5.2 – 5.6) is to assist optimisation of the plan in consideration of all the organs at risk. These guidelines should all be achievable in the majority of cases and therefore allow for the plan to be tailored to the individual case such that the patients' associated co-morbidity may be considered and doses to organs at risk modified within the guidelines given.

Region of Interest / Organ at Risk	Dose Constraint
PTV	V95% (47.5Gy) > 99.0%
PTV	PTV min > 93% (46.5Gy)
DMAX	<107% (53.5Gy)
GTV	GTV min > 100% (50.0Gy)
Spinal Cord PRV	Cord Max <80% (40Gy)
Combined Lungs	V40% (V20Gy) <25%
Heart	V80% (V40Gy) < 30%
Liver	V60% (V30Gy) < 60%
Individual kidneys	V40% (V20Gy) <25%

5.1 PTV

The aim is to encompass the PTV with the 95% isodose with the best possible conformality of the 95% isodose to the PTV. In practice 99% of the PTV should be covered by the 95% isodose. The PTV maximum should be no more than 107% of the prescribed dose to the ICRU reference point – this maximum dose is determined in accordance with ICRU definitions whereby a region of dose is considered clinically meaningful if its minimum diameter exceeds 1.5cm. These requirements for the PTV are based on the use of a pencil beam algorithm – if any other algorithm is used centres should assess dose coverage to PTV according to local experience of best possible coverage achievable.

5.2 Spinal Cord

Dose to the spinal cord PRV should be increased to a level of around 38Gy and up to a maximum point dose of 40Gy. In practice this is achieved via a high posterior beam contribution and results in best possible reduction of doses to heart & lungs. No significant advantage is expected in attempting to reduce the dose to spinal cord below 38Gy, conversely increasing the dose to this safe level will give improved dose volume results for the remaining OARs.

5.3 Lungs

The volume of lung (right and left combined) receiving 20Gy should be less than 25% i.e. $V_{20} < 25\%$. This level of dose may be achieved by judicious choice of gantry angle, optimised shielding and by limiting the percentage contribution of the lateral / lateral oblique beams.

5.4 Heart

The volume of heart receiving 40Gy should be less than 30% i.e. $V_{40} < 30\%$. A proportion of the heart may overlap with the PTV – dose reduction to the remainder of the heart volume if required may be achieved by reducing the anterior beam contribution.

5.5 Liver

The volume of liver receiving 30Gy should be less than 60% i.e. $V_{30} < 60\%$.

5.6 Kidneys

Volume of each kidney receiving 20Gy should be less than 25% i.e. $V_{20} < 25\%$. Where this is not achieved the plan should aim to spare one kidney (subject to consideration of individual kidney function as demonstrated on a renogram) as far as possible and within the $V_{20} < 25\%$ limit. This is not expected to be a problem except in some with Siewert Type 3 tumours (which are not eligible for SCOPE 1).

5.7 SCOPE 1 Radiotherapy planning using 'Type b' dose calculation algorithm

It is stated in section 5.1 that the aim is to conform the 95% isodose to the PTV with a target volume coverage of 99%. However, with increased use of type b algorithms* for dose calculation in the highly inhomogeneous region as is the thorax, the above is proven to be an unrealistic target for 95% dose coverage.

Recent work has been published² which attempted to address this issue with respect to oesophageal planning for SCOPE. The work was instigated as a result of the above issue when attempting to provide guidance to centres

returning QA and patient cases planned using type b algorithms, in which the PTV coverage would 'fail' target dose criteria.

The work included retrospectively planning 15 patients from the SCOPE trial using Oncentra Masterplan (OMP) [Nucletron, Veenendaal, The Netherlands] using the Collapsed Cone dose calculation algorithm³. The 95% dose coverage was compared with the percentage overlap of the PTV with low density tissue.

From the work it was found that a correlation could be drawn between the achievable 95% dose coverage and the percentage volume of the PTV which included low density tissue such as lung. From this correlation the following formula was derived to provide a dose coverage target:

$$V_{95\%} \geq 99\% - [0.4 \times \%PTV_{overlap}]$$

Also included in the published work was a short description of an approach to optimising a plan to achieve the above target coverage – this aspect is covered in more detail in this document:

In planning using type b algorithms it may be observed that improved coverage can be achieved through increasing the field size near the region of poor coverage. In order to avoid unnecessary increases in field size it is suggested that the initial planning is performed under full scatter conditions – inhomogeneity correction should be switched off or the patient outline set to water density. Under these conditions the plan can be quickly optimised with approximate wedging and relative beam weighting. In this way the field sizes should be set to achieve acceptable 95% isodose coverage. It is important that the relative weightings are representative of the final plan at this point as plans weighted heavily from ant post fields will result in the requirement of smaller field sizes from the lat fields, and larger on the A/P.

Final optimisation can then be conducted with inhomogeneity correction, whereby no *increase* to the field sizes should be applied. The figure derived using the formula above should be used as the target volume coverage for 95% dose.

It should be noted that the formula is based on work solely using the OMP collapsed cone algorithm on 15 patients. In using the technique for prospective planning on the same system the target coverage has been easily achieved in all cases. In which case the plan should be optimised to improve the coverage further if possible without increasing field sizes, beyond the point where the calculated target has been achieved.

Centres with an established method for planning with type b algorithms or those wishing to take a different approach can plan as preferred.

It is intended that plans calculated with type b algorithms will be assessed with respect to the target derived from the formula. As such an updated revision of the SCOPE RT plan assessment form has been produced to

include the %PTV overlap, along with the calculated target, to highlight deviations from the protocol.

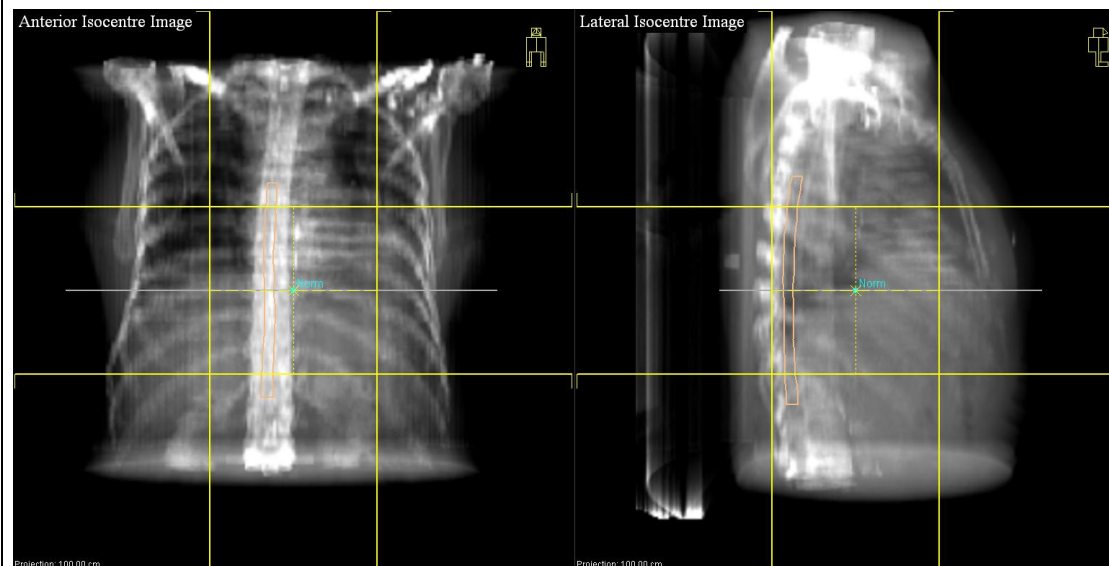
Glossary

*Type b algorithms include 'Collapsed Cone' in Pinnacle [Royal Phillips Electronics, Amsterdam, The Netherlands] and Oncentra Masterplan, 'Multigrad Superposition' in Xio [CMS Inc., St Louis, MO, USA], 'Anisotropic Analytical Algorithm' (AAA) in Eclipse [Varian Medical Systems Inc., Palo Alto, CA, USA].

5 Pre-Treatment Verification

Prior to treatment commencing, centres should follow their local protocols as regards pre-treatment verification; this may include a simulator check of the treatment, where any adjustments required should also be made according to local practice. Where simulator checks are performed, the single phase technique reduces this to one rather than two procedures.

An alternative system verifies positional accuracy on the first fraction of treatment. This may be done via the generation of 'dummy' isocentre fields (shown below) in the treatment planning system. These fields are prepared with a standard field size with zero collimator twist and are positioned at the anterior (gantry = 0°) and lateral (gantry = 90° or 270°) orientations to enable translation of any shifts seen in the comparative verification images into movements in the anterior-posterior, right-left and superior-inferior directions.



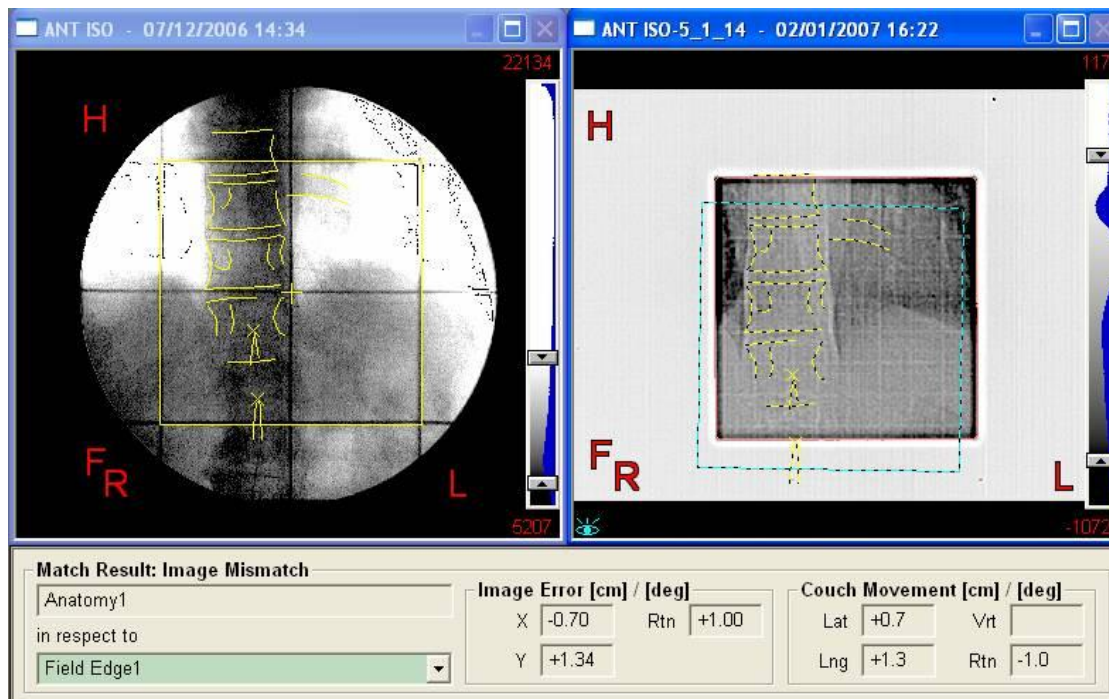
The 'dummy fields' are exported to the treatment 'record and verification' software and are used as 'reference images' with which 'on-treatment' portal images may be compared (see section 7). As such, the treatment is verified on set and a pre-treatment simulator check is not performed.

6 On-Treatment Verification

7.1 On-Treatment Verification and Adjustment of the Isocentre Position

Accuracy of delivery should be verified on the treatment set. This may be managed according to local protocols and in accordance with best practice. Our standard protocol for treatment positional verification specifies the collection of electronically acquired lateral and anterior portal isocentre images (or films where electronic means are not available) on the first three days of treatment and thereafter on a weekly basis.

Images are analysed via anatomical matching as shown in the images below: for the anterior image the vertebral bodies are outlined and matched, for the lateral image the process is repeated using the vertebral bodies and the sternum. The magnitude and direction of displacement between the 'reference' and 'on-treatment' images is then measured in the Sup-Inf, Ant-Post and Left-Right directions.



This analysis is performed and checked by suitably trained and authorised 'IRMER practitioners' For images which fall outside the accepted tolerance, action is determined based on the extent of the mismatch - three action levels are defined as follows:

- Level 1

No action is required if a portal image is less than 0.5cm displaced from the reference image.

- Level 2

If any given portal image is between 0.5 and 1.0cm displaced from the reference image then treatment may continue but set up is monitored by repeating portal images on each subsequent fraction until three sets have been acquired. At this point the average shift is calculated and the set up movements of the isocentre from the patient reference point are adapted accordingly. An off-line correction strategy is adopted i.e. a further set of images is taken on the next fraction of treatment and is analysed prior to the next day's treatment.

- Level 3

If any given portal image is more than 1.0cm displaced from the reference image, then the treatment set up is reviewed prior to further treatment being delivered. This review may be a simulator or an on-set on-line correction strategy. i.e. prior to set up, new set up isocentre movements from the patient reference mark are calculated using the known displacements from the reference image and a further set of isocentre images must be taken and analysed before the treatment is delivered.

All changes are fully documented within the patient treatment record.

7.2 On-Treatment Verification of Patient Outline

Accuracy of the patient outline should be verified on set, as changes may have occurred since the CT Planning scan was acquired. This may be done according to local protocols and will depend on the technology available at each centre. Our standard protocol requires the measurement of FSD for each treatment field for the first three fractions of treatment. The readings should reflect a consistent treatment set up i.e. if set up instructions are changed at any point during the treatment, the measurements must be taken for the three fractions following the change. Where the average reading for any field is more than 0.5cm out of tolerance, the treatment sheet is referred to Physics and the need for monitor unit correction is assessed. However if any single measurement for any given beam is more than 1.5cm different

from that planned, then the matter is investigated before further treatment is delivered.

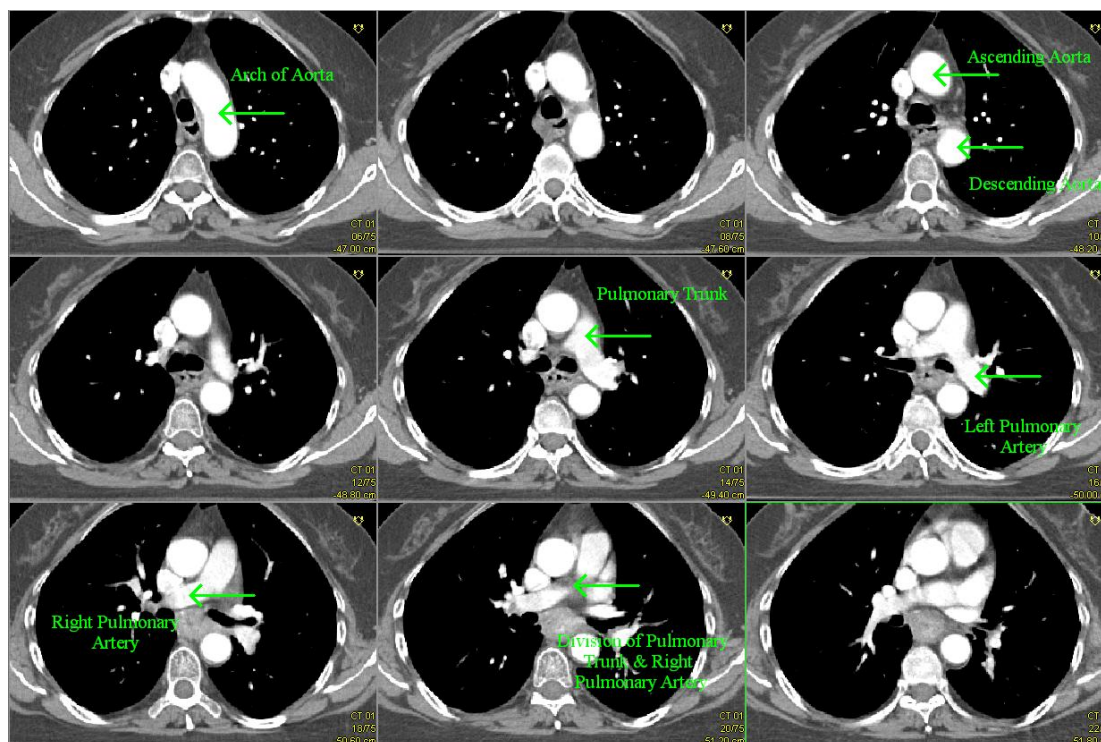
Where the patient's plan is referred for possible monitor unit correction the following guidelines are applied: If any single beams' average FSD reading is more than 1.0cm different from the planned FSD, or if any two beams' average FSD is more than 0.5cm different from that planned, then a monitor unit correction is calculated, checked and applied. Large changes in FSD (>1.5cm) may be indicative of poor set up and are investigated further to confirm treatment accuracy before a monitor unit correction is applied.

7 References

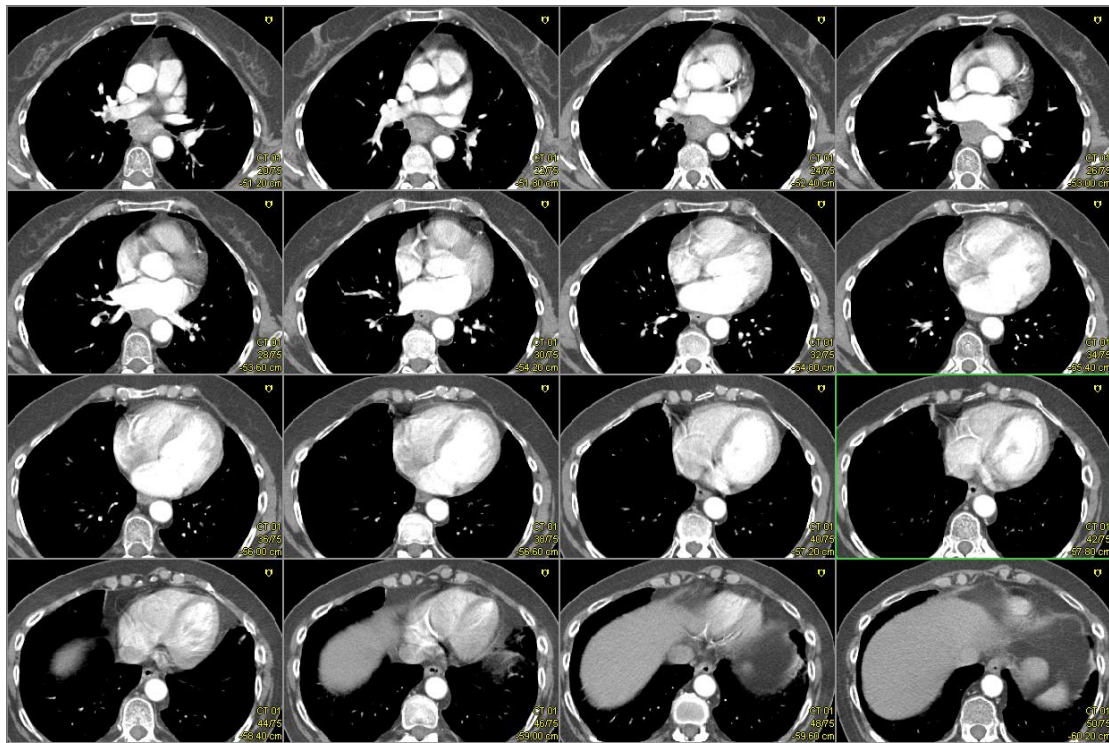
1. Board of the Faculty of Clinical Radiology, The Royal College of Radiologists (2005) *Standards For Iodinated Intravascular Contrast Agent Administration To Adult Patients* Royal College of Radiologists, London. <http://www.rcr.as.uk>
2. Wills L. The effect of planning algorithms in oesophageal radiotherapy in the context of the SCOPE 1 trial. *Radiother Oncol* 2009;93:462-467.
3. Ahnesjö A. Collapsed cone convolution of radiant energy for photon dose calculation in heterogeneous media/ *Med Phys* 1989;16:577-92.

4. Appendix 1: Delineation of Heart Volume

The whole heart is outlined to the extent of the pericardial sac (if visible). The major blood vessels (superior to the organ) and the inferior vena cava (towards the inferior extent of the heart) are excluded. The superior extent is often difficult to define and may be simplified by identification of the vessels superior to the heart. We use the point where the pulmonary trunk and the right pulmonary artery are seen as separate structures as indication of the superior extent of the heart. Shown below are alternate CT images for a scan taken at 0.3cm intervals.



For reference the non-delineated CT data set is also provided below.



8 Appendix 2: Suggested System to Reduce Posterior CTV Margin, Where Required

Where the PTV is estimated to be so close to the spinal cord PRV that its dose volume constraints cannot be met, we recommend reducing the posterior extension of CTVA to CTVB (from a maximum of 1cm to a minimum of 0.5cm). This process may be performed according to local centres' discretion yet this example gives a system of adjustment which enables the clinician to delineate PTVs for which the dose volume constraints are able to be achieved.

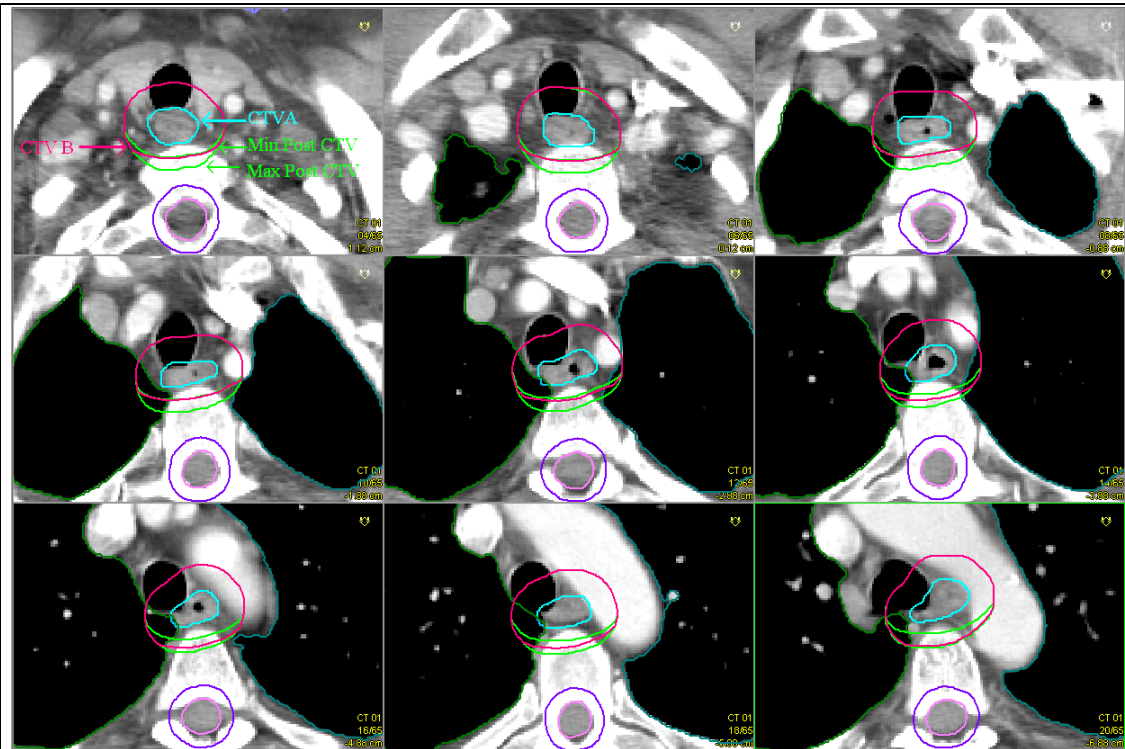
The distance between CTVB and the spinal cord PRV that will allow the cord dose volume constraints to be met is estimated (NB an additional margin is added to CTVB during creation of the PTV). Practically this cannot be easily defined, but should be evaluated at a local level with a pragmatic approach. Once the optimal distance (for each centre) between CTVB and spinal cord PRV is established, it can be applied on an individual patient basis. This distance will then be maintained by adjusting the CTVA to CTVB posterior margin on a slice-by-slice basis as follows:

Following the creation of CTVB, the distance between its posterior edge and the anterior edge of the spinal cord, PRV should be measured. At Velindre, we have noted that if CTVB lies no closer than 1.3cm from the spinal cord PRV, at any point then the CTVA to CTVB margin is kept at 1cm. However, if CTVB lies <1.3cm from the spinal cord PRV then its posterior margin is reduced on a slice-by-slice basis to a minimum 0.5cm. We recommend creating two guide structures ('Min Post CTV' and 'Max Post CTV').

Min Post CTV = CTVA + 1.0cm right, left and anteriorly and a 0.5cm margin posteriorly.

Max Post CTV = CTVA + 1.0cm right, left, anteriorly and posteriorly (i.e. the original CTVB).

CTVB is then adjusted within the range of these guide structures on a slice-by-slice to maintain the 1.3cm distance. An example of this process is shown opposite.



9 Appendix 3: Planning and Optimisation of the Single-Phase External Beam Plan

A3.1: Introduction

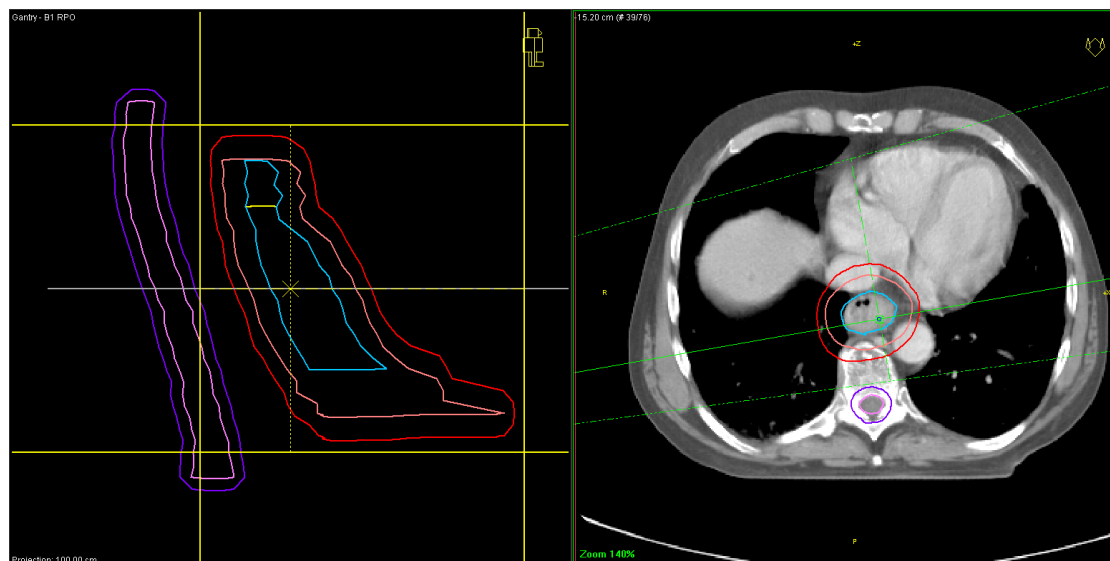
The purpose of this section is to offer guidance to centres who have not had working experience, of using a single phase technique and as such comprises a 'walk-through' example which is not intended to be prescriptive but aims to offer assistance if required. Single-phase planning had been demonstrated to offer significant cardiac dose reduction as compared to a two-phase approach (Ant-Post phase, followed by 3-field plan). Furthermore, the single-phase may offer a radiobiological advantage to organs at risk and a reduced resource requirement as compared with the two-phase approach.

A3.2: Beam Orientations

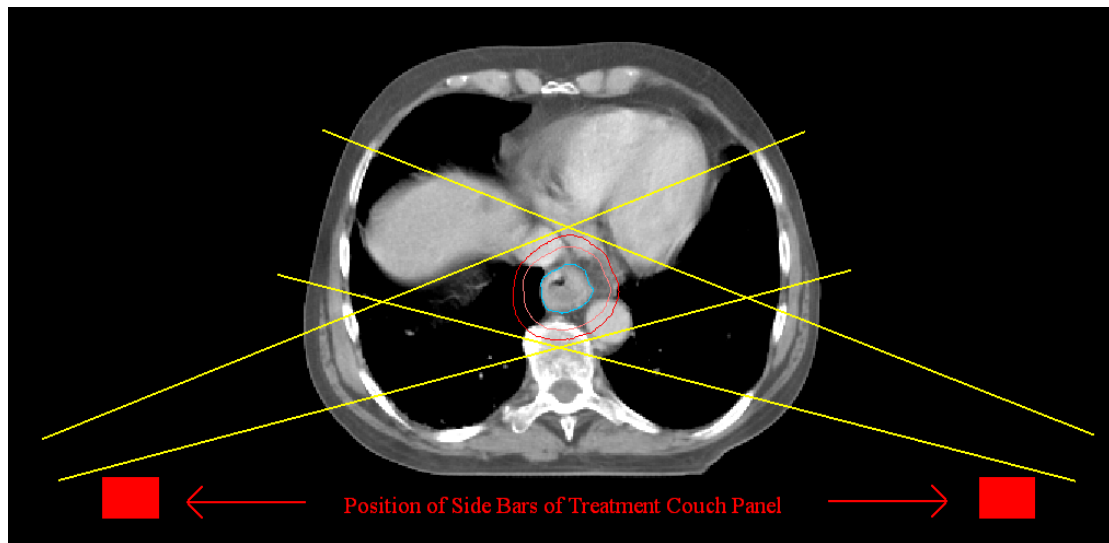
The exact number of beams and gantry angles are not explicitly defined – each patient will require an optimised arrangement. It is up to the individual centres to decide the beam arrangement. However, four primary beam orientations: anterior, posterior, right lateral (or lateral oblique) and left lateral (or lateral oblique), are usually satisfactory. This section describes how an unproblematic patient plan may be produced. Appendix 4 explores methods for planning more difficult cases.

A3.3: Positioning of Lateral / Oblique Beams

These beams should be positioned firstly to avoid the spinal cord PRV. The optimal gantry angle may be selected using the beams eye view to assess where the greatest gap between the Cord PRV and the PTV is achieved. Where possible, the gantry angle which gives the narrowest apparent size of the PTV should be considered in order to spare normal tissue.



Care should be taken to avoid gantry angles which may cause beams to pass through the dense structural parts of the treatment couch panel. We have experienced such problems with the use of the Varian tennis racket panel as the presence of the posterior beam requires that the open part of the panel be used – this part of the panel contains side bars which have significant attenuation and should be avoided during treatment. This may be avoided if the elements of the couch panel are visualised in the planning system as shown below. Here the position and size of the side bars of the treatment couch panel have been measured and added to the patient data set (assumes the patient is positioned centrally on the treatment couch). With these in place, the limiting posterior extent of the lateral/oblique beams can easily be assessed and so problems avoided.

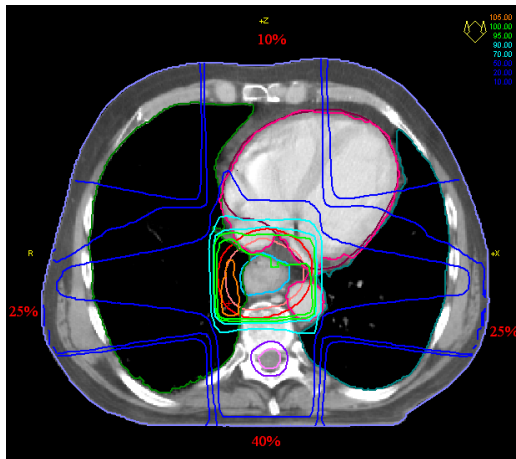
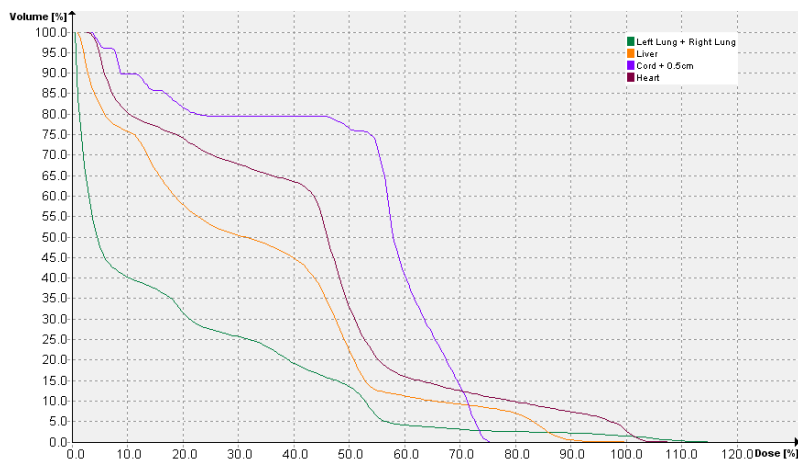


A3.4: Choice of Collimator Angle and Shielding Orientation for Lateral / Oblique Beams.

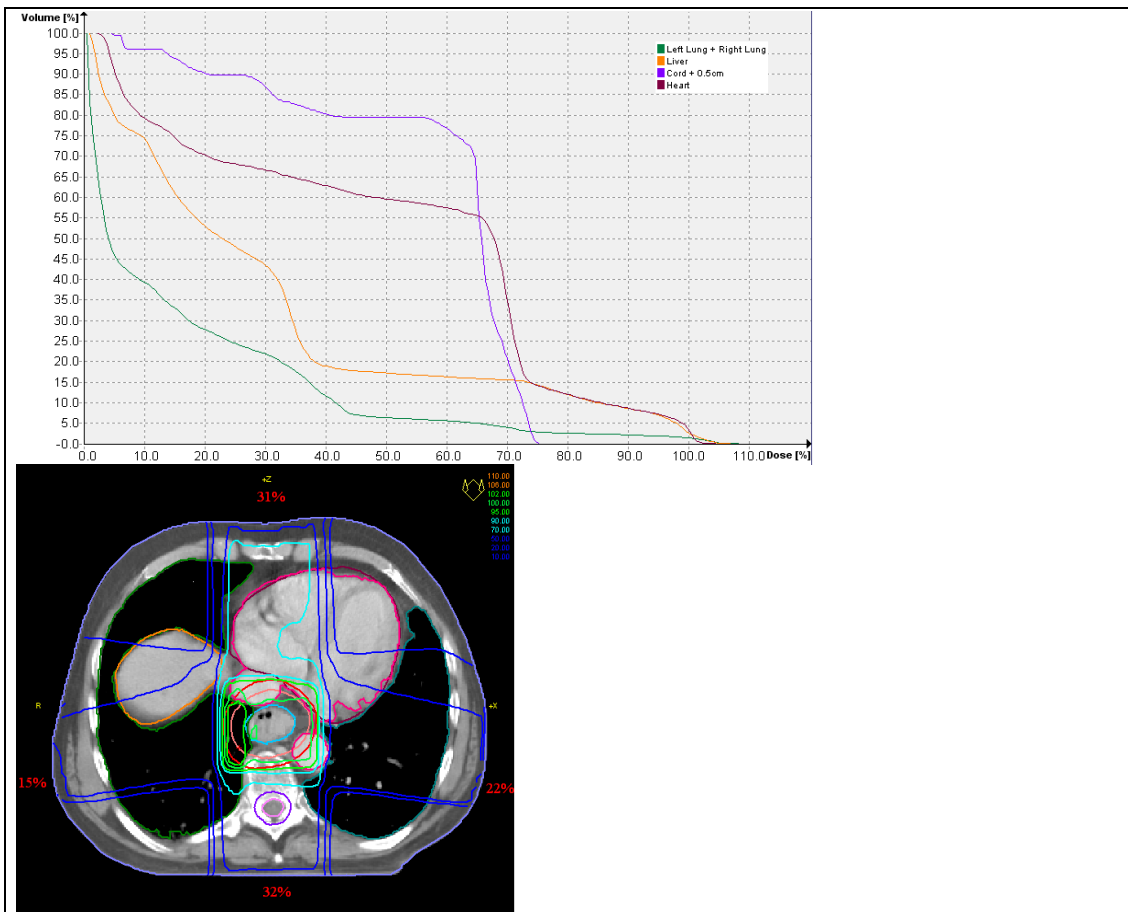
The usual 'curved' shape of the PTV from the lateral / oblique view will mean that the preferred collimator orientation for MLC shielding will often be around 0 degrees (that which enables the most conformal shielding considering the limitation of fixed MLC leaves and given their low resolution as compared to conformal shielding blocks). This position may be assessed as a starting point and approximate shielding added. For the single phase approach the lateral/oblique beams will frequently not require a wedge oriented in the ant-post direction which (if varian EDWs are used for example) would require the collimator angle to be rotated by 90 degrees. For other treatment delivery options, such as fixed or flying wedges etc. or conformal shielding blocks, this situation may not arise. However, it is undesirable to extend the treatment delivery process by their use if EDWs and MLCs are available. Where dynamic wedging is needed in the ant-post direction, the example in Appendix 4 (A4.2) shows how the loss of conformality to the PTV may be minimised.

A3.5: Establishing the Contribution of Each Beam

With the lateral / oblique beams in place, the anterior and posterior beams are added with approximate shielding and a crude calculation can then be done in order to assist in setting initial percentage contributions from each beam. At this point, the balance between the four beams can be adjusted so that the cord dose approaches the guideline of 38Gy (76% of the prescriptive dose) and that the remaining dose volume guidelines are met. The guidelines, if easily met will then allow for the plan to be tailored to the individual case such that the patient's associated co-morbidity may be considered and doses to organs at risk modified within the given guidelines. This is shown in the figures below and with reference to the dose volume guidelines given in section 5. For this example, the cord dose approaches the guideline as recommended, the lung dose volume guideline has been achieved and the heart and liver doses are considerably lower than the guideline level.



By way of example, if the patient were known to have significantly poor lung function we have the freedom within the process to increase the dose to the liver and heart in favour of the lung. This scenario is shown below.



A3.6: Coverage of the PTV

PTV coverage and the level of dose homogeneity within the PTV is assessed. In order to achieve the dose-volume requirements for the PTV given in section 5.1 the inclusion of wedges (and in some cases additional beams) may be deemed appropriate at this point. Adjustment to the relative contributions of each beam may follow. The DVH should again be referenced to check acceptability of doses to OARs.

A3.7: Fine Tuning the Plan

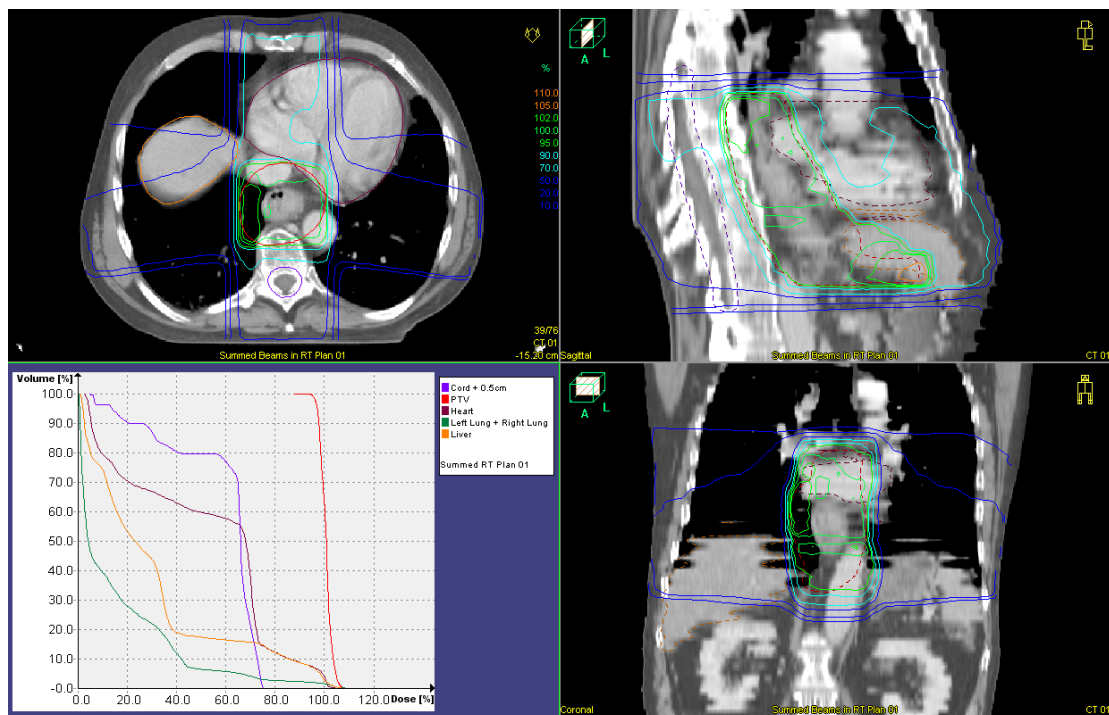
At this point a more detailed calculation is carried out (grid spacing of no greater than 0.3cm is recommended) and assessment of the overall plan is made. Subsequently MLC positions may be adjusted in order to improve the conformity of the 95% isodose to the PTV, and any of the beam parameters previously established may be modified over a number of iterations in order to fully optimise the plan.

A3.8: The Final Plan

The final plan meets the dose volume requirements for the PTV and has also achieved a suitable balance of doses to normal tissue within the guidelines

given. The plan has also taken into account the associated co-morbidities of the individual patient. The table below summarises the dose-volume information for this plan.

Region of Interest / Organ at Risk	Dose Constraint	Achieved
PTV	V95% (47.5Gy) > 99%	99.2%
PTV	PTV min > 93% (46.5Gy)	93.4%
DMAX	<107% (53.5Gy)	106%
Spinal Cord PRV	Cord Max <80% (40Gy)	75.1%
Combined Lungs	V40% (V20Gy) <25%	12%
Heart	V80% (V40Gy) < 30%	13%
Liver	V60% (V30Gy) < 60%	16%
Individual kidneys	V40% (V20Gy) <25%	N/A



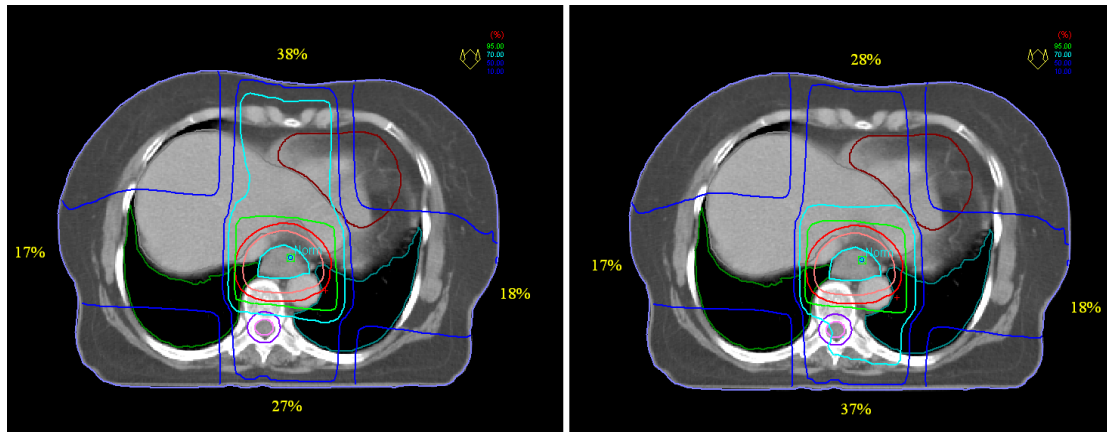
10 Appendix 4: Problem Examples

A4.1: Introduction to Problem Examples

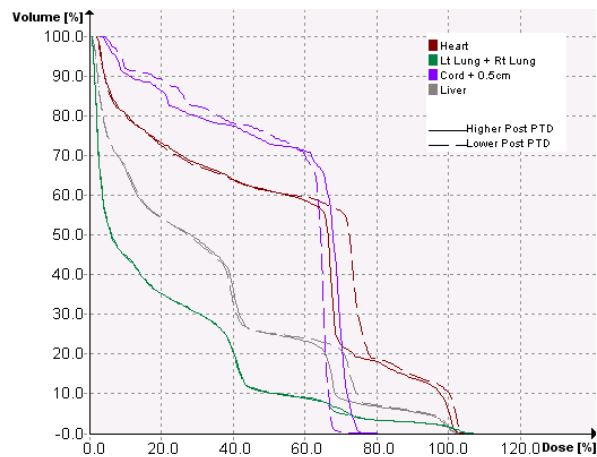
This section is intended to provide assistance to centres who may have limited experience of single phase planning and as such, attempts to illustrate and address some issues which have been found to arise in our experience. In oesophageal planning the size of the treatment site, it's proximity to multiple OARs and the inhomogeneous nature of the surrounding tissues mean that difficulties in achieving an optimal plan are often experienced. Here follows a series of examples which show how specific problems may be overcome to produce good results.

A4.2: Relative contribution of each beam

This example illustrates how increasing the relative contribution of the posterior beam in favour of the anterior beam contribution will achieve improved heart & liver sparing with no change to the lung dose. The figures below show two plans whose parameters are identical in all but one respect – the relative contributions of the anterior and posterior beams. The plan on the left has anterior and posterior beam contributions of 38% and 27% respectively whilst the plan on the right has anterior and posterior contributions of 28% and 37%.

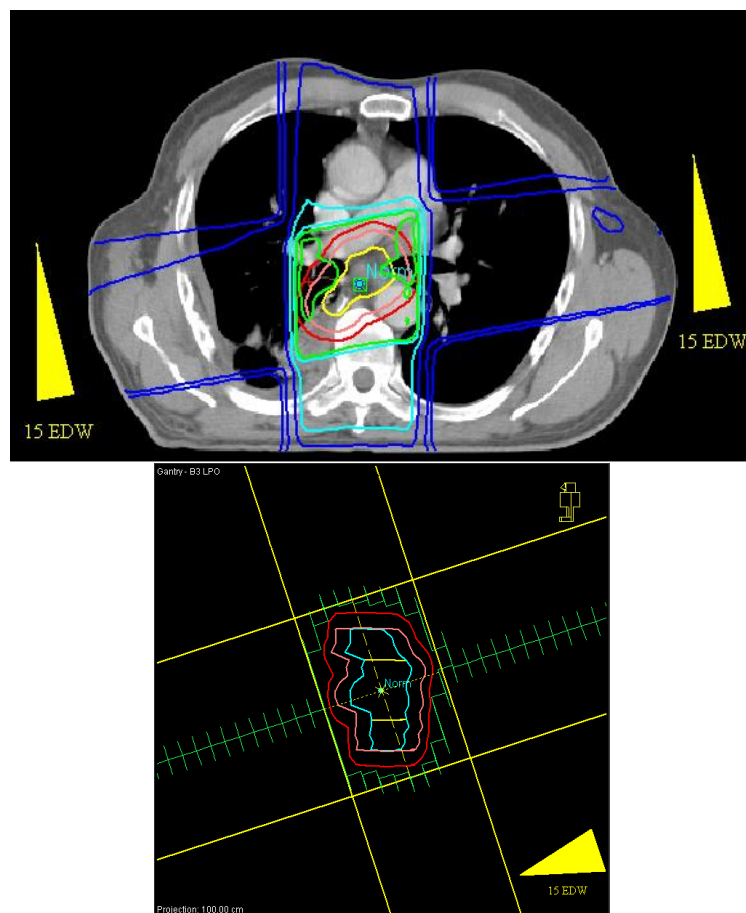


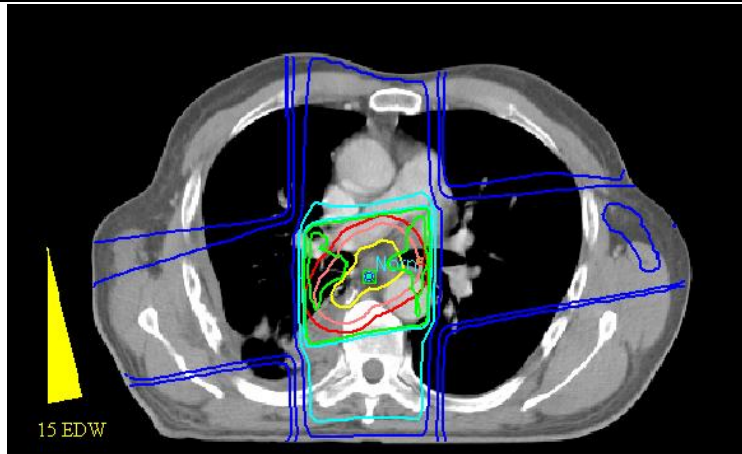
The dose volume histogram below shows a reduction in heart & liver dose, no change to the lung dose, and the cord dose remains within tolerance. In practice, increasing the cord dose to the tolerance level of 38Gy will result in the best possible sparing to the heart.



A4.3: Variations in lateral beam wedging

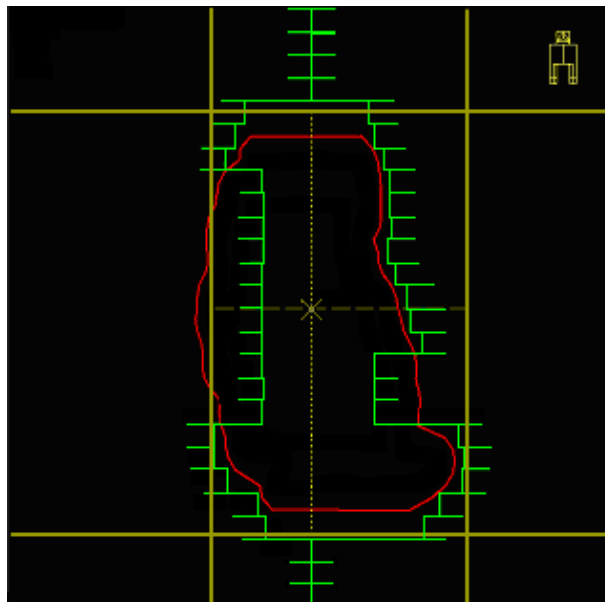
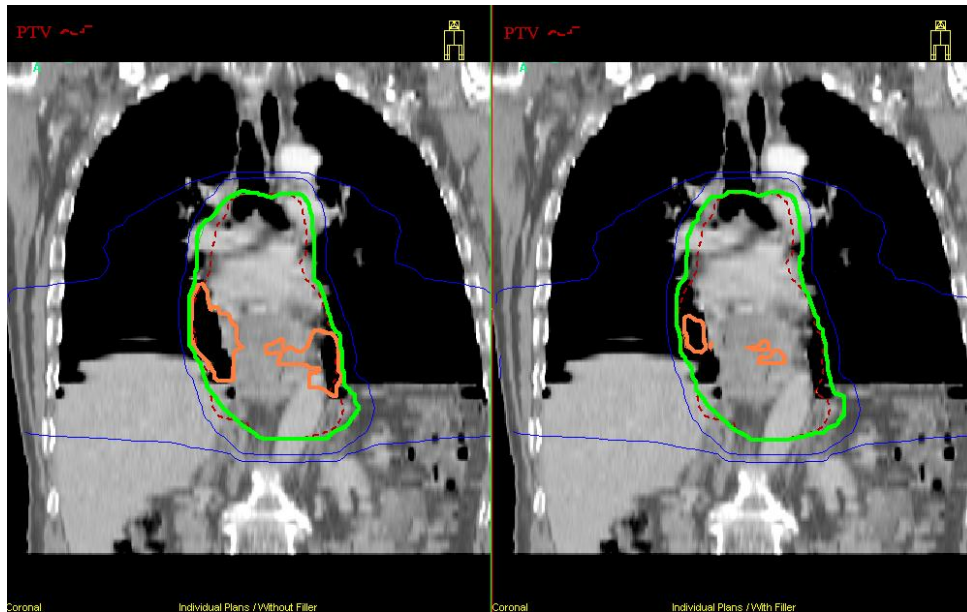
The suggested level of contribution of the posterior beam may be assisted by the use of 'anteriorly pointing' wedges on the lateral beams. However, where dynamic wedges are the preferred or are the only method of dose modulation available, their use may lead to reduced conformality of the MLCs to the PTV due to the need for the collimator to be positioned at 90° or 270° . Where EDW wedges are used, it may be possible to maintain conformality of the 95% isodose by increasing the wedge angle required on one of the lateral beams, and removing the wedge from the other. This action enables freedom of collimator angle and therefore optimal MLC positioning for one of the two lateral beams. The example below shows two plans – one having two anteriorly pointing 15 degree wedges on the lateral beams, and one having only one 30 degree wedge. The absence of the wedge on one of the lateral beams on the second plan has enabled more conformal MLC shielding and therefore improved the plan.





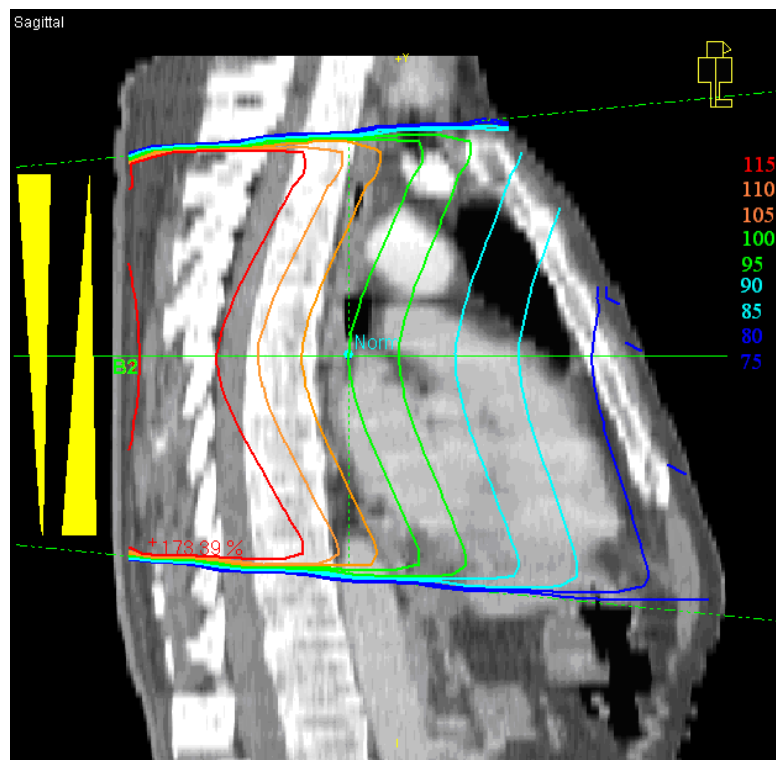
A4.4: Use of filler beams to lower hotspots within the PTV

The proximity of the oesophagus to lung tissue will often mean that difficulties are experienced in achieving a homogeneous dose throughout the PTV. The coronal sections below illustrate an example where hotspots seen in the lung tissue contained within the PTV have been reduced with the inclusion of a low weighted anterior 'filler beam' the 'beams eye view' for which is also shown below. In this case the filler beam delivers 5% of the tumour dose - the MLCs have been positioned in order to shield the hotspots and so improve the dose inhomogeneity within the PTV.



A4.5: Use of opposing superior–inferior wedged beams to improve coverage of 95% isodose and dose homogeneity within the PTV

Improvement in the coverage of the PTV with the 95% isodose may be seen by using a combination of two heavily wedged beams to replace a single unwedged beam (usually the posterior or anterior beam). To illustrate this effect the image below shows the distribution from two 60 degree wedged beams (one pointing superiorly, and one pointing inferiorly). The important thing to note is that the isodoses at depth are around 10% higher at the superior and inferior extents of the beam than at the central axis, and so the combination will deliver more dose to both extremes of the PTV than can be delivered with a single unwedged beam. Furthermore, this combination allows a greater degree of freedom in plan optimisation to achieve dose homogeneity across the PTV as the two beams can be weighted as required to achieve the best balancing of the plan.



11 A4.6: Maximising PTV coverage Vs cord dose.

A common issue raised by centres planning scope patients is how to approach the situation where the spinal cord PRV and PTV are in close proximity.

It was outlined in Appendix 2 how the posterior of CTVB may be modified in the region where it is deemed that the spinal cord PRV dose volume objective may not be met, subject to a minimum CTVA to CTVB margin of 0.5cm.

Additional advice was given in Appendix 4 covering the use of sup-inf wedges and opposed sup-inf wedges, which may be used to improve target coverage toward the furthest extent of the volume.

Further to this, the example below may be useful in optimising the posterior dose gradient to allow improved PTV coverage versus cord PRV maximum dose. The example illustrates how careful consideration of which fields to apply sup-inf wedging to can improve the distribution in this region.

Three plans were produced for the same SCOPE 1 patient. The first is based on the clinical plan in which sup wedging was used on both the anterior (45° wedge) and left lateral (15° wedge) fields. The cord PRV volume max dose was increased to a maximum, but there was still some necessary compromise to PTV coverage due to the extreme proximity of the two ROIs.

As the cord PRV and PTV are in close proximity toward the superior end of the volume further plans were created – Plan01 and Plan02 – in which the sup wedging effect was transferred from the anterior field (30° Plan01 and 15° Plan02) to the lateral field (30° Plan01 and 45° Plan02). The MU for each field was altered so that their contribution to the isocentre was constant across all plans.

The images below show the result to the dose distribution and DVH.

Figure 1

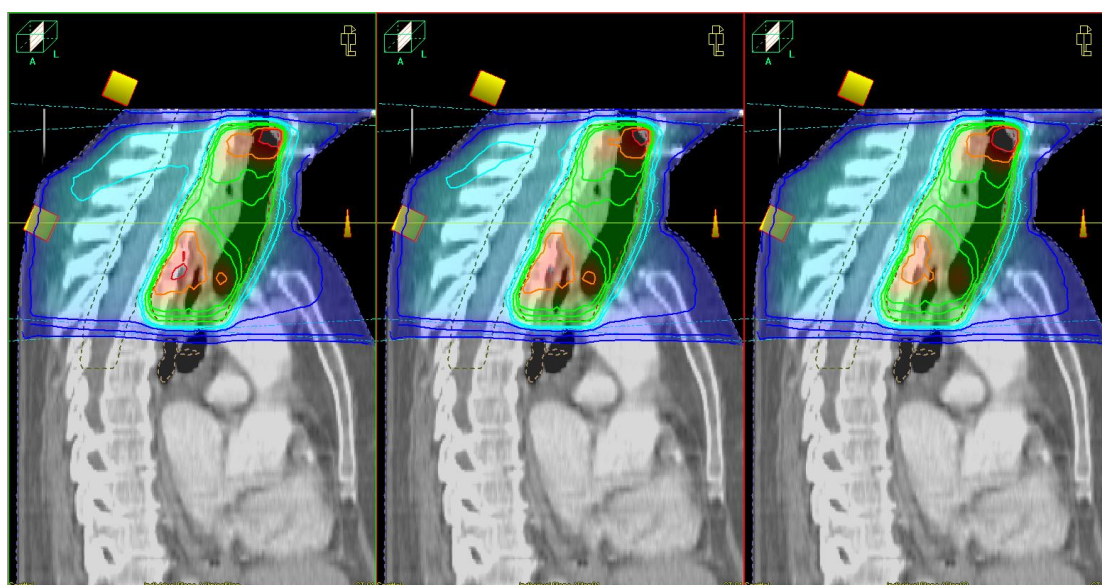
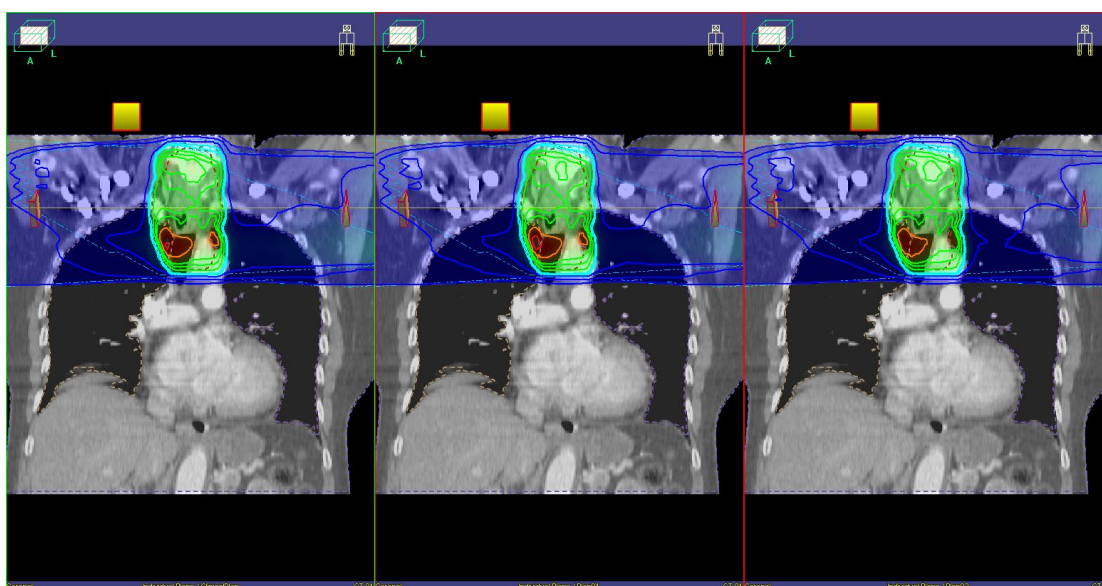


Figure 2



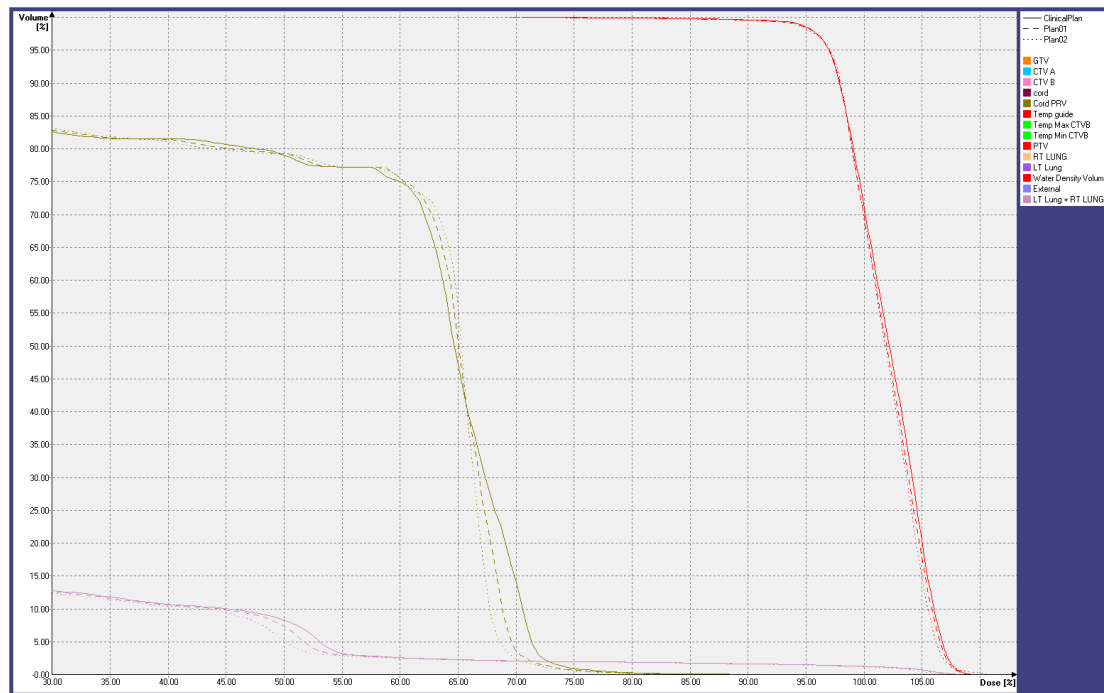
Figures 1 and 2 show sagittal and coronal views respectively of the three plans; ClinicalPlan left, Plan01 centre and Plan02 right. On the sagittal view it can be seen that with transferring the wedging from ant to lateral there is a corresponding increase in the dose gradient between the PTV and cord PRV. In the coronal sections it can be seen that there is only a small effect on the overall balance of the dose distribution throughout the length of the target.

In this particular case there is an additional benefit to the lung dose as the increased sup wedging reduces the contribution to the PTV through the lungs at the inf extent - with a resulting increase in dose to the healthy tissue

superior to the lungs and correspondingly an increase to the lower dose level at the inf extent of the cord PRV.

These changes to the distribution are reflected in the DVH in figure 3 below.

Figure 3



The DVH shows the curves for PTV, Cord PRV and combined lungs for the ClinicalPlan (solid line), Plan01 (dashed line) and Plan02 (dotted line). It can be seen that with minimal reduction in the PTV coverage (which could be improved with small alteration) there is a significant reduction in the higher dose level to the cord and an overall increase in uniformity of the dose to the cord. Small additional sparing of the lungs at the 40% (20Gy) level can be seen, along with the more considerable sparing at the 50% (25Gy) level.

In this case the increased sparing to the cord PRV is very small at the 40Gy level because of the extreme proximity, with associated PTV compromise. However, careful selection of sup-inf wedging can significantly reduce the maximum cord PRV dose and consequently improve the level of compromise in some cases.

For those cases where it has been found that a compromise is inevitable, the advice has been given that the balance of compromise should be a local clinical decision whereby the issue is for the treating consultant to balance risks and benefits of compromising PTV and exceeding cord dose constraints.

Authors

Dr T Crosby
Dr J Staffurth
Miss L Wills
Mr Rhydian Maggs

Reviewers / Contributors

Dr A Crellin
Dr I Geh
Dr D Tait
Dr K Venables (NCRI Radiotherapy Clinical Studies Quality Assurance Group)

References

1. Group MRCOCW. Surgical resection with or without preoperative chemotherapy in oesophageal cancer: a randomised controlled trial. *Lancet*. 2002;18:1727-33.
2. Zhang H, Jin G, Shen H. Epidemiologic differences in esophageal cancer between Asian and Western Populations. *Chin J Cancer*. 2012;31(6):281-6.
3. Jemal A, Bray F, Center MM, Ferlay J, Ward E, Forman D. Global Cancer Statistics. *CA Cancer J Clin*. 2011;61:69-90.
4. Gwynne S, Wijnhoven BPL, Hulshof M, Bateman A. Role of Chemoradiotherapy in Oesophageal Cancer - Adjuvant and Neoadjuvant Therapy. *Clin Oncol*. 2014;26:522-32.
5. Cunningham D, Starling N, Rao S. Capecitabine and oxaliplatin for advanced esophagogastric cancer. *N Engl J Med*. 2008;358:36-46.
6. J S Cooper MDG, A Herskovic et al. Chemotherapy of locally advanced esophageal cancer: a long term follow up of a prospective randomised trial. *JAMA*. 1999;281:1623-7.
7. Walsh TN, Noonan N, Hollywood D, Kelly A, Keeling N, Hennessy TPJ. A comparison of multimodal therapy and surgery for esophageal adenocarcinoma. *New England J Medicine*. 1996;335:462-7.
8. Gebski V, Burmeister B, Smithers BM, Foo K, Zalcborg J, Simes J. Survival benefits from neoadjuvant chemoradiotherapy or chemotherapy in oesophageal carcinoma: a meta analysis. *Lancet Oncol*. 2007;8:226-34.
9. Cooper JS, Guo MD, Herskovic A, Macdonald JS, Martenson JA, Al-Sarraf M, et al. Chemoradiotherapy of locally advanced esophageal cancer: long-term follow up

of a prospective randomized trial (RTOG 85-01). Radiation Therapy Oncology Group. JAMA. 1999;281(17):1623-7.

10. Minsky BD, Pajak TF, Ginsberg RJ, Pisansky TM, Matrenson J, Komaki R, et al. INT 0123 (Radiation Therapy Oncology Group 94-05) phase III trial of combined-modality therapy for esophageal cancer: high-dose versus standard-dose radiation therapy. J Clin Oncol. 2002;20(5):1167-74.

11. Palta JR, Kim S, Li JG, Liu C. Intensity-Modulated Radiation Therapy. The State of the Art. Madison, WI: Medical Physics Publishing; 2003.

12. Brahme A. Dosimetric precision requirements in radiation therapy. Acta Radiol Oncol. 1984;23:379-91.

13. Mijnheer BJ, Batterman JJ, Wambersie A. What degree of accuracy is required and can be achieved in photon and neutron therapy? Radiother Oncol. 1987;8:237-52.

14. Pawlik TM, Keyomarsi K. Role of cell cycle in mediating sensitivity to radiotherapy. Int J Radiat Oncol Biol Phys. 2004;59(4):928-42.

15. Mesures BIPM. The International System of Units (SI). BIPM.

16. <http://altered-states.net/barry/newsletter450/dnadamage.jpg>. DNA Damage.

17. Owadally W, Staffurth J. Principles of cancer treatment by radiotherapy. Surgery (United Kingdom). 2015.

18. Emami B, Lyman J, Brown A, Cola L, Goitein M, Munzenrider JE, et al. Tolerance of normal tissue to therapeutic irradiation. Int J Radiat Oncol Biol Phys 1991;21(1):109-22.

19. <http://health-7.com/imgs/20/7507.jpg>. Linear accelerator schematic.

20. Varian Linac Head. Available from:
https://apps.varian.com/euen/oncology/radiation_oncology/clinac/clinac_dhx_high_performance.html.
21. Webb S. The physical basis of IMRT and inverse planning. *Brit J Radiol.* 2003;76(910):678-89.
22. Teoh M, Clark CH, Wood K, Whitaker S, Nisbet A. Volumetric modulated arc therapy: a review of current literature and clinical use in practice. *Brit J of Radiol.* 2011;84(1007):967-96.
23. McGarry CK, McMahon SJ, Craft D, O'Sullivan JM, Prise KM, Hounsell AR. Inverse planned constant dose rate volumetric modulated arc therapy (VMAT) as an efficient alternative to five-field intensity modulated radiation therapy (IMRT) for prostate. *Journal of Radiotherapy in Practice.* 2014;13(1):68-78.
24. Schneider U, Pedroni E, Lomax A. The calibration of CT Hounsfield units for radiotherapy treatment planning. *Phys Med Biol.* 1996;41(1):111-24.
25. Stone HB, Coleman CN, Anscher MS, McBride WH. Effects of radiation on normal tissue: consequences and mechanisms. *The Lancet Oncology.* 4(9):529-36.
26. Drzymala RE, Mohan R, Brewster L, Chu J, Goitein M, Harms W, et al. Dose-volume histograms. *Int J Radiat Oncol Biol Phys.* 1991;21(1):71-8.
27. Pardalos, M P, Romeijn, H Edwin. *Handbook of optimization in medicine:* Springer; 2009.
28. Bewick V, Cheek L, Ball J. Statistics review 12: Survival analysis. *Critical Care.* 2004;8(5):389-94.

29. Hurt G, Nixon L, Griffiths G, Al-Mokhtar R, Gollins S, Staffurth J, et al. SCOPE1: a randomised phase II/III multicentre clinical trial of definitive chemoradiation, with or without cetuximab, in carcinoma of the oesophagus. *BMC Cancer*. 2011;11:466-78.
30. Bonner JA, Harari PM, Giralt J, Azarnia N, Shin DM, Cohen RB, et al. Radiotherapy plus cetuximab for squamous-cell carcinoma of the head and neck. *New England J Medicine*. 2006;354(6):567-78.
31. El Naqa I, Suneja G, Lindsay PE, Hope AJ, Alaly JR, Vicic M, et al. Dose response explorer: an integrated open-source tool for exploring and modelling radiotherapy dose-volume outcome relationships. *Phys Med Biol*. 2006;51:5719-35.
32. Ten Haken RK, Martel MK, Lawrence TS. Use of dose-volume-response factors in conformal high-dose therapy studies. In: A.R. Hounsell, J.M. Wilkinson, P.C. Williams, editors. *XIth International Conference on the Use of Computers in Radiation Therapy*: Handley Printers, Ltd, Manchester, UK; 1994. p. 22-3.
33. El Naqa I, Bradley J, Blanco AI, Lindsay PE, Vicic M, Hope A, et al. Multivariable modelling of radiotherapy outcomes, including dose-volume and clinical factors. *Int J Radiation Oncology Biol Phys*. 2006;64(4):1275-86.
34. Elshaikh M, Ljungman M, Ten Haken R, Lichter AS. Advances in Radiation Oncology. *Annual Review of Medicine*. 2006;57(1):19-31.
35. Griffiths EA, Brummell Z, Gorthi G, Pritchard SA, Welch IM. Tumour length as a prognostic factor in esophageal malignancy: Univariate and multivariate survival analyses. *J Surg Oncol*. 2006;93:258-67.
36. Wang BY, Goan YG, Hsu PK, Hsu WH, Wu YC. Tumour length as a prognostic factor in esophageal squamous cell carcinoma. *Ann Thorac Surg*. 2011;91:887-94.

37. Chua DTT, Sham JST, Kwong DLW, Tai KS, Wu PM, Lo M, et al. Volumetric analysis of tumor extent in nasopharyngeal carcinoma and correlation with treatment outcome. *Int J Radiat Oncol Biol Phys.* 1997;39(3):711-9.
38. Twine CP, Roberts SA, Rawlinson CE, Davies L, Escofet X, Dave BV, et al. Prognostic significance of the endoscopic ultrasound defined lymph node metastasis count in esophageal cancer. *Dis Esophagus.* 2010;23:652-9.
39. Wang S, Liao Z, Wei X, Liu H, Tucker S, Hu C, et al. Association between systematic chemotherapy before chemoradiation and increased risk of treatment-related pneumonitis in esophageal cancer patients treated with definitive chemoradiotherapy. *J Thorac Oncol.* 2008;3:277-82.
40. Weber WA, Ott K, Becker K, Dittler HJ, Helmberger H, Avril NE, et al. Prediction of response to preoperative chemotherapy in adenocarcinomas of the esophagogastric junction by metabolic imaging. *J Clin Oncol.* 2001;19:3058-65.
41. Maguire PD, Sibley GS, Zhou S, Jamieson TA, Light KL, Antoine PA, et al. Clinical and dosimetric predictors of radiation-induced esophageal toxicity. *Int J Radiat Oncol.* 1999;45:97-103.
42. Blanco AL, Chao KSC, El Naqa I, Franklin GE, Zakarian K, Vicic M, et al. Dose-volume modeling of salivary function in patients with head-and-neck cancer receiving radiotherapy. *Int J Radiat Oncology Biol Phys.* 2005;62(4):1055-69.
43. Bradley J, O'Deasay J, Bentzen S, El Naqa I. Dosimetric correlates for acute esophagitis in patients treated with radiotherapy for lung carcinoma. *Int J Radiat Oncol Biol Phys.* 2004;58(4):1106-13.
44. El Naqa I, Bradley JD, Linday PE, Hope AJ, O'Deasay J. Predicting radiotherapy outcomes using statistical learning techniques. *Phys Med Biol.* 2009;54:S9-S30.

45. El Naqa I, O'Deasy J, Mu Y, Huang E, Hope AJ, Lindsay PE, et al. Datamining approaches for modelling tumour control probability. *Acta Oncologica*. 2010;49:1363-73.
46. Olsen JR, Robinson CG, El Naqa I, Creach KM, Drzymala RE, Bloch C, et al. Dose-response for stereotactic body radiotherapy in early-stage non-small-cell lung cancer. *Int J Radiat Oncol Biol Phys*. 2011;81(4):e299-303.
47. Li XA, Alber M, O'Deasy J, Jackson A, Jee KK, Marks LR, et al. The use and QA of biologically related models for treatment planning. AAPM, 2012 Contract No.: 166.
48. O'Deasy J, Chao C, Markman J. Uncertainties in model-based outcome predictions for treatment planning. *Int J Radiat Oncol Biol Phys*. 2001;51(5):1389-99.
49. O'Deasy J, Niemierko A, Herbert D, Yan D, Jackson A, Haken RKT, et al. Methodological issues in radiation dose-volume outcome analyses: Summary of a joint AAPM/NIH workshop. *Med Phys*. 2002;29(9):2109-27.
50. Wasik MW, Yorke E, O'Deasy J, Nam J, Marks LB. Radiation dose-volume effects in the Esophagus. *Int J Radiat Oncol*. 2009;76:S86-S93.
51. Krishnankutty B, Bellary S, Naveen Kumar BR, Moodahadu LS. Data management in clinical research: An overview. *Indian Journal of Pharmacology*. 2012;44(2):168-72.
52. Gerritsen MG, Sartorius OE, vd Veen FM, Meester GT. Data management in multi-center clinical trials and the role of a nation-wide computer network. A 5 year evaluation. *Proceedings of the Annual Symposium on Computer Application in Medical Care*. 1993:659-62.
53. National Electrical Manufacturers Association.

Digital Imaging and Communications in Medicine (DICOM) Standard, (available free at <http://medical.nema.org/>). Rosslyn, VA, USA

54. Koyama-Ito H, Mizoe J. The exchange of treatment planning data using RTOG data exchange format. *Journal of JASTRO*. 2003;15(1):75-9.
55. Santanam L, Hurkmans C, Mutic S, Van Vliet-Vroegindeweij C, Brame S, Straube W, et al. Standardizing naming conventions in radiation oncology. *Int J Radiat Oncol Biol Phys*. 2012;83(4):1344-9.
56. O'Deisy J, Blanco AI, Clark VH. CERR: A computational environment for radiotherapy research. *Med Phys*. 2003;30(5):979-85.
57. Gayou O, Parida DS, Miften M. EUCLID: an outcome analysis tool for high-dimensional clinical studies. *Phys Med Biol*. 2007;52:1705-19.
58. SPSS. IBM Corp. Released 2011. IBM SPSS Statistics for Macintosh, Version 20.0. Armonk, NY: IBM Corp.
59. Feuvret L, Noel G, Mazeron JJ, Bey P. Conformity index: A review. *Int J Radiat Oncol Biol Phys*. 2006;64(2):333-42.
60. Lomax NJ, Scheib SG. Quantifying the degree of conformity in radiosurgery treatment planning. *Int J Radiat Oncol Biol Phys*. 2003;55:1409-19.
61. Wu QRJ, Wessels BW, Einstein DB, Maciunas RJ, Kim EY, Kinsella TJ. Quality of coverage: Conformity measures for stereotactic radiosurgery. *J Appl Clin Med Phys*. 2003;4(4):374-81.
62. Ohtakara K, Hayashi S, Hoshi H. The relation between various conformity indices and the influence of the target coverage difference in prescription isodose surface on these values in intracranial stereotactic radiosurgery. *Brit J Radiol*. 2012;85:e223-8.

63. Baltas D, Kolotas C, Geramani K, Mould R, Ioannidis G, Kekchidi M, et al. A conformal index (COIN) to evaluate implant quality and dose specification in brachytherapy. *Int J Radiat Oncol Biol Phys.* 1998;40(2):515-24.
64. Van Riet A, Mak CA, Moerland MA, Elders LH, Van Der Zee W. A conformation number to quantify the degree of conformality in brachytherapy and external beam irradiation: Application to the prostate. *Int J Radiat Oncol Biol Phys.* 1997;37(3):731.
65. Knoos T, Kristensen I, Nilsson P. Volumetric and dosimetric evaluation of radiation treatment plans: Radiation conformity index. *Int J Radiat Oncol Biol Phys.* 1998;42(5):1169-76.
66. Mulliez T, Speleers B, Madani I, Gersem WD, Veldeman L, Neve WD. Whole breast radiotherapy in prone and supine position: is there a place for multi-beam IMRT? *Radiat Oncol.* 2013;8:151-8.
67. Hanna GG, Hounsell AR, O'Sullivan JM. Geometrical analysis of radiotherapy target volume delineation: a systematic review of reported comparison methods. *Clin Oncol.* 2010;22:515-25.
68. Persson GF, Nygaard DE, Hollensen C, Munck af Rosenschold P, Mouritsen LS, Due AK, et al. Interobserver delinaetion variation in lung tumour stereotactic body radiotherapy. *Brit J Radiol.* 2012;85:e654-60.
69. Jena R, Kirkby NF, Burton KE, Hoole ACF, Tan LT, Burnet NG. A novel algorithm for the morphometric assessment of radiotherapy treatment planning volumes. *Brit J Radiol.* 2010;83:44-51.
70. Jena R, Kirby NF, Burton KE, Hoole ACF, Tan LT, Burnet NG. A novel algorithm for the morphometric assessment of radiotherapy treatment planning volumes. *Brit J Radiol.* 2010;83:44-51.

71. Gwynne S, Spezi E, Sebag-Montefiore D, Mukherjee S, Miles E, Conibear J, et al. Improving radiotherapy quality assurance in clinical trials: assessment of target volume delineation of the pre-accrual benchmark case. *Brit J Radiol.* 2013;86:20120398.
72. Wills L, Millin A, Paterson J, Crosby T, Staffurth J. The effect of planning algorithms in oesophageal radiotherapy in the context of the SCOPE 1 trial. *Radiother Oncol.* 2009;93:462-7.
73. Knöös T, Wieslander E, Cozzi L, Brink C, Fogliata A, Albers D, et al. Comparison of dose calculation algorithms for treatment planning in external photon beam therapy for clinical situations. *Phys Med Biol.* 2006;51(22):5785-807.
74. Ahnesjö A, Saxner M, Trepp A. A pencil beam model for photon dose calculation. *Medical Physics.* 1992;19(2):263-73.
75. Ahnesjö A. Collapsed cone convolution of radiant energy for photon dose calculation in heterogeneous media. *Medical Physics.* 1989;16(4):577-92.
76. Thomas K, Otto AS. Monte Carlo- versus pencil-beam-/collapsed-cone-dose calculation in a heterogeneous multi-layer phantom. *Phys Med Biol.* 2005;50(5):859.
77. L Wills AM, J Paterson, T Crosby, J Staffurth. The effect of planning algorithms in oesophageal radiotherapy in the context of the SCOPE 1 trial. *Radiother Oncol.* 2009;93:462-7.
78. Pöttgen C, Stuschke M. Radiotherapy versus surgery within multimodality protocols for esophageal cancer - A meta-analysis of the randomized trials. *Cancer Treatment Reviews.* 2012;38(6):599-604.
79. Measurements BICoRUa. ICRU report. Vol. 50. Bethesda: Prescribing, recording and reporting photon beam therapy. 1993;50.

80. Measurements BICoRUa. ICRU report. Vol. 62. Bethesda: Prescribing, recording and reporting photon beam therapy (supplement to ICRU report 50). 1993;62.
81. Warren S, Partridge M, Carrington R, Hurt C, Crosby T, Hawkins M. Radiobiological determination of dose escalation and normal tissue toxicity in definitive chemoradiation therapy for esophageal cancer. *Int J Radiat Oncol Biol Phys.* 2014;90:423-9.
82. Vidal M, Vieilleveigne L, Izar F, Ferrand R. Dosimetric comparison of RapidArc and 3D-Conformal RT for esophageal cancer. *Physica Medica.* 2012;28, Supplement 1(0):S2-S3.
83. Weber DC, Tomsej M, Melidis C, Hurkmans CW. QA makes a clinical trial stronger: Evidence-based medicine in radiation therapy. *Radiother Oncol.* 2012;105:4-8.
84. Button MR, Morgan CA, Croydon ES, Roberts SA, Crosby TDL. Study to Determine Adequate Margins in Radiotherapy Planning for Esophageal Carcinoma by Detailing Patterns of Recurrence After Definitive Chemoradiotherapy. *Int J Radiat Oncol Biol Phys.* 2009;73(3):818-23.
85. Gwynne S, Spezi E, Wills L, Nixon L, Hurt C, Joseph G, et al. Toward semi-automated assessment of target volume delineation in radiotherapy trials: the SCOPE 1 pretrial test case. *Int J Radiat Oncol Biol Phys.* 2012;84(4):1037-42.
86. Moore KL, Schmidt R, Moiseenko V, Olsen LA, Tan J, Xiao Y, et al. Quantifying unnecessary normal tissue complication risks due to suboptimal planning: A secondary study of RTOG 0126. *Int J Radiat Oncol Biol Phys.* 2015;92(2):228-35.

87. Kataria T, Sharma K, Subramani V, Karrthick KP, Bisht SS. Homogeneity Index: An objective tool for assessment of conformal radiation treatments. *Journal of Medical Physics*. 2012;37(4):207-13.
88. Crosby T, Hurt C, Falk S, Gollins S, Mukherjee S, Staffurth J, et al. Chemoradiotherapy with or without cetuximab in patients with oesophageal cancer (SCOPE 1): a multicentre, phase 2/3 randomised trial. *Lancet*. 2013;Online Publication.
89. Williams BA, Mandrekar JN, Mandrekar SJ, Cha SS, Furth AF. Finding Optimal Cutpoint for Continuous Covariates with Binary and Time-To-Event Outcomes. Mayo Foundation. 2006.
90. Ellingson BM, Cloughesy TF, Zaw T, Lai A, Nghiemphu PL, Harris R, et al. Functional diffusion maps (fDMs) evaluated before and after radiochemotherapy predict progression-free and overall survival in newly diagnosed glioblastoma. *NeuroOncology*. 2012;14(3):333-43.
91. Grunewald J, Dong GS, Niessen F, Wen BG, Tsao ML, Perera R, et al. Mechanistic studies of the immunochemical termination of self-tolerance with unnatural amino acids. *Proc Natl Acad Sci USA*. 2009;106(11):4337-42.
92. Sheets NC, Goldin GH, Meyer AM, Wu Y, Chang Y, Stürmer T, et al. Intensity-modulated radiation therapy, proton therapy, or conformal radiation therapy and morbidity and disease control in localized prostate cancer. *JAMA*. 2012;307(15):1611-20.
93. Bohsung J, Gillis S, Arrans R, Bakai A, De Wagter C, Knöös T, et al. IMRT treatment planning—A comparative inter-system and inter-centre planning exercise of the ESTRO QUASIMODO group. *Radiother Oncol*. 2005;76(3):354-61.

94. Chung HT, Lee B, Park E, Lu JJ, Xia P. Can All Centers Plan Intensity-Modulated Radiotherapy (IMRT) Effectively? An External Audit of Dosimetric Comparisons Between Three-Dimensional Conformal Radiotherapy and IMRT for Adjuvant Chemoradiation for Gastric Cancer. *Int J Radiat Oncol Biol Phys.* 2008;71(4):1167-74.
95. Xhaferllari I, Wong E, Bzdusek K, Lock M, Chen JZ. Automated IMRT planning with regional optimization using planning scripts. *Journal of Applied Clinical Medical Physics.* 2013;14(1):176-91.
96. Craft DL, Halabi TF, Shih HA, Bortfeld TR. Approximating convex Pareto surfaces in multiobjective radiotherapy planning. *Med Phys.* 2006;33(9):3399-407.
97. Nicolini G, Ghosh-Laskar S, Shrivastava SK, Banerjee S, Chaudhary S, Agarwal JP, et al. Volumetric Modulation Arc Radiotherapy With Flattening Filter-Free Beams Compared With Static Gantry IMRT and 3D Conformal Radiotherapy for Advanced Esophageal Cancer: A Feasibility Study. *Int J Radiat Oncol Biol Phys.* 2012;84(2):553-60.
98. Murthy KK, Shukeili KA, Kumar SS, Davis CA, Chandran RR, Namrata S. Evaluation of dose coverage to target volume and normal tissue sparing in the adjuvant radiotherapy of gastric cancers: 3D-CRT compared with dynamic IMRT. *Biomed Imaging Interv.* 2010;6:e29-36.
99. Freilich J, Hoffe SE, Almhanna K, Dinwoodie W, Yue B, Fulpo W, et al. Comparative outcomes for 3D conformal versus intensity modulated radiation therapy for esophageal cancer. *Dis Esophagus.* (in press).
100. Nahum AE, Sanchez-Nieto B. Tumour control probability modelling: Basic principles and applications in treatment planning. *Physica Medica.* 2001;17(SUPPL. 2):13-23.

101. Dhawan A, Kohandel M, Hill R, Sivaloganathan S. Tumour control probability in cancer stem cells hypothesis. *PLoS ONE*. 2014;9(5).
102. Zaider M, Hanin L. Tumor control probability in radiation treatment. *Med Phys*. 2011;38(2):574-83.
103. Brenner DJ. Point: The linear-quadratic model is an appropriate methodology for determining iso-effective doses at large doses per fraction. *Seminars in radiation oncology*. 2008;18(4):234-9.
104. Bentzen SM, Constine LS, O'Deasay J, Eisbruch A, Jackson A, Marks LB, et al. Quantitative analysis of normal tissue effects in the clinic (QUANTEC): An introduction to the scientific issues. *Int J Radiat Oncol*. 2010;76:S3-S9.
105. Burman C, Kutcher GJ, Emami B, Goitein M. Fitting of normal tissue tolerance data to an analytic function. *Int J Radiat Oncol Biol Phys*. 1991;21(1):123-5.
106. Lyman JT. Complication probability as assessed from dose-volume histograms. *Radiation Research*. 1985;104(2 II):S13-S9.
107. Kutcher GJ, Burman C, Brewster L, Goitein M, Mohan R. Three-Dimensional Photon Treatment Planning Report of the Collaborative Working Group on the Evaluation of Treatment Planning for External Photon Beam Radiotherapy Histogram reduction method for calculating complication probabilities for three-dimensional treatment planning evaluations. *Int J Radiat Oncol Biol Phys*. 1991;21(1):137-46.
108. Nahum AE, Uzan J. (Radio)Biological Optimization of External-Beam Radiotherapy. *Computational and Mathematical Methods in Medicine*. 2012;2012:13.

109. Botterweck AA, Schouten LJ, Volovics A, Dorant E, Van Den Brandt PA. Trends in incidence of adenocarcinoma of the oesophagus and gastric cardia in ten European countries. *Int J Epidemiol.* 2000;29(4):645-54.
110. Buergy D, Lorh F, Baack T, Siebenlist K, Haneder S, Michaely H, et al. Radiotherapy for tumours of the stomach and gastroesophageal junction - a review of its role in multimodal therapy. *Radiat Oncol.* 2012;7:192.
111. Settle SH, Bucci MK, Palmer MB, Liu H, Liengsawangwong R, Guerrero TM, et al. PET/CT fusion with treatment planning CT (TP CT) shows predominant pattern of locoregional failure in esophageal patients treated with chemoradiation in in GTV. *Int J Radiat Oncol Biol Phys.* 2008;72:S72-S3.
112. Fakhrian K, Oechsner M, Kampfer S, Schuster T, Molls M, Geinitz H. Advanced techniques in neoadjuvant radiotherapy allow dose escalation without increased dose to organs at risk. *Strahlenther Onkol.* 2013;189:293-300.
113. Zhang Z, Liao Z, Jin J, Ajani J, Chang JY, Jeter M, et al. Dose-Response relationship in locoregional control for patients with stage II-III esophageal cancer treated with concurrent chemotherapy and radiotherapy. *Int J Radiat Oncol Biol Phys.* 2005;61(3):656-64.
114. Geh JJ, Bond SJ, Bentzen SM, Jones RG. Systematic overview of preoperative (neoadjuvant) chemoradiotherapy trials in oesophageal cancer: Evidence of a radiation and chemotherapy dose response. *Radiother Oncol.* 2006;78:236-44.
115. Bedford JL, Viviers L, Guzel Z, Childs PJ, Webb S, Tait DM. A quantitative treatment planning study evaluating the potential of dose escalation in conformal radiotherapy of the oesophagus. *Radiother Oncol.* 2000;57:183-93.
116. Rubin P, Casarett GW. *Clinical Radiation Pathology.* Vol 1. 1968.

117. Gwynne S, Falk S, Gollins S, Wills L, Bateman A, Cummins S, et al. Oesophageal Chemoradiotherapy in the UK - A Current Practice and Future Directions. *Clin Oncol*. 2013;25:368-77.
118. Hawkins MA, Aitken A, Hansen VN, McNair HA, Tait DM. Set-up errors in radiotherapy for oesophageal cancers – Is electronic portal imaging or conebeam more accurate? *Radiother Oncol*. 2011;98(2):249-54.
119. Rapaccini GL, Aliotta A, Pompili M, Grattagliano A, Anti M, Merlino B, et al. Gastric wall thickness in normal and neoplastic subjects: a prospective study performed by abdominal ultrasound. *Gastrointest Radiol*. 1988;13(3):197-9.
120. Pickhardt PJ, Asher DB. Wall thickening of the gastric antrum as a normal finding: multidetector CT with cadaveric comparison. *AJR Am J Roentgenol*. 2003;181(4):973-9.
121. Kavanagh BD, Pan CC, Dawson LA, Das SK, Allen X, Haken RKT, et al. Radiation Dose-Volume Effectes in the Stomach and Small Bowel. *Int J Radiat Oncol Biol Phys*. 2010;76(3):S101-S7.
122. Gagliardi G, Lax I, Ottolenghi A, Rutqvist LE. Long-term cardiac mortality after radiotherapy of breast cancer - application of the relative seriality model. *Br J Radiol*. 1996;69(825):839-46.
123. De Jaeger K, Hoogeman MS, Engelsman M, Seppenwoolde Y, Damen EMF, Mijnher BJ, et al. Incorporatin an improved dose-calculation algorithm in conformal radiotherapy of lung cancer: re-evaluation of dose in normal lung tissue. *Radiother Oncol*. 2003;69(1):1-10.

124. Feng M, Normolle D, Pan CC, Dawson LA, Amarnath S, Ensminger WD, et al. Dosimetric Analysis of Radiation-Induced Gastric Bleeding. *Int J Radiat Oncol Biol Phys.* 2012;84(1):e1.
125. Roeder F, Nicolay NH, Nguyen T, Ebrahimi LS, Askoxylakis V, Bostel T, et al. Intensity modulated radiotherapy (IMRT) with concurrent chemotherapy as definitive treatment of locally advanced esophageal cancer. *Radiat Oncol.* 2014;9:191.
126. Lever FM, Lips IM, Crijns SPM, Reerink O, van Lier ALHMW, Moerland MA, et al. Quantification of Esophageal Tumor Motion on Cine-Magnetic Resonance Imaging. *Int J Radiat Oncol Biol Phys.* 2014;88(2):419-24.
127. Wang J, Lin SH, Dong L, Balter P, Mohan R, Komaki R, et al. Quantifying the Interfractional Displacement of the Gastroesophageal Junction during Radiation Therapy for Esophageal Cancer. *Int J Radiat Oncol Biol Phys.* 2012;83(2):e273-e80.
128. Langen KM, Jones DTL. Organ motion and its management. *Int J Radiat Oncol Biol Phys.* 2001;50(1):265-78.
129. Nakamura A, Shibuya K, Nakamura M, Matsuo Y, Shiinoki T, Nakata M, et al. Interfractional dose variations in the stomach and the bowels during breathhold intensity-modulated radiotherapy for pancreatic cancer: Implications for a dose-escalation strategy. *Med Phys.* 2013;40(2).
130. Kumagai M, Hara R, Mori S, Yanagi T, Asakura H, Kishimoto R, et al. Impact of Intrafractional Bowel Gas Movement on Carbon Ion Beam Dose Distribution in Pancreatic Radiotherapy. *Int J Radiat Oncol Biol Phys.* 2009;73(4):1276-81.

131. Bouchard M, McAleer MF, Starkchall G. Impact of gastric filling on radiation dose delivered to gastroesophageal junction tumours. *Int J Radiat Oncol Biol Phys.* 2010;77:292-300.
132. Urie. M. Ion beams in tumor therapy. Weinheim, Germany: Chapman & Hall; 1995.
133. Scarfe WC, Farman AG. What is Cone-Beam CT and How Does it Work? *Dental Clinics of North America.* 2008;52(4):707-30.
134. Kim D-G. Can Dental Cone Beam Computed Tomography Assess Bone Mineral Density? *J Bone Metab.* 2014;21(2):117-26.
135. Team NCA. National Radiotherapy Implementation Group Report: Image Guided Radiotherapy (IGRT) Guidance for implementation and use. 2012.
136. Watanabe M, Isobe K, Uno T, Harada R, Kobayashi H, Ueno N, et al. Intrafractional Gastric Motion and Interfractional Stomach Deformity Using CT Images. *Journal of Radiation Research.* 2011;52(5):660-5.
137. Isobe K, Uno T, Kawakami H, Ueno N, Kawata T, Ito H. A case of gastric lymphoma with marked interfractional gastric movement during radiation therapy. *International Journal of Clinical Oncology.* 2006;11(2):159-61.
138. Watanabe M, Isobe K, Takisima H, Uno T, Ueno N, Kawakami H, et al. Intrafractional gastric motion and interfractional stomach deformity during radiation therapy. *Radiother Oncol.* 2008;87:425-31.
139. Ganeshan B, Miles KA. Quantifying tumour heterogeneity with CT. *Cancer Imaging.* 2013;13(1):140-9.

140. Nelson DA, Tan TT, Rabson AB, Anderson D, Degenhardt K, White E. Hypoxia and defective apoptosis drive genomic instability and tumorigenesis. *Genes and Development*. 2004;18(17):2095-107.
141. Eccles SA, Welch DR. Metastasis: recent discoveries and novel treatment strategies. *Lancet*. 2007;369(9574):1742-57.
142. Ng F, Kozarski R, Ganeshan B, Goh V. Assessment of tumor heterogeneity by CT texture analysis: Can the largest cross-sectional area be used as an alternative to whole tumor analysis? *European Journal of Radiology*. 2013;82(2):342-8.
143. Alobaidli S, McQuaid S, South C, Prakash V, Evans P, Nisbet A. The role of texture analysis in imaging as an outcome predictor and potential tool in radiotherapy treatment planning. *Brit J Radiol*. 2014;87(1042):20140369.
144. Miles KA, Ganeshan B, Griffiths MR, Young RCD, Chatwin CR. Colorectal cancer: Texture analysis of portal phase hepatic CT images as a potential marker of survival. *Radiology*. 2009;250(2):444-52.
145. Ganeshan B, Panayiotou E, Burnand K, Dizdarevic S, Miles K. Tumour heterogeneity in non-small cell lung carcinoma assessed by CT texture analysis: A potential marker of survival. *European Radiology*. 2012;22(4):796-802.
146. Davnall F, Yip CP, Ljungqvist G, Selmi M, Ng F, Sanghera B, et al. Assessment of tumor heterogeneity: an emerging imaging tool for clinical practice? *Insights Imaging*. 2012;3(6):573-89.
147. Chowdhury R, Ganeshan B, Irshad S, Lawler K, Eisenblätter M, Milewicz H, et al. The use of molecular imaging combined with genomic techniques to understand the heterogeneity in cancer metastasis. *Brit J Radiol*. 2014;87(1038).

148. Ganeshan B, Skogen K, Pressney I, Coutroubis D, Miles K. Tumour heterogeneity in oesophageal cancer assessed by CT texture analysis: Preliminary evidence of an association with tumour metabolism, stage, and survival. *Clinical Radiology*. 2012;67(2):157-64.
149. Koller CJ, Eatough JP, Bettridge A. Variations in radiation dose between the same model of multislice CT scanner at different hospitals. *Brit J Radiol*. 2003;76(911):798-802.
150. Chalkidou A, O'Doherty MJ, Marsden PK. False discovery rates in PET and CT studies with texture features: A systematic review. *PLoS ONE*. 2015;10(5).
151. Warren S, Partridge M, Bolsi A, Lomax AJ, Hurt C, Crosby T, et al. An Analysis of Plan Robustness for Esophageal Tumors: Comparing Volumetric Modulated Arc Therapy Plans and Spot Scanning Proton Planning. *Int J Radiat Oncol Biol Phys*. 2016;95(1):199-207.
152. Fave X, Mackin D, Yang J, Zhang J, Fried D, Balter P, et al. Can radiomics features be reproducibly measured from CBCT images for patients with non-small cell lung cancer? (0094-2405 (Print)).
153. van Timmeren JE, Leijenaar RTH, van Elmpt W, Lambin P. 221 - Can we replace high quality simulation CT by simple kVcone-beam CT images to extract an externally validated radiomics signature? *Radiother Oncol*.118, Supplement 1:S107.